The role of the Wnt pathway in the regulation of the central nervous system growth

Mª Pilar Lozano Fernández

The role of the Wnt pathway in the regulation of the central nervous system growth

Mª Pilar Lozano Fernández

Barcelona, 2025

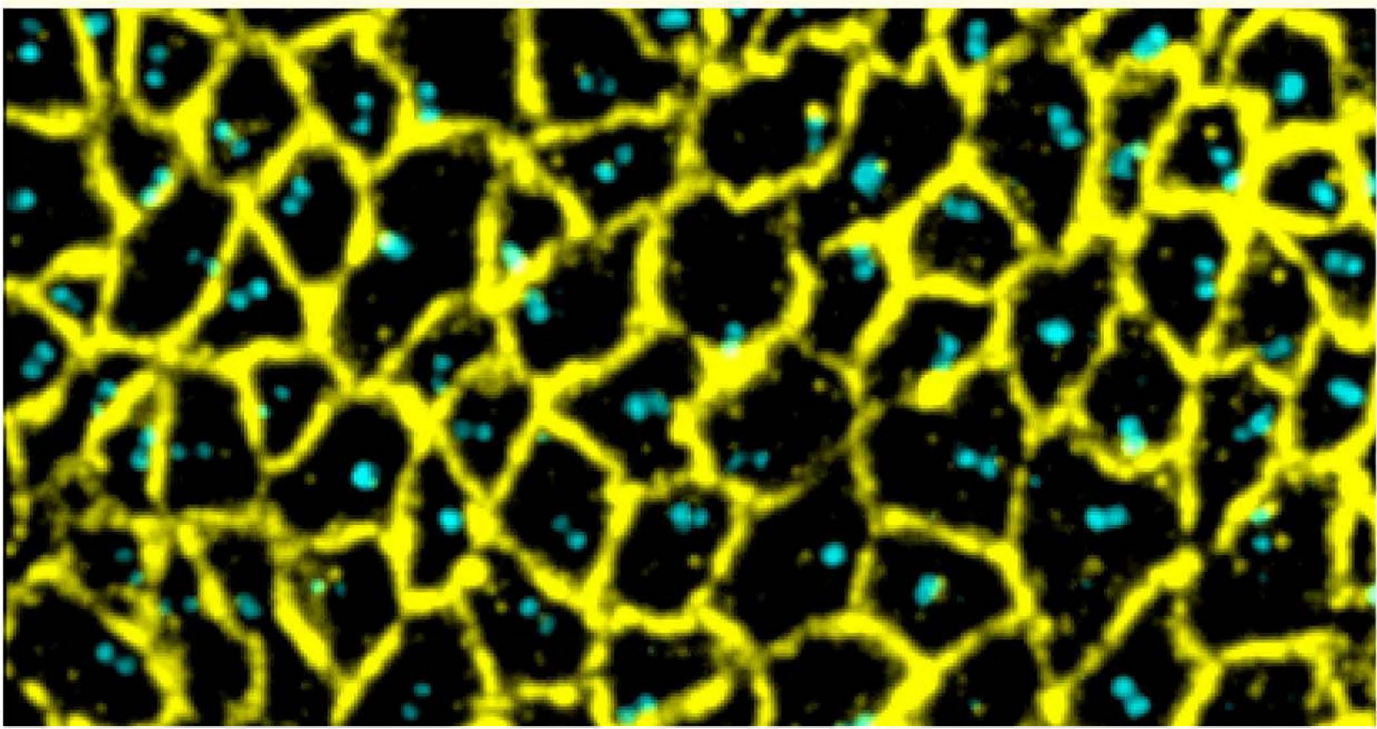

Faculty of Biology, Department of Cell Biology, Physiology and Immunology

Doctoral program in Biomedicine

Research performed at the

Institute of Molecular Biology of Barcelona, CSIC

THE ROLE OF THE WNT PATHWAY IN THE REGULATION OF THE CENTRAL NERVOUS SYSTEM GROWTH

(El paper de la via Wnt en la regulació del creixement del sistema nerviós central)

Thesis submitted by

Mª Pilar Lozano Fernández

To obtain the

Doctoral degree by the Universitat de Barcelona

Author:

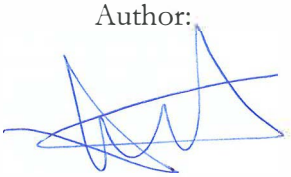

Mª Pilar Lozano Fernández

Director: Elisa Martí Gorostiza

Tutor: Marta Pascual Sánchez

Barcelona, July 2025

ABSTRACT

The central nervous system (CNS) arises from the neural tube (NT), an embryonic structure formed through highly coordinated morphogenetic processes. Proper growth and differentiation of the NT is essential to generate the diversity of cell types thar compose the mature organ. The spatiotemporal distribution of morphogens such as BMP and Wnt, secreted in the dorsal region of the NT, and Shh, secreted in the ventral region of the NT, play a critical role in establishing dorsoventral (D-V) patterning by enabling neural progenitor cells (NPCs) to acquire specific identities based of their position within NT. These signals regulate the expression of key transcriptional determinants that drive neural cell fate specification via genetic regulatory networks (GRNs). Importantly, these signals also contribute to controlling the proliferative behavior of NPCs, thereby orchestrating tissue growth. Thus, morphogen gradients integrate positional information with proliferative cues to ensure the proper expansion and organization of the embryonic neural tissue.

In this thesis, we investigate the role of the Wnt signaling pathway in regulating embryonic NT growth, using the chick embryo as a model system. We characterize the intracellular distribution of β-catenin, the key effector of Wnt signaling, and identify its accumulation at the centrosome during symmetric proliferative progenitor-progenitor divisions in early neurodevelopmental stages. Notably, we show that the centrosome pool of β-catenin corresponds to its stabilized form (S33/S37/Thr41-dephospho-β-catenin), implicating centrosome β-catenin as a downstream target of Wnt pathway activation.

Functional assays reveal that increases β-catenin levels promote symmetric PP divisions over neurogenic progenitor-neuron (PN) divisions, acting through both transcriptional and non-transcriptional mechanisms. Furthermore, we identify Nek2 kinase as a centrosome interactor of β-catenin. This interaction appears spatially restricted and enhances the promotion of symmetric PP divisions through synergistic mechanism that requires the C-terminal region of β-catenin. These findings suggest that β-catenin may exert instructive functions at the centrosome, influencing NPC division modes and contributing to the growth of the embryonic NT.

Keywords: Molecular Biology, Embryology, Physiology of the Central Nervous System, Neurosciences

SINOPSI

El sistema nerviós central (SNC) s'origina a partir del tub neural (TN), una estructura embrionària formada mitjançant processos morfogenètics altament coordinats. El creixement i la diferenciació adequats del TN són essencials per generar la diversitat de tipus cel·lulars que componen l'òrgan madur. La distribució espaciotemporal de morfògens com BMP i Wnt, secretats a la regió dorsal del TN, i Shh, secretat a la regió ventral, juga un paper fonamental en l'establiment de la regionalització dorsoventral (D-V), permetent que les cèl·lules progenitores neurals (CPNs) adquireixin identitats específiques segons la seva posició dins del TN. Aquestes senyals regulen l'expressió de determinants transcripcionals clau que dirigeixen l'especificació del destí cel·lular mitjançant xarxes reguladores gèniques (GRNs). De manera rellevant, aquestes mateixes senyals també contribueixen al control del comportament proliferatiu de les CPNs, coordinant així el creixement del teixit. Així doncs, els gradients de morfògens integren informació posicional amb senyals proliferatives per garantir l'expansió i organització adequades del teixit neural embrionari.

En aquesta tesi, investiguem el paper de la via de senyalització Wnt en la regulació del creixement del TN embrionari, utilitzant l'embrió de pollastre com a model experimental. Caracteritzem la distribució intracel·lular de la β-catenina, principal efector de la via Wnt, i identifiquem la seva acumulació al centrosoma durant les divisions simètriques proliferatives progenitor-progenitor (PP) en etapes primerenques del desenvolupament neural. En particular, mostrem que la fracció centrosòmica de β-catenina correspon a la seva forma estabilitzada (S33/S37/Thr41-desfosforilada), fet que implica la β-catenina centrosòmica com a diana directa de l'activació de la via de Wnt.

Els assaigs funcionals revelen que l'increment de nivells de β-catenina afavoreix les divisions PP simètriques en detriment de les divisions neurogèniques progenitor-neurona (PN), actuant mitjançant mecanismes tant transcripcionals com no transcripcionals. A més, identifiquem la quinasa Nek2 com a interactor centrosòmic de la β-catenina. Aquesta interacció sembla estar espacialment restringida i potencia la promoció de les divisions PP simètriques a través d'un mecanisme sinèrgic que requereix la regió C-terminal de la β-catenina. Aquests resultats suggereixen que la β-catenina podria exercir funcions instructives al centrosoma, modulant el mode de divisió de les CPNs i contribuint al creixement del TN embrionari.

Paraules clau: Biologia Molecular, Embriologia, Fisiologia del Sistema Nerviós Central, Neurociències

INDEX

LIST OF TABLES AND FIGURES 1
LIST OF ABBREVIATIONS 3
INTRODUCTION 7
1.- The formation of the CNS during embryonic development 9
1.1.- Epiblast regionalization and gastrulation: initiating morphogenetic processes in CNS formation. 9
1.2.1. Formation of the neural plate 11
1.2.2. Shaping of the neural plate 11
1.2.3. Bending the neural plate to form the neural groove and the neural folds 12
1.2.4. Fusion of the neural folds to close the neural groove and form the NT. 12
1.3.- Secondary neurulation and posterior NT specification 13
1.3.1. NMPs condense to form a solid medullary cord 13
1.3.2. NMPs undergo mesenchymal-to-epithelial transition (MET) 13
1.3.3. Formation of small lumina 13
1.3.4. Cavitation and tube formation 14
1.4.- Embryonic origin of the CNS: the NT as the foundational structure 14
2.- Dorso-ventral (D-V) patterning of the developing spinal cord: morphogenetic signals and the generation of cell diversity 17
2.1.- Graded Shh signaling controls the identity of ventral progenitors from the FP 19
2.3.- BMP controls the identity of dorsal progenitors from the RP 22
3.- NT growth: the role of the centrosome in the specialized modes of division of NPCs and their impact on CNS formation 23
3.1. Centrosome organization of symmetric divisions 26
3.2. Centrosome organization of asymmetric divisions 29
3.3. Centrosome organization of the primary cilia 31
4.- The Wnt pathway 35

4.1.- History, evolution and biological significance 35
4.2.- The canonical Wnt/β-catenin pathway 36
4.3.- The multiple roles of Wnts in NT development 39
4.3.1. Functional roles of Wnts in neural tissue growth 39
4.3.2. Functional roles of β-catenin in progenitor proliferation 40
4.3.3. Transcriptional effectors: TCF/LEF family 41
5.- The chick embryo NT as a model system 41
OBJECTIVES 43
MATERIALS AND METHODS 47
MATERIALS 49
1.- Chick embryos 49
2.- DNA constructs 49
3.- Antibodies and counterstains 51
4.- Public repositories 53
METHODS 54
1.- Chick in ovo electroporation 54
2.- En-face preparations 54
3.- Immunohistochemistry 55
3.1. En face tissue preparation for immunohistochemistry: 55
3.2. Free-floating sections preparation for immunohistochemistry: 56
4.- Luciferase-reporter Assay 56
5.- Image acquisition 57
5.1. Fluorescence microscopy 57
5.2. Confocal microscopy 57
5.3. Spinning-disk microscopy 57
6.- Image analysis and quantification 58
6.1. General Image Analysis 58
6.2. Quantification of endogenous β-catenin at the centrosome 58

6.3. Quantification of centrosome β-Catenin in electroporated embryos 59
6.4. Analysis of NPCs mode of cell division 59
6.5. Measurement of ventricular surface length 59
6.6. Nek2 localization analysis 60
6.7. Quantification of β-catenin intensity at the centrosome 60
7.- Statistical Analysis 61
8.- In silico screening for β-catenin interactors at the centrosome 61
9.- Computational docking of β-catenin-Nek2 interaction 62
RESULTS 63
1.- Centrosome localization of β-catenin in NPCs correlates with early stages of NT development 65
2.- Centrosome localization of β-catenin in NPCs correlates with Wnt pathway-dependent post-translational stabilizing modifications 68
3.- Prevention of β-catenin phosphorylation at S33 is sufficient to increase its centrosome localization, independently of junctional or transcriptional activity 71
4.- Gain-of-function (GOF) of β-catenin regulates progenitor-to-neuron ratio in the chick embryo NT through transcriptional and non-transcriptional mechanisms 72
5.- β-catenin is sufficient to shift modes of division toward self-expanding proliferative divisions in the developing NT, though transcriptional and non-transcriptional mechanisms 75
6.- β-catenin-induced aberrant growth in the chick embryo NT disrupts tissue organization through transcriptional and non-transcriptional mechanisms 78
8.- Nek2 increases the accumulation of stable β-catenin at the centrosome independently of its kinase activity 82
9.- Nek2 increases β-catenin-mediated maintenance of NPC stemness, independent of its kinase activity. 85
10.- The C- terminal region of β-catenin is required for the interaction with Nek2.. 90
DISCUSSION 95
1.- Centrosome accumulation of stabilized β-catenin during early NT development contributes to proliferation 97

2.- Nek2 as a non-catalytic modulator promoting centrosome accumulation of β-catenin 99

3. Functional importance of the C-terminal region of β-catenin for Nek2 interaction and centrosome-mediated effects 100

4. Spatially distinct but potentially coordinated roles of β-catenin at the centrosome and nucleus during neurodevelopment 101

5. Towards understanding centrosome β-catenin function: implications in NPC modes of division 103

6.- β-Catenin-mediated primary cilia elongation might link extracellular signaling to symmetric divisions through a positive feedback loop 106

7.- Proposed model and future perspectives 108

CONCLUSIONS 113

REFERENCES 117

APPENDIX 151

LIST OF TABLES AND FIGURES

Table 1. The MCPH loci, their gene products and protein functions

Table 2: Primary antibodies

Table 3: Secondary Antibodies

Figure 1. Epiblast regionalization and gastrulation initiate CNS formation.

Figure 2. Primary neurulation process.

Figure 3. Secondary neurulation process.

Figure 4. Early CNS organization and NPCs architecture along the A-P axis

Figure 5. D-V patterning of neural progenitor domains in the vertebrate developing spinal cord at early stages

Figure 6. NPC undergo INM and different modes of cell division at the apical surface of the NT.

Figure 7. Molecular mechanisms underlying the regulation of distinct modes of NPC division

Figure 8. Mature centriole organization at the basal body (BB) of the cilium and signal transduction.

Figure 9. The canonical Wnt pathway.

Figure 10. Centrosome β-catenin correlates with earlier stages of the NT development.

Figure 11. Centrosome β-catenin correlates with activation of Wnt pathway.

Figure 12. Prevention of β-catenin phosphorylation of at S33 is sufficient to increase its centrosome localization, independently of junctional or transcriptional activity.

Figure 13. β-catenin GOF increases progenitor gene Sox2 expression and decreases neurogenic gene NeuroD expression through transcriptional and non-transcriptional mechanisms.

Figure 14. β-catenin GOF increases proliferative PP divisions at the expense of neurogenic PN divisions through transcriptional and non-transcriptional mechanisms.

Figure 15. β-catenin GOF induces aberrant growth of the tissue trough transcriptional and non-transcriptional mechanisms.

Figure 16. *In silico* analysis of β-catenin interactors identify Nek2 as a centrosome partner.

Figure 17. Nek2 increases the accumulation of stable β-catenin at the centrosome independently of its kinase activity.

Figure 18. Nek2 enhances β-catenin-mediated effects independent of its kinase activity.

Figure 19. The C-terminal region of β-catenin is required for interaction with Nek2.

Figure 20. Transcriptomic analysis reveals that stabilized β-catenin regulates genes involved in proliferation and centrosome maturation.

Figure 21. Spatial distribution of stabilized β-catenin differs between proliferative and neurogenic NPC divisions.

Figure 22. Overexpression of Wnt3a or β-catenin promotes primary cilia elongation in NPCs.

Figure 23. Schematic representation of the proposed mechanism by which Wnt/β-catenin regulates proliferation of NPCs through transcriptional and non-transcriptional mechanisms.

LIST OF ABBREVIATIONS

AJ – Adherens junction

APC – Adenomatous polyposis coli

A-P – Anterior-to-posterior

aPKC – Atypical protein kinase

AVE – Anterior visceral endoderm

BB – Basal body

BM – Basement membrane

BMP – Bone morphogenetic protein

CK1 – Casein kinase 1

CNS – Central nervous system

DA – Distal appendages

D-V – Dorso-ventral

Dvl – Dishevelled

ECM – Extracellular matrix

ESC – Embryonic stem cell

FGF – Fibroblast growth factor

FOP – FGFR1 Oncogene Partner

FP – Floor plate

Fz/FZD – Frizzled

GSK3 – Glycogen Synthase Kinase 3

GRN – Gene regulatory networks

HPF – Hours post fertilization

HPE – Hours post electroporation

HSPGs – heparan sulfate proteoglycans

IFT – Intraflagellar transport

INM – Interkinetic nuclear migration

KD – Knock-down

KO – Knock-out

MCPH – Primary microcephaly

MGE – Medial ganglionic eminence

MHP – Median hinge point

MET – Mesenchymal-to-epithelial transition

MTOC – Microtubule-organizing center

MZ – Mantle zone

NMPs – Neuromesodermal progenitors

NPCs – Neural progenitor cells

NT – Neural tube

PAR3/6 – Partitioning-defective 3/6

PCM – Pericentriolar material

PCNT – Pericentrin

pH3 – Phospho-histone H3

PKA – Protein kinase A

RA – Retinoic acid

RP – Roof plate

SDA – Sub-distal appendages

Shh – Sonic Hedgehog

SVZ – Subventricular zone

TGF-β – Transforming growth factor-beta

TJ – Tight junction

VZ – Ventricular zone

VM – Ventral midbrain

Wg – Wingless

Wnt – Wingless/Int-1

WT – Wild type

INTRODUCTION

1.- The formation of the CNS during embryonic development

The central nervous system (CNS), composed of the brain and spinal cord, orchestrates both voluntary and involuntary bodily functions such as cognition, movement, emotion, sensation, respiration and learning. Its formation during embryonic development is a remarkably complex and tightly regulated process, characterized by a series of events such as the formation of the neural tube (NT), the subsequent precise growth and shaping of this embryonic structure, and the generation of cellular diversity required to produce the vast array of neural cell types necessary for constructing a functional organ.

One of the earliest and most critical morphogenetic events in CNS formation is neurulation, a dynamic process that shapes the NT, a transient embryonic structure that serves as the primordium of the entire vertebrate CNS. Although the NT is anatomically continuous along the entire anterior-to-posterior (A-P) axis, the neuroepithelial progenitor cells that line it, known as neural progenitor cells (NPCs), are highly conserved and morphologically indistinguishable. However, their embryonic origins and the molecular mechanisms underlying their genetic specification differ markedly depending on their position along this A-P axis.

The prevailing view of vertebrate CNS formation proposes that anterior and posterior NPCs arise from two different embryonic origins and are governed by different genetic regulatory programs. These developmental distinctions will be briefly explored in the following sections.

1.1.- Epiblast regionalization and gastrulation: initiating morphogenetic processes in CNS formation.

In early mammalian development, the NT formation begins shortly after gastrulation. Prior to this, the epiblast undergoes spatial regionalization, establishing the A-P axis of the embryo (Meno et al., 1996; Perea-Gomez et al., 2002; Takaoka et al., 2006; Yamamoto et al., 2004; Brennan et al., 2001; Mole, Weberling & Zernicka-Goetz, 2020). In the mouse embryo, anterior cells, destined to form the brain regions including the forebrain, midbrain and hindbrain, are specified by signals from anterior visceral endoderm (AVE), which includes transforming growth factor-beta (TGF-β) family members like Nodal, and inhibitors of both bone morphogenetic protein (BMP) and

Wingless/Int-1 (Wnt) signaling pathways (Meno et al., 1996; Perea-Gomez et al., 2002; Takaoka et al., 2006; Yamamoto et al., 2004; Brennan et al., 2001; Mole, Weberling & Zernicka-Goetz, 2020). In contrast, posterior cells, destined to form the spinal cord and caudal mesoderm, retain active Wnt signaling to promote posterior gene expression program (Metzis et al., 2018; Kimura-Yoshida et al., 2005; Blassber et al., 2022). In the human embryo, analogous processes occur, setting the stage for gastrulation (Mole, Weberling & Zernicka-Goetz, 2020; Mole et al., 2021).

This A-P regionalization of the epiblast is crucial for defining the position of the primitive streak, the region of the epiblast where cells ingress during gastrulation and, by extension, enabling gastrulation. (Metzis et al., 2028; Kimura-Yoshida et al., 2005; Mole et al., 2021). After gastrulation, anterior epiblast cells that do not ingress form the neural plate in a process known as neural induction, differentiating into ectoderm cells and choosing between either neural or non-neural ectoderm fates (Spemann & Mangold., 1924). Posterior epiblast cells do ingress through the primitive streak during gastrulation and become neuromesodermal progenitors (NMPs), bipotent stem cells contributing to both spinal cord and mesodermal tissues during body axis elongation (Metzis et al., 2018; Kimura-Yoshida et al., 2005; Blassberg et al., 2022). NMPs, maintained by Wnt activity and fibroblast growth factor (FGF) family members, gradually lose their bipotency and commit to either neural (Sox2+) or mesodermal (T/Brachryury, TbxT+) lineages, with some transiently co-expressing both at the tailbud-NT interface (Metzis et al., 2018; Kimura-Yoshida et al., 2005; Blassberg et al., 2022) (Figure 1).

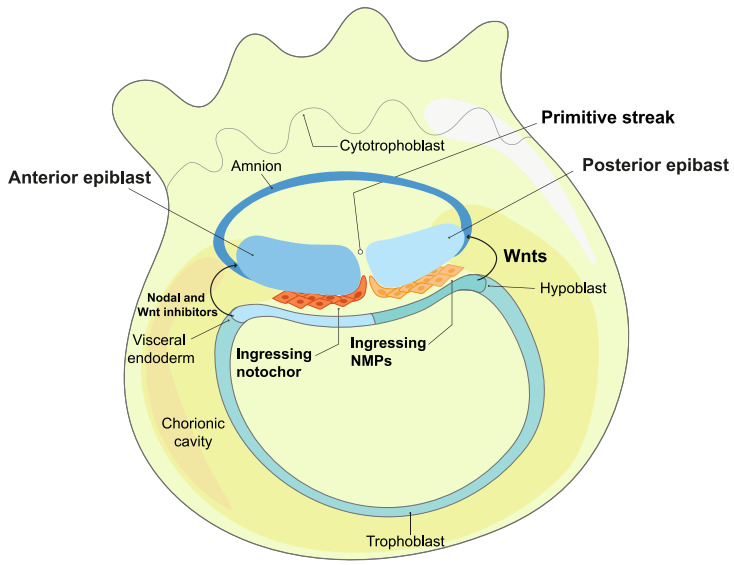

Figure 1. Epiblast regionalization and gastrulation initiate CNS formation. Schematic representation of epiblast regionalization and cell ingression during early gastrulation. Regional signaling cues such as Wnt and Nodal pattern the epiblast along the A-P axis and guide lineage specification during the initiation of CNS development.

1.2.- Primary neurulation and anterior NT specification

The vertebrate NT formation occurs in two consecutive and mechanistically different processes referred to as primary and secondary neurulation, that can be followed at different A-P levels of the developing embryo.

1.2.1. Formation of the neural plate

In the anterior NT, primary neurulation begins soon after gastrulation with the formation of the neural plate, a specialized region of the ectoderm derived from anterior epiblast cells that avoid primitive streak ingress. These cells become neural through neural induction, driven by signals from the organizer region, including BMP inhibitors and antagonists of FGF and Wnt signals. Neural plate cells undergo conserved morphogenetic changes such as apico-basal elongation, which enhances cell-cell adhesion and communication between neighboring cells, leading to the formation of a pseudostratified columnar neuroepithelium, stabilized by junctional complexes and N-cadherin expression (Canning & Cunningham, 2015; Hong & Brewster, 2006; Detrick, Dickey & Kintner, 1990; Hiraga et al., 2020). In mouse and chick, Sonic Hedgehog (Shh) signals from the notochord breaks the symmetry of the neuroepithelium by driving bending at a median hinge point (MHP), which induce the specialization of a group of overlying neuroepithelial cells to form the floor plate (FP), marked by Foxa2 expression, that coordinates subsequent morphogenesis (van Straaten, Hekking, Wiertz-Hoessels, Thors & Drukker, 1988; Placzek, Tessier-Lavigne, Yamada, Jessell & Dodd, 1990; Patten & Placzek, 2002) (Figure 2A, B).

1.2.2. Shaping of the neural plate

FP cells become shorter and wedge-shaped, with reduced proliferative activity, acting as an anchor point that supports mechanical forces during neural groove formation (van Straaten, Hekking, Wiertz-Hoessels, Thors & Drukker, 1988; Placzek, Tessier-Lavigne, Yamada, Jessell & Dodd, 1990; Patten & Placzek, 2002, Smith & Schoenwolf, 1988; Schoenwolf, 1991; Smith & Schoenwolf, 1989; Colas & Schoenwolf, 2001). Simultaneously, the lateral neural plate undergoes A-P elongation, medio-lateral narrowing and additional apico-basal thickening, setting the condition for the neural plate to generate a tubular-like structure instead of a spherical vesicle (Keller, Shook & Skoglund, 2008) (Figure 2B).

1.2.3. Bending the neural plate to form the neural groove and the neural folds

This neuroepithelium bends to form the neural groove as a basal extracellular matrix (ECM) rich in cell surface-associated glycoproteins, collagens and proteoglycans progressively deposits between the neural tissue and the underlying mesoderm, forming the basement membrane (BM), which interacts with NPCs integrins to promote cytoskeletal rearrangements (Martin-Green, 1988; Martins-Green & Erickson, 1986). The lateral edges of the neuroepithelium lift to create neural folds and are brought together to the dorsal midline (Mole et al., 2020; Pyrgaki, Trainor, Hadjantonakis & Niswander, 2010; Galea et al., 2017) (Figure 2C).

1.2.4. Fusion of the neural folds to close the neural groove and form the NT

Primary neurulation finishes with the closure of the NT when NPCs extend actin-rich protrusions (filopodia or lamellipodia), that bridge the neural folds, facilitating their fusion in a process known as "zippering" that progress in both anterio-posterior and posterior-anterior directions (Pyrgaki, Trainor, Hadjantonakis & Niswander, 2010; Galea et al., 2017) and establish a roof plate (RP) in the NT. Meanwhile, non-neural ectoderm cells reshape to form intermediate closure points (Pyrgaki, Trainor, Hadjantonakis & Niswander, 2010; Galea et al., 2017). The final stage of primary neurulation involves remodeling of dorsal surface and detachment of the closed NT from the overlying non-neural ectoderm. Proper tension control, possibly through YAP1 mechanosensing, is essential for successful NT formation and closure (Figure 2D).

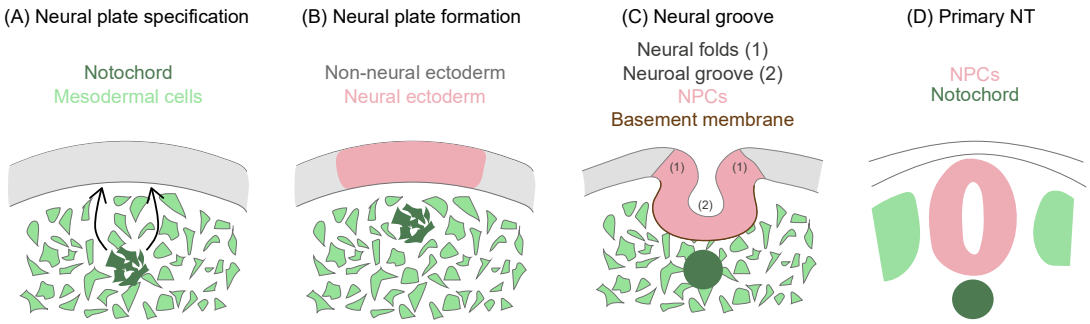

Figure 2. Primary neurulation process. Drawings represent transversal sections of an embryo undergoing primary neurulation. **(A)** Notochord signals induce the specialization of overlying ectoderm to form the neural plate through neural induction. **(B)** Neural plate cells change morphogenetically, forming a pseudostratified neuroepithelium and extending the plate. **(C)** Neural plate bends at the MHP creating a neural groove while the lateral neural folds

elevate toward the dorsal midline. **(D)** Neural folds fuse at the midline and closed NT detach from overlying ectoderm.

1.3.- Secondary neurulation and posterior NT specification

Secondary neurulation shapes the most posterior spinal cord and involves different morphogenetic events than primary neurulation (Gonzalez-Gobartt et al., 2021; Santos et al., 2023). It is a longer process that occurs concomitant to body axis elongation (Greene and Copp, 2014). This process, best studied in chick embryos, also occurs at comparable developmental stages in mouse and human embryos. It begins after more cranial regions have developed, with the transition between primary and secondary neurulation typically near to the caudal neuropore, although the location tends to vary among vertebrates (Saitsu & Shiota; 2008; Saitsu, Yamada, Uwabe Ishibashi & Shiota, 2004; Muller & O'Rahilly, 1987).

1.3.1. NMPs condense to form a solid medullary cord

NMPs ingress through the primitive streak and aggregate as mesenchymal tailbud cells along midline, forming a densely packed cylinder of cells called solid medullary cord, the precursor of the secondary NT, in a process that occurs in an anterior-posterior fashion (Schoenworld & Delongo, 1980). This condensation is concomitant with the deposition of a BM containing classical cell surface-associated glycoproteins (Gonzalez-Gobartt et al., 2021; Schoenworld & Delongo, 1980) (Figure 3A)

1.3.2. NMPs undergo mesenchymal-to-epithelial transition (MET)

Peripheral NMPs contacting the BM undergo a full MET, which result in the formation of an outer layer of neuroepithelial cells, the formation of intercellular junctions and the establishment of apico-basal cell polarity. Epithelialization propagates ventrally as the BM deposit progresses (Gonzalez-Gobartt et al., 2021; Schoenworld & Delongo, 1980). The centrally located cells retain mesenchymal features, characteristic of the medullary cord (Figure 3B).

1.3.3. Formation of small lumina

Numerous small cavities referred to as lumens appear at the junction between the peripheral epithelial and the inner cluster of mesenchymal cells, typically one cell-width from the BM (Gonzalez-Gobartt et al., 2021; Schoenworld & Delongo, 1980). These lumens vary in number, size, shape and dorso-ventral location, even though the first lumen often appears dorsally displaced (Schoenworld & Delongo, 1980) (Figure 3C).

1.3.4. Cavitation and tube formation

Different lumens finally converge to create a single continuous central cavity (Gonzalez-Gobartt et al., 2021). For that to happen, central mesenchymal cells are cleared from the luminal space (Gonzalez-Gobartt et al., 2021). In the chick embryo, this clearance is independent of apoptosis but involves the intercalation of the cells into the lateral walls of the forming NT (Gonzalez-Gobartt et al., 2021; Schoenworld & Delongo, 1980), a process dependent on TGF-β signaling via SMAD3 and YAP1 (Gonzalez-Gobartt et al., 2021), completing the formation of a hollow NT (Figure 3D).

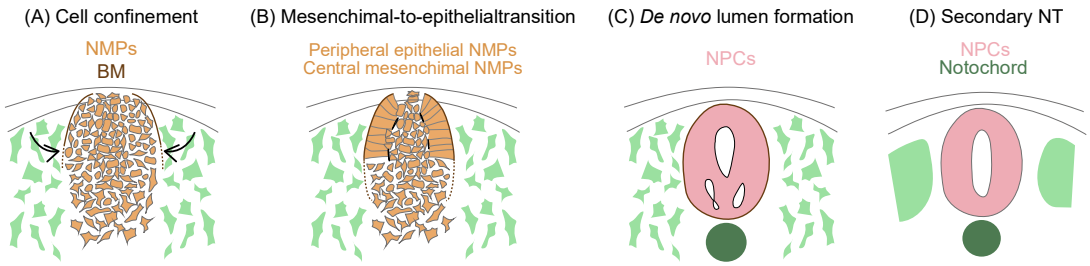

Figure 3. Secondary neurulation process. Drawings represent transversal sections of an embryo undergoing secondary neurulation. **(A)** NMPs start condensating at the midline of the tissue to form a solid medullary cord. **(B)** Dorsal cells in contact with the basement membrane (BM) undergo a complete mesenchymal-to-epithelial transition (MET) while central cells remain mesenchymal. **(C)** As MET progresses, small cavities begin to form at the interface between the epithelial and mesenchymal regions. **(D)** These cavities eventually coalesce, forming a NT with a central single lumen.

1.4.- Embryonic origin of the CNS: the NT as the foundational structure

Upon completion of the NT morphogenesis the resulting structure consists of a central cavity (ventricle) surrounded by a pseudostratified epithelium composed of Sox2 positive- neuroepithelial cells or NPCs (Figure 4A). These NPCs will proliferate and differentiate to produce neurons and glial cells. Although recent studies have revealed transcriptional diversity and molecular heterogeneity within NPC populations, suggesting that they have distinct developmental trajectories and functions (Eze, Bhaduri, Haeussler, Nowakowski & Kriegstein, 2021), these cells remain relatively uniform in terms of morphology and behavior throughout the CNS (Figure 4B, D).

Each NPC extends a basal process to the BM (or basal lamina) and an apical process toward the lumen of the NT. Their nuclei adopt distinct positions along the apico-basal

axis in coordination with cell cycle progression, a phenomenon known as interkinetic nuclear migration (INM) (Sauer, 1935; Langman, Guerrant and Freeman, 1966; Taverna & Huttner, 2010; Molina & Pituello, 2017; Saade et al., 2018) (Figure 4C).

Importantly, NPCs are fully apico-basally polarized epithelial cells. They possess an apically localized centrosome, positioned at the base of the primary cilium, which is a key structure involved in sensing environmental cues relevant to neural development. Furthermore, NPCs exhibit an organized apical plasma membrane that is structured into distinct subdomains. The adherens junction (AJ) complex, containing N-cadherin, α-catenin and β-catenin, and the tight junction (TJ) complex, containing TJP, also known as ZO-1 and/or occludin occupy sub-apical microdomains, whereas a polarity complex composed of partitioning-defective 3 (PAR3), PAR6 and atypical protein kinase (aPKC) is localized to the most apical microdomain, as demonstrated in studies using mice and chick models (Aaku-Sarastre, Hellwig & Huttner, 1996; Chenn et al., 1998; Afonso & Henrique, 2006; Martiens & Ffrench-Constant, 2009; Saade et al., 2017) (Figure 4C' and C").

The apical belt (the AJ complex) provides essential adhesive and mechanical properties to the plasma membrane that are critical to the integrity of NPCs, enabling them to resist mechanical forces associated with ventricular expansion and tissue growth. Genetic disruption of the components of the apical complex in rodent models leads to a loss of cell polarity, resulting in severe changes in NPC proliferation, morphology and function, and ultimately leading to disorganization of the ventricle (Bultje et al., 2009; Liu et al., 2018; Katayama et al., 2011). The stability of this apical end-foot architecture and the maintenance of epithelial integrity is partially regulated by the activity of the centrosome. Specifically, the appendages of the mother centriole are involved in microtubule anchoring that is essential for proper tension of the apical belt by maintaining AJ stability (Insolera, Bazzi, Shao, Anderson & Shi, 2014; Delgehyr, Sillibourne & Bornens, 2005; Shinohara, Sakayori, Takahashi & Osumi, 2013; Shao et al., 2020).

On the other hand, NPCs also connect to the BM via their basal process, which contain key ECM components and receptors, including proteoglycans, glycoproteins and integrins (Long, Moss, Laursen, Boulter & Ffrench-Constant, 2016; Copp et al., 2011; Soulintzi & Zagris, 2007) (Figure 4C). The ECM has multiple roles in NT development, providing structural support, regulating NPC proliferative capacity, and acting as a scaffold for migrating newborn neurons (Long & Huttner, 2019). *In vitro* and *in vivo* studies have demonstrated that ECM signaling plays a key role in CNS

development by supporting NPC proliferation, survival and differentiation (Drago, Nurcombe & Bartlett., 1991; Hall, Lathia, Caldwell & Ffrench-Constant, 2008; Flanagan, Rebaza, Derzic, Schwartz & Monuki, 2006; Ma et al., 2008; Campos et al., 2004), while modulation of integrin subunits in mouse and chick embryos affects NPCs proliferation (Long, Moss, Laursen, Boulter & Ffrench-Constant, 2016; Campos et al., 2004; Leone et al., 2005), underscoring the importance of ECM components in maintaining the proper structure and growth of the developing CNS.

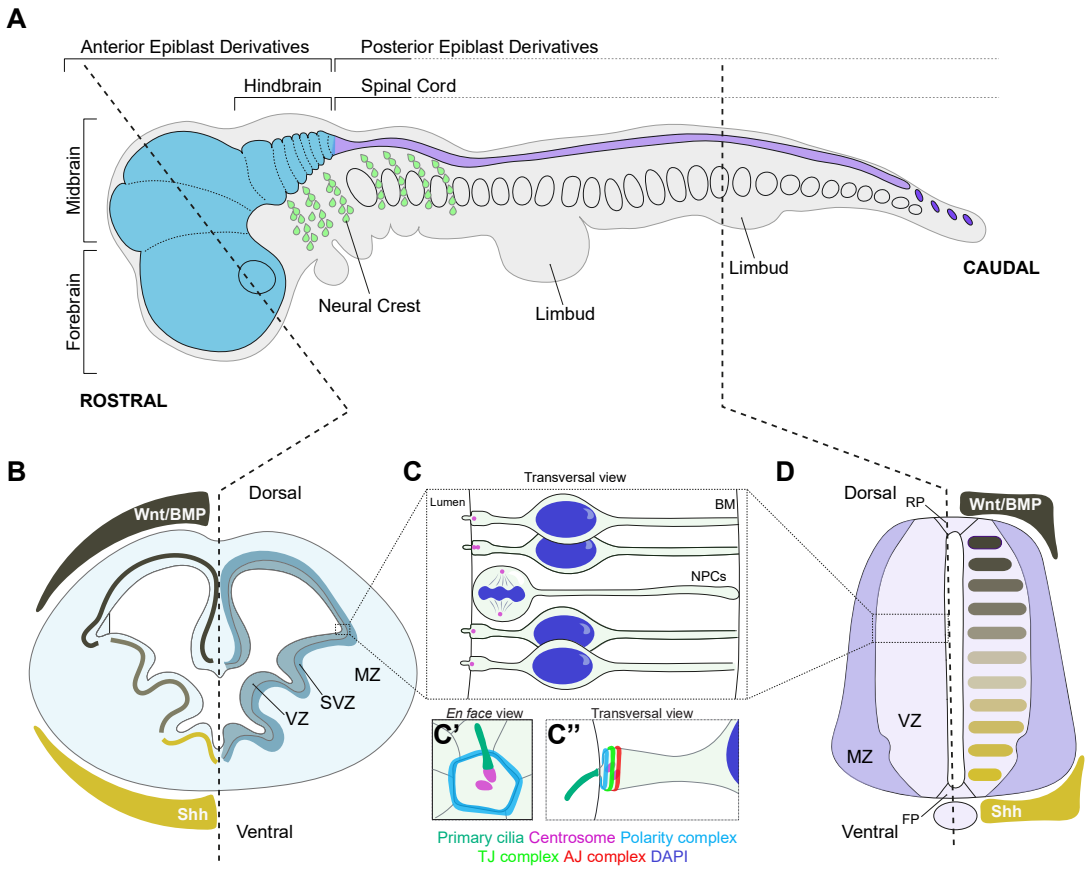

Figure 4. Early CNS organization and NPCs architecture along the A-P axis (A) Lateral view diagram of a vertebrate embryo CNS showing A-P regionalization into the forebrain, midbrain, hindbrain and spinal cord. These regions derive from spatially distinct anterior and posterior epiblast domains. Neural crest cells (green) emerge from the dorsal NT and migrate peripherally, while limb buds form laterally at trunk levels. **(B)** Diagram of transversal section through the telencephalon showing dorsal to ventral patterning driven by dorsal morphogens such as BMP and Wnt and ventral morphogen Shh. These gradients specify regional identities and drive the formation of distinct progenitor domains. The NPCs occupy the ventricular zone

(VZ), while the subventricular zone (SVZ) and mantle zone (MZ) contain differentiating and post-mitotic neurons. **(C)** Detailed view drawing of structural organization of NPCs in the VZ. These progenitors exhibit a pseudostratified neuroepithelium were elongated NPCs span from the apical (lumen) to the basal (basement membrane, BM) surfaces, undergoing INM. **(C')** En face view drawing of the apical foot of NPCs, showing centrosome (magenta), primary cilia (dark green) and polarity complex (light blue). **(C")** Transversal zoom-in drawing of the NPCs apical foot showing DAPI-stained nuclei (blue), adherens junction(AJ) compex (red), tight junction (TJ) complex (green), polarity complex (light blue), centrosome (magenta) and primary cilia (dark green). **(D)** Diagram of transversal section through the spinal cord showing patterned NPC domains from dorsal to ventral axis regulated by dorsal BMP and Wnt and ventral Shh signaling (right hemitube). NPC resides in the VZ, while post-mitotic neurons migrate into the MZ (left hemitube).

2.- Dorso-ventral (D-V) patterning of the developing spinal cord: morphogenetic signals and the generation of cell diversity

Once genetic neural specification and tissue morphogenesis have collectively coordinated the formation of a hollow NT, NPCs begin to acquire distinct identities along the D-V axis of the NT. This spatial patterning process builds upon early symmetry-breaking events, initiated during neural plate formation, and is progressively refined by three main extracellular signaling cues that emanate from specialized organizing centers within the NT.

Pattern formation refers to the process by which embryonic cells organize into spatially ordered arrangements within developing tissues. In the CNS, the generation of a vast array of neuronal and glial cells must occur in a tightly regulated temporal and spatial order to form a functional neural network. The acquisition of specific neural fates is determined by the initial spatial coordinates of each progenitor cell within the neural plate, which determines their exposure to local signaling cues. These signals progressively restrict NPC developmental potential by activating or repressing the expression of key transcriptional regulators that, in turn, control gene regulatory networks (GRNs) responsible for establishing the molecular identity and functional properties for each neural subtype.

Following NT closure, cells at the ventral midline, the FP cells, acquire the capability to promote cell diversity in the adjacent NPCs. The fate of each cell depends on its relative position with respect to the FP, the primary source of ventralizing signals. A

major breakthrough in our understanding of the molecular mechanisms underlying the polarizing activity of the FP came with the discovery that Shh, secreted by the notochord and the FP, is both required and sufficient to mimic all FP functions (Marti, Takada, Bumcrot, Sasaki & McMahon, 1995b; Marti, Bumcrot, Takada & McMahon 1995a; Echelard et al., 1993). A combination of molecular, genetic and computational modelling studies conducted mainly in chick and mouse embryos has uncovered the mechanisms through which ventral NPCs decode graded Shh signals. These insights will be explored in detail in the following sections.

At the dorsal midline, a complementary signaling center, the RP, emerges. RP cells, a cluster of specialized cells that stop proliferation earlier than any other cell population in the dorsal NT are specified under the influence of BMP signaling from the adjacent non-neural ectoderm. In the chick and mouse embryo, this induction leads to the expression of the LIM-homeodomain transcription factors Lmx1a and Lmx1b (Chizhikov & Millen, 2004; Chizhikov & Millen, 2004). As RP cells differentiate, they begin to express additional signaling molecules, including various BMP and Wnt proteins, thereby establishing a dorsal midline organizing center (Lee, Dietrich & Jessell, 2000) that orchestrates the specification and differentiation of neighboring dorsal neuronal populations (Le Dreau & Marti, 2013; Tozer, Le Dreau, Marti & Briscoe, 2013; Muroyama, Fujihara, Okeya, Kondoh & Takada, 2002; Le Dreau et al., 2012).

In addition to BMPs, other members of the TFG-β superfamily (Pituello, Yamada & Gruss, 1995; Liem, Tremml and Jessell, 1997; Garcia-Campmany and Marti, 2007) as well as retinoic acids (del Corral et al., 2003; Novitch et al., 2003; Wilson & Maden, 2005) have been implicated in the fine-tuning of D-V patterning and progenitor specification.

Because the spinal cord is the anatomically simplest and most evolutionary conserved region of the vertebrate CNS, it has been instrumental in advancing our understanding of the mechanisms that control the progressive acquisition of neural cell diversity along the D-V axis of the embryo. Key determinants of the D-V identities include members of the homeodomain and the basic-helix-loop-helix families of transcription factors (TFs), which are expressed in distinct and restricted D-V domains (Figure 5A).

Accordingly, the developing spinal cord is divided into eleven discrete domains of neural progenitors, with five ventral domains (labeled p3, pMN, p2, p1 and p0 from ventral to dorsal) and six dorsal domains (called dP1-6 from dorsal to ventral), each characterized by a unique combination of TF expression (Figure 5B). This TF code

ultimately determines the neuronal subtypes produced by each domain and depends on the activity of patterning signals secreted from the two opposed signaling centers.

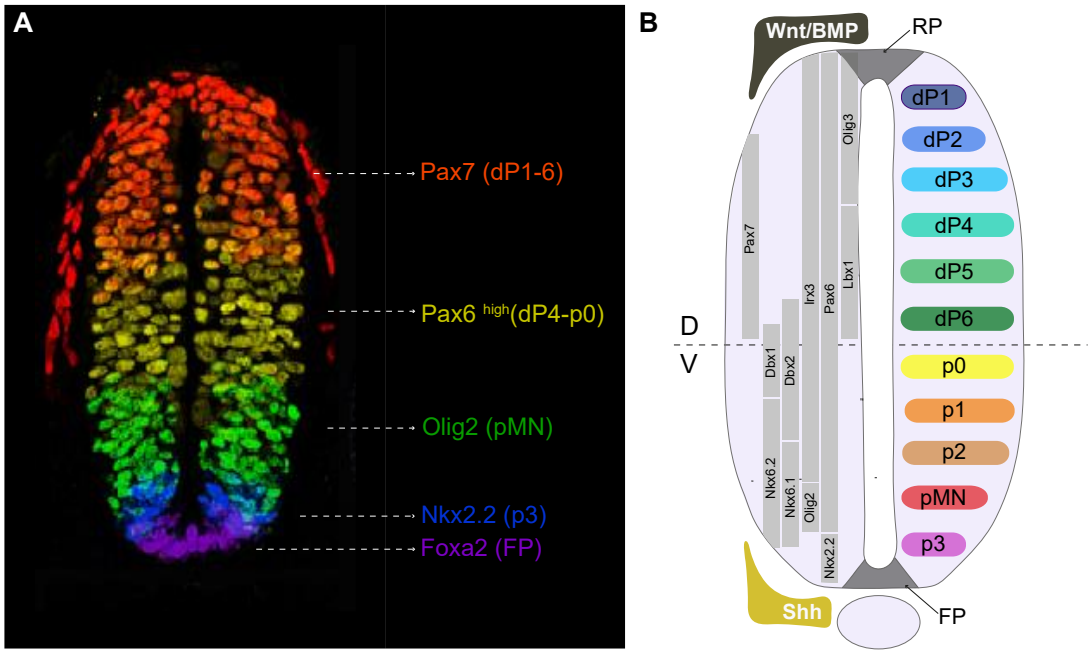

Figure 5. D-V patterning of neural progenitor domains in the vertebrate developing spinal cord at early stages. (A) Immunostaining of a transverse section of the chick NT at HH16 showing the distribution of progenitor domains along the D-V axis. Specific transcription factors label distinct progenitor populations: Pax7 (dP1–6, red), Pax6^high (dP4–p0, yellow), Olig2 (pMN, green), Nkx2.2 (p3, blue), and Foxa2 (floor plate, FP, purple). **(B)** Schematic representation of a transversal section of a NT at early stages. The left side illustrates the expression of several progenitor proteins patterning the NT along the D-V axis due to Wnt, BMP and Shh opposing gradients. The right side shows the subdivision of the NT into eleven distinct domains of neural progenitors, including (from ventral to dorsal): p3, pMN, p2-0, dP1-6, each giving rise to specific neural cell types during NT development.

2.1.- Graded Shh signaling controls the identity of ventral progenitors from the FP

During early neural development, the neural plate initially displays a dorsal character marked by the expression of paired box TFs Pax3 and Pax7, which are required for the generation of the earliest dorsal cell identity, the neural crest cells, but insufficient for the NPCs specification of dorsal neuronal subtypes (Liem et al., 1995). As the NT

closes, Shh signaling from the FP promotes the expression of ventral determinant that, among other roles, serves to restrict the expression of Pax3/7 to the dorsal region (reviewed by Ingham et al., 2011).

Shh was first identified in what were considered the two main signaling centers responsible for ventralizing the NT, the underlying notochord and the FP, precisely at the times when these centers were known to have inducing capacities (Echelard et al., 1993; Marti, Takada, Bumcrot, Sasaki & McMahon, 1995b). Subsequent gain- and loss-of-function studies demonstrated that Shh is both necessary and sufficient to induce ventral neural cell types (Marti, Bumcrot, Takada & McMahon 1995a; Roelink et al., 1995; Chiang et al., 1996). After that, Shh was postulated to function in a concentration-dependent way as a gradient morphogen, acting directly to regulate the expression of patterning determinants in the ventral NT.

Shh signaling reception occurs at the apical side of the neuroepithelial cells, where Shh proteins accumulate on the luminal surface of the NT (Marti, Bumcrot, Takada & McMahon 1995a), and specifically localize at the base of the primary cilium (Chamberlain et al., 2008). It is now well established that primary cilia are essential for intracellular Shh signal transduction, as they mediate trafficking and processing of key Hh pathway components, including Gli2 and Gli3 TFs, which regulate pathway activity by controlling the expression of target genes that determine neural cell fate (reviewed by Goetz and Anderson, 2010).

Ventral NPCs decode graded Shh through both signal concentration and duration. Higher and more sustained Shh exposure results in prolonged periods of Gli activation, leading NPCs to adopt more ventral identities (Dessaud et al., 2008). The Shh gradient within the ventral spinal cord is dynamically regulated throughout development (Chamberlain et al., 2008; Dessaud et al., 2010), linking the amount and time of Shh exposure to the timing and spatial pattern of gene induction in the NT. Consequently, ventral neural progenitor identities are established sequentially, with increasingly ventral fates requiring higher levels and longer periods of Shh signaling (reviewed by Ribes and Briscoe,2009).

The TFs Nkx2.2 and Olig2 distinguish the two most ventral progenitor domains, p3 and pMN, respectively. Their expression is initiated sequentially at the ventral midline of the NT and progressively extends to more dorsal positions as new markers appear at the midline. Thus, the Shh/Gli pathway plays a major role in patterning the ventral NT, however additional molecular mechanisms that limit target gene responses to specific progenitor domains operate from the dorsal NT to ensure proper D-V patterning.

2.2.- Wnt canonical pathway antagonizes Shh and regulates the identity of dorsal progenitors from the RP

The role of the RP in patterning the dorsal NT was initially demonstrated through explants assays (Liem et al., 1995), and later confirmed *in vivo* via genetic ablation, which resulted in severe loss of the three dorsal-most interneural populations (d1-3) and expansion of the three more ventrally located populations (d4-6) (Lee et al., 2000; Millonig et al., 2000). This prompted investigation into the secreted signals mediating RP activity, given that dorsal-most RP cells release multiple members of the Wnt and BMP families (Parr et al., 1993; Liem et al., 1997; Hollyday et al., 1995; Lee et al., 1998; Lee et al., 2000; Megason and McMahon, 2002; Robertson et al., 2004).

In both chick and mouse embryos, Wnt1 and Wnt3 are expressed in the RP and surrounding region (Parr et al., 1993; Hollyday et al., 1995; Megason and McMahon, 2002; Robertson et al., 2004). Initially described as mitogenic signals promoting NPCs proliferation (Dickinson et al., 1994; Megason and McMahon, 2002), Wnt signaling was later shown to play a crucial role in dorsal patterning of the NT (Yu et al., 2008; Alvarez-Medina et al., 2008). Specifically, upon Wnt gain-of-function, dorsal and intermediate markers such as Pax7 and Pax6 respectively were expanded and shifted ventrally at the expense of ventral progenitor markers such as Nkx6.1, Olig2 and Nkx2.2., thereby increasing the generation of dorsal neuronal subtypes with the concomitant loss of ventral neurons (Yu et al., 2008; Alvarez-Medina et al., 2008).

A key genetic interaction between the Wnt/TCF and Shh/Gli pathways involves Gli3, a dorsal TF that acts as a repressor (Gli3R) in the absence of Shh. Its expression is regulated by Wnt/β-catenin signaling through four enhancer modules within the Gli3 locus that contain consensus TCF-binding sites highly conserved throughout vertebrate species (Alvarez-Medina, 2008; Alvarez-Medina et al., 2009). Two of these enhancers, HCNR2 and HCNR3, contain sufficient information to direct expression of Gli3 in the dorsal spinal cord and are responsive to β-catenin/TCF transcriptional activity (Alvarez-Medina, 2008; Alvarez-Medina, 2009), indicating that Gli3 is a direct target of Wnt/β-catenin signaling. Since Gli3R limits Shh-dependent ventral gene expression, the balance of Shh and Wnt activities is critical for proper D-V patterning of the spinal cord. This regulatory principle also appears to be conserved in other regions of the CNS such as the telencephalon (Li et al., 2009).

While the role of primary cilia in Shh signaling is well established, growing evidence suggests that cilia also play an important role in transducing Wnt signals. Primary cilia regulate β-catenin-dependent Wnt signaling by restricting the nuclear entry of β-catenin

through sequestration of proteins like Jouberin (Lancaster et al., 2011). In addition, primary cilia participate in β-catenin-independent Wnt signaling by presenting Wnt receptors at the cilium membrane that can activate Wnt/ Glycogen Synthase Kinase 3 (GSK3) cascade and promote ciliogenesis through inhibition of PP1, a negative regulator of cilia formation (Bernatik et al., 2021). More recently, Wnt-PP1 axis has been identified, showing that Wnt-activated GSK3 signaling prevents PP1 activity, thereby facilitating ciliary biogenesis. This study demonstrated that primary cilia not only receive Wnt signals but also regulate their own formation in response (Zhang et al., 2023). Together, these findings highlight the cilium as a key cellular hub for integrating and modulating Wnt activity.

2.3.- BMP controls the identity of dorsal progenitors from the RP

Expression of BMP-ligands is highly dynamic and complex during NT development. Before NT closure, BMP2/4 are expressed in the epidermal ectoderm, while BMP4/5 are expressed in the neural folds (Liem et al., 1995; Lyons et al., 1995; Dudley and Robertson, 1997; Solloway and Robertson, 1999). At this stage, BMP7 is expressed in both the epidermal ectoderm and in the notochord (Liem et al., 1995; Lyons et al., 1995). After NT closure, BMP expression shifts to the RP where several BMPs (BMP4/5/7) as well as related molecules such as GDF7, a distant member of the BMP subfamily, and non-BMP members of the TGF-β superfamily such as Dsl-1 and Activin A/B are all expressed (Lee et al., 2000).

The initial description of a role for TGF-β/BMP in dorsal NT development was discovered through explant assays showing BMP4/5/7, Dsl1 and activin A/B have the capacity to promote the generation of two types of dorsal interneurons (dIN) identified as dI1 and dI3 (Liem et al., 1995, 1997). *In vivo* gain-of-function of BMP activity further demonstrated that increased BMP signaling result in differential responses of progenitors during patterning, favoring specification of dP1 progenitors at the expense of dP2-3 fates, whereas lower activation of the pathway promoted dP2-3 fates over dP1 (Timmer et al., 2002). These findings supported the idea that BMPs act as a classical morphogen, instructing cell fate in a concentration-dependent manner. However, genetic studies challenged model, since in BMP receptor mutant mice, the phenotype shown in dIN generation was different and dI1 neurons were absent, numbers of dI2 were reduced and dI3 neurons were unaffected (Wine-Lee et al., 2004), suggesting that BMPs may not act solely through a classical morphogen gradient but additional mechanisms may contribute to the dorsal interneuron specification.

Several lines of evidence suggest that during neural development, unlike long-range signaling demonstrated for Shh, BMPs act over a short range of action (Hogan, 1996). Most BMPs involved in NT patterning lack a specific basic amino-acid sequence that helps protein diffusion through tissues. This motif, found in BMP2/4, mediates interaction with extracellular matrix components such as heparan sulfate proteoglycans (HSPGs), which restrict BMPs diffusion as shown by a mutant version of BMP4 lacking this motif, which caused a stronger dorsalizing effect in the NT (Hu et al., 2004). Such restricted diffusion likely explain why BMP activity becomes more spatially localized as development progresses. Before NT closure, BMPs expressed broadly along the entire neural plate and can signal across the full D-V axis. However, after NT closure, BMP expression becomes restricted in and around the RP, limiting their range of action to the dorsal-most progenitor domains.

Additional evidence indicates that TGF-β/BMP family members exert qualitatively distinct, non-redundant activities during dorsal NT development. In BMP-related molecule GDF7 mutant mice, dI1A interneurons are specifically lost while the rest of the dINs remain unaffected (Lee et al., 1998). Similarly, BMP7 mutant mice maintain normal expression of key dorsal progenitor markers including Pax7, Gsh1/2 and Olig3 and RP identity marked by Lmx1b, but exhibit reduced numbers of three specific dIN subtypes (dI1, dI3 and dI5) with no compensatory increase in alternative interneuron populations, indicating that BMP7 is required for specific neuronal subtype generation but not for progenitor patterning (Le Dreau et al., 2012). In contrast, BMP4 knock-down (KD) in chick disrupts RP formation, and reduces in dI1 neurons only, confirming that BMP4 and BMP7 function non-redundantly in neural development (Le Dreau et al., 2012; extensively reviewed in Le Dreau & Marti, 2012).

3.- NT growth: the role of the centrosome in the specialized modes of division of NPCs and their impact on CNS formation

NPCs are mitotically active cells whose divisions are essential for tissue growth. The expansion of the embryonic NT depends on a finely tuned balance between cell cycle progression and cell divisions, which are tightly coordinated with the INM of the cell. During the G1 phase, the nucleus of NPCs moves in a basal direction, while during G2 phase, it returns apically to ensure that mitosis occurs at the luminal surface (Figure 6A). In species such as mice, chicken and zebrafish, NPCs maintain a slender

connection to the basal lamina throughout the cell cycle (Sauer, 1935; Langman, Guerrant and Freeman, 1966; Taverna and Huttner, 2010; Molina and Pituello, 2017; Saade et al., 2018; Kosodo et al., 2008). In contrast, humans NPCs often retract this basal process during mitosis, requiring the daughter cell to actively re-establish contact with the basal surface after division (Subramanian, Bershteyn, Paredes & Kriegstein, 2017).

INM has been classically interpreted as a spatial adaptation that allows dense packing of progenitor cells within the limited space of the NT, while maintaining their contact with both the apical and basal surfaces, an arrangement far more efficient than in a simple columnar epithelium (Sauer, 1935; Langman, Guerrant and Freeman, 1966). Beyond this structural role, INM may also influence NPC behavior. Although numerous studies correlate INM perturbations with alterations in neurogenesis (Murciano et al., 2002; Baye and Link, 2007; Del Bene et al., 2008; Del Bene, 2011; Formosa-Jordan et al. 2013; Hu et al., 2013), its instrumental role in determining the cell fate of NPCs remains unclear. Moreover, in the developing mouse spinal cord, INM has been shown to facilitate tissue growth by generating mechanical stress that alters the apical surface area of NPCs, thereby facilitating cell rearrangements and maintaining the fluidity of the neuroepithelium during growth. As development progresses, both the rate of cell divisions and INM activity decrease, leading to more restricted cellular rearrangements and tissue solidification (Bocanegra-Moreno, Singh, Hannezo, Zagorski & Kicheva, 2023).

These dynamic mechanical changes during INM are driven by the forces generated during apical nuclear migration of NPCs, which in turn rely on the microtubule cytoskeleton, organized by the apically positioned centrosome (Figure 6B). The centrosome is a small, non-membranous organelle composed of two centrioles and surrounded by a dense protein matrix known as the pericentriolar material (PCM). In vertebrate cells, centrosomes perform several critical functions which include acting as the main microtubule-organizing center (MTOC), forming the basal body (BB) of primary cilia, coordinating intracellular signaling, and organizing the mitotic spindle during cell divisions (Arquint, Gabryjonczyk and Nigg, 2014; reviewed by Blanco-Ameijerias et al., 2022). The essential role of the centrosome in apical nuclear migration has been demonstrated in rodent and zebrafish models since loss-of-function studies targeting centrosome proteins such as CEP120, PCM1, HOOK3 or members of the TACC family impair apical nuclear migration in NPCs nuclei (Ge, Frank, Calderon de Anda& Tsai, 2010; Xie et al., 2007; Yang, Want & Van Aelst, 2012). Similarly, disruption of motor protein like kinesin or dynein (Tsai, Lian, Kemal, Kriegstein &

Vallee, 2010; Hu et al., 2013) or microtubule associated regulators including TPX2 (Kosodo et al., 2011), LIS1 (Tsai, Chen, Kriegstein & Vallee, 2005; Gambello et al., 2003) DYNACTIN (Del Bene et al., 2008) Casein kinase 2, CK2 (Carneiro, Fragel-Madeira, Silva-Neto & Linden, 2008), SYNE2 (Yu et al., 2011; Zhang et al., 2009) and NUDC (Cappello, Monzo & Vallee, 2011) also lead to defective apical nuclear migration. Despite these insights, the mechanisms that drive the basal nuclear migration phase of INM remain poorly understood.

Once the nucleus reaches the apical surface, NPCs undergo mitosis, which can result in different outcomes depending on the identity of the daughter cells. Self-expanding symmetric proliferative divisions (progenitor-progenitor or PP divisions) generate two daughter cells with identical progenitor potential, ensuring the expansion of the progenitor pool and tissue growth, whereas self-renewing asymmetric divisions (progenitor-neuron or PN divisions) generate one NPC and one daughter cell that is committed to neural differentiation. Finally, self-consuming symmetric divisions (neuron-neuron or NN divisions) generate two new neurons (reviewed in Saade et al., 2018) (Figure 6A). During early stages of the development, PP divisions dominate to allow the expansion of NPCs population. Once this NPC pool has reached the critical size to generate all the neural cells required to form functional and healthy CNS, the neurogenic divisions prevail to guarantee the generation of neurons needed for proper functioning (Saade et al., 2013; Le Dreau et al., 2014). Thus, a premature switch from the symmetric proliferative to the asymmetric neurogenic mode of divisions has dramatic effects on the CNS growth and function.

Interestingly, cell division in general is intrinsically asymmetric as a consequence of differences between the centrosomes inherited by daughter cells. This asymmetry arises because only one centriole, the mother centriole, is fully mature, exhibiting two characteristic accessory structures, the Distal Appendages (DA) and the Sub-Distal Appendages (SDA). Prior to mitosis, the centrosome replicates in a semi-conservative manner, resulting in one centrosome that retains the older mother centriole and another that receives the younger daughter centriole (Blanco-Ameijerias et al., 2022). Consequently, after self-replication, centrosomes differ in structure, molecular composition and MTOC capabilities (Blanco-Ameijerias et al., 2022). This inherent asymmetry biases NPC division outcomes as demonstrated in studies on human forebrain organoids (Royall, Machado, Jessberger & Denoth-Lippuner, 2023), the developing mouse cortex (Wang et al., 2009; Paridaen, Wilsch-Brauninger and Huttner, 2013) and the developing chick spinal cord (Saade et al., 2017; Tozer et al., 2017) that show that the centrosome retaining the older mother centriole is preferentially inherited

by the daughter cell that remains as progenitor, whereas the centrosome with the newer centriole is passed to the differentiating neuron (Figure 6B).

Hence, from a centrosome perspective, the default outcome of any cell divisions should be asymmetric, which in the case of NPC is preventing tissue growth. Therefore, overcoming this intrinsic centrosome-associated asymmetry is likely required to promote symmetric proliferative divisions and embryonic CNS growth. This functional bias is thought to be regulated through centrosome maturation, a process characterized by the expansion of the PCM and a significant increase in MTOC activity. These changes may underline the instructive role of the centrosome in guiding NPC fate (Figure 6B'). Supporting this idea, the depletion of proteins involved in centrosome maturation such as NINEIN (Royall, Machado, Jessberger & Denoth-Lippuner, 2023; Wang et al., 2009), CDK5RAP2, pericentrin (PCNT) (Buchman et al., 2010), WDR62 or ASPM (Fish, Kosodo, Enard, Paabo & Huttner, 2006; Jayaraman et al., 2016) leads to the premature depletion of NPCs in the ventricular zone and impair tissue growth, ultimately resulting in a smaller CNS. Nonetheless, the molecular mechanisms through which centrosome maturation impact the outcome of NPC division remain unclear.

Moreover, centriole maturation influences the NPCs capacity to quickly reassembles a primary cilium and respond to external stimuli such as other growth factors (Anderson and Stearns, 2009), as will be discussed in greater detail in the 3.3 section. This is because, during NPCs division, a portion of the ciliary membrane is preferentially associated to the mother centrosome and is thus asymmetrically inherited by the daughter cell retaining the progenitor identity (Paridaen, Wilsch-Brauninger and Huttner, 2013).

3.1. Centrosome organization of symmetric divisions

The organization of microtubules into a bipolar mitotic spindle is a fundamental function of the centrosome and plays a crucial role in NPCs for the organization of specialized modes of division.

At the onset on mitosis, the duplicated centrosomes separate and migrate to opposite poles of the cell, where they nucleate and organize microtubules that make up the mitotic spindle (Blanco-Ameijeiras et al., 2022) (Figure 7). The organization of a bipolar mitotic spindle depends on the enhanced MTOC activity of centrosomes, which regulates the nucleation, stability and arrangement of microtubules forming the spindle. This happens because during centrosome maturation PCNT initiates the coordinated

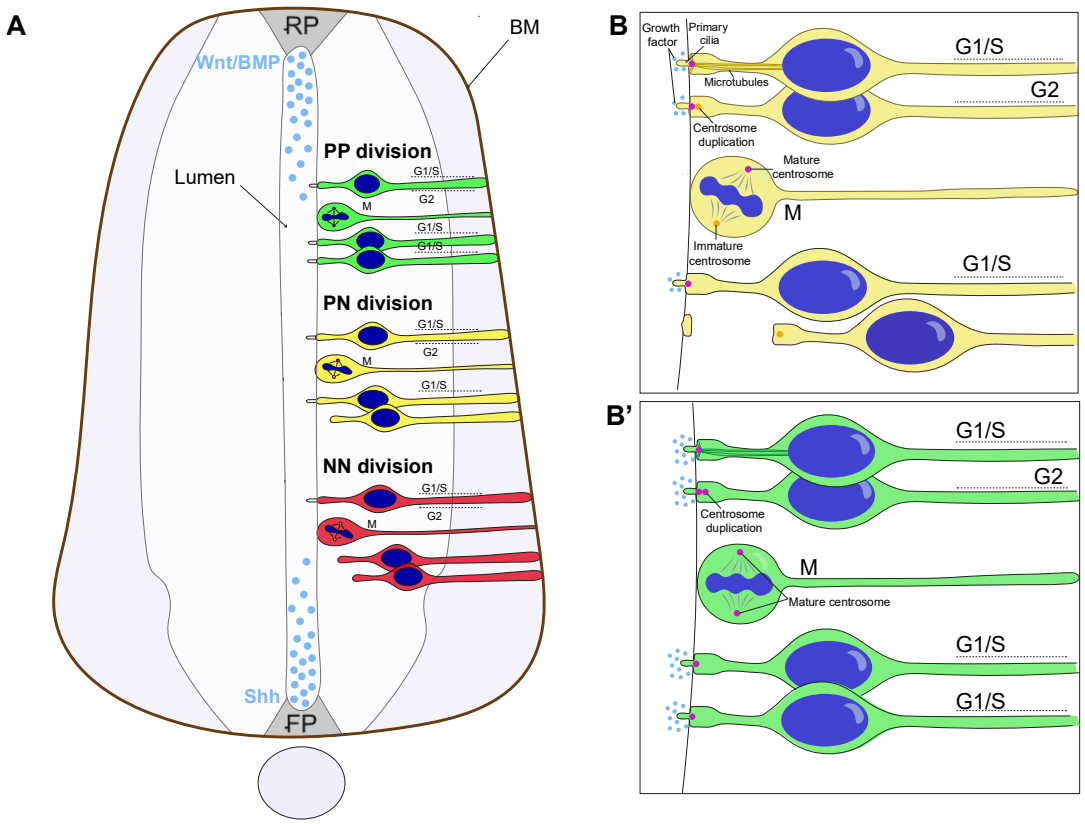

Figure 6. NPC undergo INM and different modes of cell division at the apical surface of the NT. (A) Schematic representation of a transversal section of a NT showing the direction of NPC nuclear migration along the apicobasal axis depending on the phase of the cell cycle (G1, S, G2, M), indicated by dashed arrows. NPCs divide apically at the luminal surface, undergoing distinct modes of division: PP (progenitor–progenitor) divisions (green) expand the progenitor pool, PN (progenitor–neuron) divisions (yellow) generate one progenitor and one neuron or NN (neuron–neuron) divisions (red) generate two neurons. Within NPCs, the centrosome is located at the apical region, where the older centriole gives rise to the primary cilium, which protrudes into the NT lumen and contains receptors for growth factor signaling. Additionally, during G2 phase, the centrosome replicates in a semi-conservative manner, perpetuating centrosome asymmetries. At this same phase, microtubule forces drive apical migration of the nucleus, facilitating NPC division at the ventricular (luminal) surface. **(B)** Schematic representation of an asymmetrically dividing NPC where centrosome asymmetries persist through mitosis. **(B')** Schematic representation of a symmetrically dividing NPC where intrinsic centrosome-associated asymmetry has been overcome.

assembly of additional PCM scaffold proteins such as CEP192 and CDK5RAP2, resulting in the expansion of the PCM matrix and the recruitment of additional γ-tubulin ring complexes (γ-TuRCs), facilitating microtubule nucleation and preparing centrosome to orchestrate the establishment of a mitotic spindle (Chinen et al., 2021; Jiang et al., 2021; Lawo, Hasegan, Gupta & Pelletier; 2012).

The mitotic spindle anchors to the cell cortex through astral microtubules that extend from the centrosome (di Pietro, Echard & Morin, 2016; Morin & Bellaiche, 2011). The cell cortex, located beneath the plasma membrane, contains a network of rigid, tensile actin filaments, whose assembly is locally enhanced by RHOA activation (Roszko, Afonso, Henrique & Mathis, 2006). This acting network plays a key role in orienting the mitotic spindle during cell division (Kwon, Bagonis, Danuser & Pellman, 2015). Although cortical tension is complex to study, owing the multiple roles of actin regulators in determining NPC polarization, interfering with RHOA activity in chick NPCs has demonstrated its important role in maintaining the mitotic spindle in a planar orientation (Roszko, Afonso, Henrique & Mathis, 2006).

Symmetric proliferative divisions of NPC rely on this precise regulation of the metaphase plate orientation to maintain a planar spindle alignment, ensuring the equal distribution of cellular components, particularly the apical polarity complex, between daughter cells in human (LaMonica, Lui, Hansen & Kriegstein, 2013), rodent, (Martiens & Ffrench-Constant, 2006; Kosodo et al., 2004), and chick (Saade et al., 2017, Wilcock, Swedlow & Storey, 2007; Das & Storey, 2012) models. Conversely, an oblique orientation of the metaphase plate results in the cleavage plane bypassing the apical membrane and the asymmetric inheritance of apical subdomains between daughter cells (Martiens & Ffrench-Constant, 2006; Saade et al., 2017; Kosodo et al., 2004; Das & Storey, 2012). In the developing mouse, chick and zebrafish NT, this asymmetric partitioning of apical subdomains can drive asymmetric NPC divisions (Das & Storey, 2012, Alexandre, Reugels, Barker, Blanc & Clarke, 2010). In line with this, KD of key astral microtubule factors in mouse NPCs prematurely shifts the cleavage plane to an oblique orientation, impacting the mode of NPC division (Fish, Kosodo, Enard, Paabo & Huttner, 2006; Vargas-Hurtado et al., 2019; Konno et al., 2008; Mora-Bermudez, Matsuzaki & Huttner, 2014). Thus, maintaining a planar mitotic spindle preserves symmetric NPC divisions and supports the growth of the embryonic NT (Figure 7).

3.2. Centrosome organization of asymmetric divisions

As outlined above, the positioning of the mitotic spindles, which dictated the mode of the division, is guided by interactions between astral microtubules and the polarized cell cortex (di Pietro, Echard & Morin, 2016; Morin & Bellaiche, 2011). Studies in the developing mouse cerebral cortex have shown that, at early developmental stages, astral microtubules are more abundant and longer than they are at later stages (Vargas-Hurtado et al., 2019). Additionally, live imaging in mouse model revealed that asymmetric cell division is associated with asymmetry in the size of mitotic spindles that start in metaphase and persist throughout division and that neurons preferentially arise from the daughter cell with the larger spindle pole (Delaunay, Cortay, Patti, Knoblauch & Dehay, 2014). Furthermore, a developmental transition in spindle morphology, marked by increased density and stability of inner spindle microtubules, also occurs as neurogenesis progress (Vargas-Hurtado et al., 2019) (Figure 7). Whether additional spindle functions are similarly affected during neurogenesis remains to be explored.

Following mitosis, the detachment of newly born neurons from the neuroepithelium, referred to as delamination, has a key role in ensuring the correct positioning of neurons, essential for the establishment of neuronal architecture and functional circuitry. To delaminate, NPCs must enhance their ability to organize and nucleate microtubules, which promotes apical end-foot constriction and AJ weakening. NPCs upregulate the expression of AKNA, a centrosome protein that localizes at the tip of the SDA of the mother centriole and leads to more potent MTOC activity (Camargo Ortega et al., 2019). Loss-of-function experiments of AKNA in the mouse cerebral cortex result in the retention of a greater number of NPCs in the ventricular zone, whereas its overexpression induces fast delamination (Camargo Ortega et al., 2019). During neuronal differentiation, other SDA-associated proteins, such as NINEIN and DCTN1, undergo a shift in localization from centrosome to non-centrosome sites as a result of alternative splicing (Zhang et al., 2016). This redistribution drives the anchoring and stabilization of microtubules at new cellular sites, facilitating later differentiation events such neuronal polarization 200 (Figure 7). Thus, besides maintaining NPCs integrity, changes in centrosome protein composition, which modulate MTOC activity and microtubule nucleation, also regulate the early stages of neuronal differentiation.

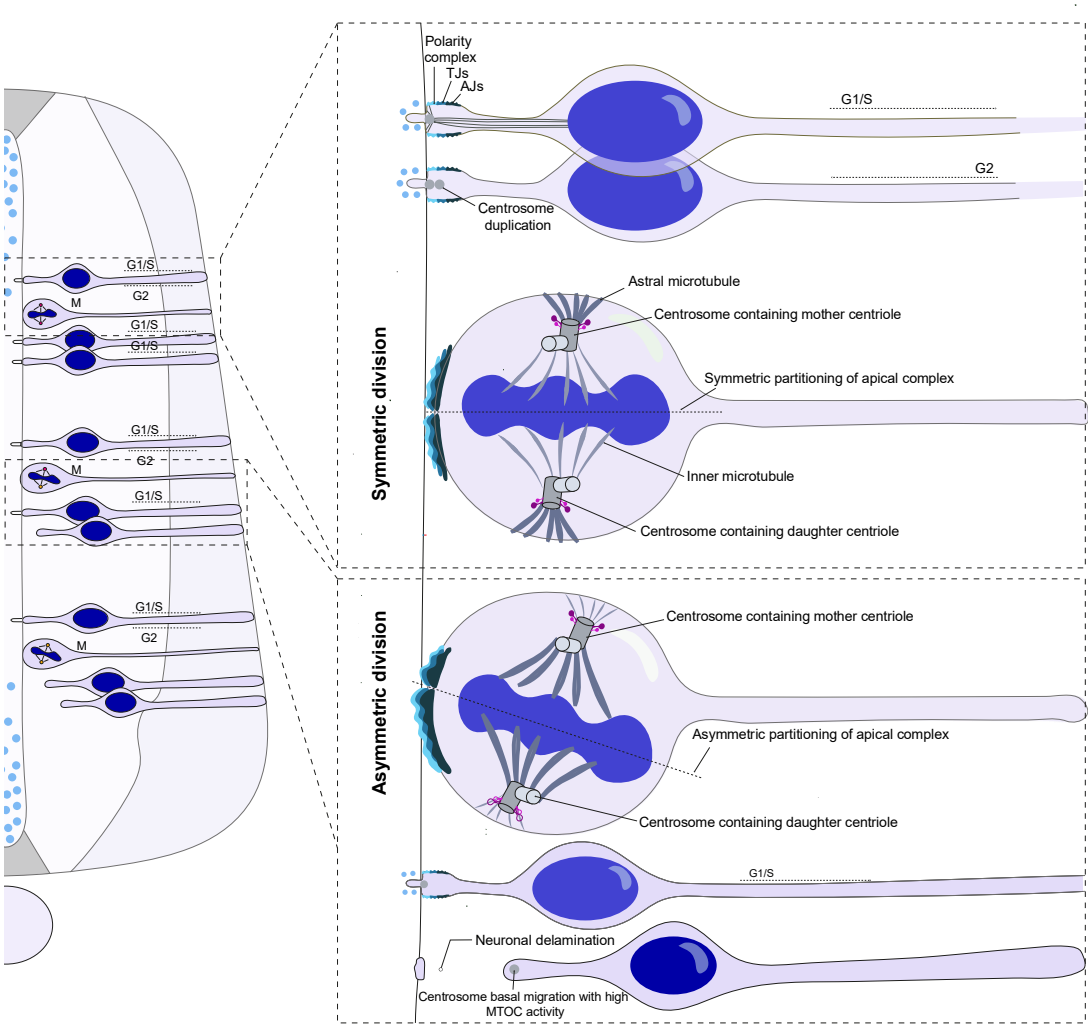

Figure 7. Molecular mechanisms underlying the regulation of distinct modes of NPC division. On the left, schematic representation of the different NPC modes of divisions. On the right, zoomed-in schematic illustrating the detailed molecular mechanisms controlling these divisions. Upon apical nuclear migration, symmetric mitosis involves the organization of a mitotic spindle that is aligned perpendicular to the lumen and stabilized by astral microtubules, ensuring equal inheritance of the apical polarity complex. In contrast, during asymmetric mitosis, the spindle pole is oblique to the NT lumen, with denser inner microtubules and fewer astral microtubules. The mother and daughter centrioles exhibit asymmetric composition, contributing to this asymmetry. The oblique spindle orientation results in unequal inheritance of the apical polarity complex. Newly formed neurons migrate basally through neuronal delamination, a process characterized by enhanced MTOC activity of the more basally located centrosome.

3.3. Centrosome organization of the primary cilia

Another feature of NPCs that relies on the centrosome is their single primary cilium, a microtubule-based organelle that protrudes from the apical cell surface that plays a central role in mediating intercellular and intracellular signaling (Caspary, Larkins & Anderson, 2007; Hwang & Mukhopadhyay, 2015; Sun, Fisher, Bowser, Pentecost & Sui, 2019; Zhang et al., 2023). Ciliogenesis begins with the conversion of the mother centriole into a basal body that is linked to the cell membrane via its distal appendages (Tanos et al., 2013; Yang et al., 2018; Anderson & Stearns, 2009). Upon docking these appendages to the cell membrane, pairs of microtubules extend from the basal body and form the ciliary axoneme, consisting of nine microtubule doublets arranged cylindrically (Sun, Fisher, Bowser, Pentecost & Sui, 2019). Despite being continuous with the cell membrane, the ciliary membrane is biochemically distinct in proteins and lipids composition, and is particularly enriched in signaling receptors, including G protein-coupled receptors for Shh, Wnt and BMP proteins (Hwang & Mukhopadhyay, 2015; Corbit et al., 2005; Rohatgi, Milenkovic & Scott, 2007; Zhang et al., 2023) (Figure 8).

In addition to orchestrate cell fate specification in the developing vertebrate CNS, Shh, Wnt and BMP signaling pathways have also a crucial role in regulating NPC cell cycle progression. Effective ciliary signaling depends on intraflagellar transport (IFT), a bidirectional trafficking process along the axoneme essential for cilia assembly, maintenance and signaling (Klena & Pigino, 2022). Disruption of IFT machinery or the structure of the ciliary axoneme in mouse embryos have been shown to interfere with Shh signaling, leading to abnormalities in NT and brain development (Caspary, Larkins & Anderson, 2007, Huangfu et al., 2003; Huangfu & Anderson, 2005; Liu, Wang & Niswander, 2005; May et al., 2005). These findings underscore the essential role of primary cilia as a hub for integrating extracellular signals in NPCs that are essential for neural development.

The arrangement of specialized modes of NPC division may also be influenced by the activity of growth factors. Early evidence supporting this notion came from studies examining Shh activity in the ventral spinal cord of chick embryos (Saade et al., 2017, Saade et al., 2013). By integrating mathematical modeling with *in vivo* tracking of NPC division modes, it was demonstrated that high Shh activity promotes symmetric proliferative divisions during early embryonic stages, while a shift to neurogenesis divisions later in development aligns with a decrease in Shh activity (Saade et al., 2013).

Thus, division mode selection is tightly regulated by morphogenic signaling pathways such as Shh during CNS development.

Appart from influencing division outcomes, Shh signaling also influences the centrosome-associated molecular machinery responsible for regulating these division modes. Specifically, Shh pathway activation in NPCs triggers the transcription of a cluster of centrosome proteins, including those involved in centriolear and PCM maturation (Saade et al., 2017), which helps to mitigate the inherent asymmetries of the centrosome. Among them, PCNT, is crucial for ensuring equal distribution of protein kinase A (PKA) at both centrosome in mitotic NPCs, a process that enables equal responsiveness to Shh in daughter cells during early development in chick embryos (Saade et al., 2017; Epstein, Marti, Scott & McMahon, 1996). As development progresses, Shh activity diminishes, PCNT expression decreases and PKA becomes associated exclusively with the centrosome containing the mother centriole, leading to differential Gli transcriptional activity and ultimately, promoting neurogenic divisions. Moreover, through downstream effectors such as Gli3, Shh signaling pathway also regulates the expression of several other centrosome proteins including CP110, ASPM, and PCM1 (Saade et al., 2017) which are crucial for centrosome maturation and symmetric divisions. Therefore, the regulation of centrosome maturation should be recognized as another critical role of Shh signaling in the CNS development.

The BMP/SMAD and Wnt/β-catenin signaling pathways are also crucial regulators of CNS growth. In particular, in both chick and mouse embryos, the mode of NPC division chosen in the developing spinal cord and cerebral cortex is influenced by the activity of canonical BMP effectors, SMAD1 and SMAD5 (Le Dreau, 2014; Najas et al., 2020). Given that components involved in both BMP and Wnt pathways have been found to localize at the centrosome, (Chilov et al., 2011; Fuentealba, Eivers, Geissert, Taelman & De Robertis, 2008), it would be valuable to investigate whether these pathways regulate cell division and centrosome dynamics through mechanisms analogous to those described by Shh signaling. However, the extent to which BMP and Wnt influence centrosome maturation and symmetry in NPCs remains to be fully elucidated.

Altogether, these data suggest that the regulation of centrosome maturation might constitute one of various functions fulfilled by growth factors in CNS development, ranging from classical roles in generating cell diversity to the maintenance of progenitor cell identity through the modulation of centrosome components and the promotion of symmetric cell divisions. Given that centrosome maturation involves the organization

of DAs and SDAs, whose main functions are in ciliogenesis, there may be a positive-feedback loop in which these growth factor signals are received and integrated by the primary cilia.

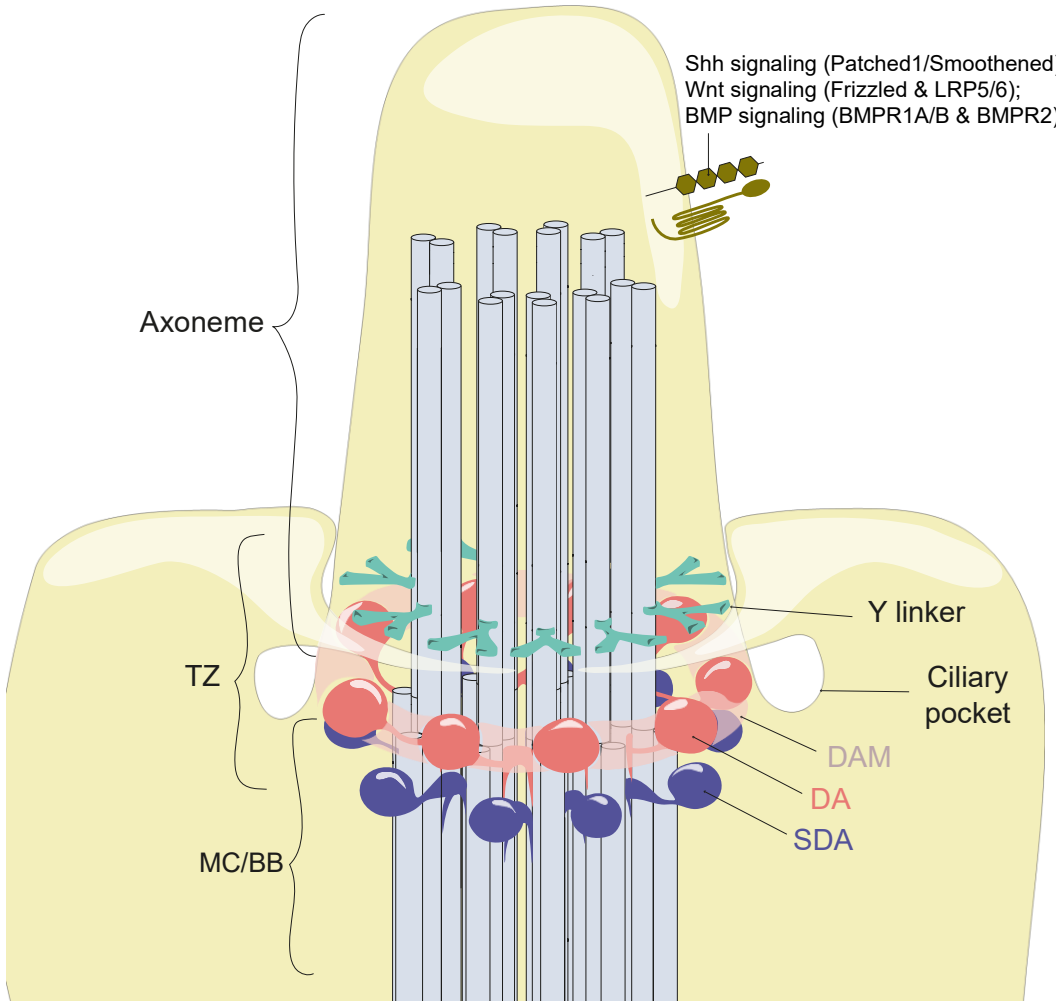

Figure 8. Mature centriole organization at the basal body (BB) of the cilium and signal transduction. The microtubule triplets of the BB, the mother centriole of the centrosome, characterized by the possession of Distal Appendages (DA), Sub-Distal Appendages (SDA) and the surrounding Distal Appendages Matrix (DAM), extend as microtubule doublets into the axoneme. This transition from triplets to doublets occurs at the transition zone (TZ), where Y-links connect the microtubules to the ciliary membrane. Along this ciliary membrane, receptors for growth factors such as Shh, BMP and Wnt localized, which facilitate intracellular signal transduction and coordinate cellular responses to external signaling cues.

3.4. Centrosome dysfunction and microcephaly

As discussed above, centrosome maturation has a central role in determining NPCs mode of division outcome and, consequently, in supporting proper brain growth. Disruption of this process is strongly linked to developmental brain disorders, particularly autosomal recessive primary microcephaly (MCPH), a genetically heterogeneous neurodevelopmental condition characterized by reduced CNS at birth.

The study of MCPH have uncovered a robust genetic association between defects in centrosome biology during development and the etiology of the disease. To date, over 30 MCPH-causative loci have been mapped across diverse populations worldwide.

Remarkably, at least 16 of these encode proteins localized to the centriole/centrosome or kinetochore/spindle poles, which are key structures for centriole biogenesis, centrosome maturation, cytokinesis and chromosome segregation. This strong enrichment underscores centrosome dysfunction as a major contributor to MCPH pathogenesis (Nano & Basto, 2017; Jayaraman, Bae and Walsh, 2018) (Table 1).

Moreover, mutations in additional centrosome-related protein such CEP63, PCNT, NIN, POC1A are also associated with microcephaly phenotypes, reinforcing the genetic link between centrosome biology and CNS growth (Table 1).

LOCUS	GENE	PROTEIN	SUBCELLULAR LOCATION	MAIN MOLECULAR FUNCTION	OMIM
MCPH1	*MCPH1*	MICROCEPHALIN	Nucleus, mitochondria	Chromosome condensation, DNA replication, DNA damage response	607117
MCHP2	*WDR62*	WDR62	Minus end of microtubules	Neuronal proliferation and migration	613583
MCPH3	*CDK5RAP2*	CDK5RAP2 (CEP125)	PCM	Microtubules nucleation, centriole disengagement after duplication	608201
MCPH4	*CASC5*	KLN1	Kinetochore	Attachment of centromeres to spindle microtubules, spindle-assembly checkpoint signaling	609173
MCPH5	*ASPM*	ASPM	Minus end of microtubule	Spindle pole organzation, microtubule dynamics at spindle pole	605481
MCPH6	*CENPJ(CPAP)*	CENPJ(CPAP)	Centriole	Centriole duplication/biogenesis	609279
MCPH7	*STIL*	STIL	Centriole cartwheel	Centriole duplication/biogenesis, primary cilium	181590
MCPH8	*CEP135*	CEP135	Centriole	Centriole biogenesis and cohesion	611423
MCPH9	*CEP152*	CEP152	Centriole	Centrioles duplication/biogenesis	613529
MCPH10	*ZNF332*	ZNF332	Nucleus	Transcription, neural progenitor proliferation	610827
MCPH11	*PHC1*	PHC1	Nucleus	Chromatin remodeling	602978
MCPH12	*CDK6*	CDK6	Nucleus, centrosome	Cell cycle control (G1/S transition)	603368
MCPH13	*CENPE*	CENPE	Plus end of microtbules, kinesin-like protein	Microtubule attachment at the kinetochore, chromosome congression	117143
MCPH14	*SAS6*	SAS6	Centriole cartwheel	Centriole duplication/biogenesis	609321
MCPH15	*MFSD2A*	MFSD2A	Cell membrane	Blood-brain barrier formation	614397
MCPH16	*ANKLE2*	ANKLE2	Endoplasmic reticulum	Nuclear envelope reassembly	616062
MCPH17	*CIT*	CIT	Midbody	Cytokinesis	605629
MCPH18	*WDFY3*	WDFY3	Nucleus	Autophagy	617485
MCPH19	*COPB2*	COPB2	Golgi, cytoplasmic vesicle	ER-to-Golgi and Golgi-ro-ER transport. Coatomer complex protein	606990
MCPH20	*KIF14*	KIF14	Mitotic spindle, midbody	Cell cycle progression, cytokinesis	611279
MCPH21	*NCAPD2*	NCAPD2	Nucleus, chromosomes	Mitotic chromosome condensation/intengrity	615638
MCPH22	*NCAPD3*	NCAPD3	Nucleus, chromosomes	Mitotic chromosome condensation/intengrity	609276
MCPH23	*NCAPH*	NCAPH	Nucleus, chromosomes	Mitotic chromosome condensation/intengrity	602332
MCPH24	*NUP37*	NUP37	Nucleus, nuclear pore complex	Kinetochore microtubule attachment, mitotic progression	609264
MCPH25	*MAP11*	MAP11	Mitotic spindle, midbody	Mitotic spindle dynamics, cytokinesis	618350
MCPH26	*LMNB1*	LMNB1	Nucleus, inner nuclear membrane	Nuclear shape, spindle assembly	150340
MCPH27	*LMNB2*	LMNB2	Nucleus, inner nuclear membrane	Nuclear shape, spindle assembly	150341
MCPH28	*RRP7A*	RRP7A	Nucleus, cilium, microtubules	Ribosome biogenesis, cilium resorption	619449
MCPH29	*PDCD6IP*	PDCD6IP	Cytoplasmic vesicle membrane	Cytokinses, apoptosis	608074
MCPH30	*BUB1*	BUB1	Chromosomes, kinetochore	Spindle-assembly checkpoint signaling, chromosome segregation	602452
MOPD2	*PCNT*	PCNT	PCM	PCM formation and centrosome cohesion	605925
SCKL1	*ATR*	ATR	Nucleus, chromosomes	DNA damage response	601215
SCKL2	*RBBP8 (CTIP)*	RBBP8	Nucleus, chromosomes	DNA double-strand break repair-homologous recombination	604124
SCKL6	*CEP63*	CEP63	Mother centriole	Centriole integrity/assembly	614724
SCKL7	*NIN*	NINEIN	Sub-distal appendage of mother centriole	Microtubule anchoring at mother centriole	608684
SCKL8	*DNA2*	DNA2	Nucleus, mitochondria	DNA replication/repair	601810
SCKL9	*TRAIP*	TRAIP	Nucleus	Replication stress response	605958
SCKL10	*NSMCE2*	NSMCE2	Nucleus	DNA double-strand break repair-homologous recombination	617246
MCCRP1	*TUBGCP6*	TUBGCP6	PCM/MTOC	Microtubule nucleation	610053
MCCRP2	*PLK4*	PLK4	Centriole	Centriole duplication/biogenesis	605031
MCCRP3	*TUBGCP4*	TUBGCP4	PCM/MTOC	Microtubule nucleation	609610
MCLRM	*KIF11*	KIF11	Plus end of microtubules	Bipolar spindle establishment	148760
CDCMB/SMELED	*DYNC1H1*	DYNC1H1	Microtubules	Transporter of cargo towards the minus ends of microtubules	600112
Bloom (BLM) syndrome	*RECQL3*	RECQL3	Nucleus	DNA replication/repair	604610
LilG4 syndrome	*LIG4*	LIG4	Nucleus	DNA repair	601837
SSMED	*XRCC4*	XRCC4	Nucleus	DNA repair	194363
Meyer Gorlin syndrome 1	*ORC1*	ORC1	Nucleus	DNA replication	601902
Meyer Gorlin syndrome 2	*ORC4*	ORC4	Nucleus	DNA replication	603056
Meyer Gorlin syndrome 3	*ORC6*	ORC6	Nucleus	DNA replication	607213
Meyer Gorlin syndrome 4	*CDT1*	CDT1	Nucleus, chromosomes, kinetochore	DNA replication, mitosis	605525
Meyer Gorlin syndrome 5	*CDC6*	CDC6	Nucleus	DNA replication	602627
Meyer Gorlin syndrome 6	*GMNN*	GMNN	Nucleus	DNA replication	602842

Table 1. The MCPH loci, their gene products and protein functions

4.- The Wnt pathway

4.1.- History, evolution and biological significance

The journey of Wnt research began in 1982, when Roel Nusse and Harold Varmus identified the int-1 gene in mice infected with the mouse mammary tumor virus (MMTV) Nusse & Varmus, 1982). This gene, activated by the viral insertion, was found to be a proto-oncogene, marking the first discovery of a mammalian Wnt gene. Just a few years later, in 1987, researchers discovered that the *Drosophila* gene Wingless (wg), one of the segment polarity genes, was homologous to the mouse int-1 gene (Rijsewijk et al., 1987a). Moreover, functional studies in *Xenopus* demonstrated that ectopic expression of int-1 induces the formation of a secondary dorsal axis of the embryos, suggesting a role for int-1 as an organizer, a hallmark function of developmental morphogens (McMahon and Moon, 1989). These findings demonstrated that a gene initially identified in the context of cancer biology had a crucial role in normal development.

The developmental importance of Wnt signaling was reinforced when int-1 became one of the first genes to be knocked out (KO) by homologous gene targeting in mice. KO models exhibited a dramatically reduced cerebellum and midbrain, resulting in severe ataxia and embryonic lethality (Thomas & Capecchi, 1990, McMahon & Bradley, 1990). The recognition that int-1 and wg were evolutionary conserved genes performing similar functions across species shifted the scientific perspective: these genes were not isolated curiosities of cancer or fly development but part of a broader, evolutionarily conserved signaling mechanism. To reflect this shared identity, int-1 was renamed Wnt1 — a fusion of Wingless and int — and became the foundation of the Wnt gene family (Nusse et al., 1991).

The renaming prompted the discovery of additional Wnt genes across diverse species. Researchers rapidly identified Wnt genes in *Xenopus*, mice, and humans. All these genes shared key structural features, encoding secreted proteins with conserved cysteine-rich domains, hinting at a common mode of action (Gavin et al. 1990; Roelink et al., 1990; Kimelman et al., 1992; Gallahan & Callahan, 1997).

Over time, it became evident that Wnt proteins constituted a large family of secreted signaling molecules with roles in development, cell proliferation, and tissue homeostasis. By the early 1990s, the Wnt family had expanded to include at least 19 Wnt genes in mammals, with orthologs found in invertebrates like *Drosophila*, C. elegans, and even in basal metazoans such as Hydra (Gavin et al., 1990; Kusserow et al., 2005, Gurley et al., 2010). This broad evolutionary conservation underscores their ancient and fundamental role in organizing the body plan across the animal kingdom (Petersen & Reddien, 2009; Niehrs, 2010; Holstein, 2012, reviewed in Nusse & Varmus, 2012).

4.2.- The canonical Wnt/β-catenin pathway

As the developmental importance of Wnt genes became evident, researchers began to investigate how Wnt signals are transduced from the cell surface to the nucleus. Unlike other signaling pathways of the time, the Wnt cascade was not unraveled in a linear fashion but it was assembled from a mosaic of findings across model systems like *Drosophila*, *Xenopus* and mammalian cell. This experimental patchwork helped define what is now known as the canonical Wnt/β-catenin pathway.

A major turning point came from cancer research in the early 1990s, when mutations in the large tumor suppressor gene Adenomatous Polyposis Coli (APC) were found to cause familial adenomatous polyposis, a hereditary form of colon cancer (Groden et al., 1991; Kinzler et al., 1991). Similar truncating mutations were found in the Min mouse model, an established model for intestinal tumorigenesis (Su et al., 1993), but the molecular basis remained unclear until APC was shown to bind β-catenin, a protein previously known for its role in cell adhesion (Rubinfeld et al., 1993; Su et al., 1993). Around the same time, β-catenin was identified as the vertebrate homolog of *Drosophila* Armadillo gene, a segment polarity gene involved in the Wingless pathway (McCrea et al., 1991; Peifer & Wieschaus, 1990). These findings suggested that Wnt signaling might intersect with cell adhesion and developmental regulation through β-catenin.

Experiments in *Xenopus* showed that manipulating β-catenin levels could induce or suppress dorsal axis formation (McCrea et al., 1993; Heasman et al., 1994) suggesting that Wnt signaling might regulate β-catenin through protein stabilization rather than synthesis. This led to the identification of GSK3 as a key negative regulator (Siegfried et al., 1992). This kinase was found to form a complex with β-catenin and APC, where it phosphorylates β-catenin, marking it for degradation via the ubiquitin-proteasome

pathway (Rubinfeld et al., 1996; Yost et al., 1996; Aberle et al., 1997; Orford et al., 1997). In the absence of Wnt signals, this degradation is continuous, preventing β-catenin accumulation. Upon Wnt binding, GSK3 activity is inhibited, allowing β-catenin to stabilize, accumulate in the cytoplasm and translocate into the nucleus to activate gene transcription. This mechanistic framework was further refined by identifying Dishevelled (Dvl) as an upstream inhibitor of GSK3 (Peifer et al., 1991; Noordermeer et al., 1994), and Axin as a scaffold protein originally identified in mouse mutant as a limiting component of the β-catenin destruction complex (Zeng et al., 1997; Behrens et al., 1998; Ikeda et al., 1998; Lee et al., 2003). This multiprotein complex, composed of APC, AXIN, GSK3 and β-catenin, became a central concept in canonical Wnt signaling. Loss of any of these components results in β-catenin stabilization and aberrant target gene activation. This molecular insight provided a mechanistic explanation for how APC mutations drive colon cancer and why mutations in β-catenin or Axin are found in other cancers (Korinek et al., 1997; Morin et al., 1997; Satoh et al., 2000) (Figure 9A).

By the mid-1990s, the core of the canonical Wnt pathway was established, but two key gaps remained: the identity of the Wnt receptors and the nuclear partner of β-catenin. A major breakthrough in understanding cell surface transduction of Wnt signaling came with the discovery of the Frizzled (Fz) family, seven-pass transmembrane receptors first identified in *Drosophila* as genes involved in planar cell polarity (Gubb & Garcia-Bellido, 1982; Vinson et al., 1989). Later, Fz gene Dfz2 was shown to bind Wg protein directly (Bhanot et al., 1996) and its expression in cultured cells led to β-catenin/Armadillo stabilization. Inside the cell, Fz interacts with Dvl, linking receptor activation to downstream signaling (Perrimon & Mahowald, 1987). The receptor complex also includes a second essential component, the co-receptors from the LRP family, particularly LRP5/6 (Arrow in *Drosophila*) (Wehrli et al., 2000; Tamai et al., 2000). Upon Wnt binding, LRP5/6 becomes phosphorylated at its cytoplasmic tail, which triggers recruitment of Axin and GSK3 to the membrane, thereby disrupting destruction complex and allowing stabilization of β-catenin and its accumulation in the cytoplasm (Figure 9B).

On the other hand, β-catenin's mechanism of action in the nucleus remained elusive until the identification of the TCF/LEF1 family of transcription factors. Initially studied in T-cell gene regulation (van de Wetering et al., 1991; Waterman et al., 1991), TCF/LEF1 proteins were later shown to directly bind β-catenin through its Armadillo repeat domain (Molenaar et al., 1996; Behrens et al., 1996). This interaction converts TCF from a transcriptional repressor into an activator by displacing co-repressors like

Groucho (Cavallo et al., 1998). Studies across species, including *Drosophila* (Brunner et al., 1997; Riese et al., 1997) and C. elegans (Rocheleau et al., 1997) revealed conserved roles of TCF homologs in mediating Wnt-driven transcriptional programs. The β-catenin–TCF complex regulates expression of those direct targets of the Wnt canonical pathway with functional TCF binding sites. They are known to be involved in cell proliferation and differentiation, including proto-oncogenes like c-myc (He et al., 1998) or key regulators of the G1/S transition of cell cycle like cyclin D1 (Tetsu & McCormick, 1999) (Figure 9A, B).

These discoveries closed the loop of the canonical pathway, marking a turning point in Wnt biology by linking membrane events to gene regulation and, by piecing together data from these various systems, scientists mapped out a core cascade of events that serves as the foundational framework for studying Wnt function in both development and disease.

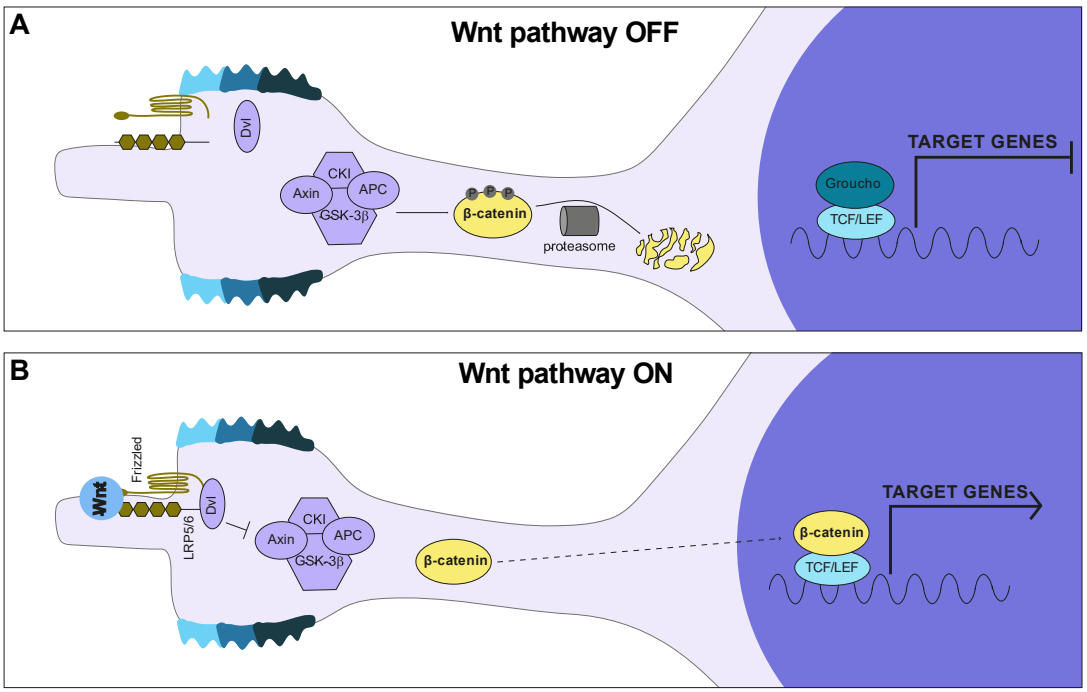

Figure 9. The canonical Wnt pathway. (A) Wnt pathway OFF: In the absence of Wnt signaling, the destruction complex composed of AXIN, APC, GSK-3β and CKI phosphorylates β-catenin, targeting it for ubiquitination and degradation by the proteasome. This prevents β-catenin from accumulating in the cytoplasm or entering the nucleus, and Wnt target genes remain transcriptionally repressed. **(B)** Wnt pathway ON: Upon binding of Wnt

ligands the Frizzled (Fz) receptor and LRP5/6 co-receptor, the destruction complex is disrupted, leading to the stabilization of β-catenin in the cytoplasm. Stabilized β-catenin then translocate to the nucleus, where it acts as a transcriptional co-activator of TCF/LEF transcription factors, enabling the transcription of Wnt signaling target genes and driving cellular processes such as proliferation and differentiation.

4.3.- The multiple roles of Wnts in NT development

Wnts are a large family of highly conserved, secreted signaling glycoproteins related to the *Drosopholila* Wg protein that mediate in intercellular communication and play crucial roles in numerous developmental processes including cell polarity, adhesion, motility, proliferation, apoptosis, developmental differentiation, patterning and morphogenesis (Dale, 1998; Wodarz & Nusse, 1998; Smalley & Dale, 1999; Widelitz, 2005; Mikels & Nusse, 2006).

During NT development, Wnt ligands exhibit highly dynamic and region-specific expression patterns. Wnt1, Wnt3, Wnt3a, Wnt4, and Wnt7b are predominantly expressed in dorsal regions of the NT, contributing to dorsal neural identity and patterning, often in cooperation with BMP (Megason & McMahon, 2002). In contrast, Wnt4, Wnt5a and Wnt7a have been found in more ventral regions, suggesting their potential involvement in integrating with other signaling pathways such as Shh and FGF to influence ventral patterning and neurogenesis (Agalliu et al., 2009).

4.3.1. Functional roles of Wnts in neural tissue growth

Genetic studies support the critical role for Wnts in regional specification and neural tissue growth in multiple areas of the developing CNS. Wnt1 KO mice lack a properly developed midbrain and cerebellum (McMahon & Bradley, 1990; Thomas & Cappechi, 1990) while Wnt3a mutant mice (Lee et al., 2000) exhibit a profound loss of the hippocampus. Moreover, Wnt1/Wn3a double mutant mice have an additional reduction in caudal diencephalon, rostral hindbrain, and spinal cord regions (Ikeya et al., 1997; Muroyama et al., 2002), indicating their semi redundant roles in CNS development.

In the chick NT, Wnt1 and Wnt3a, expressed in the dorsal midline, form a dorsal-to-ventral mitogenic gradient via β-catenin, promoting G1–S progression by upregulating cyclin D and facilitating NPC re-entry into the cell cycle (Megason & McMahon, 2002). Ectopic overexpression of Wnt1 or Wn3a, or activation of a constitutively active form of β-catenin in the chick and mouse embryos, results in enhanced NPC proliferation

and delayed neuronal differentiation (Dickinson et al., 1994; Megason & McMahon, 2002; Panhuysen et al., 2004). These manipulations lead to significant tissue overgrowth without major alterations in D-V patterning, although these effects appear dose- and timing-dependent as, higher or earlier overexpression of Wnts may cross a threshold that begins to influence fate specification, as demonstrated in other studies (Alvarez-Medina et al., 2008).

Loss-of-function studies in chick embryos indicates that Shh acts upstream of Wnt signaling to regulate cyclin D1 expression and G1 progression. Independently, the Shh pathway via Gli TFs also controls G2-M transition by modulating late cyclins and CDC25B phosphatase (Alvarez-Medina et al., 2009; Jayaraman et al., 2019), highlighting a coordinates control of cell cycle phases by multiple growth factors during CNS development to ensure correct size, shape and symmetry of the tissue.

4.3.2. Functional roles of β-catenin in progenitor proliferation

Further insight into the mechanism underlying Wnt-dependent neuroepithelial cell proliferation comes from the genetic manipulations of β-catenin, the central mediator of canonical Wnt signaling. Loss- and gain-of-function mutations introduced into the mouse β-catenin locus (Machon et al., 2003; Zechner et al., 2003) showed that the tissue mass in the spinal cord and several brain areas, including cerebral cortex and hippocampus, is reduced after ablation of β-catenin, accompanied by a failure to maintain the neural precursor pool. In contrast, chick spinal cords and mouse brains expressing activated β-catenin exhibited enlarged tissue mass and a corresponding increase in population of neural precursors (Megason and McMahon, 2002; Zechner et al., 2003).

These findings suggest that canonical Wnt/β-catenin signaling is essential for maintaining the proliferative capacity of neural progenitors, regulating both the size of the progenitor pool and influencing the decision of NPCs to proliferate or differentiate. Interestingly, enhancement of β-catenin signaling in embryonic stem cell (ESC), particularly when combined with retinoic acid (RA) treatment, significantly increases the numbers of neuron generated (Otero et al., 2004), suggesting a context-dependent effect of β-catenin signalilng, particularly during early neuronal differentiation.

At the transcriptional level, canonical Wnt signaling promotes the expression of cyclin D1 in the developing spinal cord, consistent with a role in promoting cell cycle progression and delaying cell cycle exit of NPCs (Megason and McMahon, 2002;

Panhuysen et al., 2004). Thus, Wnt/β-catenin signaling regulates both the maintenance of the progenitor pool and the timing of neuronal differentiation.

4.3.3. Transcriptional effectors: TCF/LEF family

Beyond Wnt ligands, the spatial and temporal expression of core components of the canonical Wnt/β-catenin pathway further support its role in NT development and growth. The TCF/LEF family of TFs, which includes TCF1(Tcf7), TCF3 (Tcf7l1), TCF4 (Tcf7l2) and LEF1 are expressed in the developing NT, albeit with distinct regional and temporal patterns (Galceran et al., 1999; Galceran et al., 2000; Kim & Dorsky, 2011, Merrill et al., 2004; Yi et al., 2011; Alvarez-Medina et al., 2008). Notably, LEF1, TCF1 and TCF4 show strong expression in dorsal regions of the NT, overlapping with regions of active Wnt signaling and Wnt ligand expression (Galceran et al., 1999; Galceran et al., 2000; Alvarez-Medina et al., 2008). In contrast, TCF3, a known repressor of target genes, is more broadly expressed and may help keep Wnt signaling tightly regulated in less active regions (Merrill et al., 2004; Yi et al., 2011).

One of the best-characterized transcriptional targets and feedback regulators of canonical Wnt signaling is AXIN2, which is itself acts as a negative feedback regulator of the pathway. AXIN2 expression has been used as a sensitive readout of Wnt/β-catenin signaling activity and is enriched in the dorsal NT during key stages of neurogenesis (Jho et al., 2002; Lustig et al., 2002). The localized expression of AXIN2 correlates strongly with areas of LEF1 and Wnt1 expression, further supporting a model in which canonical Wnt signaling plays a role in dorsal NT proliferation.

The specific expression patterns of Wnt ligands and intracellular components ensure that canonical Wnt signaling is precisely regulated in the developing NT, allowing coordinated control of progenitor proliferation, patterning, and differentiation along the D-V axis.

5.- The chick embryo NT as a model system

The use of chick embryos as animal model dates back to classical Greece, when Aristotle first recognized the chick embryo as the ideal subject for embryological studies. Since then, it has been widely used as a classical embryological model for developmental biology due to its ready availability, similarity to early human embryos, and amenability to embryological and surgical manipulations.

In the 1950s, an exhaustive preparation of a series of normal stages of the chick embryo, following its development all along the incubation, served the practical purpose of identifying and designating embryonic developmental stages on the basis of external morphological characters (Hamburguer and Hamilton, 1951).

However, with the arrival of the molecular era, certain experimental limitations of the model became apparent, mostly due to the difficulty of performing targeted mutagenesis or generating stable transgenic lines. Fortunately, from the 1990s to the present day, a number of new methods for transient transgenesis have been developed (Itasaki, Bel-Vialar & Krumlauf, 1999; Ishii & Mikawa, 2005; Morin et al., 2017) and the sequencing of the chicken genome (Hillier et al., 2004) has greatly expanded its utility.

Thus, although stable germline transgenesis remains challenging, these advances in transient, spatiotemporally targeted gene manipulation combined with genomic data have re-established the chick embryo as a powerful model system, allowing researchers to integrate genetics approaches with classical embryological techniques and providing a unique tool to explore the role of developmentally important GRN.

In recent times other model organisms such as the mouse and zebrafish have been in greater demand because of more extensive genetic toolkits (Burt, 2005). However, the chick embryo genetic tool available for the chick embryo are catching up with these models while presenting some important advantages: it is easy to manipulate without in utero surgery, has a fast embryonic developmental timeline, requires minimal maintenance and it is cost-effective.

Despite not being a mammalian model, the chick embryo remains highly relevant for understanding human biology. As an evolutionary conserved system, it provides valuable insights into CNS development and neural cell diversity.

OBJECTIVES

The aim of this thesis is to elucidate the cellular and molecular mechanisms by which the Wnt pathway regulates the growth of the CNS, using the chick embryo as *in vivo* model.

The specific objectives of this thesis are:

- To characterize the subcellular distribution of key components of the Wnt pathway within NPCs, with particular focus on β-catenin, during NT development.
- To dissect how modulation of Wnt/β-catenin signaling affects the balance between proliferative and neurogenic divisions of NPCs.
- To investigate the potential instructive role of the centrosome as a regulatory site in β-catenin-mediated NPC fate decisions.
- To identify intracellular modulators that influence β-catenin subcellular localization and function during neurodevelopment.

MATERIALS AND METHODS

MATERIALS

1.- Chick embryos

Fertilized eggs from the White-Leghorn strain of chickens were incubated horizontally at 38.5°C in an atmosphere of 70% humidity. Embryonic development was staged according to the morphological criteria established by Hamburger and Hamilton (1951).

2.- DNA constructs

The endogenous transcriptional activity of Wnt canonical pathway was measured using TOPFLASH reporter construct (Korinek et al., 1998). This TCF-responsive plasmid contains two sets (with the second set in the reverse orientation) of three tandem TCF-binding sites repeats (wild-type sequence) positioned upstream of a minimal thymidine kinase (TK) promoter, driving the expression of the luciferase open reading frame.

Sox2 expression was monitored using two different reporter constructs: a pSox2-GFP and a pSox2-Luc. Both reporters contain chicken genomic fragments spanning the 7.6–14 kb regulatory region of the Sox2 locus, which encompasses key enhancers for neural progenitor expression (Uchikawa et al., 2003). These regulatory elements were initially cloned into the pTK:EGFP vector. Subsequently, the Sox2 promoter region was removed and inserted into the pGL4.12(luc2CP) vector to generate a luciferase-based version of the reporter (Saade et al., 2013, 2017).

Tis21 expression was analyzed with the pTis21-RFP reporter construct, that corresponds to the Tis21 promoter region (from −442 to +65 nucleotides to the transcription start site) (Iacopetti et al., 1999) amplified by PCR from the mouse genome and then cloned into the pTK:RFP vector (Uchikawa et al., 2003).

NeuroD expression was studied with the NeuroD-Luc reporter construct, which contains a fragment of the NeuroD1 promoter known to include binding sites for proneural transcription factors such as Neurogenin (Ngn) and Mash1(Ascl1) (Gao et al., 2009). This promoter fragment was cloned into a pGL3 backbone

The pCAGGS-IRES-GFP (PCIG) and its derivate pCIEGO (pCIG lacking the IRES-GFP region) were used as control for electroporation (Megason and McMahon, 2002).

The following DNAs were inserted into pCIG or pCIEGO for genetic manipulation:

- β-cateninWT-FLAG: a wild-type form of human β-catenin (Addgene, 16518), subcloned in-house into the pCIEGO-FlAG vector. Cloning was performed by EcoR321 (V) digestion (ThermoFisher #FD0303) followed by recombination with the β-catenin sequence using the In-Fusion HD (Takara, 638909).
  Primers used:
  F: ATCGATAAGCTTGATATGGCTACTCAAGCTGATTTGATGG.
  R: GTAATCGAATTCGATTTACAGGTCAGTATCAAACCAGGCC.

- β-cateninS33Y-FLAG: a stabilized mutant form of human β-catenin in which serine 33, one of the residues critical of its degradation, is mutated to tyrosine, impairing recognition by the destruction complex hence working as a degradation-resistant mutant form (Kolligs et al., 1999).

- β-cateninS33YΔα-catBS-FLAG: a truncated form of human β-catenin lacking the α-catenin-binding domain, which disrupts its ability to link to α-catenin (Herrera et al., 2014). This construct was subcloned in-house into the pCIEGO-FLAG vector via EcoR321 (V) digestion (ThermoFisher #FD0303) and In-Fusion® HD (Takara, 638909) recombination (primers as above).

- β-cateninS33YΔCT-FLAG: a truncated version of the human β-catenin lacking the C-terminal domain where β-catenin binds to the transcription factors of the TCF/LEF family, resulting in loss of transcriptional co-activator activity (Valenta et al., 2011). This sequence was subcloned in-house into the pCIEGO-FLAG vector using EcoR321 (V) digestion and In-Fusion® HD (Takara, 638909) recombination.
  Primers used:
  F: ATCGATAAGCTTGATATGGCTACTCAAGCTGATTTGATGG.
  R: CTGCAGGAATTCGATTTACCGTTTCTTGTAATCTTGTGGC.

- β-cateninΔNT (CA- β-catenin): a mutant form of β-catenin lacking amino acids 29-48 and therefore lacking phosphorylation sites necessary for degradation, thus acting as a constitutively active mutant form (Tetsu & McCormick, 1999).

- Nek2-GFP: a wild-type version of the human Nek2 kinase fused to GFP (Fry et al., 1995; Fry et al., 1998).

- Nek2K37R-GFP: a catalytically inactive mutant of Nek2 fused to GFP, in which the critical lysine at position 37 in the Nek2 catalytic domain is replaced by arginine (Fry et al., 1995; Fry et al., 1998).

DNA amplification was performed using indicated primers and Phusion High-Fidelity DNA Polymerase (Fisher, 10024537). Restriction enzyme digestions were carried out according to the manufacturers' protocol. All constructs were validated by restriction enzyme digestions and/or Sanger sequencing.

For plasmid DNA amplification, chemically competent *E.coli* DH5α cells were transformed, and single colonies were inoculated into into LB medium. Cultures were grown overnight, and DNA was extracted using either a standard miniprep kit (NZYMiniprep) for analytical purposes, or the NucleoBond Xtra Midi Plus EF kit (Machery-Nagel, 740422), when large-scale plasmid preparations were required for electroporation into the chick embryos. Depending on the desired DNA yield, 4 mL (miniprep) or 100 mL (midiprep) cultures were used.

3.- Antibodies and counterstains

The following antibodies and counterstains were used for immunohistochemical analyses.

Antibody	Source	#Catalogue	Host Sp	Conc
β-catenin	Sigma	C7207	Mouse monoclonal	1:500
FOP (FGFR1OP)	O.Rosnet	Gift	Rabbit monoclonal	1:1000
Phospho-β-catenin (S33/S37/Thr41)	Cell Signaling	9561	Rabbit polyclonal	1:250
Active β-catenin/ dephospho- β-catenin (S37/Thr41)	Milipore	05-665	Mouse monoclonal	1:500
N-cadherin	ZYMED	13-2100	Rat monoclonal	1:500

Flag	Merck	F3165-2MG	Mouse monoclonal	1:1000
Phospho-Histone 3	Sigma	H9908	Rat monoclonal	1:500
Sox2	Invitrogen	481400	Rabbit polyclonal	1:1000
HuC/D	Molecular probes	A-21271	Mouse monoclonal	1:1000
GFP	AvesLabs	GFP-1010	Chicken polyclonal	1:500
Centrin	Merck	04-1624	Mouse monoclonal	1:250

Table 2: Primary antibodies

Antibody	Source	#Catalogue	Host Sp	Conc
Alexa 488 anti-mouse	ThermoFisher Sci.	A-21202	Donkey IgG	1:1000
Alexa 488 anti-rabbit	ThermoFisher Sci.	A-21206	Donkey IgG	1:1000
Alexa 488 anti-chick	ThermoFisher Sci.	A-11039	Goat IgG	1:1000
Alexa 555 anti-rat	ThermoFisher Sci.	A-78945	Donkey IgG	1:1000
Alexa 555 anti-rabbit	ThermoFisher Sci.	A-31572	Donkey IgG	1:1000
Alexa 647 anti-mouse	ThermoFisher Sci.	A-21235	Goat IgG	1:1000
Alexa 633 anti-rat	ThermoFisher Sci.	A-21434	Goat IgG	1:1000
Alexa 633 anti-rabbit	ThermoFisher Sci.	A-21070	Goat IgG	1:1000
Alexa 647 anti-rabbit	ThermoFisher Sci.	A-21245	Goat IgG	1:1000

Table 3: Secondary Antibodies

Counter-stains were added during incubation with secondary antibody. DAPI (1:1000) was used to visualize nuclei (Sigma-Aldrich, #D9542).

Primary and secondary antibodies were used as explained in detail in the immunohistochemistry section.

4.- Public repositories

The BioGRID database (version 4.4.245, May 2025) was used for the protein interaction analysis as part of the β-catenin centrosome-partner screening. BioGRID is a comprehensive, manually curated repository of biological interactions that aggregates experimentally validated data from a wide range of high-throughput and low-throughput studies, encompassing both physical and genetic interactions across multiple species.

At the time of access, the database included approximately 2.8 million non-redundant protein and genetic interactions, with extensive coverage of data specific to *Homo sapiens* (Oughtred et al., 2021).

METHODS

1.- Chick in ovo electroporation

In ovo electroporation and embryo recovery were performed at the indicated developmental stages. Embryos were electroporated with purified plasmid DNA (0,1-1μg/ml in H20; Sigma-Aldrich, W4502) supplemented with Fast Green FCF (50ng/ml; Sigma-Aldrich, F7258) to visualize the injection. Before manipulation, 7ml of albumen were removed from the egg using a syringe and a window was opened at the top of the shell to visualize the embryo (Stern 1993; Selleck 1996).

The DNA solution was injected into the lumen of the NT using a glass capillary (GD-1, Narishige) made with Narishige PC-10 glass capillary puller, by blowing air through an aspirator tube (Sigma-Aldrich, A5177-5EA). 200μl of 1% Penicillin/Streptomycin (P/S) (Gibco, 15070063) were poured on top of the embryo to improve electrode conductivity. Subsequently, platinum commercial electrodes (CUY610P1.5-1, Nepagene) were flanking the NT of the embryo to perform the electroporation using an Intracel Dual Pulse (TSS-20 Ovodyne) electroporator, delivering five pulses of 23V at intervals of 50 ms.

After electroporation, the window in the sell was finally sealed with plastic tape, and embryos were returned to the incubator until they reached the desired developmental stage.

2.- En-face preparations

For better visualization of the apical surfaces ("apical feet") of NPCs, *en face* or open-book dissections were performed. Chick embryos were collected at the desired developmental stage from the egg and fixed either in 4% paraformaldehyde (PFA; Sigma-Aldrich, 16005) prepared in 1x PBS for 2h at 4ºC, or pre-chilled with methanol (HPLC grade 99.8%; VWR, 1.06018.2500) overnight at -20ºC.

Following fixation, the embryos were pinned dorsal side up onto dissection pad made of Sylgard Silicone Elastomer (World Precision Instruments #SYLG184). Using two

homemade tungsten wire tools, the NT was incised along the RP to subsequently be separated from the adjacent paraxial mesoderm and the ventral non-neural tissue to facilitate flat mounting of the tissue.

Opened NTs exposing the apical surfaces of the NPCs were then collected and processed for downstream applications.

3.- Immunohistochemistry

3.1. En face tissue preparation for immunohistochemistry:

Immunohistochemistry of *en face* samples was carried out as follows:

- Chick embryos were removed from the egg at desired stage and fixed in either 4% PFA in 1xPBS for 2 hours at 4°C, or pre-chilled with methanol (HPLC 99.8%; VWR, 1.06018.2500) overnight at -20ºC.
- Dissected NTs were permeabilized PBS containing 0.1% SDS for 1h at room temperature (RT).
- Dissected NTs were then incubated in blocking solution (PBS, 0.5% Trinton-X-100, 10% bovine serum albumin, BSA) for at least 30min at RT.
- Dissected NTs were incubated with primary antibodies diluted in antibody solution (1% BSA in PBT [PBS + 0.5% Triton X-100]) at least overnight at 4ºC with gently shaking.
- Following primary incubation, dissected NTs were washed 3 times for 10 min in PBT.
- Samples were then incubated with secondary antibodies diluted in antibody solution overnight at 4ºC with gently shaking.
- After secondary incubation, dissected NTs were washed again 3 times for 10 min in PBT-
- NTs were transferred onto a glass coverslip to be manipulated using tungsten wire tools to orient the apical surface toward the coverslip.
- Excess liquid was removed as much as possible and mounting media (Mowiol; Sigma-Aldrich, 81381) was added on top.
- Finally, with a µwell sticker (iSpacer 0.25mm SUNJin Lab #IS016) and a second glass coverslip were placed on top of the tissue to seal the sample.

3.2. Free-floating sections preparation for immunohistochemistry:

Immunostaining of transversal vibratome sections was carried out as follows:

- Chick embryos were removed from the egg at desired stage and fixed in 4% PFA in 1xPBS for 2 hours at 4°C, or pre-chilled with methanol (HPLC 99.8%; VWR, 1.06018.2500) overnight at -20ºC.
- Embryos were embedded in plastic moulds with a warm agarose/sucrose matrix (5% agarose + 10% sucrose in distilled water) and cooled down to solidify at RT.
- Solidified blocks were sectioned at 50µm thickness using a Leica Vibratome (VT1000S) to generate free-floating transversal sections.
- Sections were washed 3 times for 5min in PBT (PBS+0.1% Triton-X-100).
- Sections were incubated in blocking solution (10% BSA in PBT) for at least 30 min at RT.
- Sections were incubated with primary antibodies diluted in antibody solution (1% BSA in PBT) overnight at 4ºC with gentle shaking.
- Following primary incubation, sections were washed 3 times for 10min in PBT.
- Sections were then incubated in secondary antibodies diluted in antibody solution for at least 2h at RT.
- Following secondary incubation, sections were washed 3 times for 10min in PBT.
- Sections were transferred to water for glass-slide mounting, and covered with Mowiol (Sigma- Aldrich, 81381) and a glass coverslip.

Primary antibodies used are listed in Table 2 and were visualized using Alexa® Fluor conjugated secondary antibodies (Table 3). All samples were stored at 4 °C in the dark until imaging, and care was taken throughout the protocol to minimize photobleaching and preserve tissue morphology.

4.- Luciferase-reporter Assay

Chick embryos were electroporated with indicated DNA constructsor the PCIG/pCIEGO vectors as control, together with the specified Firefly-Luciferase reporter constructs and a Renilla-Luciferase reporter construct driven by the CMV immediate-early enhancer promoter (Promega) for normalization purposes.

Embryos were harvested at the indicated hours post electroporation (hpe) following *in ovo* incubation. Spinal cords from the NTs were isolated and homogenized using a

douncer in 50 µL of Passive Lysis Buffer (Promega) for 30 minutes. The lysates were subsequently transferred to ice to halt enzymatic activity.

Firefly and Renilla luciferase activities were quantified sequentially from the same sample using the Dual Luciferase® Reporter (DLR™) Assay System (Promega) on a Sirius Luminometer (Berthold) operated with FB12 Sirius Software. Firefly luciferase values were normalized to Renilla luciferase activity to account for variability in electroporation efficiency and to enable accurate comparison across experimental conditions.

5.- Image acquisition

5.1. Fluorescence microscopy

Samples were imaged on an inverted Leica DMI8 microscope equipped with Spectra-X Light Engine featuring 6 solid-state LEDs. The objective used was a LEICA 25X (IMM, NA 0.80, 0.25mm working distance).

Instant computational clearing algorithm were applied in image post-processing to remove out-of-focus light in real-time, enhancing optical sectioning and image clarity.

5.2. Confocal microscopy

Samples were imaged on an inverted Zeiss LSM-780 confocal microscope equipped with a multiline Argon laser (458/488/514nm), a DPSS laser (561 nm) and a HeNe laser (633 nm). The objectives used were a ZEISS 25X (IMM, NA 0.80, 0.57mm working distance) and a ZEISS 63X (oil, NA 1.4, 0.18mm working distance).

5.3. Spinning-disk microscopy

Samples were imaged on an inverted Nikon Ti-E microscope integrated with an Andor Dragonfly 505 spinning-disk confocal system and equipped with 405, 488, 561 and 637 nm laser lines. The objectives used were a Nikon CFI Plan Apo IR 20X (IMM, NA 0.80, 0.51mm working distance), a Nikon CFI Plan Apochromat Lambda 60X (Oil, NA

1.40, 0.13mm working distance) and Nikon CFI SR HP Apo TIRF 100x (Oil, NA 1.49, 0.12mm working distance).

Fluorophore combinations were carefully selected to minimize spectral overlap and reduce channel crosstalk, ensuring accurate signal detection.

6.- Image analysis and quantification

6.1. General Image Analysis

Raw confocal microscopy data were exported to ImageJ/FiJi (http://rsbweb.nih.gov/ij/; RRID: SCR_003070) for subsequent image processing and analysis (Rueden et al., 2017; Schindelin et al., 2012). The raw Z-stack data were processed to generate appropriate projections, including single optical sections, maximum intensity projections, or sum intensity projections, depending on the experimental requirements.

Image processing steps such as background subtraction and contrast enhancement were performed to ensure optimal visualization and accurate analysis. Figures, diagrams, and schematic representations were generated using Adobe Illustrator CC2018 (RRID: SCR_014199) for final representation.

6.2. Quantification of endogenous β-catenin at the centrosome

Whole-mount *en face* preparations of fixed WT embryos were stained with antibodies against endogenous β-catenin and anti-FOP to mark centrosomes. Confocal images were acquired at two distinct developmental stages using identical microscope settings- including laser intensity, pinhole aperture and detector gain- to ensure comparability across all samples. For each embryo, random dorsal and ventral regions were selected for analysis.

Sum intensity projections were generated for each region using ImageJ, applying the same projections settings across all samples. The resulting fluorescence intensity data were quantified by calculating the percentage of centrosomes exhibiting β-catenin

localization. Data are presented as mean ± SEM, and visualized as bar graphs using GraphPad Prism 8.

6.3. Quantification of centrosome β-Catenin in electroporated embryos

β-catenin expression vectors carrying different mutations were electroporated and fixed embryos were stained with antibodies against the vectors' tag (FLAG), endogenous N-cadherin to mark the apical belt of NPCs, and anti-FOP to identify centrosomes. Confocal images were acquired using identical microscope settings to ensure consistency across all samples.

For each embryo, random regions were selected for analysis. Sum intensity projections were generated using ImageJ, with uniform projection parameters applied to all images. Electroporated cells were identified based on vector-derived cytoplasmic fluorescence or characteristic apical membrane morphology. Centrosome β-catenin was quantified by determining the percentage of centrosomes positive for β-catenin within electroporated cells. Data are presented as mean± SEM and visualized as bar graphs using GraphPad Prism 8.

6.4. Analysis of NPCs mode of cell division

HH14 embryos were electroporated with the progenitor reporter pSox2-GFP and the neurogenic reporter pTis21-RFP. Fixed tissue sections were stained with an anti-phospho-histone H3 (pH3) antibody to identify mitotic cells. Confocal images were acquired using identical microscope settings across all sample to ensure consistency.

pH3-positive cells were classified according to reporter expression: green, orange or red. The proportion of cells in each category was quantified to calculate the percentage of cells undergoing distinct modes of division. Data are represented as mean± SEM and visualized as stacked bar graphs using GraphPad Prism 8.

6.5. Measurement of ventricular surface length

Transversal sections of fixed HH23 embryos were stained with anti-Sox2 and anti-HuC/D antibodies to label NPCs and differentiated neurons, respectively. The length of ventricular surface was measured using the Segmented Line tool in ImageJ. For each

embryo, ventricular surface on the electroporated side of the NT was measured and normalized to the corresponding length on the non-electroporated (control) side. Data are presented as mean± SEM and visualized as bar graphs using GraphPad Prism 8.

6.6. Nek2 localization analysis

Fixed transversal sections of embryos electroporated with Nek2 vectors were stained with anti-FOP antibody to visualized centrosomes. To assess the spatial distribution of Nek2 relative to the centrosome, the Straight Line tool of ImageJ was used to draw a line across the centrosome region in each image. Fluorescence intensity profiles for both FOP and Nek2 signals were extracted along this line. The resulting intensity data were plotted as XY line graphs using GraphPad Prism 8.

6.7. Quantification of β-catenin intensity at the centrosome

En face preparations of fixed embryos were stained with anti-FOP antibody to label centrosomes, together with antibodies specific to either phosphorylated (S33/S37/Thr41) or dephosphorylated forms of endogenous β-catenin. In embryos electroporated with β-catenin vectors, the protein was detected using an anti-FLAG antibody, which recognizes the epitope tag from the vector rather than endogenous β-catenin.

For each embryo, random regions were selected for analysis. Within these regions, individual centrosomes were manually outlined using the Oval Selection tool in ImageJ. Sum intensity projections were generated using identical projection settings across all samples, and the integrated fluorescence density within each selected centrosome was measured.

Quantification was performed in both control and electroporated embryos, including conditions with or without co-electroporation of Nek2 overexpression vectors. Confocal images were acquired using identical microscope settings- laser intensity and detector gain- to ensure consistency across samples. Data are presented as mean± SEM and visualized as bar graphs using GraphPad Prism 8.

7.- Statistical Analysis

Statistical analysis was performed using the GraphPad Prism 8 (RRID: SCR_002798).

For comparisons between two groups, either the Mann-Whitney test or the Kolmogórov-Smirnov test was used. For comparisons involving more than two groups, the Kruskal-Wallis or two-way ANOVA was applied, followed by Dunn's multiple comparisons test when appropriate.

The normality of data distributions was evaluated using the D'Agostino Pearson omnibus normality test.

Statistical significance was represented as follows: * $p<0.05$, ** $p<0.01$, *** $p<0.001$ and **** $p<0.0001$.

8.- In silico screening for β-catenin interactors at the centrosome

To explore the functional landscape of β-catenin (CTNNB1) protein-protein interactions, interactome data were obtained from the BioGRID database (version 4.4.245, May 2025; https://thebiogrid.org), a manually curated repository of experimentally validated protein and genetic interactions. The full set of CTNNB1 interactors was downloaded and used as the input gene list for functional enrichment analysis.

Gene Ontology (GO) term enrichment was performed using the PANTHER Classification System (http://pantherdb.org). Initially, the complete list of interactors was analyzed to identify significantly enriched Cellular Component GO terms. This analysis allowed for the clustering of the interactors based on their subcellular localization and protein complex association.

From the top-enriched cellular components, proteins annotated with the *centrosome* term were selected for further investigation, given the focus of this study on centrosome-related functions. The subset of centrosome interactors was then re-analyzed using PANTHER, this time identify enrichment in Biological Process GO terms. This second-level analysis aimed to classify centrosome β-catenin interactors based on their

putative roles in cellular pathways. This stepwise GO enrichment approach enabled the prioritization of centrosome-associated β-catenin interactors for downstream analyses.

Bubble plots were generated in Microsoft Excel, where dot size reflects statistically significant (-log10 adjusted p-value) and the x-axis indicates the enrichment factor (also referred to as rich factor). In addition, protein interaction networks were further visualized and explored using Cytoscape.

9.- Computational docking of β-catenin-Nek2 interaction

To investigate the potential interaction between β-catenin (CTNNB1) and NEK2 kinase, protein-protein docking simulations were performed using the HADDOCK2.4 web server (High Ambiguity Driven DOCKing) available through the WeNMR platform (https://wenmr.science.uu.nl/haddock2.4/).

Three-dimensional structures of CTNNB1 and NEK2 were obtained from the AlphaFold Protein Structure Database, which provides high-confidence structural predictions based on deep learning algorithms. The AlphaFold models were used as input structures for docking.

To guide the docking process, active residues were selected based on predicted surface accessibility and presumed involvement in protein-protein interaction interfaces. These residues were manually defined in the HADDOCK interface, which required specification of both "active" (interacting) and "passive" (neighbouring surface) residues for each protein. No additional experimental restraints were applied.

The HADDOCK docking protocol consisted of three stages: (1) an initial rigid-body energy minimization, (2) a semi-flexible refinement in torsion angle space, and (3) a final refinement in explicit solvent. The resulting models were clustered based on root-mean-square deviation (RMSD) and scored using the HADDOCK score, a weighted sum of the van der Waals, electrostatic, desolvation, and restraint energies.

From the generated output, the top-ranking cluster- defined by the lowest HADDOCK score and z-score- was selected for further analysis.

Visualization and structural evaluation of the docking poses were performed using PyMOL (Schrödinger, LLC), focusing on the interaction interface and residue contacts.

RESULTS

1.- Centrosome localization of β-catenin in NPCs correlates with early stages of NT development

During the early development of the chick embryo NT (HH12 chick embryos, 17-19 hours post fertilization, hpf), NPCs primarily undergo proliferative symmetric divisions. These divisions result in both daughter cells remaining as NPCs, thereby promoting tissue growth. Later in development (HH21 chick embryos, 50-52hpf) there is a shift towards primary neurogenesis so that upon cell division, at least one daughter cell will undergo neuronal differentiation instead of remaining as two NPCs (Saade et al., 2013; Le Dréau et al., 2014). The mechanisms that control these specialized cell divisions of the NPCs have been correlated with the maturation of the centrosome, marked by the acquisition of appendages and enhanced microtubule-organizing capacity (Wang et al., 2009; Paridaen, Wilsch-Brauninger & Huttner, 2013; Saade et al., 2017; Tozer et al., 2017).

To begin to study a possible role for β-catenin in the regulation of NT growth, we first aimed to explore the subcellular distribution of β-catenin within NPCs, including the possible localization at the centrosome.

To address this question, we generated *en face* chick embryo NT preparations (See Materials and Methods) (Figure 10A) at these two developmental stages (HH12 and HH21) to examine the distribution of endogenous β-catenin. As expected, we observed an abundant pool of β-catenin localizing with at the apical belt of the NPCs at both early HH12 and late HH21 developmental stages (Figure 10B, C). This observation aligns with the well-known roles of β-catenin in epithelial cell polarity and the structural organization of the apical complex (Baum et al., 2011; Oda et al., 2011).

We used anti-FOP (FGFR1 Oncogene Partner) immunostaining as a centriole marker (Andersen et al., 2003), which appears as a single dot during the G1 phase and as two dots during the S/G2 phases, given that FOP immunostaining cannot resolve individual centrioles by confocal microscopy. This analysis demonstrate that β-catenin also co-localizes with centrosomes during both the G1 and G2 phases of the cell cycle (Figure 1B, B', C, C'), consistent with previous reports of its localization at the base of the cilia in hTERT-RPE cells (Kyun et al., 2020). Additionally, we observed that this centrosome localization of β-catenin is preserved during mitosis (Figure 10B", C"). Since mitosis is the critical moment when cells determine their mode of division, the

presence of β-catenin at the centrosome during this phase might suggest a potential role in the control of the division mode.

To assess the possible dynamics of the centrosome pool of β-catenin, we quantified its levels during the G1phase at the two developmental time points. Additionally, we assessed whether the distribution of centrosome β-catenin varied between dorsal and ventral cells of the NT, considering that the secretion of the Wnt ligands, and therefore the activation of the pathway, differs along the dorsal to ventral axis of the developing NT.

At early developmental stages (HH12), up to 45% of the centrosomes analyzed exhibited β-catenin association, predominantly at one of the two centrioles, in both dorsal and ventral regions of the NT (39.16±2.73% of centrosomes in dorsal NT cells and 28.39±3.99% in ventral NT cells displayed β-catenin at a single centriole while only 3.87±1.11% of centrosomes in dorsal NT cells and 2.82±0.76% in ventral NT cells showed β-catenin associated with both centrioles). Notably, the proportion of cells with centrosome β-catenin was higher in the dorsal NT (around 45%) compared to the ventral NT (around 30%) (Figure 10D). This result suggests that the centrosome pool of β-catenin might depend on the activation of the Wnt-pathway by Wnt ligands.

In contrast, at later developmental stages (HH21), the centrosome pool of β-catenin in G1 phase was still primarily associated with one centriole (8.21±1.89% of centrosomes in dorsal NT cells and 10.02±6.39% in ventral NT cells displayed β-catenin at a single centriole while only 1.33±1.33% of centrosomes in dorsal NT cells and 0% in ventral NT cells showed β-catenin associated with both centrioles). However, its overall prevalence decreased significantly in both dorsal and ventral NT regions when compared with earlier stages (from 40% to around 9% in dorsal NT cells and from 30% to 8% in ventral NT cells) (Figure 10E).

Taken together these results show a temporal (at early developmental stages) and spatial (at the dorsal NT) association of β-catenin to the centrosome, that prompted us to investigate its dependence on the Wnt pathway activation.

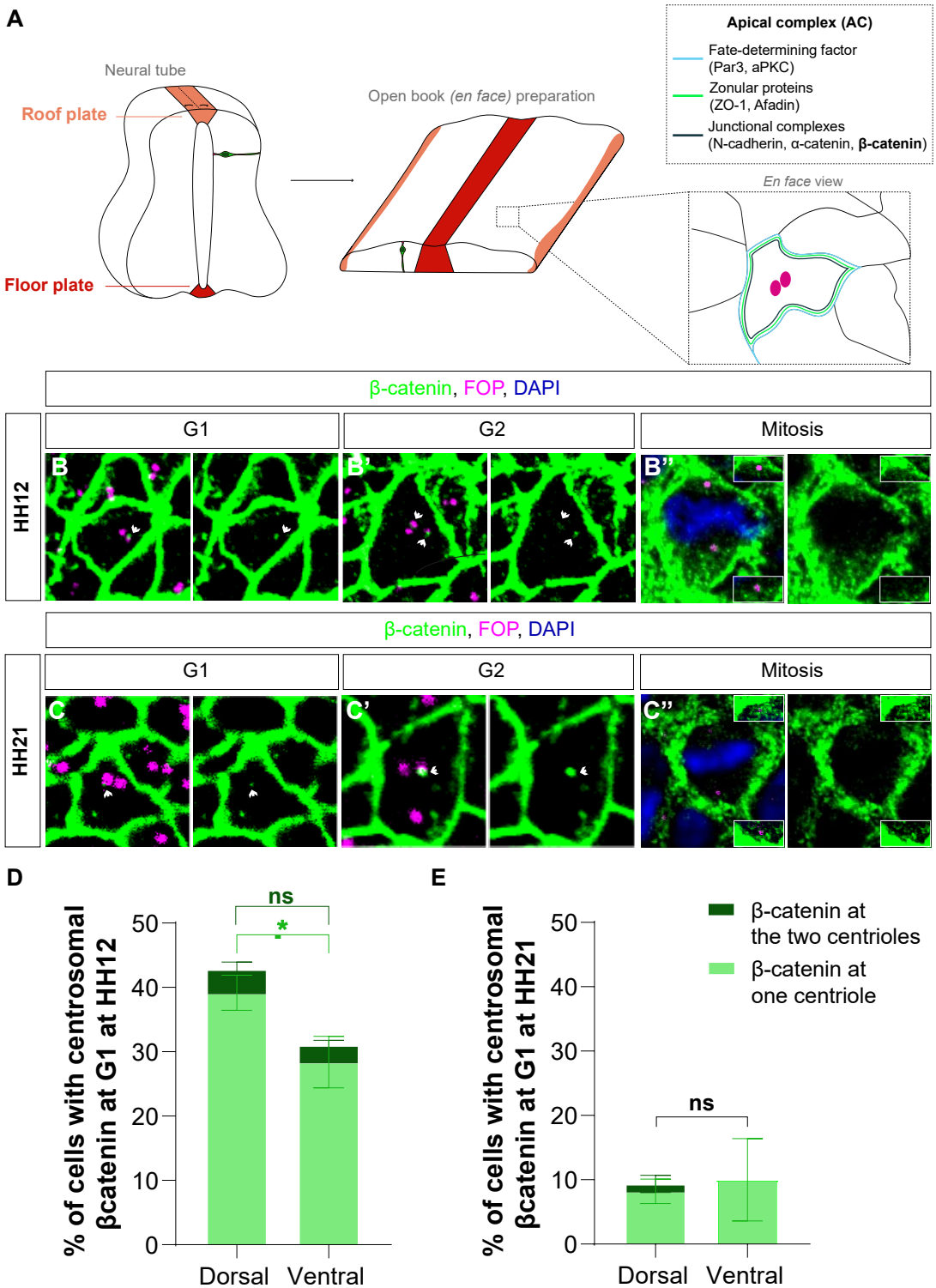
A
Neural tube
Roof plate
Floor plate
Open book (en face) preparation
Apical complex (AC)
Fate-determining factor (Par3, aPKC)
Zonular proteins (ZO-1, Afadin)
Junctional complexes (N-cadherin, α-catenin, β-catenin)
En face view
β-catenin, FOP, DAPI
G1
G2
Mitosis
HH12
B
B'
B''
β-catenin, FOP, DAPI
G1
G2
Mitosis
HH21
C
C'
C''
D
% of cells with centrosomal βcatenin at G1 at HH12
ns
*
50
40
30
20
10
0
Dorsal
Ventral
E
% of cells with centrosomal βcatenin at G1 at HH21
β-catenin at the two centrioles
β-catenin at one centriole
ns
50
40
30
20
10
0
Dorsal
Ventral

Figure 10. Centrosome β-catenin correlates with earlier stages of the NT development. **(A)** Schematic representation of chick embryo NT *en face* dissection. These preparations allow the apical view of the feet of NPCs where the centrosome and the apical complex localizes. Representative images of chick embryo NT at early stages of development (HH12) **(B-B")** and later stages of development (HH21) **(C-C")** show the subcellular distribution of β-catenin during the indicated cell cycles phases: G1, G2 and mitosis. The pancentrosomal marker FOP (magenta) highlights the centrosome, while β-catenin (green) marks both apical and centrosome regions. **(D,E)** Quantification of centrosome β-catenin at G1 phase at both early (HH12) and late (HH21) stages of development, comparing dorsal versus ventral cells in the NT since Wnt ligands are secreted at the dorsal region. The analysis accounts for whether centrosome β-catenin is more associated with one or both centrioles. Two-way ANOVA test and multiple comparison test was performed. n=350 cells per condition. Errors bar show the means±SEM. *, $P<0.05$; ns = not significate.

2.- Centrosome localization of β-catenin in NPCs correlates with Wnt pathway-dependent post-translational stabilizing modifications

Activation of the Wnt canonical pathway occurs when Wnt ligands bind to transmembrane receptors, leading to the inhibition of the kinase activity of the destruction complex. This results in the stabilization of β-catenin in the cytoplasm and its subsequent translocation to the nucleus, where it functions as a transcriptional cofactor. In contrast, in the absence of Wnt ligands, β-catenin is first phosphorylated by Casein Kinase 1 (CK1) at serine 45, which primes it for further phosphorylation by GSK3β at threonine 41, serine 37, and serine 33. These sequential phosphorylations target β-catenin for ubiquitin-mediated proteasomal degradation (Figure 11A, B).

To investigate whether Wnt pathway-dependent post-translational modifications influence the subcellular distribution of β-catenin, we analyzed the endogenous localization of distinct β-catenin pools. To this end, we performed immunostaining on transversal sections and *en face* preparations of the chick embryo NTs using two different antibodies: one specific for S33/S37/Thr41-phosphorylated-β-catenin, which is associated with pathway inactivation, and one that recognizes the stable, S33/S37/Thr41-dephosphorylated form of β-catenin, corresponding to the active state of the pathway (See Materials and Methods).

Transversal sections of wild-type (WT) chick embryo NT revealed distinct spatial distributions of these two β-catenin pools. The (S33/S37/Thr41) phosphorylated form

exhibited a ubiquitous distribution throughout NPCs (Figure 11C), whereas the dephosphorylated form was predominantly enriched at the apical region of the NT (Figure 11D). These observations are consistent with the hypothesis that the Wnt canonical pathway may play a key role in regulating the subcellular distribution of β-catenin within NPCs.

Furthermore, we used *en face* preparations of WT chick embryo NT to analyse the subcellular distribution of these two β-catenin pools at the apical region of NPCs, identified by the adherent protein N-cadherin (Chenn et al., 1998), and the pan-centrosomal marker FOP. Results showed that the (S33/S37/Thr41) phosphorylated pool of β-catenin showed a punctate distribution, lacking a consistent pattern within the apical region, despite the presence of ring-like structures at varying distances from the centrosome (Figure 11E).

In contrast, the (S33/S37/Thr41) dephosphorylated pool of β-catenin showed a clear association with the apical NPC belt co-localizing with N-Cadherin. In addition, this form of β-catenin appeared associated to FOP- labelled centrosomes (Figure 11F). This distribution is consistent with previous reports about the centrosome dynamics of β-catenin during interphase, in which β-catenin exchanges between centrosome and non-centrosome pools with kinetics similar to those of other centrosome components, while stabilized β-catenin exhibits reduced turnover at the centrosome (Bahmanyar et al., 2008). These findings support the idea that the centrosome-associated pool of β-catenin is the more stable one, which correlates with an activation of the Wnt canonical pathway.

Together, these findings suggest that β-catenin may perform a Wnt-depedent, non-canonical function at the centrosome-particularly during early developmental stages. Therefore, we next set to investigate whether this might be distinct from its well-characterized roles in either the adherens junctions and the Wnt signaling transcriptional activation, and whether it might be related to the control of symmetric proliferative division, and hence the growth of the neural tissue.

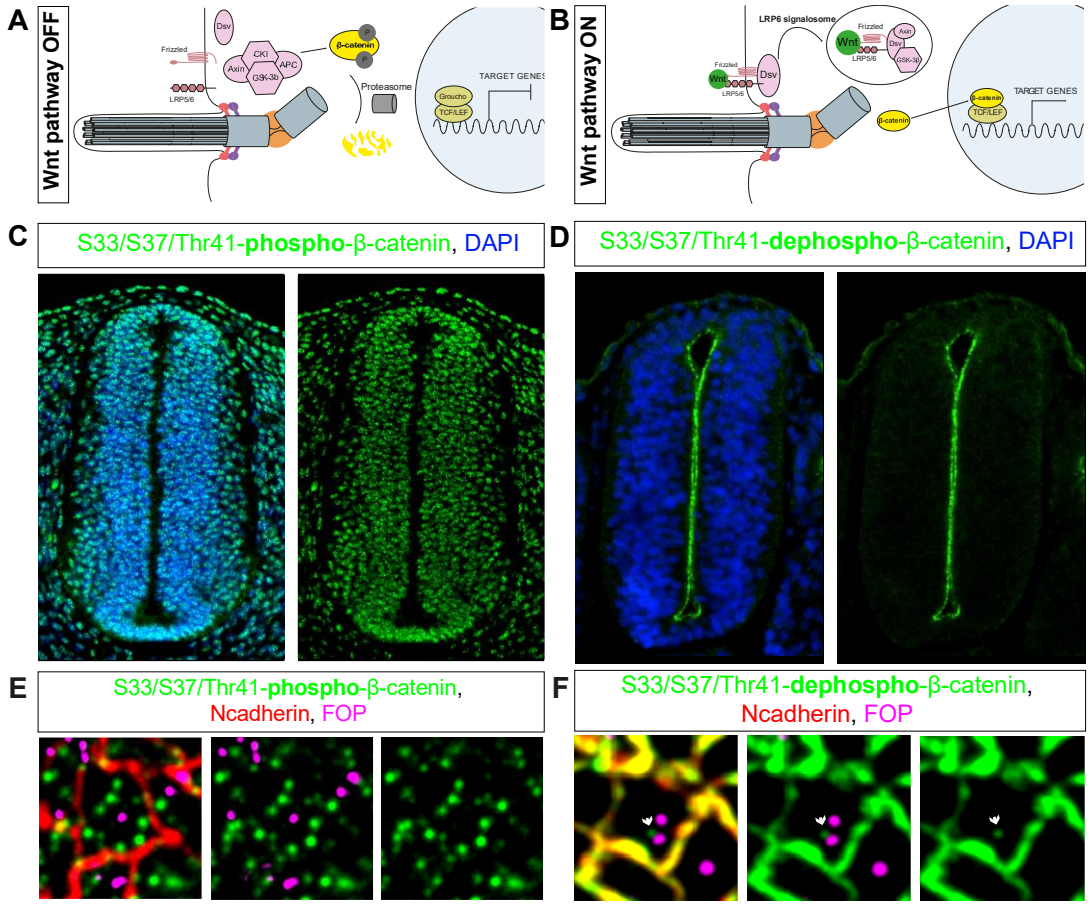

Figure 11. Centrosome β-catenin correlates with activation of Wnt pathway. (A, B) Schematic representation of Wnt canonical pathway in the absence of Wnt ligands (OFF) and in the presence of Wnt ligands (ON), respectively. In the absence of Wnt ligands, the kinase activity of GSK3β/CKI phosphorylates β-catenin. The presence of Wnt ligands quench the kinase activity, to stabilize β-catenin. Representative images of transverse sections of the developing spinal cord of a HH21 chick embryo show ubiquitous localization of S33/S37/Thr41-phosphorylated β-catenin (green) **(C)** while stable S33/S37/Thr41-dephosphorylated β-catenin (green) accumulates at the apical end of NPCs **(D).** Representative images of *en face* preparation of the chick embryo NT show the most apical region of NPCs where the pancentrosomal marker FOP (magenta) marks the centrosome and the adherent protein N-cadherin (red) marks the apical belt. **(E)** The S33/S37/Thr41-phosphorylated pool of β-catenin (green) exhibited a variable distribution pattern within this region. **(F)** The S33/S37/Thr41-dephosphorylated pool of β-catenin (green) shows co-localization with N-cadherin and FOP.

3.- Prevention of β-catenin phosphorylation at S33 is sufficient to increase its centrosome localization, independently of junctional or transcriptional activity

The temporal correlation between centrosome β-catenin accumulation and symmetric proliferative stages of the development raises the possibility that β-catenin's localization to the centrosome may contribute directly to centrosome maturation and, consequently, to the determination of the mode of cell division.

To begin to address the functional implications of this centrosome association, we analyzed the centrosome recruitment of different β-catenin variants in the developing chick NT: (i) a wild-type form of the protein (β-cateninWT), (ii) a stable form in which one of the residues responsible of its degradation is inactive (β-cateninS33Y) hence working as a stabilized version of the protein (Kolligs et al., 1999), (iii) a truncated form of β-catenin lacking the α-catenin-binding domain (β-cateninS33YΔα-catBS), which disrupts its ability to link to α-catenin (Herrera et al., 2014) and (iv) a truncated version of the protein lacking the C-terminal domain were β-catenin binds to the transcription factors of the TCF/LEF family (β-cateninS33YΔCT) thus deficient in its transcriptional co-activator activity (Valenta et al., 2011) (Figure 12A).

We electroporated all four β-catenin variants into the chick embryo NT at very low concentrations (50 ng) to minimize potential overexpression effect and to ensure that the resulting protein levels closely resembled endogenous β-catenin expression. *En face* preparations of the chick embryo developing NT revealed that β-cateninWT, β-cateninS33Y and β-cateninS33YΔCT co-localized with the adherent protein N-cadherin at the apical belt of NPCs. In contrast, β-cateninS33YΔα-catBS did not show junctional localization, validating the loss of its α-catenin-binding domain. Additionally, all β-catenin variants were found to localize with the pan-centrosomal marker FOP (Figure 12B-F), however, the proportion of electroporated cells exhibiting centrosome association of β-catenin-positive varied significantly.

Embryos electroporated with β-cateninWT exhibited centrosome localization in approximately 15% of analyzed NPCs (14.34±4.94% of analyzed cells), whereas embryos electroporated with stabilized forms of β-catenin (β-cateninS33Y, β-cateninS33YΔα-catBS and β-cateninS33YΔCT) resulted in a marked increase, with around 30% of analyzed cells displaying centrosome β-catenin-positive results (27.39±1.70% of analyzed cells in β-cateninS33Y condition, 30.42±2.60% of analyzed

cells in β-cateninS33YΔα-catBS condition and 23.74±1.30% of analyzed cells in β-cateninS33YΔCT condition) (Figure 12G).

These findings indicate that S33Y β-catenin point mutation, responsible for its stabilization, is sufficient to increase β-catenin accumulation at the centrosome, independently of its junctional or transcriptional functions.

Altogether, these results support the hypothesis that Wnt pathway activity may facilitate the accumulation of stabilized, non-phosphorylated β-catenin at the centrosome which may in turn promote centrosome maturation and prompted us to test whether this might influence the NPCs division mode and hence CNS growth.

4.- Gain-of-function (GOF) of β-catenin regulates progenitor-to-neuron ratio in the chick embryo NT through transcriptional and non-transcriptional mechanisms

In order to investigate the functional implications of the differential subcellular pools of β-catenin, we first assessed the transcriptional activity of these β-catenin variants taking advantage of the TOP-FLASH luciferase reporter system (Korinek et al., 1998). This system is composed of three multimerized consensus TCF/LEF binding motifs located upstream of the firefly luciferase gene. The induction of luciferase activity from this reporter construct is dependent on the presence of both β-catenin and TCF, making it a faithful reporter of Wnt canonical pathway activity (See Materials and Methods) (Figure 13A). Moreover, previous studies from the group have demonstrated that TCFs transcription factors are differentially expressed in the developing spinal cord, Tcf1, Tcf3 and Tcf4 distributed along the entire dorso-ventral axis of the NT, where they regulate dorsal-ventral patterning (Alvarez-Medina et al., 2008). Hence, the electroporated forms of β-catenin are sufficient to activate transcriptional responses, most likely through binding with endogenous TCFs.

We co-electroporated chick embryo NT at HH14 with the indicated forms of β-catenin together with the reporter of the transcriptional activity of the Wnt pathway TOP-FLASH. Twenty-four hpe, luciferase assays revealed a high transcriptional activity following the electroporation of β-catenin, β-cateninS33Y and β-cateninS33YΔα-catBS (control vector = 0.95±0.07 vs. β-cateninWT = 31.74±4.81, β- cateninS33Y = 66.52±11.91, β-cateninS33YΔα-catBS = 35.37±11.92), while the β- cateninS33YΔCT

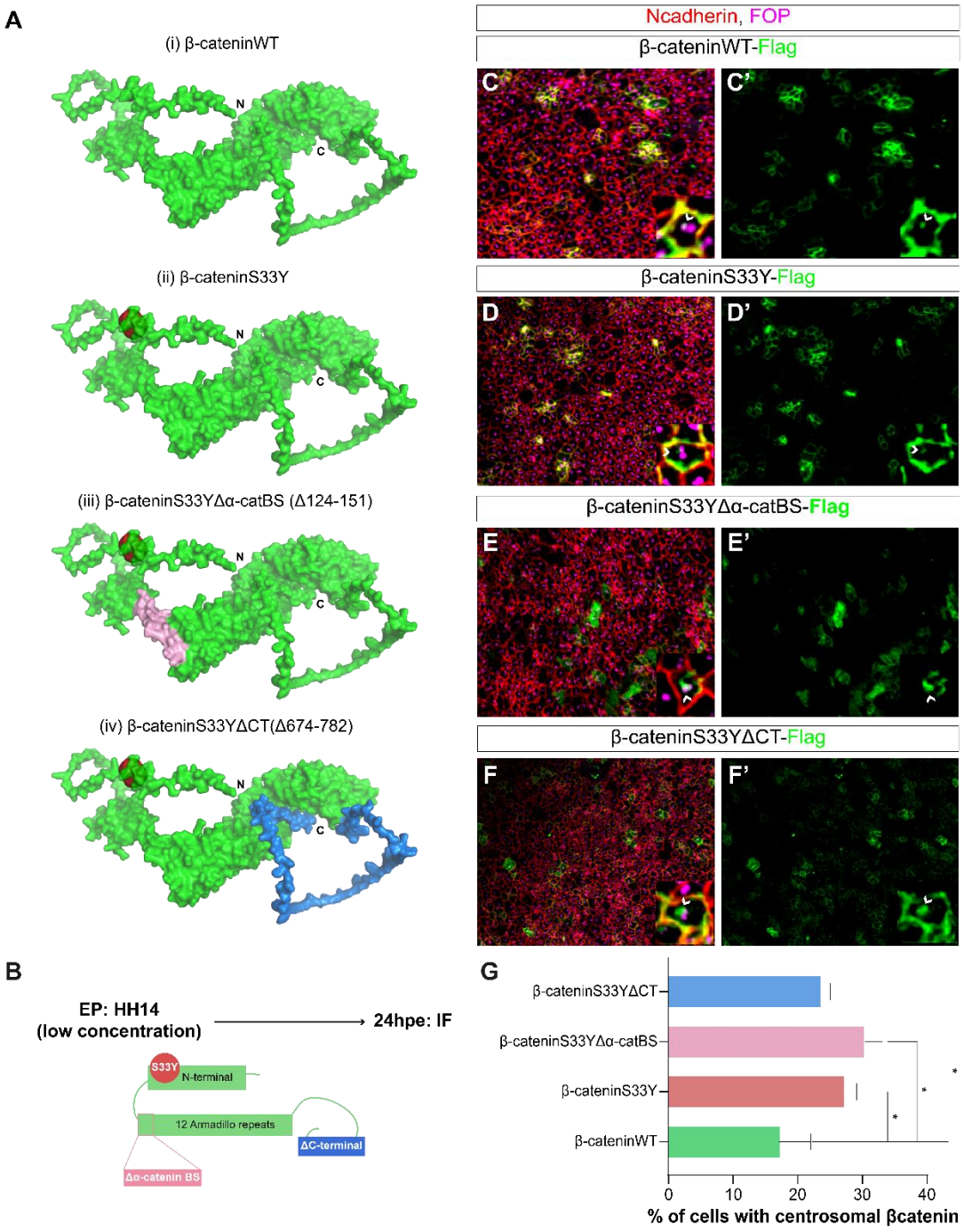

Figure 12. Prevention of β-catenin phosphorylation of at S33 is sufficient to increase its centrosome localization, independently of junctional or transcriptional activity. (A) Alpha Fold structures of different β-catenin variants: (i) β-cateninWT: full-length β-catenin, (ii)

β-catenin S33Y: stable β-catenin with a point mutation in which serine at position 33 has been replaced with tyrosine (indicated in red spheres), (iii) β-cateninS33YΔα-catBS: stabilized for of β-catenin with the serine to tyrosine point mutation at position 33 (depicted in red) and a deletion of the amino acids 124-151 (shown in pinck), disrupting its ability to link to α-catenin, (iv) β-cateninS33YΔCT: stable β-catenin with a serine to tyrosine point mutation at position 33 (highlighted in red) and a deletion of amino acids 674-782 (indicated in blue) which are crucial binding to TCF transcription factors. **(B)** Schematic representation of the electroporation (EP) of distinct β-catenin variants into the spinal cord of chick embryos at low concentrations to investigate their subcellular localization. **(C-F)** Representative images of *en face* preparations of the chick embryo NT show the apical part of NPCs labeled with N-cadherin (red) and FOP (magenta), highlighting centrosome distribution of all four electroporated β-catenin variants (β-cateninWT, β-cateninS33Y, β-cateninS33YΔα-catBS and β-cateninS33YΔCT). Loss of the α-catenin binding domain in the β-cateninS33YΔα-catBS variant impairs localization to the apical belt identified by N-cadherin (red). **(G)** Quantification of centrosome β-catenin at G1 phase. One-way ANOVA test and multiple comparison test werw performed. Three independent experiments, n=300 cells per condition. Error bars show the means±SEM. *, $P<0.05$.

truncated version was unable to activate the reporter (control vector = 0.95±0.07 vs. β-cateninS33YΔCT = 1.69±0.30) (Figure 13B), therefore validating that, in the chick embryo NT, this latter form of β-catenin is deficient as a transcriptional co-activator.

To explore the potential role of these β-catenin variants in the regulation of the maintenance of NPC stemness, we co-electroporated them with a reporter of the neural progenitor gene Sox2 (Uchikawa et al., 20043), in which a fragment of the enhancer region of the gene controls the expression of the luciferase enzyme (Saade et al., 2013) (See Materials and Methods) (Figure 13C) thus allowing us to determine the activation status of the Sox2 gene.

We electroporated HH14 chick embryo NT and collected them 24hpe. Quantification of luciferase activity for each β-catenin variant showed a significant increase in the luciferase activity promoted by all four variants of the protein (control vector = 1.00±0.06 vs. β-cateninWT = 3.47±0.93, β-cateninS33Y = 7.56±0.93, β-cateninS33YΔα-catBS = 5.23±0.37, β-cateninS33YΔCT = 2.73±0.36) (Figure 13D).

These findings indicate that β-catenin is sufficient to activate the expression of the Sox2 neural progenitor gene, either directly through transcriptional co-activation of TCFs or indirectly, through the regulation of additional genes responsible for maintaining the neural progenitor state. Interestingly, the electroporation of the β-cateninS33YΔCT mutant, which lacks transcriptional activity, was sufficient to increase luciferase activity,

although at lower levels. This observation prompted us to propose that additional, mechanisms independent of β-catenin's transcriptional activity might contribute to the regulation of Sox2 expression and/or stemness, that might be involving β-catenin non-canonical role linked to the centrosome.

Next, we investigated whether β-catenin might play a role in the loss of stemness. To this end, we utilized the NeuroD luciferase reporter, which contains a fragment of the NeuroD promoter known to activate the pan-neurogenic differentiation program. This reporter drives the expression of a luciferase enzyme, allowing us to assess the activation state of the NeuroD gene through luciferase activity (Gao et al., 2009) (see Materials and Methods) (Figure 13C).

We electroporated HH14 chick embryo NT and collected samples 24hpe. Analysis showed a significant reduction of NeuroD expression following the electroporation of the four β-catenin variants (control vector = 1.00±0.04 vs. β-cateninWT = 0.52±0.03, β-cateninS33Y = 0.80±0.03, β-cateninS33YΔα-catBS = 0.27±0.03, β-cateninS33YΔCT = 0.50±0.03) (Figure 13E).

Our results show that, similarly to Sox2 gene expression, β-catenin is sufficient to decrease the expression of the NeuroD neural differentiation gene through both transcriptional-dependent and transcriptional-independent mechanisms, as it is shown by β-cateninS33YΔCT mutant, which lacks transcriptional activity yet still suppresses NeuroD expression, suggesting that β-catenin may regulate neural differentiation and the loss of stemness through both direct and indirect mechanisms.

5.- β-catenin is sufficient to shift modes of division toward self-expanding proliferative divisions in the developing NT, though transcriptional and non-transcriptional mechanisms

Next, to further investigate the mechanisms by which β-catenin might regulate the stemness of NPCs at the cellular level, we took advantage of two fluorescent reporters, generated and validated in the laboratory, that unequivocally identify and distinguish the three modes of divisions of NPCs in the chick embryo NT depending on the outcome of the cell division. The pSox2-GFP reporter, where the pSox2 enhancer element (Uchikawa et al., 2003) allow us to track proliferative PP progenitors through GFP expression (Saade et al., 2013, Le Dreau et al., 2014), and the pTis21-RFP

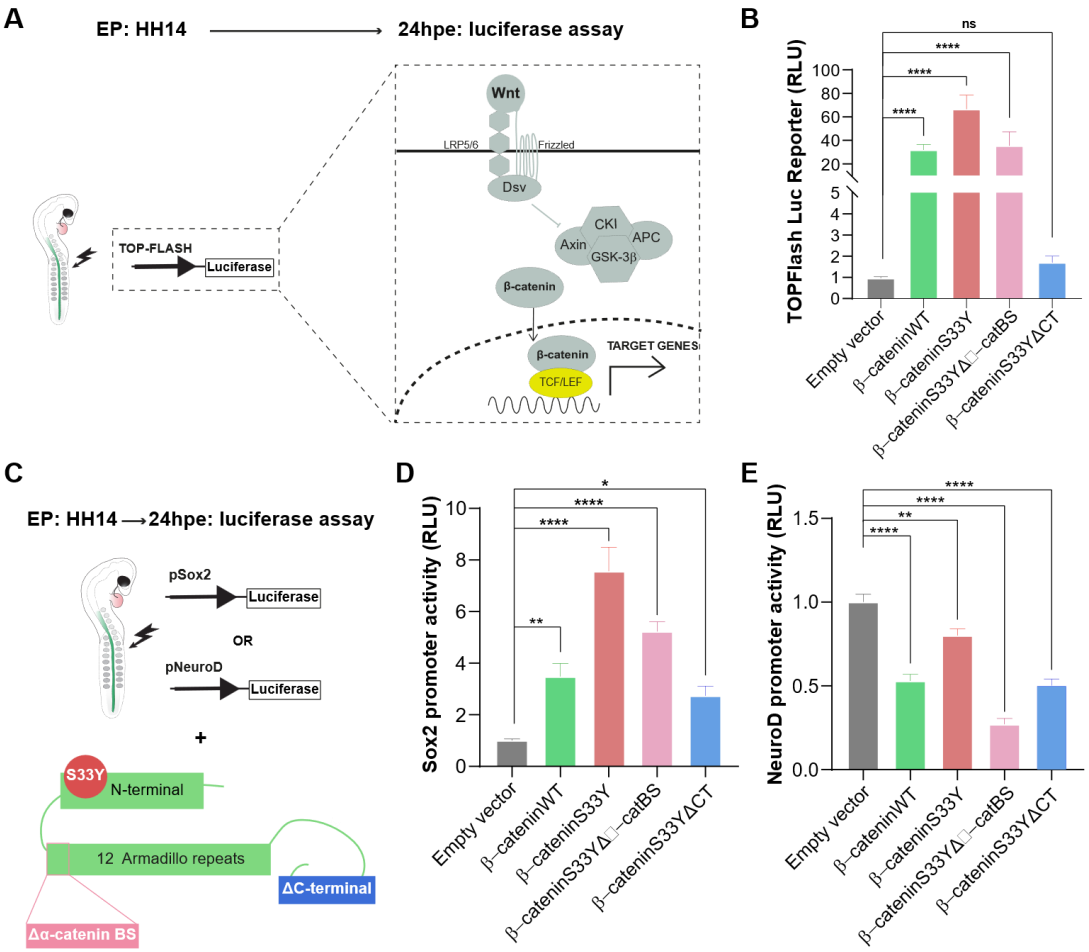

Figure 13. β-catenin GOF increases progenitor gene Sox2 expression and decreases neurogenic gene NeuroD expression through transcriptional and non-transcriptional mechanisms. **(A)** Scheme representing the TOP-FLASH luciferase reporter system electroporation in the chick embryo NT at HH14 for in vivo luciferase assay 24hpe. The dotted box represents TOPFLASH construct, in which three multimerized consensus TCF/LEF binding motifs control the expression of a luciferase enzyme. **(B)** Quantification of Luciferase/Renilla activity at 24hpe of control or β-catenin variants (β-cateninWT, β-cateninS33Y, β-cateninS33YΔα-catBS and β-cateninS33YΔCT). One-way ANOVA test and multiple comparison test were performed. Three independent experiments, n= 30 embryos per condition. Errors bars show the means±SEM. ****, P<0.0001; ns = not significate. **(C)** Scheme representing Sox2 and NeuroD reporters' electroporation in the chick embryo NT at HH14 for in vivo luciferase assay 24hpe together with the different β-catenin variants marked by a color code. **(D)** Quantification of Sox2-Luciferase/Renilla activity at 24hpe of either control or β-catenin variants (β-cateninWT, β-cateninS33Y, β-cateninS33YΔα-catBS and β-

cateninS33YΔCT). One-way ANOVA test and multiple comparison test were performed. Three independent experiments, n= 30 embryos per condition. Errors bar show ±SEM. *, P<0.05; **, P<0.01; ****, P<0.0001. **(E)** Quantification of NeuroD-Luciferase/Renilla activity at 24hpe of control or β-catenin variants (β-cateninWT, β-cateninS33Y, β-cateninS33YΔα-catBS and β-cateninS33YΔCT). One-way ANOVA test and multiple comparison test were performed. Three independent experiments, n= 30 embryos per condition. Errors bars show means±SEM. **, P<0.01; ****, P<0.0001.

reporter, in which the promoter region of the anti-proliferative gene Tis21 (Iacopetti et al., 1999), whose expression is restricted to neurogenic progenitors (Haubensak et al., 2004), allow us to specifically track neurogenic PN/NN progenitors through RFP expression (Saade et al., 2013, Le Dreau et al., 2014) (Figure 14A, B).

We co-electroporated HH14 chick embryo NT with these two reporters alongside the different β-catenin variants and labelled mitosis by immunostaining with the anti-pH3 antibody. 24hpe results show the coexistence of progenitors (i) only expressing pSox2-GFP (PP progenitors), (ii) co-expressing pSox2-GFP and pTis21-RFP (PN progenitors) and (iii) only expressing pTis21-RFP (NN progenitors) (Figure 14C). Quantification of mitotic figures, based on the expressed fluorochrome (green for PP divisions, orange for PN divisions or red for NN divisions), revealed that overexpression of all four β-catenin variants increased the number of pH3+ mitotic cells expressing only pSox2-GFP reporter (PP divisions). This was accompanied by a reduction in the number of pH3+ mitotic cells co-expressing pSox2-GFP and pTis21-RFP reporters (PN divisions) when compared to the control (control vector = PP: 25.67±1.48; PN: 63.17±1.74; NN: 11.28±1.34 vs. β-cateninWT = PP: 45.20±3.41; PN: 49.00±3.92; NN: 5.90±1.15, β-cateninS33Y = PP: 59.10±2.78; PN: 34.50±2.33; NN: 6.40±1.96, β-cateninS33YΔα-catBS = PP: 32.00±1.52; PN: 61.33±0.66; NN: 7.33±1.76, β-cateninS33YΔCT = PP: 38.25±3.45; PN: 52.50±2.66; NN: 4.00±1.76) (Figure 14D).

Altogether, these results indicate that β-catenin is sufficient to promote symmetric proliferative PP divisions while reducing neurogenic divisions. This effect appears to involve both transcriptional and non-transcriptional mechanisms, as evidenced by the β-cateninS33YΔCT variant, which lacks transcriptional activity yet still increases PP divisions at the expense of neurogenic outcomes, consistent with the findings presented in Figure 13.

Interestingly, the interaction between β-catenin and α-catenin also seems to be dispensable for the observed effect, as electroporation of β-cateninS33YΔα-catBS vector was similarly able to promote PP divisions in detriment of PN divisions. This finding, in agreement with the results in Figure 13, suggests that β-catenin's role in modulating the progenitor-to-neuron transition does not only depend on its association with α-catenin.

Overall, our functional experiments demonstrate that β-catenin enhances the proportion of symmetric PP divisions in NPCs, even when its canonical functions, such as its role as a transcriptional co-factor or as a component of the apical complex, are disrupted. These results correlate however with β-catenin's localization at the centrosome and support the hypothesis that this pool may contribute to the regulation of the mode of division. Nevertheless, given the β-catenin multifunctional nature, it remains possible that compensatory mechanisms are at play. Further experiments specifically targeting its centrosome pool will be critical to clarify the specific contribution of this localization to the control of the mode of the division.

6.- β-catenin-induced aberrant growth in the chick embryo NT disrupts tissue organization through transcriptional and non-transcriptional mechanisms

To investigate the long-term impact of the overexpressing all four β-catenin variants on the NT development, we analyzed chick embryo NT 48hpe for the expression of key protein markers. Specifically, we examined Sox2, a classical progenitor marker (Uchikawa et al., 1997; Graham et al., 2003), which is typically localized in the apical region of the NT within the ventricular zone and pan-neural marker HuC/D (Okano et al., 1997), which is predominantly found in the basal region of the NT. This basal region corresponds to the mantle zone, where NPCs have lost their stemness, detached from the apical surface and migrated laterally to differentiate into neurons.

Results indicated that in control electroporated embryos, HuC/D+ neurons were correctly localized laterally, while Sox2+ NPCs were positioned medially. In contrast, embryos electroporated with all four β-catenin variants exhibited disrupted tissue organization, with occasional formation of ectopic small NT-like structures (Figure 15A-E). Quantification of ventricular length of the two hemi tubes that form

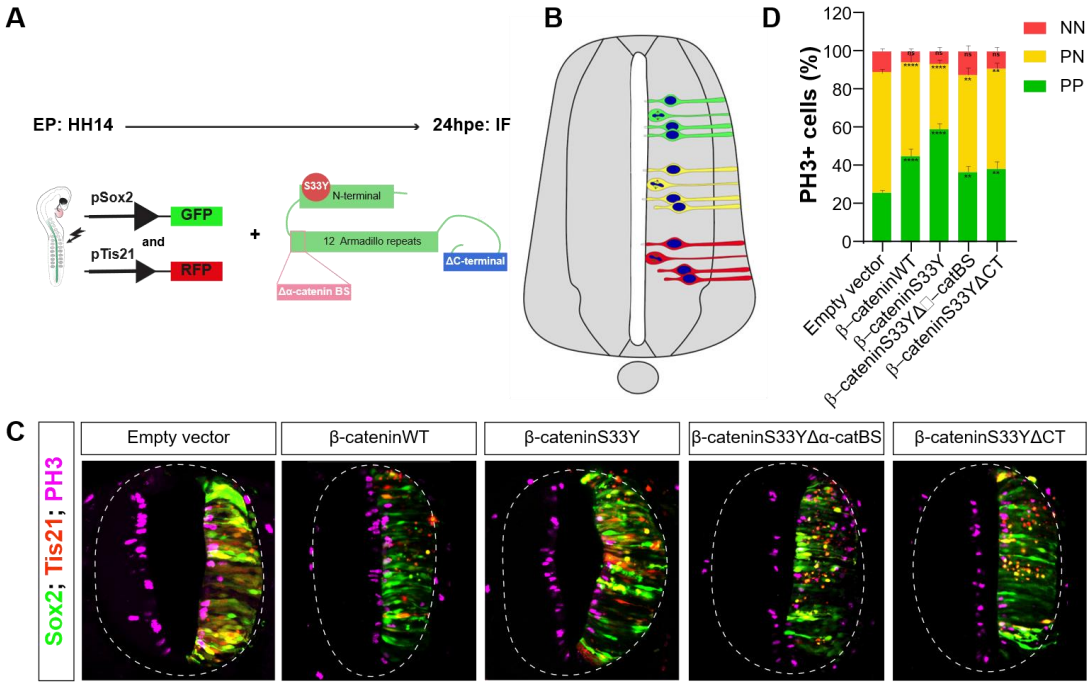

Figure 14. β-catenin GOF increases proliferative PP divisions at the expense of neurogenic PN divisions through transcriptional and non-transcriptional mechanisms. **(A, B)** Schematic representations of reporters pSox2-GFP and pTis21-RFP electroporated into the chick embryo NT to mark NPCs according to their mode of division (either green for proliferative PP divisions, orange for neurogenic PN divisions and red for neurogenic NN divisions) alongside the different β-catenin variants. **(C)** In vivo analysis of the modes of division. HH14 embryos were electroporated with either control plasmid or β-catenin variants (β-cateninWT, β-cateninS33Y, β-cateninS33YΔα-catBS and β-cateninS33YΔCT) together with the pSox2-GFP and the pTis21-RFP reporters. Transverse sections were stained at 24hpe for pH3 (magenta) to identify mitotic progenitors. **(D)** Quantification of pH3+ cells according to their modes of divisions (PP: green, PN: orange or NN: red). Two-way ANOVA test and multiple comparison test were performed. Three independent experiments, n= 21 embryos per condition. Error bars show means ± SEM. **, P<0.01; ****, P < 0.0001; ns = not significate.

the NT (electroporated/no-electroporated side) showed an up to 2-fold increase in the tissue growth after electroporation of all four β-catenin variants (control vector = 0.95±0.02 vs. β-cateninWT = 1.12±0.06, β-cateninS33Y = 1.73±0.20, β-cateninS33YΔα-catBS = 2.19±0.18, β-cateninS33YΔCT = 1.12±0.06) (Figure 15F, G).

These results indicate that β-catenin is sufficient to induce an aberrant growth of the tissue and are consistent with the published role of β-catenin contributing to the maturation of N-cadherin and the establishment of apical AJs through its structural function (Herrera et al., 2021). In addition, Wnt/β-catenin signaling transcriptionally regulates the expression of cell cycle genes such as Cyclin D1, which is essential for G1 progression in NPCs, thereby promoting NPCs proliferation and tissue expansion (Alvarez-Medina et al., 2008).

Interestingly, our data point to a novel mechanism as the same disrupted tissue organization was observed following electroporation of the β-cateninS33YΔCT variant or the β-cateninS33YΔα-catBS variant, which lacks transcriptional and apical activity respectively, but localize at the centrosome. This support our hypothesis that mechanisms beyond the transcriptional or apical functions of β-catenint may regulate apical organization and tissue growth.

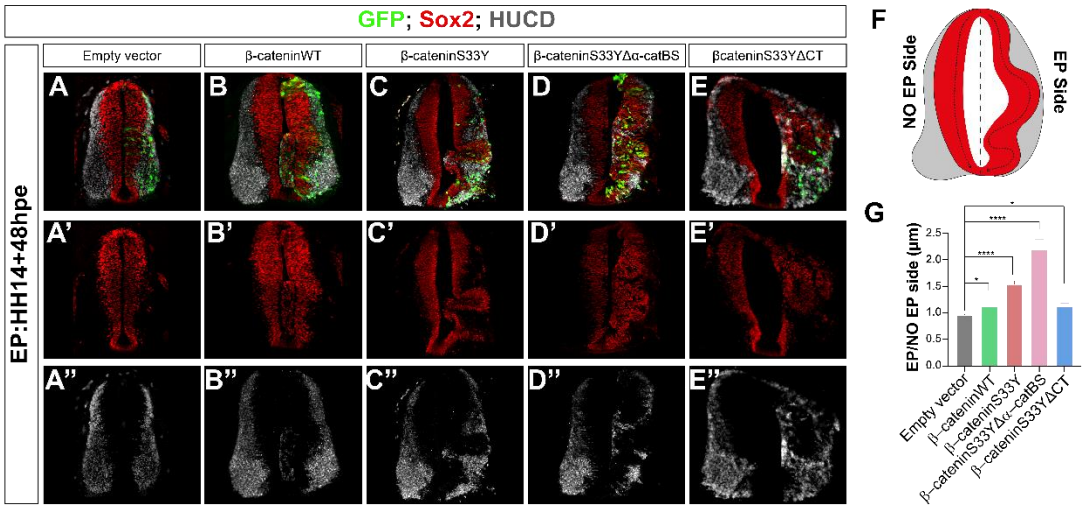

Figure 15. β-catenin GOF induces aberrant growth of the tissue trough transcriptional and non-transcriptional mechanisms. (A-E) Representative images of transverse sections of the developing spinal cord of the chick embryo stained 48hpe for Sox2 (red) and HUC/D (grey). HH14 embryos were electroporated with either control **(A-A")** plasmid or β-catenin variants: (β-cateninWT **(B-B"),** β-cateninS33Y **(C-C"),** β-cateninS33YΔα-catBS **(D-D")** and β-cateninS33YΔCT **(E-E")** together with a control of electroporation (H2B-GFP) (green). **(F)** Schematic representation of ventricular length quantification following Sox2+ cells line. **(G)** Quantification of Sox2+ cells line distribution along the DV axis of the NT. One-way ANOVA test and multiple comparison test were performed. Three independent experiments, n= 15 embryos per condition. Error bars show means ± SEM. *, P<0.05; ****, P < 0.0001.

7.- A search for β-catenin interactors at the centrosome identifies the kinase Nek2 as a potential centrosome regulator

Our results showed that β-catenin regulates NPC stemness maintenance and CNS growth through both transcriptional and non-transcriptional mechanisms. We hypothesize that the non-transcriptional role might be likely linked to the β-catenin localization and/or function at the centrosome; however, the molecular mechanisms underlying this association remain to be elucidated.

To explore potential regulators of β-catenin at the centrosome, we first conducted an *in silico* analysis of its interactors using the Biological General Repository for Interation Datasets (BioGRID) (Oughtred et al., 2021) (See Materials and Methods), a curated biological database of protein and genetic interactions across multiple species, including *Homo sapiens*. We used the most recent gene identifier list to annotate protein-protein interaction (PPI) networks.

We identified a total of 961 proteins with physical interaction evidence with β-catenin. To assess their subcellular distribution, we performed a clustering analysis based on Gene Ontology (GO) terms associated with their cellular component. This analysis revealed that β-catenin interactors are distributed across 345 distinct subcellular compartments. From these, we selected the 20 most significantly enriched compartments based on false discovery rate (FDR). Notably, this list included centrosome-related terms, confirming the presence of β-catenin interactors at the centrosome (Figure 16A).

To further characterize this centrosome subset, we conducted an additional GO enrichment analysis focused on biological process terms of the proteins within this cluster. This approach allowed us to identify a set of centrosome-associated β-catenin interactors functionally linked to cell cycle regulation and mitotic progression (Figure 16B). We identified several serine/threonine kinases known to play key roles in the regulation of cell cycle and mitotic progression, including CDK1, CDK2, CDK6 (reviewed by Malumbres and Barbacid, 2009), PLK1, AURKA, AURKB (Lera et al., 2012; Bruisma et al., 2014; Macůrek et al., 2008; reviewed in Goldenson & Crispino, 2015), NEK2 (Fry et al., 1995; Fry et al., 1998) (Figure 16C).

We selected Nek2 as a candidate for further investigation, since it is reported to physical interact with β-catenin at the centrosome, promoting β-catenin stabilization in HEK293 cells (Bahmanyar et al., 2008; Mbom et al., 2014). Moreover, Nek2 has an

established role in centrosome separation and spindle dynamics (Bahmanyar et al., 2008).

Hence, we set to test the hypothesis that Nek2 may function as a critical modulator of β-catenin recruitment at the centrosome. To begin to assess the subcellular localization of Nek2 in NPCs, we used a low concentration (200ng) of both Nek2 and its kinase-dead mutant form (Nek2K37R), an inactive mutant, in which the critical lysine at position 37 in the Nek2 catalytic domain is replaced by arginine (Fry et al., 1995; Fry et al., 1998). We electroporated the expression vectors into the NT of the chick embryo and prepared transversal sections of the developing spinal cord. Results revealed that Nek2 and Nek2K37R form localizes to the centrosome, as indicated by its co-localization with the pan-centrosomal marker FOP (Figure 16D, E). This centrosome localization was further confirmed in *en face* preparations of electroporated chick embryo NTs, were the apical belt of NPCs, recognized by adherent protein N-cadherin, is more clearly visualized. In line with the previous observations, both Nek2 and Nek2K37R accumulates in the apical part of the cell, co-localizing with FOP (Figure 16F).

These results show a clear association of Nek2 with the centrosome in the context of developing NT, which does not depend on its kinase activity.

8.- Nek2 increases the accumulation of stable β-catenin at the centrosome independently of its kinase activity

Given the reported physical interaction between Nek2 and β-catenin, we next set to analyze whether Nek might contribute to the β-catenin localization at the centrosome in NPCs.

To this end, we first generated *en-face* preparation of the chick embryo NT to examine the distribution of endogenous (S33/S37/Thr41) phosphorylated and (S33/S37/Thr41) dephosphorylated pools of β-catenin following Nek2 overexpression.

Control electroporations showed that while the (S33/S37/Thr41) phosphorylated pool of β-catenin did not show a consistent pattern of localization at the centrosome (Figure 17A), the (S33/S37/Thr41) dephosphorylated pool of β-catenin associated with pan-centrosomal market FOP (Figure 17B). Interestingly, Nek2 overexpression did not affect the distribution of the (S33/S37/Thr41) phosphorylated pool of β-catenin while

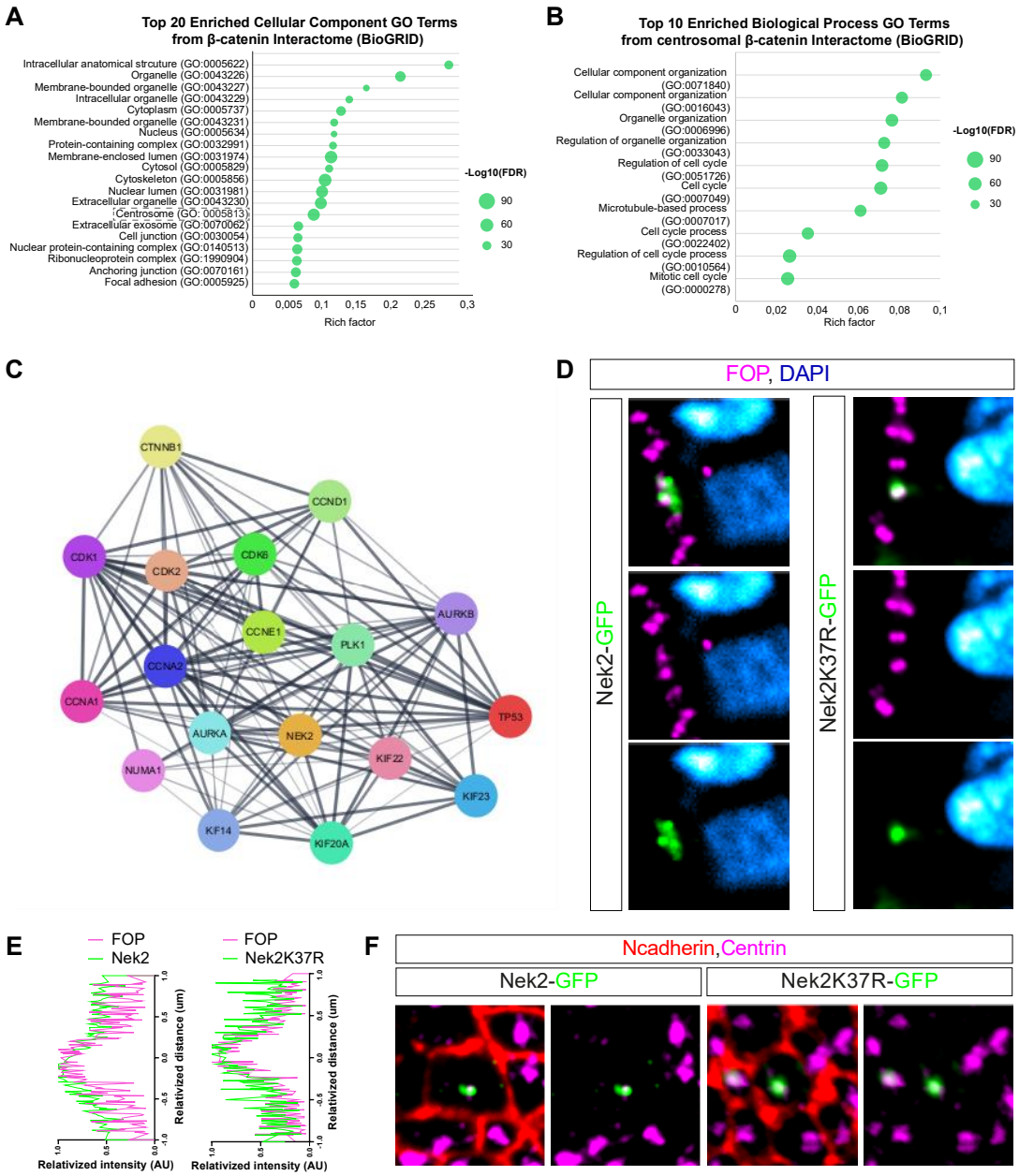

Figure 16. ***In silico*** **analysis of β-catenin interactors identify Nek2 as a centrosome partner. (A)** GO analysis of the Top 20 Cellular Component GO terms associated with β-catenin interactors (source: www.biogrid.com) identifies the centrosome (highlighted with the dotted box) as one of the subcellular locations where β-catenin-associated proteins are localized. **(B)** GO analysis of the Top 10 β-catenin Biological Process of just interactors localized at the centrosome reveals an enrichment of biological processes related to cell cycle

regulation. These findings suggest a potential role for centrosome β-catenin in the regulation of cell cycle and mitosis progression. **(C)** Analysis of centrosome β-catenin interactors involved in cell cycle regulation identifies proteins that serve as key regulators of mitotic progression and proliferation, such as Nek2. In NPC, Nek2 localizes to the centrosome **(D)** Representative images of transversal sections of the chick embryo NT show that Nek2-GFP (green) and its kinase-dead mutant (Nek2K37R-GFP) (green) co-localize with the centrosome, marked by the pancentrosomal marker FOP (magenta), in the spinal cord of the chick embryo. **(E)** Histogram plot showing co-localization between the centrosome (FOP) and both Nek2 and Nek2K37R. **(F)** Representative images of *en face* preparations of the chick embryo NT confirm co-localization of both Nek2 and Nek2K37R (green) with the centrosome, highlighted with FOP (magenta), in the most apical part of NPCs, recognized with the adherent protein N-cadherin (red).

the accumulation at the centrosome of the (S33/S37/Thr41) dephosphorylated pool of β-catenin increased almost twofold (β-catenin intensity at the centrosome in Nek2-GFP- cells = 1±0.02 AU vs. S33/S37/Thr41-phospho-β-catenin intensity at the centrosome in Nek2-GFP+ cells = 0.97± 0.05 and S33/S37/Thr41-dephospho-β-catenin intensity at the centrosome in Nek2-GFP+ cells = 1.61±0.07) (Figure 17A', B', D).

We confirmed these results by generating *en-face* chick embryo NT preparations after co-electroporation of Nek2 construct with β-cateninS33Y, that is the equivalent of the (S33/S37/Thr41) dephosphorylated pool of β-catenin. As expected, β-cateninS33Y localized at the centrosome, and its centrosome accumulation increased nearly threefold when co-expressed with Nek2 (β-cateninS33Y intensity at the centrosome in GFP- cells = 1±0.02 vs. β-cateninS33Y intensity at the centrosome in Nek2-GFP + cells = 2.55±0.18) (Figure 17C, C', D). These results show that Nek2 promotes the centrosome accumulation of stable β-catenin.

We aimed to determine whether the effects of Nek2 on β-catenin require its kinase activity. To address this, we overexpressed a kinase-dead mutant form of Nek2 (Nek2K37R) in the chick embryo NT and generated *en face* preparations to analyze the distribution of the different β-catenin pools. Result showed that overexpression of Nek2K37R did not alter the distribution of (S33/S37/Thr41) phosphorylated pool of β-catenin. However, it significantly increased the centrosome accumulation of S33/S37/Thr41-dephospho-β-catenin and stabilized β-cateninS33Y up to nearly threefold (β-catenin intensity at the centrosome in Nek2K37R-GFP- cells = 1±0.03 AU vs. S33/S37/Thr41-phospho-β-catenin intensity at the centrosome in Nek2K37R-

GFP+ cells = 1.00± 0.11, S33/S37/Thr41-dephospho-β-catenin intensity at the centrosome in Nek2K37R-GFP+ cells = 2.15±0.14 and β-cateninS33Y intensity at the centrosome in Nek2K37R-GFP + cells = 2.85±0.15) (Figure 17E-H). These findings indicate that Nek2 promotes the centrosome accumulation of stable β-catenin, independently of its kinase activity, in agreement with previous observations in *in vitro* systems (Mbom et al., 2014).

To assess whether overexpression of Nek2 or Nek2K37R might also influence the transcriptional activity of β-catenin, we co-electroporated chick embryo NTs at HH14 with Nek2 or Nek2K37R, either alone or in combination with β-cateninS33Y, together with the Wnt pathway transcriptional activity reporter TOP-FLASH (Figure 17I). 24hpe, luciferase assay revealed that neither Nek2 nor Nek2K37R significantly activated transcriptional activity of the pathway. As expected, β-cateninS33Y strongly activated transcriptional activity but this activation was not further enhanced by the co-expression of either Nek2 or Nek2K37R (control vector = 1.00±0.10 vs. Nek2 = 0.85±0.16, Nek2K37R= 0.75±.13, β-cateninS33Y = 58.56±7.74, β-cateninS33Y+Nek2 = 58.98±5.83 and β-cateninS33Y+Nek2K37R = 54.07±12.38) (Figure 17J).

These results suggest that Nek2's effects on β-catenin do not extend to its nuclear transcriptional activity and may instead reflect a localized, non-transcriptional role.

9.- Nek2 increases β-catenin-mediated maintenance of NPC stemness, independent of its kinase activity.

Our previous results indicate a dual β-catenin role in the regulation of neural differentiation and the loss of stemness through both transcriptional and non-transcriptional mechanisms. Hence, we next sought to test whether the Nek2 enhanced accumulation of β-catenin to the centrosome, might have an impact on the regulation of NPC stemness.

To test this hypothesis, we co-electroporated HH14 chick embryo NTs with Nek2 constructs and two different variants of β-catenin (β-cateninWT and β-cateninS33Y), together with Sox2-Luciferase reporter (Figure 18A). 24hpe, results showed that overexpression of either Nek2 or Nek2K37R alone was insufficient to increase Sox2 expression. As expected, β-cateninS33Y led to a marked upregulation of Sox2

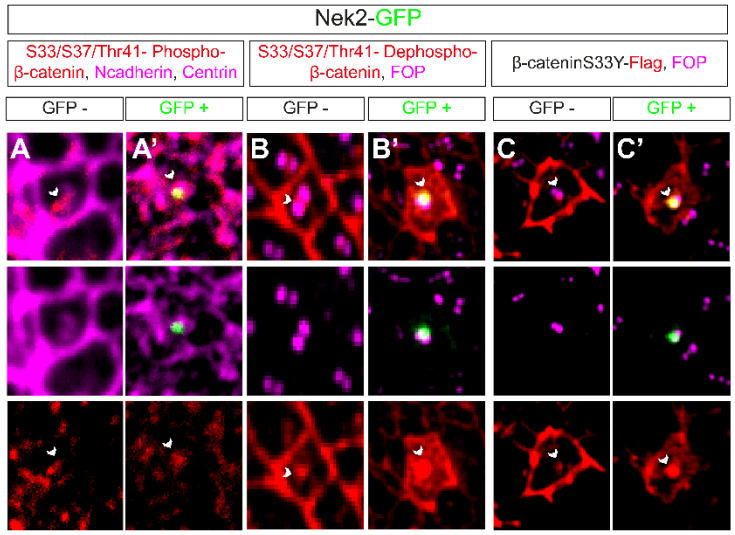
Nek2-GFP
S33/S37/Thr41- Phospho-β-catenin, Ncadherin, Centrin
S33/S37/Thr41- Dephospho-β-catenin, FOP
β-cateninS33Y-Flag, FOP
GFP -
GFP +
A
A'
B
B'
C
C'

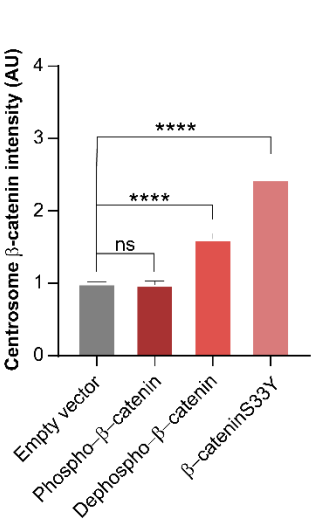
D
Centrosome β-catenin intensity (AU)
0
1
2
3
4
****
****
ns
Empty vector
Phospho-β-catenin
Dephospho-β-catenin
β-cateninS33Y

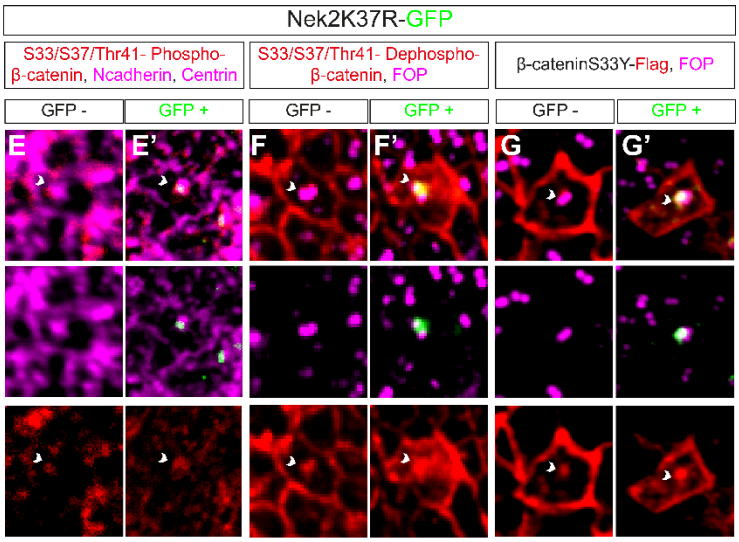
Nek2K37R-GFP
S33/S37/Thr41- Phospho-β-catenin, Ncadherin, Centrin
S33/S37/Thr41- Dephospho-β-catenin, FOP
β-cateninS33Y-Flag, FOP
GFP -
GFP +
E
E'
F
F'
G
G'

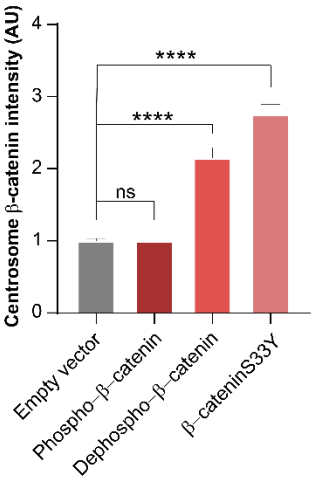
H
Centrosome β-catenin intensity (AU)
0
1
2
3
4
****
****
ns
Empty vector
Phospho-β-catenin
Dephospho-β-catenin
β-cateninS33Y

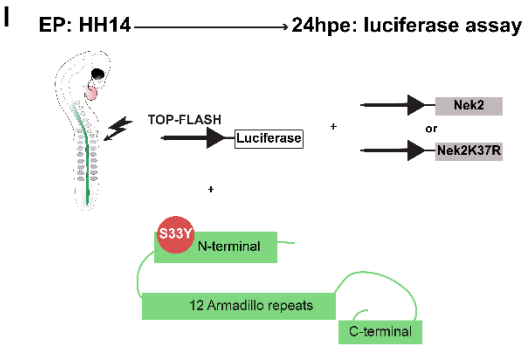
I
EP: HH14
24hpe: luciferase assay
TOP-FLASH
Luciferase
Nek2
or
Nek2K37R
S33Y
N-terminal
12 Armadillo repeats
C-terminal

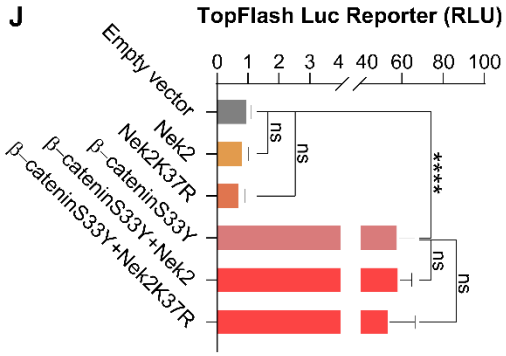
J
TopFlash Luc Reporter (RLU)
0
1
2
3
4
40
60
80
100
Empty vector
Nek2
Nek2K37R
β-cateninS33Y
β-cateninS33Y+Nek2
β-cateninS33Y+Nek2K37R
ns
ns
****
ns
ns

Figure 17. Nek2 increases the accumulation of stable β-catenin at the centrosome independently of its kinase activity. Nek2 increases the accumulation of stable β-catenin at the centrosome**.** Representative images of *en face* preparations of the chick embryo NT show that while overexpression of Nek2-GFP (green) does not lead to increased accumulation of endogenous S33/S37/Thr41-phospho- β-catenin (red) **(A-A'),** it does increase the accumulation of endogenous S33/S37/Thr41-dephospho- β-catenin (red) **(B-B')** and stabilized form of β-catenin (β-catenin S33Y) (red) **(C-C')** at the centrosome (magenta). **(D)** Quantification of S33/S37/Thr41-phospho- β-catenin, S33/S37/Thr41-dephospho- β-catenin and β-catenin S33Y intensity at the centrosome during G1 phase in control versus Nek2 + cells. One-way ANOVA test and multiple comparison test was performed. Three independent experiments n=50 cells per condition. Error bars show the means±SEM. ****, P<0.0001; ns, P< not significate. Nek2 increases the accumulation of stable β-catenin independently of its kinase activity. Representative images of en face preparations of the chick embryo NT show that overexpression of kinase-dead Nek2 mutant (Nek2K37R-GFP) (green) does not enhance the accumulation of endogenous S33/S37/Thr41-phospho- β-catenin (red) **(E-E'),** but does promote accumulation of endogenous S33/S37/Thr41-dephospho- β-catenin (red) **(F-F')** and stable β-catenin S33Y (red) **(G-G')** at the centrosome (magenta). **(H)** Quantification of S33/S37/Thr41-phospho-β-catenin, S33/S37/Thr41-dephospho- β-catenin and β-catenin S33Y intensity at the centrosome during G1 phase in control versus Nek2K37R + cells. One-way ANOVA test and multiple comparison test was performed. Three independent experiments n=40 cells per condition. Error bars show the means±SEM. ****, P<0.0001; ns, P< not significate. Nek2 is insufficient to modulate TCF-mediated transcriptional responses. **(I)** Scheme representation of the electroporation of the TOP-FLASH luciferase reporter in the chick embryo NT at HH14 for in vivo luciferase assay 24hpe. The reporter was co-electroporated together with Nek2, Nek2K37R or Nek2/Nek2K37R combined with stable β-catenin (β-cateninS33Y) to assess their impact on Wnt pathway transcripcional activity. **(J)** Quantification of TOPFLASH-Luciferase/Renilla activity at 24hpe of control, Nek2, Nek2K37R and/or stabilized β-catenin (βcateninS33Y). One-way ANOVA test and multiple comparison test was performed. Three independent experiments, n= 12 embryos per condition. Errors bar show the means±SEM. ****, P<0.0001; ns = not significate.

expression, in agreement with our previous results. Interestingly, co-electroporation of Nek2 with β-cateninS33Y led to a further increase is Sox2 expression levels suggesting a synergistic effect (control vector = 1.00±0.05 vs. Nek2 = 0.99±0.08, Nek2K37R = 0.81±0.05, β-cateninS33Y = 10.63±1.18, β-cateninS33Y + Nek2 = 15.94±1.47) (Figure 18B).

Since β-cateninS33Y cannot be phosphorylated by Nek2 due to its point mutation in residue S33, where Nek2 kinase activity normally exerts its kinase activity (Mbom et al.,

2014), these results indicate that Nek2 synergistic effect on β-catenin is independent on its kinase activity.

To further confirm this kinase-independent mechanism, we co-electroporated β-cateninWT with either Nek2 or Nek2K37R. At 24hpe, both Nek2 and Nek2K37R enhanced Sox2 expression levels in the presence of β-cateninWT, surpassing the levels of β-cateninWT alone (control vector = 1.00±0.05 vs. β-cateninWT = 4.19±0.59, β-cateninWT + Nek2 = 10.22±0.99, β-cateninWT + Nek2K37R = 8.18±1.10) (Figure 18B).

Taken together, these findings support the idea that Nek2 enhances β-catenin-mediated effects on maintaining NPCs stemness through a mechanism that is independent of its kinase activity.

To further understand the mechanisms by which the Nek2-β-catenin complex regulate the stemness of NPCs at the cellular level, we took advantage of two fluorescent reporters, previously introduced in chapter 5, that unequivocally identify and distinguish the three modes of divisions of NPCs in the chick spinal cord depending on the expressed fluorochrome of the division. We co-electroporated HH14 chick embryo NT with these two reporters alongside with Nek2 construct alone or in combination with β-cateninS33Y and labelled mitosis by immunostaining with the anti-pH3 antibody (Figure 18C). 24hpe, results show the coexistence of progenitors (i) only expressing pSox2-GFP (PP progenitors), (ii) co-expressing pSox2-GFP and pTis21-RFP (PN progenitors) and (iii) only expressing pTis21-RFP (NN progenitors) (Figure 18D). Quantification of mitotic figures based on the expressed fluorochrome (green for PP divisions, orange for PN divisions or red for NN divisions), revealed that overexpression of Nek2 did not change the mode of divisions rate of NPCs while β-cateninS33Y increase the rate of proliferative PP divisions in detriment of PN ones (Figure 14C, 18E). Importantly, the co-expression of Nek2 and β-cateninS33Y further increase proliferative PP divisions in detriment of neurogenic PN divisions, compared to β-cateninS33Y alone (control vector = PP: 25.36±1.28; PN: 62.68±1.55; NN: 12.14±1.28 vs. Nek2 = PP: 24.63±1.49; PN: 64.50±2.90; NN: 11.00±2.41, β-cateninS33Y = PP: 57.39±2.28; PN: 37.33±1.86; NN: 7.44±1.94, β-cateninS33Y+Nek2 = PP: 68.93± 3.53; PN: 27.64± 2.09; NN: 2.50±1.42) (Figure 18E).

These results indicate that β-catenin-mediated increase in symmetric proliferative PP divisions is further enhanced when combined with Nek2, supporting the cooperative role for Nek2 and β-catenin in maintaining NPCs stemness.

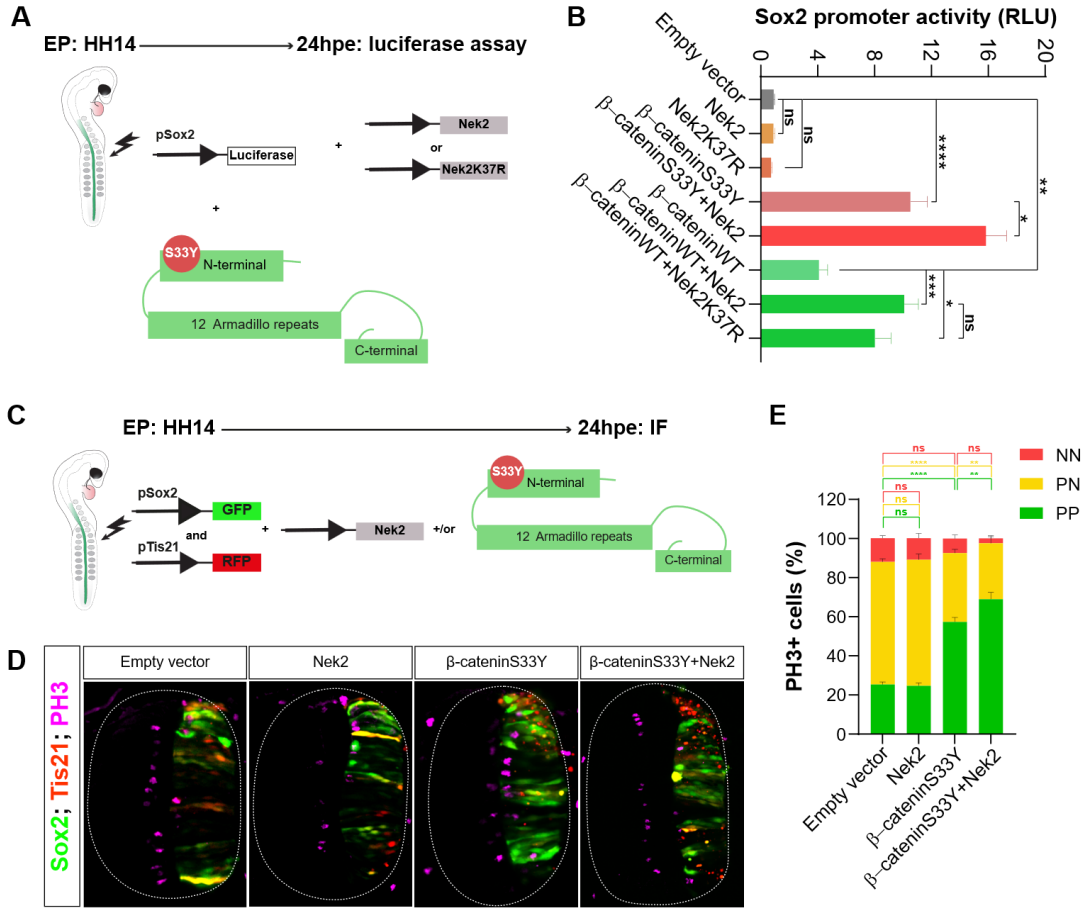

Figure 18. Nek2 enhances β-catenin-mediated effects independent of its kinase activity. **(A)** Scheme representing Sox2 reporters' electroporation in the chick embryo NT at HH14 for in vivo luciferase assay 24hpe together with different β-catenin variants (β-cateninS33Y and β-cateninWT) marked by a color code. **(B)** Quantification of Sox2-Luciferase/Renilla activity at 24hpe of either control or β-catenin variants (β-cateninS33Y and β-cateninWT). One-way ANOVA test, multiple comparison test and t-test were performed. Three independent experiments, n= 24 embryos per condition Errors bar show ±SEM. *, P<0.05; **, P<0.01; ***, P<0.001; ****, P<0.0001. **(C)** Schematic representations of reporters electroporated into the chick embryo NT to mark NPCs according to their mode of division (either green for proliferative PP divisions, orange for neurogenic PN divisions and red for neurogenic NN divisions) alongside Nek2, stable β-catenin (β-cateninS33Y) or Nek2 combined with stable β-catenin (β-cateninS33Y). **(D)** In vivo analysis of the modes of division. HH14 embryos were electroporated with either control plasmid, Nek2 and/or stable β-catenin (β-cateninS33Y), together with the pSox2-GFP and the pTis21-RFP reporters. Transverse sections were stained at 24hpe for pH3 (magenta) to identify mitotic progenitors. **(E)** Quantification of pH3+ cells

according to their modes of divisions (PP: green, PN: orange or NN: red). Two-way ANOVA test, multiple comparison test and t-test were performed. Three independent experiments, n= 15 embryos per condition. Error bars show means ± SEM. **, P<0.01; ****, P < 0.0001; ns = not significate.

10.- The C- terminal region of β-catenin is required for the interaction with Nek2.

In order to elucidate the molecular basis of the interaction between Nek2 and β-catenin, we performed an *in silico* structural analysis aimed at identifying their binding interface. For this purpose, we used the HADDOCK (High Ambiguity Driven protein–protein DOCKing) server (Honorato et al., 2021; Honorato et al., 2024), an information-driven, flexible docking platform designed for modeling biomolecular complexes. The docking protocol generated 9 clusters of potential Nek2- β-catenin complexes. From these, we selected the cluster with the most favorable HADDOCK score (Z-score: -1.5) as the most reliable model, based on energetic and structural criteria. Structural analysis of this top-ranking cluster suggested that the C-terminal region of β-catenin is the primary site of interaction with Nek2 (Figure 19A).

To experimentally validate the *in silico* finding, we follow the same rationale applied in previous chapter and hypothesize that if Nek2 enhances β-catenin-mediated effects through direct interaction, deletion of the interacting region should abolish any Nek2's effect.

To test this hypothesis, we electroporated HH14 chick embryo NTs with different β-catenin variants lacking specific domains known to be implicated in protein-protein interactions, and therefore likely candidates for mediating Nek2 binding: β-cateninS33YΔα-catBS, lacking the α-catenin binding site; β-cateninS33YΔC, deficient in the C-terminal region, which contains TCF binding domains and β-cateninΔN, a mutant form of β-catenin lacking amino acids 29-48 (N-terminal region) and therefore lacking phosphorylation sites necessary for degradation, thereby functioning as a stabilized mutant (Tetsu & McCormick, 1999). Each construct was co-electroporated with a Sox2-Luciferase reporter plasmid to assess Sox2 expression levels (Figure 19B).

At 24hpe, luciferase assays showed that both β-cateninS33YΔα-catBS and β-cateninΔN were capable of upregulating Sox2 expression, and this effect was significantly

enhanced upon co-expressed with Nek2. In contrast, β-cateninS33YΔC also increased Sox2 levels- consistent with our previous results- but its effect was not further enhanced upon Nek2 co-expression (control vector = 0.97±0.12 vs. β-cateninS33YΔα-catBS = 3.60±0.23, β-cateninS33YΔα-catBS + Nek2 = 5.59±0.43, β-cateninS33YΔC = 3.73±0.29, β-cateninS33YΔC + Nek2 = 3.46±0.23, β-cateninΔN = 5.80±0.38, β-cateninΔN + Nek2 = 9.22±0.67) (Figure 19C).

These results provided experimental support for the *in silico* model, confirming that the C-terminal region of β-catenin is necessary for the enhancement of β-catenin-mediated effects on maintaining stemness of NPCs.

To assess whether the β-catenin C-terminal region was also required for the Nek2-mediated centrosome recruitment, we generated *en-face* preparations of chick embryo NTs that were previously co-electroporated with β-cateninS33YΔC and Nek2 constructs. Results showed that, as expected, β-cateninS33YΔC localized at the centrosome, however, its centrosome accumulation did not change upon Nek2 overexpression (β-cateninS33YΔC intensity at the centrosome in GFP- cells = 1±0.06 vs. β-cateninS33YΔC intensity at the centrosome in Nek2-GFP + cells = 1.11±0.12) (Figure 19D, E).

These results show that the C-terminal region of β-catenin is required for its Nek2-mediated recruitment at the centrosome.

Furthermore, we co-electroporated of HH14 chick embryo NTs with the progenitor reporter pSox2-GFP and the neurogenic reporter pTis21-RFP alongside the β-cateninS33YΔC construct alone or in combination with Nek2 (Figure 19F) and labelled mitosis by immunostaining with the anti-pH3. 24hpe, results showed the coexistence of progenitors (i) only expressing pSox2-GFP (PP progenitors), (ii) co-expressing pSox2-GFP and pTis21-RFP (PN progenitors) and (iii) only expressing pTis21-RFP (NN progenitors) (Figure 9G). Quantification of mitotic figures, based on the expressed fluorochrome (green for PP divisions, orange for PN divisions or red for NN divisions), revealed that overexpression of β-cateninS33YΔC increases the proportion of proliferative PP divisions at the expense of PN divisions, consistent with our previous findings. However, no synergistic effect was observed when Nek2 was co-expressed (control vector = PP: 25.36±1.28; PN: 62.68±1.55; NN: 12.14±1.28 vs. β-cateninS33YΔC = PP: 43.79±2.64; PN: 45.54±2.30; NN: 10.29±3.75, β-cateninS33YΔC + Nek2= PP: 50.14±3.08; PN: 39.71±1.52; NN: 10.29±3.75) (Figure 19H).

These results confirm that the C-terminal region of β-catenin is essential for the Nek2-mediated effects in the modulation of NPCs mode of division.

Figure 19. The C-terminal region of β-catenin is required for interaction with Nek2. The C-terminal region of β-catenin is required for the Nek2-mediated co-activation of Sox2 expression **(A)** *In silico* prediction of the interaction between Nek2 and β-catenin identifies C-terminal region of β-catenin as the primary interaction interface (source: HADDOCK) **(B)** Scheme representing Sox2 reporters' electroporation in the chick embryo NT at HH14 for in vivo luciferase assay 24hpe together with different β-catenin variants (β-cateninS33YΔα-catBS, β-cateninS33YΔCT and β-cateninS33YΔNT) marked by a color code aiming to experimentally validate the *in silico* predition. **(C)** Quantification of Sox2-Luciferase/Renilla activity at 24hpe of either control or β-catenin variants (β-cateninS33YΔα-catBS, β-cateninS33YΔCT and β-cateninS33YΔNT). One-way ANOVA test, multiple comparison test and t-test were performed. Three independent experiments, n= 21 embryos per condition Errors bar show ±SEM. **, P<0.01; ***, P<0.001; ****, P<0.0001, ns = not significate. The C-terminal region of β-catenin is required for the Nek2-mediated centrosome localization and indirect increase of PP divisions. **(D)** Representative images of *en face* preparations of the chick embryo NT show a loss of Nek2- dependent increase in β-catenin intensity around the centrosome (magenta) when the C-terminal region of the protein is deleted, as seen with the electroporation of β-cateninS33YΔCT mutant (red). **(E)** Quantification of β-cateninS33YΔCT intensity at the centrosome during G1 phase in control versus Nek2 + cells. T-test was performed. Three independent experiments, n=40 cells per condition. Error bars show the means±SEM. ns = not significate. **(F)** Schematic representations of reporters electroporated into the chick embryo NT to mark NPCs according to their mode of division (either green for proliferative PP divisions, orange for neurogenic PN divisions and red for neurogenic NN divisions) alongside β-cateninS33YΔCT and β-cateninS33YΔCT combined with Nek2. **(G)** In vivo analysis of the modes of division. HH14 embryos were electroporated with either control plasmid, β-cateninS33YΔCT and β-cateninS33YΔCT + Nek2, together with the pSox2-GFP and the pTis21-RFP reporters. Transverse sections were stained at 24hpe for pH3 (magenta) to identify mitotic progenitors. **(H)** Quantification of pH3+ cells according to their modes of divisions (PP: green, PN: orange or NN: red). Two-way ANOVA test and multiple comparison test were performed. Three independent experiments, n= 5 embryos per condition. Error bars show means ± SEM. ***, P < 0.001; ns = not significate.

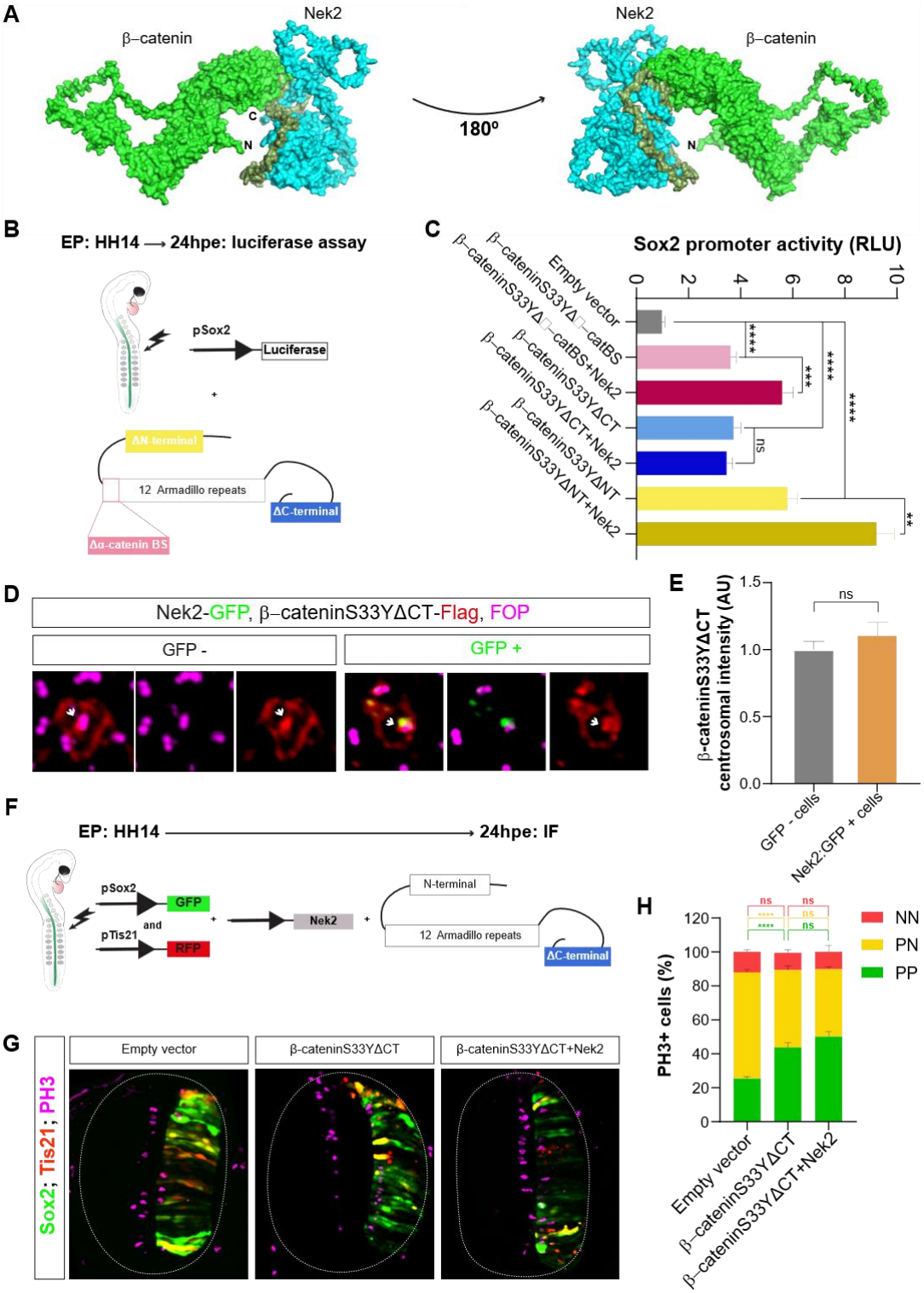
A
β–catenin
Nek2
C
N
180º
Nek2
β–catenin
N
B
EP: HH14 ⟶ 24hpe: luciferase assay
pSox2
Luciferase
+
ΔN-terminal
12 Armadillo repeats
ΔC-terminal
Δα-catenin BS
C
Sox2 promoter activity (RLU)
Empty vector
β–cateninS33YΔβ–catBS
β–cateninS33YΔβ–catBS+Nek2
β–cateninS33YΔCT
β–cateninS33YΔCT+Nek2
β–cateninS33YΔNT
β–cateninS33YΔNT+Nek2
0
2
4
6
8
10
****
***
****
****
ns
**
D
Nek2-GFP, β–cateninS33YΔCT-Flag, FOP
GFP -
GFP +
E
β-cateninS33YΔCT centrosomal intensity (AU)
1.5
1.0
0.5
0.0
ns
GFP - cells
Nek2:GFP + cells
F
EP: HH14
24hpe: IF
pSox2
GFP
and
pTis21
RFP
+
Nek2
+
N-terminal
12 Armadillo repeats
ΔC-terminal
G
Sox2; Tis21; PH3
Empty vector
β-cateninS33YΔCT
β-cateninS33YΔCT+Nek2
H
PH3+ cells (%)
120
100
80
60
40
20
0
ns
ns
****
ns
****
ns
NN
PN
PP
Empty vector
β–cateninS33YΔCT
β–cateninS33YΔCT+Nek2

DISCUSSION

Understanding how NPCs coordinate proliferative and neurogenic divisions during development is fundamental to elucidating how the CNS acquires its complex architecture. This thesis investigates the role of Wnt pathway, particularly its key effector β-catenin, in regulating NPC fate decisions during early stages of chick NT development. It specifically explores how post-translational modifications and subcellular localization of β-catenin influence its instructive potential.

While β-catenin is widely known for its transcriptional role within the Wnt canonical pathway and its structural function in adherens junctions, our work reveals additional, non-canonical functions that contribute to the NPC proliferation. In particular, this study identifies the centrosome as a critical site for β-catenin accumulation during NT development and explores the molecular mechanisms underlying this localization, including a novel role for the kinase Nek2.

1.- Centrosome accumulation of stabilized β-catenin during early NT development contributes to proliferation

Our results show that during the early NT development, β-catenin is not uniformly distributed throughout the cytoplasm of NPCs but instead accumulates specifically at the centrosome. Notably, this localization is most prominent during developmental windows characterized by a predominance of proliferative symmetric PP divisions, particularly in the dorsal region of the chick NT.

We further demonstrate that the pool of β-catenin at the centrosome corresponds to the stable, non-phosphorylated form of the protein (dephosphorylated at S33/S37/Thr41), which is the active species in the canonical Wnt signaling cascade. Whereas, the phosphorylated, degradation-targeted form of β-catenin (phosphorylated at S33/S37/Thr41) remains diffusely distributed throughout the cytoplasm. Importantly, blocking phosphorylation at critical degradation residues such as through mutation of S33, lead to of β-catenin stabilization and its preferential accumulation at the centrosome, even in the absence of transcriptional or apical localization cues. This suggest that β-catenin stabilization, potentially downstream of Wnt pathway activation, promotes its preferential localization to the centrosome.

Previous studies have reported centrosome localization of β-catenin in vitro and in early embryonic models, linking it to centrosome cohesion and spindle orientation

(Bahmanyar et al., 2008). Notably, in the mouse neocortex, Chilov et al. (2011) demonstrated that β-catenin KO leads to increased neurogenic divisions, in part due to altered spindle orientation. While these studies suggested a centrosome-related function for β-catenin, our work builds upon them by providing in vivo evidence in the chick NT that stabilized β-catenin accumulates at the centrosome, and that this enrichment correlates with regions and time points of proliferative divisions. These findings suggest a potential instructive role for centrosome β-catenin not just in spindle positioning, but more broadly in modulating NPC division modes during early neurodevelopment.

The centrosome is increasingly recognized as a multifunctional signaling hub that integrates polarity cues, mitotic spindle orientation and cell cycle regulation (Nigg & Raff., 2009; Bornens, 2012). Our findings support a model in which stabilized β-catenin accumulates at the centrosome to locally promote proliferative divisions, thereby contributing to the expansion of the progenitor pool during early CNS development. This pool of β-catenin at the centrosome may act by locally enhancing microtubule nucleation or spindle stability, thereby promoting mitotic configurations that maintain progenitor identity of cells. Through such localized control, Wnt signaling activity could be spatially translated into distinct type of cell division, enabling progenitor domains with higher Wnt signaling, and consequently more β-catenin at the centrosome, to sustain proliferation longer or expand more rapidly than those regions with lower pathway activation. This mechanism could fine-tune the pace of regional neural tissue growth during development.

However, it remains to be determined whether centrosome β-catenin plays an instructive role in promoting proliferative divisions, or whether its accumulation is a secondary effect of broader Wnt signaling activity or apico-basal polarity dynamics. Additionally, we cannot yet rule out the possibility that centrosome localization serves a buffering or sequestration role, as proposed in other systems (Lancaster et al., 2011), rather than acting as an active instructive role.

Clarifying these possibilities will require precise strategies to manipulate centrosome pool of β-catenin without interfering with transcriptional and junctional roles. This includes the identification and CRISPR/Cas9-mediated disruption of domains responsible for centrosome targeting, the use of phospho-mimetic mutants that prevent centrosome accumulation and the identification of centrosome interactors through co-immunoprecipitation followed by mass spectrometry or proximity labeling approaches to manipulate this centrosome signaling. Ultimately, dissecting the instructive potential of centrosome β-catenin will benefit from tools that allow its selective overexpression

at the centrosome such as fusion constructs with centrosome anchor proteins, enabling a more direct assessment of its instructive potential in regulating NPC fate during early neurogenesis.

2.- Nek2 as a non-catalytic modulator promoting centrosome accumulation of β-catenin

Our data reveal that Nek2, a kinase traditionally known for its role in centrosome cohesion and mitotic regulation, also has a crucial non-catalytic role in stabilizing and promoting the accumulation of the stabilized pool of β-catenin at the centrosome during early NT development. This suggests that Nek2 acts as a modulatory scaffold, facilitating localization of β-catenin at the centrosome. Importantly, catalytic inhibition of Nek2 does not abolish accumulation of β-catenin at the centrosome, indicating that its role in this process does not require its enzymatic activity.

Previous studies have primarily characterized Nek2 as a mitotic kinase regulating centrosome separation (Faragher & Fry, 2003; reviewed by Fry et al., 2012). More recent evidence has shown that β-catenin is a physiological substrate of Nek2, and that Nek2 plays a role in regulating the centrosome cycle (Bahmanyar et al., 2008, Mbom et al., 2014). Moreover, the Nek2- β-catenin interaction appears to inhibit binding of the E3 ligase β-TrCP, thereby preventing β-catenin ubiquitination and degradation (Mbom et al., 2014). Our findings extend these observations by demonstrating *in vivo* that Nek2 can stabilized β-catenin specifically the centrosome, a context not previously explored. This contributes to the growing understanding of proteins of the centrosome as integrators of signaling beyond their classical roles in mitosis.

The ability of Nek2 to promote β-catenin accumulation at the centrosome independently of its catalytic activity defines a regulatory mechanism that results in the enhancement of NPC proliferation, likely by modulating centrosome dynamics, which in turn bias cell fate decisions toward symmetric proliferative PP divisions.

However, it is important to note that we have not yet demonstrated a direct or necessary requirement of endogenous Nek2 in β-catenin centrosome targeting, nor confirmed a clear physical interaction between the two proteins *in vivo*. This leaves open the possibility that additional centrosome partners could be involved in this effect.

Consequently, the precise molecular mechanisms and broader relevance of the scaffold role of Nek2 remain unclear.

Future studies should aim to identify the domains of Nek2 required for β-catenin binding using targeted mutagenesis and structure-function analysis. Proteomic approaches such as BioID or Appex could reveal additional interactors implicated in the centrosome complex, and functional experiments that selectively disrupt Nek2- β-catenin interaction will be essential to establish causality. Nonetheless, understanding this novel non-catalytic function of Nek2 could reveal new layers of regulation in NPC fate control and potentially identify targets to modulate NPC proliferation in regenerative medicine or disease.

3. Functional importance of the C-terminal region of β-catenin for Nek2 interaction and centrosome-mediated effects

Although C-terminal region of β-catenin is dispensable for its intrinsic ability to promote symmetric proliferative PP divisions in NPCs, our findings demonstrate that this domain is essential for its functional cooperation with Nek2, as shown by structure-function analyses. The loss of synergistic behavior coincides with impaired accumulation of β-catenin at the centrosome, suggesting that the C-terminal region mediates either a specific protein-protein interaction or a conformational requirement necessary for cooperative behavior.

This role extends beyond the well-characterized transcriptional functions of the C-terminal region of β-catenin, which include interactions with co-activators such as CBP/p300 (Hecht et al., 2000; Miyabayashi et al., 2007) to activate the TCF/LEF-mediated transcription of Wnt target genes. Here, we reveal a non-transcriptional function of this domain in mediating β-catenin accumulation at the centrosome and functional cooperation with Nek2. Whereas previous studies have largely focused on the N-terminal domain of β-catenin in regulating its stability via phosphorylation and degradation (Aberle et al., 1997; Yost et al., 1996; Liu et al., 1999; Rubinfeld et al., 1996; Xing et al., 2004), our findings highlight a distinct and previously unappreciated role for the C-terminal region of β-catenin in enabling spatially restricted, non-canonical protein interactions.

These results support the idea that β-catenin operates as a modular scaffold, whose domain-specific functions are dictated by subcellular context and partner availability, influencing centrosome dynamics and, consequently, NPC fate decisions.

Nonetheless, we cannot yet exclude alternative explanations for this cooperative behavior such as indirect effects of the truncation on protein folding or stability. Additionally, biochemical validation of a direct interaction will be required to clarify the molecular basis of this cooperation. Defining the precise residues mediating the interaction could guide the development of targeted mutations or inhibitors that selectively uncouple non-canonical (centrosome) and canonical (transcriptional) functions of β-catenin.

4. Spatially distinct but potentially coordinated roles of β-catenin at the centrosome and nucleus during neurodevelopment

While this thesis primarily focuses on the non-canonical role of stabilized β-catenin at the centrosome mediated by Nek2, with no comparable enhancement observed in the nucleus, which suggests a spatially restricted interaction between these two proteins, it is important to consider how these pathways may intersect or operate in parallel to regulate NPCs fate.

To explore this, we analyzed published bulk RNA-Seq data from medial ganglionic eminence (MGE) progenitors (GSE112714) (Ma et al., 2019) in which overexpression of the stabilized β-catenin mutant (β-cateninS33Y) resulted in 521 upregulated genes and 587 downregulated genes (Figure 20 A, B). Among these, 88 genes were annotated to proliferation-related processes, including transcriptional regulators such as TCF7L2 (Korinek et al., 1998), JUN (Shaulian & Karin, 2001; Eferl & Wagner, 2003), NOTCH1 (Artavanis-Tsakonas, Rand & Lake, 1999), ASLC1(Huang, Chan & Schuurmans, 2014), STAT5B (Nosaka et al., 1999), RUNX1 (Okuda et al., 1996) (Figure 20C). These data reinforce canonical transcriptional role of β-catenin in activating proliferative programs in neural progenitors.

Importantly, we also identified a subset of differentially expressed genes: TUBA1A, TUBB4A, PRKAR2B and CNTRL that are components of the centrosome maturation pathway (as annotated in Reactome.org) and transcriptionally regulated by Wnt/ β-catenin signaling (Figure 20D). This suggest that canonical Wnt signaling may influence

centrosome composition or function through transcriptional regulation, indirectly impacting the non-canonical role of β-catenin at this organelle.

Further support for dual regulation came from reanalysis of published RNA-Seq from ventral midbrain (VM) progenitors (GSE241041) (Yang et al., 2024) comparing Wnt pathway activation via Wnt agonist CHIR99021 versus receptor-level activation via FZD5 receptor. CHIR-mediated activation upregulated proliferation-associated factors such as CSF1R (Morandi et al., 2011), MMP2 (Dong et al., 2011) and TNIK (Shitashige et al., 2010), consistent with canonical activation of Wnt target genes. Conversely, receptor-mediated activation via FZD5 showed upregulation of genes including numerous neuronal differentiation markers such as NEUROD4 (Hardwick & Philpott, 2015), SOX21 (Whittington et al., 2015) and BMP2 (Rios et al., 2004), alongside with genes involved centrosome/microtubule regulation such as DCLK1 (Agulto et al., 2021; reviewed in Ramkumar et al., 2018), MARK2 (Zulkipli et al., 2018) and MAP2 (reviewed in Ramkumar et al., 2018), which are critical for spindle positioning and microtubule dynamics.

Together, these findings suggest that Wnt/β-catenin signaling governs NPCs fate through both transcriptional and centrosome mechanisms, according to our hypothesis. While nuclear β-catenin activates transcriptional programs that drive proliferation and potentially repress differentiation, it also appears to regulate the expression of proteins related to centrosome biology. Moreover, receptor-mediated activation, which potentially enhance centrosome β-catenin, seems to favor neurogenesis but modulate mitotic spindle dynamics. These spatially distinct roles may converge on the regulation of symmetric versus asymmetric divisions.

While β-catenin and Nek2 interact locally at the centrosome to regulate division mode, likely by influencing mitotic spindle dynamics as both proteins have been independently implicated in spindle assembly, microtubule anchoring and spindle orientation (Faragher & Fry, 2003, Huang et al., 2007; Chilov et al. 2011, Kaplan et al., 2004), the transcriptomic data point toward possible upstream transcriptional regulatory programs that may influence centrosome localization of β-catenin (among other proteins), and/or downstream gene expression changes that may be driven by these centrosome-associated cues. This raises the possibility of a feedback loop whereby nuclear and centrosome β-catenin pools are coordinated, integrating spatially restricted signals with broader transcriptional regulation during neurodevelopment.

Understanding this dual functionality underscores the complexity of the role of β-catenin in NPCs and encourages further studies to dissect how centrosome and nuclear β-catenin pools coordinate to regulate neurogenesis.

5. Towards understanding centrosome β-catenin function: implications in NPC modes of division

Our data demonstrate that β-catenin promotes symmetric proliferative PP divisions in NPCs through a combination of transcription-dependent and transcription-independent mechanisms. While the classical role of β-catenin as a transcriptional co-activator in the Wnt pathway is well established and known to regulate proliferation of NPCs (Megason & McMahon, 2002; Machon et al., 2003; Zechner et al., 2003), and its apical localization has been linked to tissue growth (Herrera et al., 2013), our findings highlight a distinct centrosome pool of β-catenin that influence NPC modes of division in cooperation with Nek2.

At the transcriptional level, β-catenin regulates genes critical for cell cycle progression and proliferation (He et al., 1998; Tetsu & McCormick, 1999). At the centrosome, however, β-catenin may exert non-transcriptional functions by modulating mitotic spindle organization, microtubule nucleation, or spindle orientation which could locally bias the outcome of NPC division towards the proliferative PP mode (Kaplan et al., 2004; Huang et al., 2007; Bahmanyar et al., 2008; Chilov et al., 2011).

Preliminary data suggest that the spatial distribution of stabilized β-catenin during mitosis differs between proliferative (Tis21-) and neurogenic (Tis21+) divisions. In proliferative divisions, β-catenin partially overlaps with the metaphase plate, localizing near the plus ends of microtubules (Figure 21A, B) while in neurogenic divisions, β-catenin is largely excluded from this region (Figure 21C, D). Although these observations require further validation, they support the hypothesis that β-catenin may differentially interact with components of the mitotic machinery depending on the division mode. This spatially regulated localization could reflect a functional role for β-catenin in modulating microtubule dynamics or spindle positioning specific to proliferative divisions.

Although no prior studies have described this precise behavior of β-catenin at the spindle, previous reports have documented β-catenin interaction with microtubules and

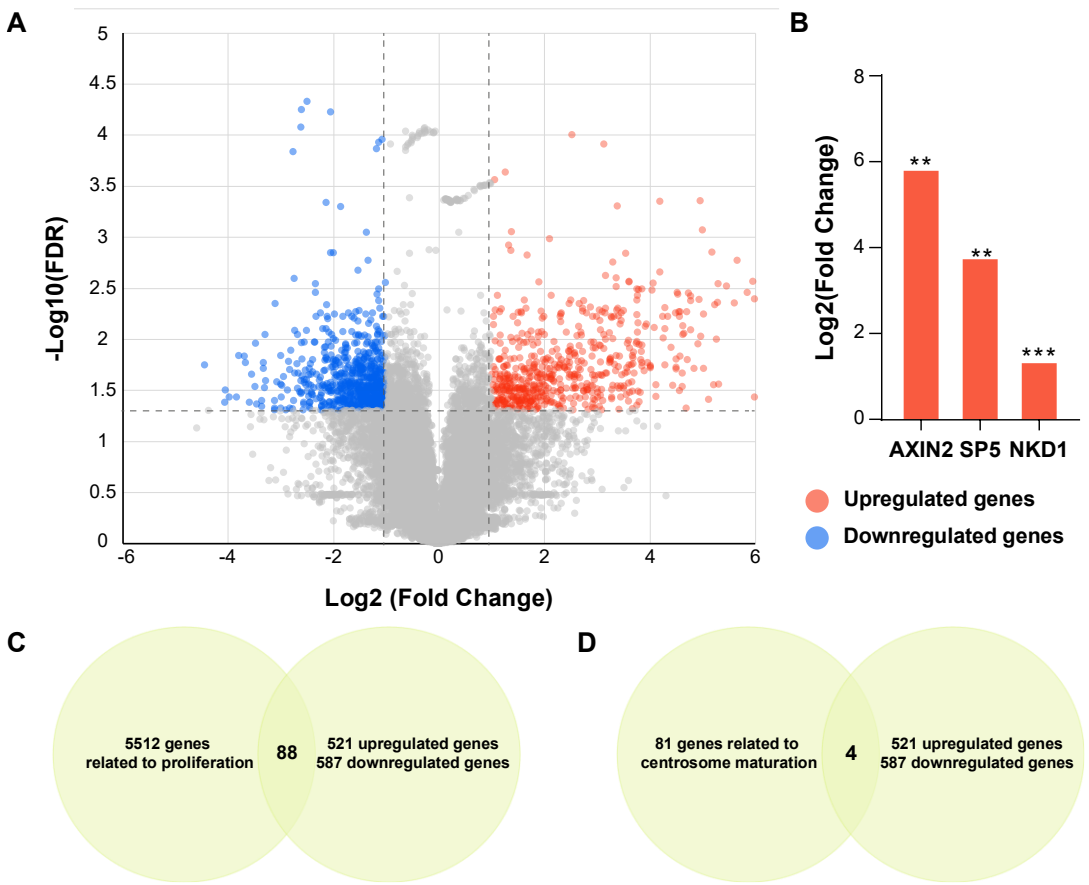

Figure 20. Transcriptomic analysis reveals that stabilized β-catenin regulates genes involved in proliferation and centrosome maturation. (A) Volcanos plot showing differentially expressed genes (DEGs) in MGE progenitors overexpressing stabilized β-catenin (β-cateninS33Y) versus control (RNA-Seq data from Ma et al., 2019; GSE112714. Significantly upregulated genes (Log2Fold Change>1, FDR<0.05) are shown in red, and significantly downregulated genes (Log2Fold Change<-1, FDR<0.05) in blue. (B) Expression changes of selected Wnt canonical pathway target genes serve as internal positive controls, confirming activation of Wnt signaling in β-cateninS33Y-overexpressing cells. (C) Venn diagram showing the number of DEGs overlapping with genes annotated under the Gene Ontology (GO) biological process term "proliferation" (GO: 0008283). A total of 88 proliferation-related genes were differentially expressed. (D) Venn diagram showing the number of DEGs overlapping with genes annotated for "centrosome maturation" as defined in Reactome.org (R-HSA-380270). Four centrosome-related genes were found to be transcriptionally regulated by stabilized β-catenin.

microtubule-associated proteins (Huang et al., 2007, Kaplan et al., 2004) supporting the plausibility of a centrosome- and spindle-associated role. Furthermore, the cooperative interaction with Nek2 may further fine-tune the local function of β-catenin during mitosis.

In conclusion, although the precise molecular mechanisms remain to be elucidated, we propose that β-catenin not only functions as a nuclear transcriptional co-activator but also as a spatially restricted scaffold at the centrosome that, together with Nek2, fine-tunes mitotic spindle behavior and contributes to the regulation of the division modes. This dual role may allow NPCs to integrate global transcriptional programs with local cytoskeletal cues, ensuring proper balance between proliferation and differentiation required during early CNS development.

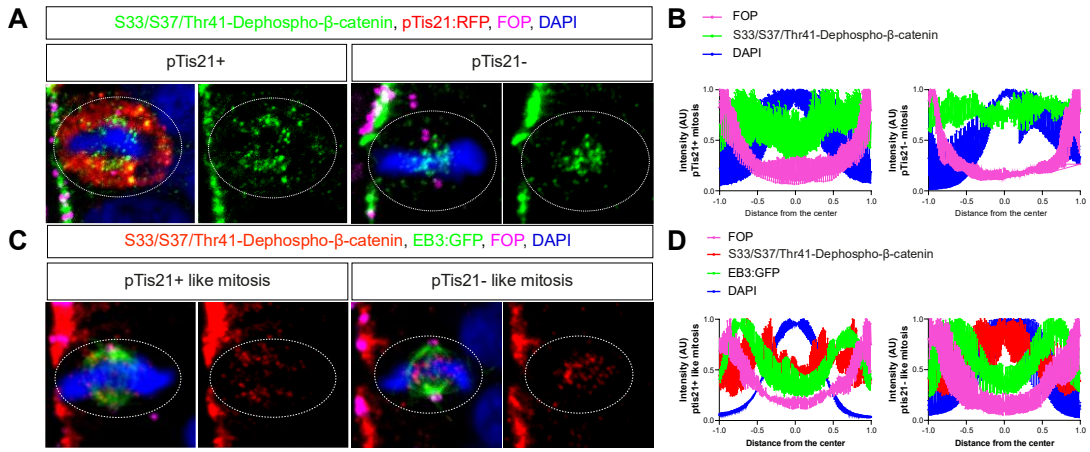

Figure 21. Spatial distribution of stabilized β-catenin differs between proliferative and neurogenic NPC divisions. (A) Representative images of a NPC undergoing either proliferative (Tis21-) or neurogenic (Tis21+) divisions, visualized using the pTis21:RFP reporter. Cells are immunostained with the centrosomal marker FOP (magenta), stabilized β-catenin (S33/S37/Thr41-dephospho- β-catenin, green) and DAPI (blue). In Tis21- division, stabilized β-catenin partially overlaps with the metaphase plate whereas in Tis21+ divisions, it is largely excluded from this region. **(B)** Fluorescence intensity profiles drawn from one FOP-positive centrosome to the other across the metaphase plate in Tis21- and Tis21+ divisions, showing relative distribution of FOP (magenta), S33/S37/Thr41-dephospho-β-catenin (green) and DAPI (blue). **(C)** Representative images of $Tis21^{-}$-like and $Tis21^{+}$-like divisions stained for S33/S37/Thr41-dephospho-β-catenin (red) and microtubule plus-end marker EB3:GFP (green). In $Tis21^{-}$-like divisions, β-catenin is concentrated at the metaphase plate and excluded from microtubule plus-ends whereas in $Tis21^{+}$-like divisions, β-catenin localizes along microtubule plus-ends and is largely excluded from the metaphase plate. **(D)** Fluorescence

intensity profiles drawn from one FOP-positive centrosome to the other across the metaphase plate in Tis21^{-}-like and Tis21^{+}-like divisions, showing showing relative distribution of FOP (magenta)S33/S37/Thr41-dephospho-β-catenin (red), EB3:GFP (green) and DAPI (blue).

6.- β-Catenin-mediated primary cilia elongation might link extracellular signaling to symmetric divisions through a positive feedback loop

Preliminary observations from our study revealed that overexpression of either Wnt ligand (Wnt3a) and β-catenin leads to elongation of the primary cilia in NPCs (Figure 22 A, B).

Primary cilia are known to act as sensory organelles that integrate a wide array of extracellular signals, including Shh, Wnt and BMP (Goetz & Anderson, 2010; reviewed by Lancaster & Gleeson, 2009). Ciliary length is a dynamic feature that has been shown to modulate signal sensitivity, duration and downstream cellular responses (Wang & Dynlacht, 2018).

While Wnt/β-catenin canonical signaling is generally thought to be negatively regulated by primary cilia (Corbit et al., 2008), more recent studies suggest a more complex interplay, in which bidirectional interaction whereby Wnt signaling can influence ciliary architecture and cilia can, in turn, regulate aspects of Wnt pathway activity (Lancaster et al., 2011; Kyun et al., 2020). Our preliminary data add to this emerging view by showing that increased Wnt and β-catenin levels correlate with primary cilia elongation, suggesting a potential feedback mechanism.

The elongation of cilia may enhance the capacity of NPCs to sense and integrate morphogenetic cues, thereby promoting proliferative outcomes. Specifically, extended cilia might increase the surface area or prolonged dwell time for receptor-ligand interactions, potentially amplifying the reception and transduction of morphogens such as Wnt. This, in turn, could reinforce β-catenin activity through both transcriptional and non-transcriptional (centrosome-associated) mechanisms. It is therefore plausible that this cilia elongation functions as a structural interface linking extracellular cues and intracellular machinery controlling the mode of the division of NPCs. This structural modification may establish a positive feedback loop that maintains the proliferative

state of NPCs during critical windows of neurodevelopment, ensuring adequate expansion of the progenitor pool prior to differentiation.

Despite the potential significance of these findings, it is important to note that our observations are based on overexpression models and should be interpreted with caution. The precise molecular mechanisms through which β-catenin promotes this ciliary elongation remain to be identified, and the functional consequences of this structural change on NPCs behavior, such as changes in responsiveness to signaling have not yet been directly tested.

Future work should aim to identify the molecular mediators of this ciliary phenotype and assess whether elongation causally alters Wnt signaling activity or NPC fate. In addition, experiments manipulating ciliary length independently of β-catenin are needed to clarify whether cilia themselves causally affect NPC division mode.

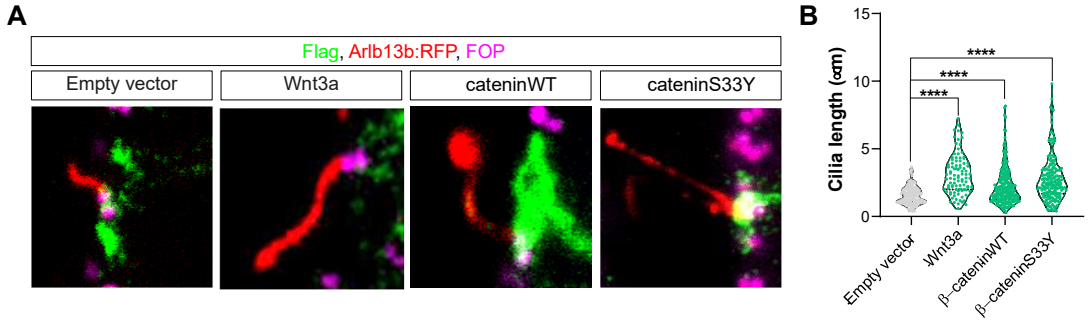

Figure 22. Overexpression of Wnt3a or β-catenin promotes primary cilia elongation in NPCs. (A) Representative images of the chick embryo NT showing primary cilia of NPCs marked by the ciliary membrane protein Arlb13b:RFP (red) at the basal body marker FOP (magenta). Embryos were previously electroporated with control, Wnt3a, β-catenin WT or stabilized β-catenin (β-cateninS33Y) plasmids (green). **(B)** Violin plot showing cilia lengh quantification in control versus Wnt3a**,** β-catenin WT and β-cateninS33Y conditions. One-way ANOVA test and multiple comparison test were performed- Three independent experiments, n=100 primary cilia per conditions. Error bar show the means±SEM. ****, P<0.00001.

7.- Proposed model and future perspectives

Our data supports a model in which β-catenin functions as a multifaceted regulator of NPC behavior, combining both its canonical transcriptional activity with a non-canonical, centrosome-associated role, in cooperation with Nek2.

We show that β-catenin localizes to the centrosome of NPCs predominantly at early developmental stages, coinciding with the time window of symmetric proliferative PP divisions. This centrosome pool is enriched in stabilized β-catenin, which is the S33/S37/Thr41-dephosphorylated pool of β-catenin, likely reflecting an activation of the Wnt signaling pathway by its ligand. Importantly, prevention of its S33 phosphorylation leads to increased accumulation of β-catenin at the centrosome, confirming a role for post-translational stabilization in regulating this localization, independently of transcriptional or apical activity.

Functionally, β-catenin overexpression promotes proliferative PP divisions at the expense of neurogenic PN divisions, acting through both transcriptional and non-transcriptional mechanisms. This shift correlates with transcriptional upregulation of progenitor gene Sox2 and repression of proneural gene NeuroD, ultimately resulting in aberrant tissue overgrowth.

Mechanistically, we identified Nek2 as a β-catenin binding partner at the centrosome. Nek2 overexpression increases the levels of stabilized β-catenin at the centrosome and synergistically enhances the pro-proliferative effect on NPC divisions. Importantly, this interaction requires the C-terminal region of β-catenin, supporting a domain-specific, transcriptional independent function of β-catenin at the centrosome.

While these data define key aspects of a dual role of β-catenin, several questions remain open.

First, although Wnt/β-catenin pathway is well known to activate proliferative targets such as MYC, CCND1, and AXIN2, our preliminary transcriptomic analysis suggest that β-catenin may also transcriptionally regulates the expression of genes involved in centrosome maturation such as TUBA1A, TUBB4A, PRKAR2B and CNTRL Additionally, further analysis suggest that receptor-mediated Wnt signaling may support the regulation of proliferation through non-transcriptional mechanisms that regulate genes implicated in spindle orientations and microtubules dynamics. This duality raises the possibility that β-catenin coordinates both transcriptional and local, non-

transcriptional mechanisms to fine-tune mitotic events. However, whether these two axes act in parallel, converge on shared targets or are temporally ordered in a hierarchical manner remains to be clarified.

Second, although we have shown that centrosome β-catenin and its interaction with Nek2 affect NPCs mode of division, the precise mechanisms by which they influence spindle orientation or microtubule behavior remain to be elucidated. Preliminary data suggest that β-catenin may act locally as a structural scaffold or signaling hub at the spindle apparatus, potentially modulating microtubule dynamics and contributing to the symmetric outcome of the division. Future studies are required to dissect how β-catenin-mediated centrosome cues coordinate spindle organization to determine the mode of the division.

Lastly, we observed that the overexpression of both Wnt ligand (Wnt3a) and β-catenin (β-cateninWT and β-cateninS33Y) correlates with elongation of the primary cilium. This structural alteration could modulate the sensitivity and integration of key developmental pathways such as Wnt, Shh or BMP, potentially forming a positive feedback loop into both the transcriptional and centrosome functions of β-catenin that stabilizes the proliferative state. However, whether cilia elongation is a direct consequence of Wnt/β-catenin signaling activation, and whether it functionally contribute to symmetric proliferative PP divisions represents an intriguing but still speculative aspect of this model.

Altogether, we propose a model in which β-catenin integrates spatial cues from the centrosome and the primary cilium with temporal transcriptional programs, to fine-tune the balance between NPC proliferation and differentiation. This spatiotemporal control is likely essential for ensuring tissue growth during early CNS formation.

Understanding how this coordination between distinct but interconnected processes is achieved is key to deciphering the mechanisms underlying NPC divisions, especially those that include multifunctional proteins like β-catenin, that participate in diverse subcellular contexts.

Moreover, this model may also provide a framework to investigate similar dual roles in other stem cell systems or disease models.

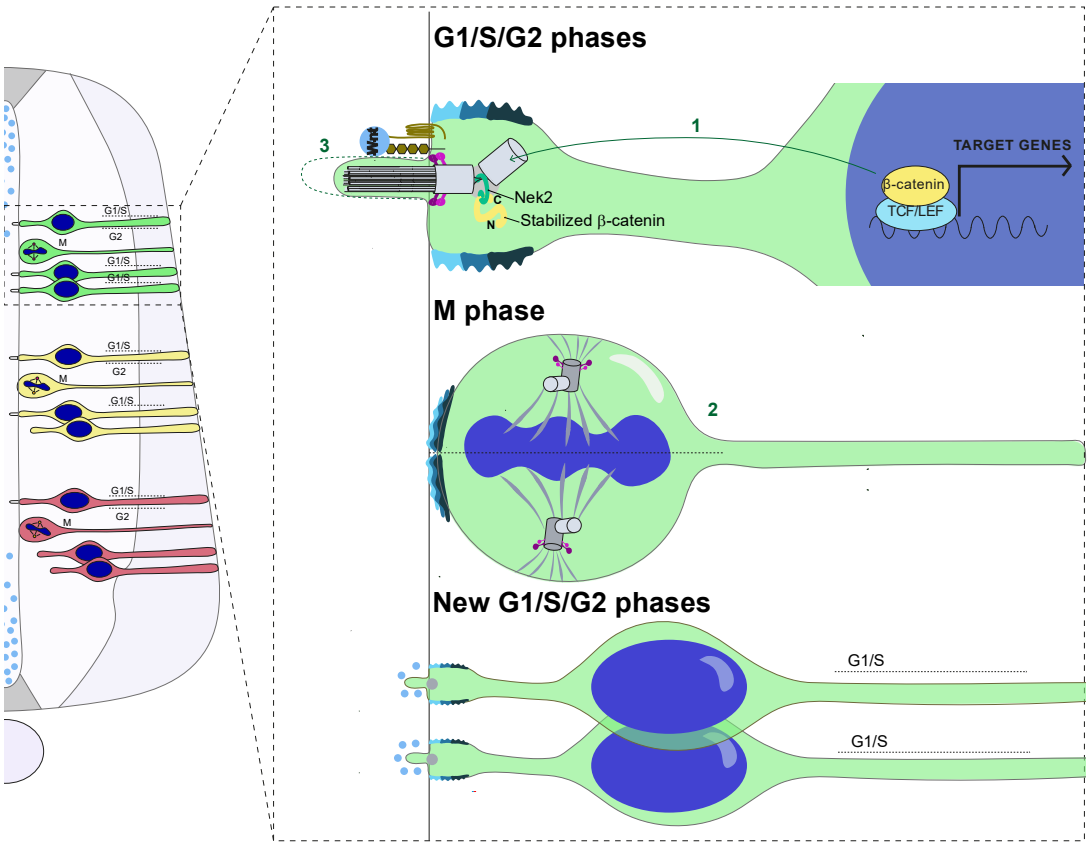

Figure 23. Schematic representation of the proposed mechanism by which Wnt/β-catenin regulates proliferation of NPCs through transcriptional and non-transcriptional mechanisms. β-catenin promotes symmetric proliferative PP divisions of NPCs through both transcriptional and non-transcriptional mechanisms. At the transcriptional level, β-catenin promotes expression of proliferation-associated genes such as Sox2 and represses neuronal differentiation by downregulating proneural genes like NeuroD. Independently, a centrosome-localized pool of β-catenin, identified as a stabilized form lacking phosphorylation marks at residues S33/S37/Thr41, correlates with similar pro-proliferative effects. This centrosome accumulation of stabilized β-catenin is potentially regulated by Nek2, which requires the C-terminal region of β-catenin for their interaction. Nek2 overexpression promotes the accumulation of stabilized β-catenin at the centrosome and cooperates with β-catenin to further enhance PP divisions. **(1)** While these findings support parallel transcriptional and non-transcriptional functions for β-catenin, whether these axes converge on shared targets or operate independently remain to be determined . **(1, 2)** Moreover, the contribution of Wnt/β-catenin signaling to centrosome maturation or MTOC activity and how these structural changes

influence spindle behavior to bias divisions outcomes remains unresolved. **(3)** Finally, preliminary evidence suggests that both Wnt3a and β-catenin overexpression leads to primary cilia elongation, raising the possibility that this structural change could enhance signaling reception and establish a positive feedback loop that would sustain proliferative signaling. However, whether elongated cilia play a causal role in regulating symmetric division remains an open question.

CONCLUSIONS

1.- β-catenin localizes to the centrosome of neural progenitor cells (NPCs), and this localization correlates with symmetric proliferative progenitor-progenitor (PP) divisions during early developmental stages.

2.- The pool of β-catenin localized at the centrosome is the stabilized form (S33/S37/Thr41-dephospho- β-catenin), supporting regulation of centrosome β-catenin by Wnt pathway activity.

3.- Preventing phosphorylation at S33 is sufficient to enhance centrosome localization of β-catenin.

4.- Overexpression of β-catenin promotes symmetric proliferative (PP) divisions at the expense of neurogenic (PN) divisions, mediated through both transcriptional and non-transcriptional mechanisms.

5.- Nek2 is a centrosome binding partner of β-catenin with potential role in regulating NPC division.

6.- Nek2 overexpression increases the levels of stabilized β-catenin at the centrosome, without a corresponding effect in the nucleus, suggesting a spatially restricted interaction.

7.- β-catenin-Nek2 interaction enhances symmetric proliferative PP divisions through synergistic effects.

8.- The C-terminal region of β-catenin is required for Nek2 interaction.

REFERENCES

Aaku-Saraste, E. Hellwig, A. and Huttner, W.B. Loss of occluding and functional tight junctions, but not ZO-1, during neural tube closure-remodeling of the neuroepithelium prior to neurogenesis. Developmental biology 180(2), 664-679. (1996). https://doi.org/10.1006/dbio.1996.0336

Aberle H, Bauer A, Stappert J, Kispert A, Kemler R. Beta-catenin is a target for the ubiquitin-proteasome pathway. EMBO J 16: 3797-3804 (1997). https://doi.org/10.1093/emboj/16.13.3797

Anderson, C. T. & Stearns, T. Centriole age underlies asynchronous primary cilium growth in mammalian cells. Curr. Biol. 19, 1498-1502 (2009). https://doi.org/10.1016/j.cub.2009.07.034

Afonso, C. and Henrique, D. PAR3 acts as a molecular organizar to define the apical domain of the chick neuroepithelial cells. J Cell Sci. 119(20) 4293-4305 (2006). https://doi.org/10.1242/jcs.03170

Agalliu D, Takada S, Agalliu I, McMahon AP, Jessell TM. Motor neurons with axial muscle projections specified by Wnt4/5 signaling. Neuron. Mar 12;61(5):708-20 (2009). https://doi.org/10.1016/j.neuron.2008.12.026

Agulto RL, Rogers MM, Tan TC, Ramkumar A, Downing AM, Bodin H, Castro J, Nowakowski DW, Ori-McKenney KM. Autoregulatory control of microtubule binding in doublecortin-like kinase 1. Elife. Jul 26;10:e60126 (2021). https://doi.org/10.7554/eLife.60126

Alexandre, P., Reugels, A. M., Barker, D., Blanc, E. & Clarke, J. D. Neurons derive from the more apical daughter in asymmetric divisions in the zebrafish neural tube. Nat. Neurosci. 13, 673-679 (2010). https://doi.org/10.1038/nn.2547

Alvarez-Medina R., Cayuso J., Okubo T., Takada S., Marti E. Wnt canonical pathway restricts graded Shh/Gli patterning activity through the regulation of Gli3 expression. Development 135:237-247 (2008). https://doi.org/10.1242/dev.012054

Alvarez-Medina R., Le Dreau G., Ros M., Marti E. Hedgehog activation is required upstream of Wnt signalling to control neural progenitor proliferation. Development 136:3301-3309 (2009). https://doi.org/10.1242/dev.041772

Andersen JS, Wilkinson CJ, Mayor T, Mortensen P, Nigg EA, Mann M. Proteomic characterization of the human centrosome by protein correlation profiling. Nature. Dec 4;426(6966):570-4 (2003). https://doi.org/10.1038/nature02166

Arquint, C., Gabryjonczyk, A.M. and Nigg, E.a. Centrosome as signaling centres. Philos. Trans. R. Soc. B. Biol. Sci. 369(1650) (2014). https://doi.org/10.1098/rstb.2013.0464

Artavanis-Tsakonas S, Rand MD, Lake RJ. Notch signaling: cell fate control and signal integration in development. Science. Apr 30;284(5415):770-6 (1999) https://doi.org/10.1126/science.284.5415.770

Bruinsma W, Macurek L, Freire R, Lindqvist A, Medema RH. Bora and Aurora-A continue to activate Plk1 in mitosis. J Cell Sci. Feb 15;127(Pt 4):801-11 (2014). https://doi.org/10.1242/jcs.137216

Bahmanyar S, Kaplan DD, Deluca JG, Giddings TH Jr, O'Toole ET, Winey M, Salmon ED, Casey PJ, Nelson WJ, Barth AI. beta-Catenin is a Nek2 substrate involved in centrosome separation. Genes Dev. Jan 1;22(1):91-105 (2008). https://doi.org/10.1101/gad.1596308

Baum B, Georgiou M. Dynamics of adherens junctions in epithelial establishment, maintenance, and remodeling. J Cell Biol. Mar 21;192(6):907-17 (2011). https://doi.org/10.1083/jcb.201009141

Baye, L.M. & Link, B.A. Interkinetic nuclear migration and the selection of neurogenesis cell divisions during vertebrate retinogenesis. Journal of Neuroscience. 27(38), 10143-10152 (2007). https://doi.org/10.1523/JNEUROSCI.2754-07.2007

Behrens J, Jerchow BA, Wurtele M, Grimm J, Asbrand C, Wirtz R, Kuhl M, Wedlich D, Birchmeier W. Functional interaction of an axin homolog, conductin, with beta-catenin, APC, and GSK3beta. Science 280: 596-599 (1998). https://doi.org/10.1126/science.280.5363.596

Behrens J, von Kries JP, Kuhl M, Bruhn L, Wedlich D, Grosschedl R, Birchmeier W. Functional interaction of beta-catenin with the transcription factor LEF-1. Nature 382: 638-642 (1996). https://doi.org/10.1038/382638a0

Bernatik O., Paclikova P., Kotrbova A., Bryja V., Cajanek L. Primary Cilia Formation Does Not Rely on WNT/β-Catenin Signaling. Front Cell Dev Biol. Feb 26;9:623753 (2021). https://doi.org/10.3389/fcell.2021.623753

Bhanot P, Brink M, Samos CH, Hsieh JC, Wang Y, Macke JP, Andrew D, Nathans J, Nusse R. A new member of the frizzled family from Drosophila functions as a Wingless receptor. Nature 382: 225-230 (1996). https://doi.org/10.1038/382225a0

Blanco-Ameijeiras J., Lozano-Fernández P., Martí E. Centrosome maturation - in tune with the cell cycle. J Cell Sci. Jan 15;135(2):jcs259395 (2022). https://doi.org/10.1242/jcs.259395

Blassberg, R. et al. Sox2 levels regulate the chromatin occupancy of WNT mediators in epiblast progenitors responsible for vertebrate body formation. Nat. Cell Biol. 24, 633-644 (2022). https://doi.org/10.1038/s41556-022-00910-2

Bocanegra-Moreno, L., Singh, A., Hannezo, E., Zagorski, M. & Kicheva, A. Cell cycle dynamics control fluidity of the developing mouse neuroepithelium. Nat. Phys. 19, 1050-1058 (2023). https://doi.org/10.1038/s41567-023-01977-w

Bornens M. The centrosome in cells and organisms. Science. Jan 27;335(6067):422-6 (2012). https://doi.org/10.1126/science.1209037

Brennan, J. et al. Nodal signalling in the epiblast patterns the early mouse embryo. Nature 411, 965-969 (2001). https://doi.org/10.1038/35082103

Brunner E, Peter O, Schweizer L, Basler K. Pangolin encodes a Lef-1 homologue that acts downstream of Armadillo to transduce the Wingless signal in Drosophila. Nature 385: 829-833 (1997). https://doi.org/10.1038/385829a0

Buchman, J. J. et al. Cdk5rap2 interacts with pericentrin to maintain the neural progenitor pool in the developing neocortex. Neuron 66, 386-402 (2010). https://doi.org/10.1016/j.neuron.2010.03.036

Bultje, R. S. et al. Mammalian Par3 regulates progenitor cell asymmetric division via notch signaling in the developing neocortex. Neuron 63, 189-202 (2009). https://doi.org/10.1016/j.neuron.2009.07.004

Burt, D.W. Chicken genome: Current status and future opportunities. Genome Research. 15(12) 1692-1698 (2005) https://doi.org/10.1101/gr.4141805

Camargo Ortega, G. et al. The centrosome protein AKNA regulates neurogenesis via microtubule organization. Nature 567, 113-117 (2019). https://doi.org/10.1038/s41586-019-0962-4

Campos, L. S. et al. ß1 integrins activate a MAPK signalling pathway in neural stem cells that contributes to their maintenance. Development 131, 3433-3444 (2004). https://doi.org/10.1242/dev.01199

Canning, D. R. & Cunningham, R. L. Cell adhesion properties of neural stem cells in the chick embryo. In Vitro Cell Dev. Biol. Anim. 51, 507-514 (2015). https://doi.org/10.1007/s11626-014-9851-1

Cappello, S., Monzo, P. & Vallee, R. B. NudC is required for interkinetic nuclear migration and neuronal migration during neocortical development. Dev. Biol. 357, 326-335 (2011). https://doi.org/10.1016/j.ydbio.2011.07.001

Carneiro, A. C., Fragel-Madeira, L., Silva-Neto, M. A. & Linden, R. A role for CK2 upon interkinetic nuclear migration in the cell cycle of retinal progenitor cells. Dev. Neurobiol. 68, 620-631 (2008). https://doi.org/10.1002/dneu.20613

Caspary, T., Larkins, C. E. & Anderson, K. V. The graded response to Sonic hedgehog depends on cilia architecture. Dev. Cell 12, 767-778 (2007). https://doi.org/10.1016/j.devcel.2007.03.004

Cavallo RA, Cox RT, Moline MM, Roose J, Polevoy GA, Clevers H, Peifer M, Bejsovec A. Drosophila Tcf and Groucho interact to repress Wingless signalling activity. Nature 395: 604-608 (1998). https://doi.org/10.1038/26982

Chamberlain C.E., Jeong J., Guo C., Allen B.L., McMahon A.P. Notochord-derived Shh concentrates in close association with the apically positioned basal body in neural target cells and forms a dynamic gradient during neural patterning. Development 135:1097-1106 (2008). https://doi.org/10.1242/dev.013086

Chenn, A. et al. Intrinsic polarity of mammalian neuroepithelial cells. Molecular and cellular neurosciences, 11(4) 183-193 (1998). https://doi.org/10.1006/mcne.1998.0680

Chiang C., Litingtung Y., Lee E., Young K.E., Corden J.L., Westphal H., Beachy P.A. Cyclopia and defective axial patterning in mice lacking Sonic hedgehog gene function. Nature 383:407-413 (1996). https://doi.org/10.1038/383407a0

Chilov, D. et al. Phosphorylated ß-catenin localizes to centrosomes of neuronal progenitors and is required for cell polarity and neurogenesis in developing midbrain. Dev. Biol. 357, 259-268 (2011). https://doi.org/10.1016/j.ydbio.2011.06.029

Chinen, T. et al. Centriole and PCM cooperatively recruit CEP192 to spindle poles to promote bipolar spindle assembly. J. Cell Biol. 220, e202006085 (2021). https://doi.org/10.1083/jcb.202006085

Chizhikov, V. V. & Millen, K. J. Control of roof plate formation by Lmx1a in the developing spinal cord. Development 131, 2693-2705 (2004). https://doi.org/10.1242/dev.01139

Colas, J. F. & Schoenwolf, G. C. Towards a cellular and molecular understanding of neurulation. Dev. Dyn. 221, 117-145 (2001). https://doi.org/10.1002/dvdy.1144

Copp, A. J. et al. Regional differences in the expression of laminin isoforms during mouse neural tube development. Matrix Biol. 30, 301-309 (2011). https://doi.org/10.1016/j.matbio.2011.04.001

Corbit, K. C. et al. Vertebrate smoothened functions at the primary cilium. Nature 437, 1018-1021 (2005). https://doi.org/10.1038/nature04117

Corbit K.C., Shyer A.E., Dowdle W.E., Gaulden J., Singla V., Chen M.H., Chuang P.T., Reiter J.F. Kif3a constrains beta-catenin-dependent Wnt signalling through dual ciliary and non-ciliary mechanisms. Nat Cell Biol. Jan;10(1):70-6 (2008). https://doi.org/10.1038/ncb1670

Dale TC. Signal transduction by the Wnt family of ligands. Biochem J. Jan 15;329 (Pt 2)(Pt 2):209-23 (1998). https://doi.org/10.1042/bj3290209

Das, R. M. & Storey, K. G. Mitotic spindle orientation can direct cell fate and bias Notch activity in chick neural tube. EMBO Rep. 13, 448-454 (2012). https://doi.org/10.1038/embor.2012.42

Del Bene, F. et al. Regulation of neurogenesis by interkinetic nuclear migration through an apical-basal notch gradient. Cell. 134(6) 1055-165 (2008). https://doi.org/10.1016/j.cell.2008.07.017

Del Bene, F. et al. Assembly of functionally integrated human forebrain spheroids. Nature. 545(7652) 54-59 (2011). https://doi.org/10.1038/nature22330

del Corral, R.D. et al. Opposing FGF and retinoid pathways control ventral neural pattern, neuronal differentiation and segmentation during body axis extension. Neuron. 40(1) 65-79 (2003). https://doi.org/10.1016/S0896-6273(03)00565-8

Delaunay, D., Cortay, V., Patti, D., Knoblauch, K. & Dehay, C. Mitotic spindle asymmetry: a Wnt/PCP-regulated mechanism generating asymmetrical division in cortical precursors. Cell Rep. 6, 400-414 (2014). https://doi.org/10.1016/j.celrep.2013.12.026

Delgehyr, N., Sillibourne, J. & Bornens, M. Microtubule nucleation and anchoring at the centrosome are independent processes linked by ninein function. J. Cell Sci. 118, 1565-1575 (2005). https://doi.org/10.1242/jcs.02302

Dessaud E., McMahon A.P., Briscoe J. 2008. Pattern formation in the vertebrate neural tube: A sonic hedgehog morphogen-regulated transcriptional network. Development 135:2489-2503 (2008). https://doi.org/10.1242/dev.009324

Dessaud E., Ribes V., Balaskas N., Yang L.L., Pierani A., Kicheva A., Novitch B.G., et al. Dynamic assignment and maintenance of positional identity in the ventral neural tube by the morphogen sonic hedgehog. PLoS Biol 8:e1000382 (2010). https://doi.org/10.1371/journal.pbio.1000382

Detrick, R. J., Dickey, D. & Kintner, C. R. The effects of N-cadherin misexpression on morphogenesis in Xenopus embryos. Neuron 4, 493-506 (1990). https://doi.org/10.1016/0896-6273(90)90108-R

di Pietro, F., Echard, A. & Morin, X. Regulation of mitotic spindle orientation: an integrated view. EMBO Rep. 17, 1106-1130 (2016). https://doi.org/10.15252/embr.201642292

Dickinson M.E., Krumlauf R., McMahon A.P. Evidence for a mitogenic effect of Wnt-1 in the developing mammalian central nervous system. Development 120:1453-1471 (1994). https://doi.org/10.1242/dev.120.6.1453

Dong W, Li H, Zhang Y, Yang H, Guo M, Li L, Liu T. Matrix metalloproteinase 2 promotes cell growth and invasion in colorectal cancer. Acta Biochim Biophys Sin (Shanghai). Nov;43(11):840-8 (2011). https://doi.org/10.1093/abbs/gmr085

Drago, J., Nurcombe, V. & Bartlett, P. F. Laminin through its long arm E8 fragment promotes the proliferation and differentiation of murine neuroepithelial cells in vitro. Exp. Cell Res. 192, 256-265 (1991). https://doi.org/10.1016/0014-4827(91)90184-V

Dudley A.T., Robertson E.J. Overlapping expression domains of bone morphogenetic protein family members potentially account for limited tissue defects in BMP7 deficient embryos. Dev Dyn 208:349-362 (1997). https://doi.org/10.1002/(SICI)1097-0177(199703)208:3<349::AID-AJA6>3.3.CO;2-9

Echelard, Y. et al. Sonic hedgehog, a member of a family of putative signaling molecules, is implicated in the regulation of CNS polarity. Cell 75, 1417-1430 (1993). https://doi.org/10.1016/0092-8674(93)90627-3

Eferl R, Wagner EF. AP-1: a double-edged sword in tumorigenesis. Nat Rev Cancer. Nov;3(11):859-68 (2003). https://doi.org/10.1038/nrc1209

Epstein, D. J., Marti, E., Scott, M. P. & McMahon, A. P. Antagonizing cAMP-dependent protein kinase A in the dorsal CNS activates a conserved Sonic hedgehog signaling pathway. Development 122, 2885-2894 (1996). https://doi.org/10.1242/dev.122.9.2885

Eze, U. C., Bhaduri, A., Haeussler, M., Nowakowski, T. J. & Kriegstein, A. R. Single-cell atlas of early human brain development highlights heterogeneity of human neuroepithelial cells and early radial glia. Nat. Neurosci. 24, 584-594 (2021). https://doi.org/10.1038/s41593-020-00794-1

Faragher AJ, Fry AM. Nek2A kinase stimulates centrosome disjunction and is required for formation of bipolar mitotic spindles. Mol Biol Cell. Jul;14(7):2876-89 (2003). https://doi.org/10.1091/mbc.e03-02-0108

Fish, J. L., Kosodo, Y., Enard, W., Paabo, S. & Huttner, W. B. Aspm specifically maintains symmetric proliferative divisions of neuroepithelial cells. Proc. Natl Acad. Sci. USA 103, 10438-10443 (2006). https://doi.org/10.1073/pnas.0604066103

Flanagan, L. A., Rebaza, L. M., Derzic, S., Schwartz, P. H. & Monuki, E. S. Regulation of human neural precursor cells by laminin and integrins. J. Neurosci. Res. 83, 845-856 (2006). https://doi.org/10.1002/jnr.20778

Formosa-Jordan, P.A.U et al. Lateral inhibition and neurogénesis: Novel aspects in motion. International Journal of Developmental Biology. 57(5) 341-350 (2013) https://doi.org/10.1387/ijdb.120259jf

Fry AM, Meraldi P, Nigg EA. A centrosomal function for the human Nek2 protein kinase, a member of the NIMA family of cell cycle regulators. EMBO J. Jan 15;17(2):470-81 (1998). https://doi.org/10.1093/emboj/17.2.470

Fry AM, Schultz SJ, Bartek J, Nigg EA. Substrate specificity and cell cycle regulation of the Nek2 protein kinase, a potential human homolog of the mitotic regulator NIMA of Aspergillus nidulans. J Biol Chem. May 26;270(21):12899-905 (1995). https://doi.org/10.1074/jbc.270.21.12899

Fry AM, O'Regan L, Sabir SR, Bayliss R. Cell cycle regulation by the NEK family of protein kinases. J Cell Sci. Oct 1;125(Pt 19):4423-33 (2012). https://doi.org/10.1242/jcs.111195

Fuentealba, L. C., Eivers, E., Geissert, D., Taelman, V. & De Robertis, E. M. Asymmetric mitosis: unequal segregation of proteins destined for degradation. Proc. Natl Acad. Sci. USA 105, 7732-7737 (2008). https://doi.org/10.1073/pnas.0803027105

Galceran J, Fariñas I, Depew MJ, Clevers H, Grosschedl R. Wnt3a-/--like phenotype and limb deficiency in Lef1(-/-)Tcf1(-/-) mice. Genes Dev. Mar 15;13(6):709-17 (1999). https://doi.org/10.1101/gad.13.6.709

Galceran J, Miyashita-Lin EM, Devaney E, Rubenstein JL, Grosschedl R. Hippocampus development and generation of dentate gyrus granule cells is regulated by LEF1. Development. Feb;127(3):469-82 (2000). https://doi.org/10.1242/dev.127.3.469

Galea, G. L. et al. Biomechanical coupling facilitates spinal neural tube closure in mouse embryos. Proc. Natl Acad. Sci. USA 114, E5177-E5186 (2017). https://doi.org/10.1073/pnas.1700934114

Gallahan D, Callahan R. The mouse mammary tumor associated gene INT3 is a unique member of the NOTCH gene family (NOTCH4). Oncogene 14: 1883-1890 (1997). https://doi.org/10.1038/sj.onc.1201035

Gambello, M. J. et al. Multiple dose-dependent effects of Lis1 on cerebral cortical development. J. Neurosci. 23, 1719-1729 (2003). https://doi.org/10.1523/JNEUROSCI.23-05-01719.2003

Gao Z, Ure K, Ables JL, Lagace DC, Nave KA, Goebbels S, Eisch AJ, Hsieh J. Neurod1 is essential for the survival and maturation of adult-born neurons. Nat Neurosci. Sep;12(9):1090-2 (2009). https://doi.org/10.1038/nn.2385

Garcia-Campmany, L. and Marti, E. The TGFbeta intracellular effector Smad3 regulates neuronal differentiation and cell fate specification in the developing spinal cord. Development. 134(1) 65-75 (2007). https://doi.org/10.1242/dev.02702

Gavin BJ, McMahon JA, McMahon AP. Expression of multiple novel Wnt-1/int-1-related genes during fetal and adult mouse development. Genes Dev 4: 2319-2332 (1990). https://doi.org/10.1101/gad.4.12b.2319

Ge, X., Frank, C. L., Calderon de Anda, F. & Tsai, L. H. Hook3 interacts with PCM1 to regulate pericentriolar material assembly and the timing of neurogenesis. Neuron 65, 191-203 (2010). https://doi.org/10.1016/j.neuron.2010.01.011

Goetz S.C., Anderson K.V. The primary cilium: A signalling centre during vertebrate development. Nat Rev Genet 11:331-344 (2010). https://doi.org/10.1038/nrg2774

Goldenson B, Crispino JD. The aurora kinases in cell cycle and leukemia. Oncogene. Jan 29;34(5):537-45 (2015). https://doi.org/10.1038/onc.2014.14

Gonzalez-Gobartt, E. et al. Cell intercalation driven by SMAD3 underlies secondary neural tube formation. Dev. Cell 56, 1147-1163.e6 (2021). https://doi.org/10.1016/j.devcel.2021.03.023

Graham V, Khudyakov J, Ellis P, Pevny L. SOX2 functions to maintain neural progenitor identity. Neuron. Aug 28;39(5):749-65 (2003). https://doi.org/10.1016/S0896-6273(03)00497-5

Greene ND, Copp AJ. Neural tube defects. Annu Rev Neurosci. 37:221-42 (2014). https://doi.org/10.1146/annurev-neuro-062012-170354

Groden J, Thliveris A, Samowitz W, Carlson M, Gelbert L, Albertsen H, Joslyn G, Stevens J, Spirio L, Robertson M, Sargeant L, Krapcho K, Wolff E, Burt R, Hughes JP, Warrington J, McPherson J, Wasmuth J, Le Paslier D, Abderrahim H et al. Identification and characterization of the familial adenomatous polyposis coli gene. Cell 66: 589-600 (1991). https://doi.org/10.1016/0092-8674(81)90021-0

Gubb D, Garcia-Bellido A. A genetic analysis of the determination of cuticular polarity during development in Drosophila melanogaster. J Embryol Exp Morphol 68: 37-57 (1982). https://doi.org/10.1242/dev.68.1.37

Gurley KA, Elliott SA, Simakov O, Schmidt HA, Holstein TW, Alvarado AS. Expression of secreted Wnt pathway components reveals unexpected complexity of the planarian amputation response. Dev Biol 347: 24-39 (2010). https://doi.org/10.1016/j.ydbio.2010.08.007

Hall, P. E., Lathia, J. D., Caldwell, M. A. & Ffrench-Constant, C. Laminin enhances the growth of human neural stem cells in defined culture media. BMC Neurosci. 9, 71 (2008). https://doi.org/10.1186/1471-2202-9-71

Hamburger V, Hamilton HL. A series of normal stages in the development of the chick embryo. Dev Dyn. 1992 Dec;195(4):231-72 (1951). https://doi.org/10.1002/aja.1001950404

Hardwick LJ, Philpott A. Multi-site phosphorylation regulates NeuroD4 activity during primary neurogenesis: a conserved mechanism amongst proneural proteins. Neural Dev. Jun 18;10:15 (2015). https://doi.org/10.1186/s13064-015-0044-8

Haubensak W, Attardo A, Denk W, Huttner WB. Neurons arise in the basal neuroepithelium of the early mammalian telencephalon: a major site of neurogenesis. Proc Natl Acad Sci U S A. Mar 2;101(9):3196-201 (2004). https://doi.org/10.1073/pnas.0308600100

He TC, Sparks AB, Rago C, Hermeking H, Zawel L, da Costa LT, Morin PJ, Vogelstein B, Kinzler KW. Identification of c-MYC as a target of the APC pathway. Science 281: 1509-1512 (1998). https://doi.org/10.1126/science.281.5382.1509

Heasman J, Crawford A, Goldstone K, Garner-Hamrick P, Gumbiner B, McCrea P, Kintner C, Noro CY, Wylie C. Overexpression of cadherins and underexpression of beta-catenin inhibit dorsal mesoderm induction in early Xenopus embryos. Cell 79: 791-803 (1994). https://doi.org/10.1016/0092-8674(94)90069-8

Hecht A, Vleminckx K, Stemmler MP, van Roy F, Kemler R. The p300/CBP acetyltransferases function as transcriptional coactivators of beta-catenin in vertebrates. EMBO J. Apr 17;19(8):1839-50 (2000). https://doi.org/10.1093/emboj/19.8.1839

Herrera A, Saade M, Menendez A, Marti E, Pons S. Sustained Wnt/β-catenin signalling causes neuroepithelial aberrations through the accumulation of aPKC at the apical pole. Nat Commun. Jun 19;5:4168 (2014). https://doi.org/10.1038/ncomms5168

Hillier, L.W. et al. Sequence and comparative analysis of the chicken genome provide unique perspectives on vertebrate evolution. Nature, 432(7018) 695-716 (2004). https://doi.org/10.1038/nature03154

Hiraga, K. et al. Redundant type II cadherins define neuroepithelial cell states for cytoarchitectonic robustness. Commun. Biol. 3, 574 (2020). https://doi.org/10.1038/s42003-020-01297-2

Hogan B.L. Bone morphogenetic proteins in development. Curr Opin Genet Dev 6:432-438 (1996). https://doi.org/10.1016/S0959-437X(96)80064-5

Hollyday M., McMahon J.A., McMahon A.P. Wnt expression patterns in chick embryo nervous system. Mech Dev 52:9-25 (1995). https://doi.org/10.1016/0925-4773(95)00385-E

Holstein T. The evolution of the Wnt pathway. Cold Spring Harb Perspect Biol (in press) (2012). https://doi.org/10.1101/cshperspect.a007922

Hong, E. & Brewster, R. N-cadherin is required for the polarized cell behaviors that drive neurulation in the zebrafish. Development 133, 3895-3905 (2006). https://doi.org/10.1242/dev.02560

Honorato RV, Trellet ME, Jiménez-García B, Schaarschmidt JJ, Giulini M, Reys V, Koukos PI, Rodrigues JPGLM, Karaca E, van Zundert GCP, Roel-Touris J, van Noort CW, Jandová Z, Melquiond ASJ, Bonvin AMJJ. The HADDOCK2.4 web server for integrative modeling of biomolecular complexes. Nat Protoc. Nov;19(11):3219-3241 (2024). https://doi.org/10.1038/s41596-024-01011-0

Honorato RV, Koukos PI, Jiménez-García B, Tsaregorodtsev A, Verlato M, Giachetti A, Rosato A, Bonvin AMJJ. Structural Biology in the Clouds: The WeNMR-EOSC Ecosystem. Front Mol Biosci. Jul 28;8:729513 (2021). https://doi.org/10.3389/fmolb.2021.729513

Hu, D.J. et al. Dynein recruitment to nuclear pores activates apical nuclear migration and mitotic entry in brain progenitors cells. Cell. 154(6) 1300-1313 (2013). https://doi.org/10.1016/j.cell.2013.08.024

Hu Q., Ueno N., Behringer R.R. Restriction of BMP4 activity domains in the developing neural tube of the mouse embryo. EMBO Rep 5:734-739 (2004). https://doi.org/10.1038/sj.embor.7400184

Huang C, Chan JA, Schuurmans C. Proneural bHLH genes in development and disease. Curr Top Dev Biol.110:75-127 (2014). https://doi.org/10.1016/B978-0-12-405943-6.00002-6

Huang P, Senga T, Hamaguchi M. A novel role of phospho-beta-catenin in microtubule regrowth at centrosome. Oncogene. Jun 28;26(30):4357-71 (2007). https://doi.org/10.1038/sj.onc.1210217

Huangfu, D. et al. Hedgehog signalling in the mouse requires intraflagellar transport proteins. Nature 426, 83-87 (2003). https://doi.org/10.1038/nature02061

Huangfu, D. & Anderson, K. V. Cilia and hedgehog responsiveness in the mouse. Proc. Natl Acad. Sci. USA 102, 11325-11330 (2005). https://doi.org/10.1073/pnas.0505328102

Hwang, S. H. & Mukhopadhyay, S. G-protein-coupled receptors and localized signaling in the primary cilium during ventral neural tube patterning. Birth Defects Res. A Clin. Mol. Teratol. 103, 12-19 (2015). https://doi.org/10.1002/bdra.23267

Iacopetti P, Michelini M, Stuckmann I, Oback B, Aaku-Saraste E, Huttner WB. Expression of the antiproliferative gene TIS21 at the onset of neurogenesis identifies single neuroepithelial cells that switch from proliferative to neuron-generating division. Proc Natl Acad Sci U S A. Apr 13;96(8):4639-44 (1999). https://doi.org/10.1073/pnas.96.8.4639

Ikeda S, Kishida S, Yamamoto H, Murai H, Koyama S, Kikuchi A. Axin, a negative regulator of the Wnt signaling pathway, forms a complex with GSK-3beta and beta-catenin and promotes GSK-3beta-dependent phosphorylation of beta-catenin. EMBO J 17: 1371-1384 (1998). https://doi.org/10.1093/emboj/17.5.1371

Ikeya M, Lee SM, Johnson JE, McMahon AP, Takada S. Wnt signalling required for expansion of neural crest and CNS progenitors. Nature. Oct 30;389(6654):966-70 (1997). https://doi.org/10.1038/40146

Ingham P.W., Nakano Y., Seger C. Mechanisms and functions of Hedgehog signalling across the metazoa. Nat Rev Genet 12:393-406 (2011). https://doi.org/10.1038/nrg2984

Insolera, R., Bazzi, H., Shao, W., Anderson, K. V. & Shi, S. H. Cortical neurogenesis in the absence of centrioles. Nat. Neurosci. 17, 1528-1535 (2014). https://doi.org/10.1038/nn.3831

Ishii, Y. & Mikasa, T. Somatic transgenesis in the avian model system. Birth Defects Research Part C: Embryo Today: Reviews. 75(1) 19-27 (2005). https://doi.org/10.1002/bdrc.20033

Itasaki, N., Bel-Vialar, S. & Krumlauf, R. Shocking developments in chick embryology: electroporation and in ovo gene expression. Nature Cell Biology. 1(8) E203-E207 (1999). https://doi.org/10.1038/70231

Jayaraman, D. et al. Microcephaly proteins Wdr62 and Aspm define a mother centriole complex regulating centriole biogenesis, apical complex, and cell fate. Neuron 92, 813-828 (2016). https://doi.org/10.1016/j.neuron.2016.09.056

Jayaraman, D., Bae, B.-I. and Walsh, C.A. The generics of primary Microcephaly. Annual Review of Genomics and Human Genetics (19) 177-200 (2018). https://doi.org/10.1146/annurev-genom-083117-021441

Jho EH, Zhang T, Domon C, Joo CK, Freund JN, Costantini F. Wnt/beta-catenin/Tcf signaling induces the transcription of Axin2, a negative regulator of the signaling pathway. Mol Cell Biol. Feb;22(4):1172-83 (2002). https://doi.org/10.1128/MCB.22.4.1172-1183.2002

Jiang, X. et al. Condensation of pericentrin proteins in human cells illuminates phase separation in centrosome assembly. J. Cell Sci. 134, jcs258897 (2021). https://doi.org/10.1242/jcs.258897

Kaplan DD, Meigs TE, Kelly P, Casey PJ. Identification of a role for beta-catenin in the establishment of a bipolar mitotic spindle. J Biol Chem. Mar 19;279(12):10829-32 (2004). https://doi.org/10.1074/jbc.C400035200

Katayama, K. et al. Loss of RhoA in neural progenitor cells causes the disruption of adherens junctions and hyperproliferation. Proc. Natl Acad. Sci. USA 108, 7607-7612 (2011). https://doi.org/10.1073/pnas.1101347108

Keller, R., Shook, D., Skoglund, P. The forces that shape embryos: physical aspects of convergent extension by cell intercalation. Phys Biol. Apr 10;5(1) (2008). https://doi.org/10.1088/1478-3975/5/1/015007

Kim HS, Dorsky RI. Tcf7l1 is required for spinal cord progenitor maintenance. Dev Dyn. Oct;240(10):2256-64 (2011). https://doi.org/10.1002/dvdy.22716

Kimelman D, Christian JL, Moon RT. Synergistic principles of development: overlapping patterning systems in Xenopus mesoderm induction. Development 116: 1-9 (1992). https://doi.org/10.1242/dev.116.1.1

Kimura-Yoshida, C. et al. Canonical Wnt signaling and its antagonist regulate anterior-posterior axis polarization by guiding cell migration in mouse visceral endoderm. Dev. Cell 9, 639-650 (2005). https://doi.org/10.1016/j.devcel.2005.09.011

Kinzler KW, Nilbert MC, Su LK, Vogelstein B, Bryan TM, Levy DB, Smith KJ, Preisinger AC, Hedge P, McKechnie D, Finniear R, Markham A, Groffen J, Boguski M, Altschul S, Horii A, Ano H, Miyoshi Y, Miki Y, Nishsho I et al. Identification of FAP locus genes from chromosome 5q21. Science 253: 661-665 (1991). https://doi.org/10.1126/science.1651562

Klena, N. & Pigino, G. Structural biology of cilia and intraflagellar transport. Annu. Rev. Cell Dev. Biol. 38, 103-123 (2022). https://doi.org/10.1146/annurev-cellbio-120219-034238

Kolligs FT, Hu G, Dang CV, Fearon ER. Neoplastic transformation of RK3E by mutant beta-catenin requires deregulation of Tcf/Lef transcription but not activation of c-myc expression. Mol Cell Biol. Aug;19(8):5696-706 (1999). https://doi.org/10.1128/MCB.19.8.5696

Konno, D. et al. Neuroepithelial progenitors undergo LGN-dependent planar divisions to maintain self-renewability during mammalian neurogenesis. Nat. Cell Biol. 10, 93-101 (2008). https://doi.org/10.1038/ncb1673

Korinek V, Barker N, Morin PJ, van Wichen D, de Weger R, Kinzler KW, Vogelstein B, Clevers H. Constitutive transcriptional activation by a beta-catenin-Tcf complex in APC-/- colon carcinoma. Science 275: 1784-1787 (1997). https://doi.org/10.1126/science.275.5307.1784

Korinek V, Barker N, Willert K, Molenaar M, Roose J, Wagenaar G, Markman M, Lamers W, Destree O, Clevers H. Two members of the Tcf family implicated in Wnt/beta-catenin signaling during embryogenesis in the mouse. Mol Cell Biol. Mar;18(3):1248-56 (1998). https://doi.org/10.1128/MCB.18.3.1248

Kosodo, Y. et al. Cytokinesis of neuroepithelial cells can divide their basal process before anaphase. EMBO J. 27, 3151-3163 (2008). https://doi.org/10.1038/emboj.2008.227

Kosodo, Y. et al. Asymmetric distribution of the apical plasma membrane during neurogenic divisions of mammalian neuroepithelial cells. EMBO J. 23, 2314-2324 (2004). https://doi.org/10.1038/sj.emboj.7600223

Kosodo, Y. et al. Regulation of interkinetic nuclear migration by cell cycle-coupled active and passive mechanisms in the developing brain. EMBO J. 30, 1690-1704 (2011). https://doi.org/10.1038/emboj.2011.81

Kusserow A, Pang K, Sturm C, Hrouda M, Lentfer J, Schmidt HA, Technau U, von Haeseler A, Hobmayer B, Martindale MQ, Holstein TW. Unexpected complexity of the Wnt gene family in a sea anemone. Nature 433: 156-160 (2005). https://doi.org/10.1038/nature03158

Kwon, M., Bagonis, M., Danuser, G. & Pellman, D. Direct microtubule-binding by myosin-10 orients centrosomes toward retraction fibers and subcortical actin clouds. Dev. Cell 34, 323-337 (2015). https://doi.org/10.1016/j.devcel.2015.06.013

Kyun ML, Kim SO, Lee HG, Hwang JA, Hwang J, Soung NK, Cha-Molstad H, Lee S, Kwon YT, Kim BY, Lee KH. Wnt3a Stimulation Promotes Primary Ciliogenesis through β-Catenin Phosphorylation-Induced Reorganization of Centriolar Satellites. Cell Rep. Feb 4;30(5):1447-1462 (2020). https://doi.org/10.1016/j.celrep.2020.01.019

LaMonica, B. E., Lui, J. H., Hansen, D. V. & Kriegstein, A. R. Mitotic spindle orientation predicts outer radial glial cell generation in human neocortex. Nat. Commun. 4, 1665 (2013). https://doi.org/10.1038/ncomms2647

Lancaster M.A., Schroth J., Gleeson J.G. Subcellular spatial regulation of canonical Wnt signalling at the primary cilium. Nat Cell Biol 13:700-707 (2011). https://doi.org/10.1038/ncb2259

Lancaster MA, Schroth J, Gleeson JG. Subcellular spatial regulation of canonical Wnt signaling at the primary cilium. Nat Cell Biol. Jun;13(6):700-7 (2011). https://doi.org/10.1038/ncb2259

Lancaster MA, Gleeson JG. The primary cilium as a cellular signaling center: lessons from disease. Curr Opin Genet Dev. Jun;19(3):220-9 (2009). https://doi.org/10.1016/j.gde.2009.04.008

Langman, J., Guerrant, R.L. and Freeman, B.G. Behavior of neuro-epithelial cells during closure of the neural tube. J. Comp. Neurol. 127, 399-411 (1966). https://doi.org/10.1002/cne.901270308

Lawo, S., Hasegan, M., Gupta, G. D. & Pelletier, L. Subdiffraction imaging of centrosomes reveals higher-order organizational features of pericentriolar material. Nat. Cell Biol. 14, 1148-1158 (2012). https://doi.org/10.1038/ncb2591

Le Dreau, G. et al. Canonical BMP7 activity is required for the generation of discrete neuronal populations in the dorsal spinal cord. Development 139, 259-268 (2012). https://doi.org/10.1242/dev.074948

Le Dréau G., Martí E. Dorsal-ventral patterning of the neural tube: a tale of three signals. Dev Neurobiol. Dec;72(12):1471-81 (2012). https://doi.org/10.1002/dneu.22015

Le Dreau, G. & Marti, E. The multiple activities of BMPs during spinal cord development. Cell. Mol. Life Sci. 70, 4293-4305 (2013). https://doi.org/10.1007/s00018-013-1354-9

Le Dreau, G., Saade, M., Gutierrez-Vallejo, I. & Marti, E. The strength of SMAD1/5 activity determines the mode of stem cell division in the developing spinal cord. J. Cell Biol. 204, 591-605 (2014). https://doi.org/10.1083/jcb.201307031

Lee, K. J., Dietrich, P. & Jessell, T. M. Genetic ablation reveals that the roof plate is essential for dorsal interneuron specification. Nature 403, 734-740 (2000). https://doi.org/10.1038/35001507

Lee E, Salic A, Kruger R, Heinrich R, Kirschner MW. The roles of APC and Axin derived from experimental and theoretical analysis of the Wnt pathway. PLoS Biol 1: E10 (2003). https://doi.org/10.1371/journal.pbio.0000010

Lee K.J., Mendelsohn M., Jessell T.M. Neuronal patterning by BMPs: A requirement for GDF7 in the generation of a discrete class of commissural interneurons in the mouse spinal cord. Genes Dev 12:3394-3407 (1998). https://doi.org/10.1101/gad.12.21.3394

Leone, D. P. et al. Regulation of neural progenitor proliferation and survival by β1 integrins. J. Cell Sci. 118, 2589-2599 (2005). https://doi.org/10.1242/jcs.02396

Lera RF, Burkard ME. High mitotic activity of Polo-like kinase 1 is required for chromosome segregation and genomic integrity in human epithelial cells. J Biol Chem. Dec 14;287(51):42812-25 (2012). https://doi.org/10.1074/jbc.M112.412544

Li X.J., Zhang X., Johnson M.A., Wang Z.B., Lavaute T., Zhang S.C. Coordination of sonic hedgehog and Wnt signaling determines ventral and dorsal telencephalic neuron types from human embryonic stem cells. Development 136:4055-4063 (2009). https://doi.org/10.1242/dev.036624

Liem, K.F., Tremml, G.and Jessell, T.M. A role for the roof plate and its resident TGF-β-related proteins in neuronal patterning in the dorsal spinal cord. Cell. 91(1) 127-138 (1997). https://doi.org/10.1016/S0092-8674(01)80015-5

Liem K.F. Jr., Tremml G., Roelink H., Jessell T.M. Dorsal differentiation of neural plate cells induced by BMP-mediated signals from epidermal ectoderm. Cell 82:969-979 (1995) https://doi.org/10.1016/0092-8674(95)90276-7

Liu, W. A. et al. PARD3 dysfunction in conjunction with dynamic HIPPO signaling drives cortical enlargement with massive heterotopia. Genes Dev. 32, 763-780 (2018). https://doi.org/10.1101/gad.313171.118

Liu, A., Wang, B. & Niswander, L. A. Mouse intraflagellar transport proteins regulate both the activator and repressor functions of Gli transcription factors. Development 132, 3103-3111 (2005). https://doi.org/10.1242/dev.01894

Liu C, Kato Y, Zhang Z, Do VM, Yankner BA, He X. beta-Trcp couples beta-catenin phosphorylation-degradation and regulates Xenopus axis formation. Proc Natl Acad Sci U S A. May 25;96(11):6273-8 (1999). https://doi.org/10.1073/pnas.96.11.6273

Long, K., Moss, L., Laursen, L., Boulter, L. & Ffrench-Constant, C. Integrin signalling regulates the expansion of neuroepithelial progenitors and neurogenesis via Wnt7a and Decorin. Nat. Commun. 7, 10354 (2016). https://doi.org/10.1038/ncomms10354

Long, K. R. & Huttner, W. B. How the extracellular matrix shapes neural development. Open Biol. 9, 180216 (2019). https://doi.org/10.1098/rsob.180216

Lustig B, Jerchow B, Sachs M, Weiler S, Pietsch T, Karsten U, van de Wetering M, Clevers H, Schlag PM, Birchmeier W, Behrens J. Negative feedback loop of Wnt signaling through upregulation of conductin/axin2 in colorectal and liver tumors. Mol Cell Biol. Feb;22(4):1184-93 (2002). https://doi.org/10.1128/MCB.22.4.1184-1193.2002

Lyons K.M., Hogan B.L., Robertson E.J. Colocalization of BMP 7 and BMP 2 RNAs suggests that these factors cooperatively mediate tissue interactions during murine development. Mech Dev 50:71-83 (1995). https://doi.org/10.1016/0925-4773(94)00326-I

Ma, W. et al. Cell-extracellular matrix interactions regulate neural differentiation of human embryonic stem cells. BMC Dev. Biol. 8, 90 (2008). https://doi.org/10.1186/1471-213X-8-90

Ma L, Wang Y, Hui Y, Du Y, Chen Z, Feng H, Zhang S, Li N, Song J, Fang Y, Xu X, Shi L, Zhang B, Cheng J, Zhou S, Liu L, Zhang X. WNT/NOTCH Pathway Is Essential for the Maintenance and Expansion of Human MGE Progenitors. Stem Cell Reports. May 14;12(5):934-949 (2019). https://doi.org/10.1016/j.stemcr.2019.04.007

Machon O, van den Bout CJ, Backman M, Kemler R, Krauss S. Role of beta-catenin in the developing cortical and hippocampal neuroepithelium. Neuroscience.122(1):129-43 (2003). https://doi.org/10.1016/S0306-4522(03)00519-0

Macůrek L, Lindqvist A, Lim D, Lampson MA, Klompmaker R, Freire R, Clouin C, Taylor SS, Yaffe MB, Medema RH. Polo-like kinase-1 is activated by aurora A to promote checkpoint recovery. Nature. Sep 4;455(7209):119-23 (2008). https://doi.org/10.1038/nature07185

Marti, E., Takada, R., Bumcrot, D. A., Sasaki, H. & McMahon, A. P. Distribution of Sonic hedgehog peptides in the developing chick and mouse embryo. Development 121, 2537-2547 (1995a). https://doi.org/10.1242/dev.121.8.2537

Marti, E., Bumcrot, D. A., Takada, R. & McMahon, A. P. Requirement of 19 K form of Sonic hedgehog for induction of distinct ventral cell types in CNS explants. Nature 375, 322-325 (1995b). https://doi.org/10.1038/375322a0

Martiens, V. and Ffrench-Constant, C. Adherens junction domains are split by asymmetric division of embryonic neural stem cells. EMBO Rep. 10(5) 515-520 (2009). https://doi.org/10.1038/embor.2009.36

Martins-Green, M. Origin of the dorsal surface of the neural tube by progressive delamination of epidermal ectoderm and neuroepithelium: implications for neurulation and neural tube defects. Development 103, 687-706 (1988). https://doi.org/10.1242/dev.103.4.687

Martins-Green, M. & Erickson, C. A. Development of neural tube basal lamina during neurulation and neural crest cell emigration in the trunk of the mouse embryo. J. Embryol. Exp. Morphol. 98, 219-236 (1986). https://doi.org/10.1242/dev.98.1.219

May, S. R. et al. Loss of the retrograde motor for IFT disrupts localization of Smo to cilia and prevents the expression of both activator and repressor functions of Gli. Dev. Biol. 287, 378-389 (2005). https://doi.org/10.1016/j.ydbio.2005.08.050

Mbom BC, Siemers KA, Ostrowski MA, Nelson WJ, Barth AI. Nek2 phosphorylates and stabilizes β-catenin at mitotic centrosomes downstream of Plk1. Mol Biol Cell. Apr;25(7):977-91 (2014). https://doi.org/10.1091/mbc.e13-06-0349

McCrea PD, Brieher WM, Gumbiner BM. Induction of a secondary body axis in Xenopus by antibodies to beta-catenin. J Cell Biol 123: 477-484 (1993). https://doi.org/10.1083/jcb.123.2.477

McCrea PD, Turck CW, Gumbiner B. A homolog of the armadillo protein in Drosophila (plakoglobin) associated with E-cadherin. Science 254: 1359-1361 (1991). https://doi.org/10.1126/science.1962194

McMahon A.P., Bradley A. The Wnt-1 (int-1) proto-oncogene is required for development of a large region of the mouse brain. Cell 62: 1073-1085 (1990). https://doi.org/10.1016/0092-8674(90)90385-R

McMahon A.P. & Moon R.T. Ectopic expression of the proto-oncogene int-1 in Xenopus embryos leads to duplication of the embryonic axis. Cell 58: 1075-1084 (1989). https://doi.org/10.1016/0092-8674(89)90506-0

Megason S.G., McMahon A.P. A mitogen gradient of dorsal midline Wnts organizes growth in the CNS. Development 129:2087-2098 (2002). https://doi.org/10.1242/dev.129.9.2087

Meno, C. et al. Left-right asymmetric expression of the TGFβ-family member lefty inmouse embryos. Nature 381, 151-155 (1996). https://doi.org/10.1038/381151a0

Merrill BJ, Pasolli HA, Polak L, Rendl M, García-García MJ, Anderson KV, Fuchs E. Tcf3: a transcriptional regulator of axis induction in the early embryo. Development. Jan;131(2):263-74 (2004). https://doi.org/10.1242/dev.00935

Metzis, V. et al. Nervous system regionalization entails axial allocation before neural differentiation. Cell 175, 1105-1118.e17 (2018). https://doi.org/10.1016/j.cell.2018.09.040

Millonig J.H., Millen K.J., Hatten M.E. The mouse Dreher gene Lmx1a controls formation of the roof plate in the vertebrate CNS. Nature 403:764-769 (2000) https://doi.org/10.1038/35001573

Miyabayashi T, Teo JL, Yamamoto M, McMillan M, Nguyen C, Kahn M. Wnt/beta-catenin/CBP signaling maintains long-term murine embryonic stem cell pluripotency. Proc Natl Acad Sci U S A. Mar 27;104(13):5668-73 (2007). https://doi.org/10.1073/pnas.0701331104

Mole, M. A., Weberling, A. & Zernicka-Goetz, M. Comparative analysis of human andmouse development: from zygote to pre-gastrulation. Curr. Top. Dev. Biol. 136, 113-138 (2020). https://doi.org/10.1016/bs.ctdb.2019.10.002

Mole, M. A. et al. A single cell characterisation of human embryogenesis identifies pluripotency transitions and putative anterior hypoblast centre. Nat. Commun. 12, 3679 (2021). https://doi.org/10.1038/s41467-021-23758-w

Mole, M. A. et al. Integrin-mediated focal anchorage drives epithelial zippering during mouse neural tube closure. Dev. Cell 52, 321-334.e6 (2020). https://doi.org/10.1016/j.devcel.2020.01.012

Molenaar M, van de Wetering M, Oosterwegel M, Peterson-Maduro J, Godsave S, Korinek V, Roose J, Destree O, Clevers H. XTcf-3 transcription factor mediates beta-catenin-induced axis formation in Xenopus embryos. Cell 86: 391-399 (1996). https://doi.org/10.1016/S0092-8674(00)80112-9

Molina, A. and Pituello, F. Playing with the cell cycle to build the spinal cord. Dev. Biol, 432(1), 14-23 (2017). https://doi.org/10.1016/j.ydbio.2016.12.022

Mora-Bermudez, F., Matsuzaki, F. & Huttner, W. B. Specific polar subpopulations of astral microtubules control spindle orientation and symmetric neural stem cell division. eLife 3, e02875 (2014). https://doi.org/10.7554/eLife.02875

Morandi A, Barbetti V, Riverso M, Dello Sbarba P, Rovida E. The colony-stimulating factor-1 (CSF-1) receptor sustains ERK1/2 activation and proliferation in breast cancer cell lines. PLoS One. 6(11):e27450 (2011). https://doi.org/10.1371/journal.pone.0027450

Morin, X. & Bellaiche, Y. Mitotic spindle orientation in asymmetric and symmetric cell divisions during animal development. Dev. Cell 21, 102-119 (2011). https://doi.org/10.1016/j.devcel.2011.06.012

Morin PJ, Sparks AB, Korinek V, Barker N, Clevers H, Vogelstein B, Kinzler KW. Activation of b-catenin-Tcf signaling in colon cancer by mutations in b-catenin or APC. Science 275: 1787-1790 (1997). https://doi.org/10.1126/science.275.5307.1787

Morin V, Véron N, Marcelle C. CRISPR/Cas9 in the Chicken Embryo. Methods Mol Biol. 1650:113-123 (2017). https://doi.org/10.1007/978-1-4939-7216-6_7

Muller, F. & O'Rahilly, R. The development of the human brain, the closure of the caudal neuropore, and the beginning of secondary neurulation at stage 12. Anat. Embryol. 176, 413-430 (1987). https://doi.org/10.1007/BF00310083

Murciano et al. Interkinetic nuclear movement may provide spatial cues to the regulation of neurogenesis. Moecular and Cellular Neuroscience. 21(2) 285-300 (2002). https://doi.org/10.1006/mcne.2002.1174

Muroyama, Y., Fujihara, M., Ikeya, M., Kondoh, H. & Takada, S. Wnt signaling plays an essential role in neuronal specification of the dorsal spinal cord. Genes Dev. 16, 548-553 (2002). https://doi.org/10.1101/gad.937102

Muroyama Y, Fujihara M, Ikeya M, Kondoh H, Takada S. Wnt signaling plays an essential role in neuronal specification of the dorsal spinal cord. Genes Dev. Mar 1;16(5):548-53 (2002). https://doi.org/10.1101/gad.937102

Najas, S. et al. A SMAD1/5-YAP signalling module drives radial glia self-amplification and growth of the developing cerebral cortex. Development 147, dev187005 (2020). https://doi.org/10.1242/dev.187005

Nano, M. & Basto, R. Consequences of cenrtrosome dysfunction during brain development. Adv exp Med Biol, 1002, 19.45 (2017). https://doi.org/10.1007/978-3-319-57127-0_2

Niehrs C. On growth and form: a Cartesian coordinate system of Wnt and BMP signaling specifies bilaterian body axes. Development (Cambridge, England) 137: 845-857 (2010). https://doi.org/10.1242/dev.039651

Nigg EA, Raff JW. Centrioles, centrosomes, and cilia in health and disease. Cell. Nov 13;139(4):663-78 (2009). https://doi.org/10.1016/j.cell.2009.10.036

Noordermeer J, Klingensmith J, Perrimon N, Nusse R. dishevelled and armadillo act in the wingless signalling pathway in Drosophila. Nature 367: 80-83 (1994). https://doi.org/10.1038/367080a0

Nosaka T, Kawashima T, Misawa K, Ikuta K, Mui AL, Kitamura T. STAT5 as a molecular regulator of proliferation, differentiation and apoptosis in hematopoietic cells. EMBO J. Sep 1;18(17):4754-65 (1999). https://doi.org/10.1093/emboj/18.17.4754

Novitch, B.G. et al. A requirement for retinoic acid-mediated transcriptional activation in ventral neural patterning and motor neuron specification. Neuron. 40(1) 81-95 (2003). https://doi.org/10.1016/j.neuron.2003.08.006

Nusse R, Varmus H. Three decades of Wnts: a personal perspective on how a scientific field developed. EMBO J. Jun 13;31(12):2670-84 (2012). https://doi.org/10.1038/emboj.2012.146

Nusse R., Varmus H.E. Many tumors induced by the mouse mammary tumor virus contain a provirus integrated in the same region of the host genome. Cell 31: 99-109 (1982). https://doi.org/10.1016/0092-8674(82)90409-3

Nusse R., Brown A., Papkoff J., Scambler P., Shackleford G., McMahon A., Moon R., Varmus H. A new nomenclature for int-1 and related genes: the Wnt gene family. Cell 64: 231 (1991). https://doi.org/10.1016/0092-8674(91)90633-A

Oda H, Takeichi M. Evolution: structural and functional diversity of cadherin at the adherens junction. J Cell Biol. Jun 27;193(7):1137-46 (2011). https://doi.org/10.1083/jcb.201008173

Okano HJ, Darnell RB. A hierarchy of Hu RNA binding proteins in developing and adult neurons. J Neurosci. May 1;17(9):3024-37 (1997). https://doi.org/10.1523/JNEUROSCI.17-09-03024.1997

Okuda T, van Deursen J, Hiebert SW, Grosveld G, Downing JR. AML1, the target of multiple chromosomal translocations in human leukemia, is essential for normal fetal liver hematopoiesis. Cell. Jan 26;84(2):321-30 (1996). https://doi.org/10.1016/S0092-8674(00)80986-1

Orford K, Crockett C, Jensen JP, Weissman AM, Byers SW .Serine phosphorylation-regulated ubiquitination and degradation of beta-catenin. J Biol Chem 272: 24735-24738 (1997). https://doi.org/10.1074/jbc.272.40.24735

Otero JJ, Fu W, Kan L, Cuadra AE, Kessler JA. Beta-catenin signaling is required for neural differentiation of embryonic stem cells. Development. Aug;131(15):3545-57 (2004). https://doi.org/10.1242/dev.01218

Panhuysen M, Vogt Weisenhorn DM, Blanquet V, Brodski C, Heinzmann U, Beisker W, Wurst W. Effects of Wnt1 signaling on proliferation in the developing mid-/hindbrain region. Mol Cell Neurosci. May;26(1):101-11 (2004). https://doi.org/10.1016/j.mcn.2004.01.011

Paridaen, J. T., Wilsch-Brauninger, M. & Huttner, W. B. Asymmetric inheritance of centrosome-associated primary cilium membrane directs ciliogenesis after cell division. Cell 155, 333-344 (2013). https://doi.org/10.1016/j.cell.2013.08.060

Parr B.A., Shea M.J., Vassileva G., McMahon A.P. Mouse Wnt genes exhibit discrete domains of expression in the early embryonic CNS and limb buds. Development 119:247-261 (1993). https://doi.org/10.1242/dev.119.1.247

Patten, I. & Placzek, M. Opponent activities of Shh and BMP signaling during floor plate induction in vivo. Curr. Biol. 12, 47-52 (2002). https://doi.org/10.1016/S0960-9822(01)00631-5

Peifer M, Wieschaus E. The segment polarity gene armadillo encodes a functionally modular protein that is the Drosophila homolog of human plakoglobin. Cell 63: 1167-1176 (1990). https://doi.org/10.1016/0092-8674(90)90413-9

Peifer M, Rauskolb C, Williams M, Riggleman B, Wieschaus E. The segment polarity gene armadillo interacts with the wingless signaling pathway in both embryonic and adult pattern formation. Development 111: 1029-1043 (1991). https://doi.org/10.1242/dev.111.4.1029

Perea-Gomez, A. et al. Nodal antagonists in the anterior visceral endoderm prevent theformation of multiple primitive streaks. Dev. Cell 3, 745-756 (2002). https://doi.org/10.1016/S1534-5807(02)00321-0

Perrimon N, Mahowald AP. Multiple functions of segment polarity genes in Drosophila. Dev Biol 119: 587-600 (1987). https://doi.org/10.1016/0012-1606(87)90061-3

Petersen CP, Reddien PW. Wnt signaling and the polarity of the primary body axis. Cell 139: 1056-1068 (2009). https://doi.org/10.1016/j.cell.2009.11.035

Pituello, F., Yamada, G. and Gruss, P. activin A inhibits Pax-6 expression and perturbs cell differentiation in the developing spinal cord in vitro. Proceedings of the national Academy of Sciences of the United States of America. 92(15), 6952-6956 (1995). https://doi.org/10.1073/pnas.92.15.6952

Placzek, M., Tessier-Lavigne, M., Yamada, T., Jessell, T. & Dodd, J. Mesodermal control of neural cell identity: floor plate induction by the notochord. Science 250, 985-988 (1990). https://doi.org/10.1126/science.2237443

Pyrgaki, C., Trainor, P., Hadjantonakis, A. K. & Niswander, L. Dynamic imaging of mammalian neural tube closure. Dev. Biol. 344, 941-947 (2010). https://doi.org/10.1016/j.ydbio.2010.06.010

Ramkumar A, Jong BY, Ori-McKenney KM. ReMAPping the microtubule landscape: How phosphorylation dictates the activities of microtubule-associated proteins. Dev Dyn. Jan;247(1):138-155 (2018). https://doi.org/10.1002/dvdy.24599

Ribes V., Briscoe J. Establishing and interpreting graded Sonic Hedgehog signaling during vertebrate neural tube patterning: The role of negative feedback. Cold Spring Harb Perspect Biol 1:a002014 (2009). https://doi.org/10.1101/cshperspect.a002014

Riese J, Yu X, Munnerlyn A, Eresh S, Hsu SC, Grosschedl R, Bienz M. LEF-1, a nuclear factor coordinating signaling inputs from wingless and decapentaplegic. Cell 88: 777-787 (1997). https://doi.org/10.1016/S0092-8674(00)81924-8

Rijsewijk F., Schuermann M., Wagenaar E., Parren P., Weigel D., Nusse R. The Drosophila homolog of the mouse mammary oncogene int-1 is identical to the segment polarity gene wingless. Cell 50: 649-657 (1987a). https://doi.org/10.1016/0092-8674(87)90038-9

Rios I, Alvarez-Rodríguez R, Martí E, Pons S. Bmp2 antagonizes sonic hedgehog-mediated proliferation of cerebellar granule neurones through Smad5 signalling. Development. Jul;131(13):3159-68 (2004). https://doi.org/10.1242/dev.01188

Robertson C.P., Braun M.M., Roelink H. Sonic hedgehog patterning in chick neural plate is antagonized by a Wnt3-like signal. Dev Dyn 229:510-519 (2004). https://doi.org/10.1002/dvdy.10501

Rocheleau CE, Downs WD, Lin R, Wittmann C, Bei Y, Cha YH, Ali M, Priess JR, Mello CC. Wnt signaling and an APC-related gene specify endoderm in early C. elegans embryos. Cell 90: 707-716 (1997). https://doi.org/10.1016/S0092-8674(00)80531-0

Roelink H, Wagenaar E, Lopes da Silva S, Nusse R. Wnt-3, a gene activated by proviral insertion in mouse mammary tumors, is homologous to int-1/Wnt-1 and is normally expressed in mouse embryos and adult brain. Proc Natl Acad Sci USA 87: 4519-4523 (1990). https://doi.org/10.1073/pnas.87.12.4519

Roelink H., Porter J.A., Chiang C., Tanabe Y., Chang D.T., Beachy P.A., Jessell T.M. Floor plate and motor neuron induction by different concentrations of the aminoterminal cleavage product of sonic hedgehog autoproteolysis. Cell 81:445-455 (1995). https://doi.org/10.1016/0092-8674(95)90397-6

Rohatgi, R., Milenkovic, L. & Scott, M. P. Patched1 regulates hedgehog signaling at the primary cilium. Science 317, 372-376 (2007). https://doi.org/10.1126/science.1139740

Roszko, I., Afonso, C., Henrique, D. & Mathis, L. Key role played by RhoA in the balance between planar and apico-basal cell divisions in the chick neuroepithelium. Dev. Biol. 298, 212-224 (2006). https://doi.org/10.1016/j.ydbio.2006.06.031

Royall, L. N., Machado, D., Jessberger, S. & Denoth-Lippuner, A. Asymmetric inheritance of centrosomes maintains stem cell properties in human neural progenitor cells. eLife 12, e83157 (2023). https://doi.org/10.7554/eLife.83157

Rubinfeld B, Souza B, Albert I, Müller O, Chamberlain SH, Masiarz FR, Munemitsu S, Polakis P. Association of the APC gene product with beta-catenin. Science (New York, NY) 262: 1731-1734 (1993). https://doi.org/10.1126/science.8259518

Rubinfeld B, Albert I, Porfiri E, Fiol C, Munemitsu S, Polakis P. Binding of GSK3beta to the APC-beta-catenin complex and regulation of complex assembly. Science (New York, NY) 272: 1023-1026 (1996). https://doi.org/10.1126/science.272.5264.1023

Saade, M. et al. A centrosomal view of the CNS growth. Development (Cambridge, England), 145(21) (2018). https://doi.org/10.1242/dev.170613

Saade, M., Gonzalez-Gobartt, E., Escalona, R., Usieto, S. & Marti, E. Shh-mediated centrosomal recruitment of PKA promotes symmetric proliferative neuroepithelial cell division. Nat. Cell Biol. 19, 493-503 (2017). https://doi.org/10.1038/ncb3512

Saade M, Gutiérrez-Vallejo I, Le Dréau G, Rabadán MA, Miguez DG, Buceta J, Martí E. Sonic hedgehog signaling switches the mode of division in the developing nervous system. Cell Rep. Aug 15;4(3):492-503. (2013) doi: 10.1016/j.celrep.2013.06.038. Epub 2013 Jul 25. https://doi.org/10.1016/j.celrep.2013.06.038

Saitsu, H. & Shiota, K. Involvement of the axially condensed tail bud mesenchyme in normal and abnormal human posterior neural tube development. Congenit. Anom. 48, 1-6 (2008). https://doi.org/10.1111/j.1741-4520.2007.00178.x

Saitsu, H., Yamada, S., Uwabe, C., Ishibashi, M. & Shiota, K. Development of the posterior neural tube in human embryos. Anat. Embryol. 209, 107-117 (2004). https://doi.org/10.1007/s00429-004-0421-2

Santos, C. et al. Spinal neural tube formation and regression in human embryos. eLife 12, RP88584 (2023). https://doi.org/10.7554/eLife.88584.3

Satoh S, Daigo Y, Furukawa Y, Kato T, Miwa N, Nishiwaki T, Kawasoe T, Ishiguro H, Fujita M, Tokino T, Sasaki Y, Imaoka S, Murata M, Shimano T, Yamaoka Y, Nakamura Y. AXIN1 mutations in hepatocellular carcinomas, and growth suppression in cancer

cells by virus-mediated transfer of AXIN1. Nat Genet 24: 245-250 (2000). https://doi.org/10.1038/73448

Sauer, F.C. Mitosis in the neural tube. J. Comp. Neurol. 62, 377-405 (1935). https://doi.org/10.1002/cne.900620207

Schoenwolf, G. C. Cell movements driving neurulation in avian embryos. Dev. Suppl. Suppl 2, 157-168 (1991). https://doi.org/10.1242/dev.113.Supplement_2.157

Schoenwolf, G. C. & Delongo, J. Ultrastructure of secondary neurulation in the chick embryo. Am. J. Anat. 158, 43-63 (1980). https://doi.org/10.1002/aja.1001580106

Shao, W. et al. Centrosome anchoring regulates progenitor properties and cortical formation. Nature 580, 106-112 (2020). https://doi.org/10.1038/s41586-020-2139-6

Shaulian E, Karin M. AP-1 in cell proliferation and survival. Oncogene. Apr 30;20(19):2390-400 (2001). https://doi.org/10.1038/sj.onc.1204383

Shinohara, H., Sakayori, N., Takahashi, M. & Osumi, N. Ninein is essential for the maintenance of the cortical progenitor character by anchoring the centrosome to microtubules. Biol. Open 2, 739-749 (2013). https://doi.org/10.1242/bio.20135231

Shitashige M, Satow R, Jigami T, Aoki K, Honda K, Shibata T, Ono M, Hirohashi S, Yamada T. Traf2- and Nck-interacting kinase is essential for Wnt signaling and colorectal cancer growth. Cancer Res. Jun 15;70(12):5024-33 (2010). https://doi.org/10.1158/0008-5472.CAN-10-0306

Siegfried E, Chou TB, Perrimon N. Wingless signaling acts through zeste-white 3, the Drosophila homolog of glycogen synthase kinase-3, to regulate engrailed and establish cell fate. Cell 71: 1167-1179 (1992). https://doi.org/10.1016/S0092-8674(05)80065-0

Smalley MJ, Dale TC. Wnt signalling in mammalian development and cancer. Cancer Metastasis Rev. 18(2):215-30 (1999). https://doi.org/10.1023/A:1006369223282

Smith, J. L. & Schoenwolf, G. C. Role of cell-cycle in regulating neuroepithelial cell shape during bending of the chick neural plate. Cell Tissue Res. 252, 491-500 (1988). https://doi.org/10.1007/BF00216636

Smith, J. L. & Schoenwolf, G. C. Notochordal induction of cell wedging in the chick neural plate and its role in neural tube formation. J. Exp. Zool. 250, 49-62 (1989). https://doi.org/10.1002/jez.1402500107

Solloway M.J., Robertson E.J. Early embryonic lethality in Bmp5;Bmp7 double mutant mice suggests functional redundancy within the 60A subgroup. Development 126:1753-1768 (1999). https://doi.org/10.1242/dev.126.8.1753

Soulintzi, N. & Zagris, N. Spatial and temporal expression of perlecan in the early chick embryo. Cell Tissues Organs 186, 243-256 (2007). https://doi.org/10.1159/000107948

Spemann, H. & Mangold, H. Induction of embryonic primordia by implantation of organizers from a different species. Int. J. Dev. Biol. 100, 599-638 (1924). https://doi.org/ 10.1016/j.cdev.2024.203940

Su LK, Vogelstein B, Kinzler KW. Association of the APC tumor suppressor protein with catenins. Science 262: 1734-1737 (1993). https://doi.org/10.1126/science.8259519

Subramanian, L., Bershteyn, M., Paredes, M. F. & Kriegstein, A. R. Dynamic behaviour of human neuroepithelial cells in the developing forebrain. Nat. Commun. 8, 14167 (2017) https://doi.org/10.1038/ncomms14167

Sun, S., Fisher, R. L., Bowser, S. S., Pentecost, B. T. & Sui, H. Three-dimensional architecture of epithelial primary cilia. Proc. Natl Acad. Sci. USA 116, 9370-9379 (2019). https://doi.org/10.1073/pnas.1821064116

Takaoka, K. et al. The mouse embryo autonomously acquires anterior-posterior polarity at implantation. Dev. Cell 10, 451-459 (2006). https://doi.org/10.1016/j.devcel.2006.02.017

Tamai K, Semenov M, Kato Y, Spokony R, Liu C, Katsuyama Y, Hess F, Saint-Jeannet JP, He X. LDL-receptor-related proteins in Wnt signal transduction. Nature 407: 530-535 (2000). https://doi.org/10.1038/35035117

Tanos, B. E. et al. Centriole distal appendages promote membrane docking, leading to cilia initiation. Genes Dev. 27, 163-168 (2013). https://doi.org/10.1101/gad.207043.112

Taverna, E. and Huttner, W.B. Neural progenitor nuclei in motion. Neuron, 67(6), 906-914. (2010). https://doi.org/10.1016/j.neuron.2010.08.027

Tetsu O, McCormick F. Beta-catenin regulates expression of cyclin D1 in colon carcinoma cells. Nature. Apr 1;398(6726):422-6 (1999). https://doi.org/10.1038/18884

Thomas K.R. & Capecchi M.R. Targeted disruption of the murine int-1 proto-oncogene resulting in severe abnormalities in midbrain and cerebellar development. Nature 346: 847-850 (1990). https://doi.org/10.1038/346847a0

Timmer J.R., Wang C., Niswander L. BMP signaling patterns the dorsal and intermediate neural tube via regulation of homeobox and helix-loop-helix transcription factors. Development 129:2459-2472 (2002). https://doi.org/10.1242/dev.129.10.2459

Tozer, S., Le Dreau, G., Marti, E. & Briscoe, J. Temporal control of BMP signalling determines neuronal subtype identity in the dorsal neural tube. Development 140, 1467-1474 (2013). https://doi.org/10.1242/dev.090118

Tozer, S., Baek, C., Fischer, E., Goiame, R. & Morin, X. Differential routing of mindbomb1 via centriolar satellites regulates asymmetric divisions of neural progenitors. Neuron 93, 542-551.e4 (2017). https://doi.org/10.1016/j.neuron.2016.12.042

Tsai, J. W., Lian, W. N., Kemal, S., Kriegstein, A. R. & Vallee, R. B. Kinesin 3 and cytoplasmic dynein mediate interkinetic nuclear migration in neural stem cells. Nat. Neurosci. 13, 1463-1471 (2010). https://doi.org/10.1038/nn.2665

Tsai, J. W., Chen, Y., Kriegstein, A. R. & Vallee, R. B. LIS1 RNA interference blocks neural stem cell division, morphogenesis, and motility at multiple stages. J. Cell Biol. 170, 935-945 (2005). https://doi.org/10.1083/jcb.200505166

Uchikawa M, Ishida Y, Takemoto T, Kamachi Y, Kondoh H. Functional analysis of chicken Sox2 enhancers highlights an array of diverse regulatory elements that are conserved in mammals. Dev Cell. Apr;4(4):509-19 (2003). https://doi.org/10.1016/S1534-5807(03)00088-1

Uchikawa M, Kamachi Y, Kondoh H. Two distinct subgroups of Group B Sox genes for transcriptional activators and repressors: their expression during embryonic organogenesis of the chicken. Mech Dev. Jun;84(1-2):103-20 (1999). https://doi.org/10.1016/S0925-4773(99)00083-0

Valenta T, Gay M, Steiner S, Draganova K, Zemke M, Hoffmans R, Cinelli P, Aguet M, Sommer L, Basler K. Probing transcription-specific outputs of β-catenin in vivo. Genes Dev. Dec 15;25(24):2631-43 (2011). https://doi.org/10.1101/gad.181289.111

van de Wetering M, Oosterwegel M, Dooijes D, Clevers H. Identification and cloning of TCF-1, a T lymphocyte-specific transcription factor containing a sequence-specific

HMG box. EMBO J 10: 123-132 (1991). https://doi.org/10.1002/j.1460-2075.1991.tb07928.x

van Straaten, H. W., Hekking, J. W., Wiertz-Hoessels, E. J., Thors, F. & Drukker, J. Effect of the notochord on the differentiation of a floor plate area in the neural tube of the chick embryo. Anat. Embryol. 177, 317-324 (1988). https://doi.org/10.1007/BF00315839

Vargas-Hurtado, D. et al. Differences in mitotic spindle architecture in mammalian neural stem cells influence mitotic accuracy during brain development. Curr. Biol. 29, 2993-3005.e9 (2019). https://doi.org/10.1016/j.cub.2019.07.061

Vinson CR, Conover S, Adler PN. A Drosophila tissue polarity locus encodes a protein containing seven potential transmembrane domains. Nature 338: 263-264 (1989). https://doi.org/10.1038/338263a0

Wang, X. et al. Asymmetric centrosome inheritance maintains neural progenitors in the neocortex. Nature 461, 947-955 (2009). https://doi.org/10.1038/nature08435

Wang L, Dynlacht BD. The regulation of cilium assembly and disassembly in development and disease. Development. Sep 17;145(18):dev151407 (2018). https://doi.org/10.1242/dev.151407

Waterman ML, Fischer WH, Jones KA. A thymus-specific member of the HMG protein family regulates the human T cell receptor C alpha enhancer. Genes Dev 5: 656-669 (1991). https://doi.org/10.1101/gad.5.4.656

Wehrli M, Dougan ST, Caldwell K, O'Keefe L, Schwartz S, Vaizel-Ohayon D, Schejter E, Tomlinson A, DiNardo S. arrow encodes an LDL-receptor-related protein essential for Wingless signalling. Nature 407: 527-530 (2000). https://doi.org/10.1038/35035110

Whittington N, Cunningham D, Le TK, De Maria D, Silva EM. Sox21 regulates the progression of neuronal differentiation in a dose-dependent manner. Dev Biol. Jan 15;397(2):237-47 (2015). https://doi.org/10.1016/j.ydbio.2014.11.012

Widelitz R. Wnt signaling through canonical and non-canonical pathways: recent progress. Growth Factors. Jun;23(2):111-6 (2005). https://doi.org/10.1080/08977190500125746

Wilcock, A. C., Swedlow, J. R. & Storey, K. G. Mitotic spindle orientation distinguishes stem cell and terminal modes of neuron production in the early spinal cord. Development 134, 1943-1954 (2007). https://doi.org/10.1242/dev.002519

Wilson, L. & Maden, M. The mechanisms of dorsoventral patterning in the vertebrate neural tube. Developmental Biology. 282(1) 1-13 (2005). https://doi.org/10.1016/j.ydbio.2005.02.027

Wine-Lee L., Ahn K.J., Richardson R.D., Mishina Y., Lyons K.M., Crenshaw E.B III. Signaling through BMP type 1 receptors is required for development of interneuron cell types in the dorsal spinal cord. Development 131:5393-5403 (2004). https://doi.org/10.1242/dev.01379

Wodarz A, Nusse R. Mechanisms of Wnt signaling in development. Annu Rev Cell Dev Biol.14:59-88 (1998). https://doi.org/10.1146/annurev.cellbio.14.1.59

Xie, Z. et al. Cep120 and TACCs control interkinetic nuclear migration and the neural progenitor pool. Neuron 56, 79-93 (2007). https://doi.org/10.1016/j.neuron.2007.08.026

Xing Y, Clements WK, Le Trong I, Hinds TR, Stenkamp R, Kimelman D, Xu W. Crystal structure of a beta-catenin/APC complex reveals a critical role for APC phosphorylation in APC function. Mol Cell. Aug 27;15(4):523-33 (2004). https://doi.org/10.1016/j.molcel.2004.08.001

Yamamoto, M. et al. Nodal antagonists regulate formation of the anteroposterior axis of the mouse embryo. Nature 428, 387-392 (2004). https://doi.org/10.1038/nature02418

Yang, Y. T., Wang, C. L. & Van Aelst, L. DOCK7 interacts with TACC3 to regulate interkinetic nuclear migration and cortical neurogenesis. Nat. Neurosci. 15, 1201-1210 (2012). https://doi.org/10.1038/nn.3171

Yang, T. T. et al. Super-resolution architecture of mammalian centriole distal appendages reveals distinct blade and matrix functional components. Nat. Commun. 9, 2023 (2018). https://doi.org/10.1038/s41467-018-04469-1

Yang A, Chidiac R, Russo E, Steenland H, Pauli Q, Bonin R, Blazer LL, Adams JJ, Sidhu SS, Goeva A, Salahpour A, Angers S. Exploiting spatiotemporal regulation of FZD5 during neural patterning for efficient ventral midbrain specification. Development. Mar 1;151(5):dev202545 (2024). https://doi.org/10.1242/dev.202545

Yi F, Pereira L, Hoffman JA, Shy BR, Yuen CM, Liu DR, Merrill BJ. Opposing effects of Tcf3 and Tcf1 control Wnt stimulation of embryonic stem cell self-renewal. Nat Cell Biol. Jun 19;13(7):762-70 (2011). https://doi.org/10.1038/ncb2283

Yost C, Torres M, Miller JR, Huang E, Kimelman D, Moon RT. The axis-inducing activity, stability, and subcellular distribution of beta-catenin is regulated in Xenopus embryos by glycogen synthase kinase 3. Genes Dev 10: 1443-1454 (1996). https://doi.org/10.1101/gad.10.12.1443

Yu, J. et al. KASH protein Syne-2/Nesprin-2 and SUN proteins SUN1/2 mediate nuclear migration during mammalian retinal development. Hum. Mol. Genet. 20, 1061-1073 (2011). https://doi.org/10.1093/hmg/ddq549

Yu W., McDonnell K., Taketo M.M., Bai C.B. Wnt signaling determines ventral spinal cord cell fates in a time-dependent manner. Development 135:3687-3696 (2008). https://doi.org/10.1242/dev.021899

Zechner D, Fujita Y, Hülsken J, Müller T, Walther I, Taketo MM, Crenshaw EB 3rd, Birchmeier W, Birchmeier C. beta-Catenin signals regulate cell growth and the balance between progenitor cell expansion and differentiation in the nervous system. Dev Biol. Jun 15;258(2):406-18 (2003). https://doi.org/10.1016/S0012-1606(03)00123-4

Zeng L, Fagotto F, Zhang T, Hsu W, Vasicek TJ, Perry WL III, Lee JJ, Tilghman SM, Gumbiner BM, Costantini F. The mouse Fused locus encodes Axin, an inhibitor of the Wnt signaling pathway that regulates embryonic axis formation. Cell 90: 181-192 (1997). https://doi.org/10.1016/S0092-8674(00)80324-4

Zhang, X. et al. SUN1/2 and Syne/Nesprin-1/2 complexes connect centrosome to the nucleus during neurogenesis and neuronal migration in mice. Neuron 64, 173-187 (2009). https://doi.org/10.1016/j.neuron.2009.08.018

Zhang, X. et al. Cell-type-specific alternative splicing governs cell fate in the developing cerebral cortex. Cell 166, 1147-1162.e15 (2016). https://doi.org/10.1016/j.cell.2016.07.025

Zhang K., Da Silva F., Seidl C., Wilsch-Bräuninger M., Herbst J., Huttner W.B., Niehrs C. Primary cilia are WNT-transducing organelles whose biogenesis is controlled by a WNT-PP1 axis. Dev Cell. Jan 23;58(2):139-154.e8 (2023). https://doi.org/10.1016/j.devcel.2022.12.006

Zulkipli I, Clark J, Hart M, Shrestha RL, Gul P, Dang D, Kasichiwin T, Kujawiak I, Sastry N, Draviam VM. Spindle rotation in human cells is reliant on a MARK2-mediated equatorial spindle-centering mechanism. J Cell Biol. Sep 3;217(9):3057-3070 (2018). https://doi.org/10.1083/jcb.201804166

APPENDIX

© 2022. Published by The Company of Biologists Ltd | Journal of Cell Science (2022) 135, jcs259395. doi:10.1242/jcs.259395

REVIEW

SUBJECT COLLECTION: CILIA AND FLAGELLA

Centrosome maturation – in tune with the cell cycle

Jose Blanco-Ameijeiras, Pilar Lozano-Fernández and Elisa Martí*

ABSTRACT

Centrosomes are the main microtubule-organizing centres, playing essential roles in the organization of the cytoskeleton during interphase, and in the mitotic spindle, which controls chromosome segregation, during cell division. Centrosomes also act as the basal body of cilia, regulating cilium length and affecting extracellular signal reception as well as the integration of intracellular signalling pathways. Centrosomes are self-replicative and duplicate once every cell cycle to generate two centrosomes. The core support structure of the centrosome consists of two molecularly distinct centrioles. The mother (mature) centriole exhibits accessory appendages and is surrounded by both pericentriolar material and centriolar satellites, structures that the daughter (immature) centriole lacks. In this Review, we discuss what is currently known about centrosome duplication, its dialogue with the cell cycle and the sequential acquisition of specific components during centriole maturation. We also describe our current understanding of the mature centriolar structures that are required to build a cilium. Altogether, the built-in centrosome asymmetries that stem from the two centrosomes inheriting molecularly different centrioles sets the foundation for cell division being an intrinsically asymmetric process.

KEY WORDS: Cell division, Centrosome asymmetries, Primary cilium, Centrosome maturation

Introduction

The centrosome is a small, non-membranous organelle capable of self-replication. Centrosomes perform several critical functions in animal cells, which include serving as the main microtubule-organizing centre (MTOC), the basal body of cilia and a platform for intracellular signalling, as well as organizing the mitotic spindle during cell division (Arquint et al., 2014). The centrosome was first identified at the end of the 19th century, and at the time described as a moderately and uniformly stained sphere interspersed with a filamentous scaffold (Boveri, 1900). More recently, genomics and proteomics has helped us better define the components and understand the biology of the centrosome, and some of the diseases associated with centrosome dysfunction. In addition, in the past decade, technological breakthroughs, which include super-resolution microscopy, have helped researchers to characterize the composition and 3D organization of the centrosome at the molecular level. Here, we provide an up-to-date view of the 3D organization of the centrosome and the asymmetries between mother and daughter centrioles, as well as discuss how centrosome replication is coordinated with the cell cycle. We will also highlight the dynamics of centriole maturation, involving the recruitment of proteins required for appendage assembly, as well as centriole 'dematuration', which involves the partial disassembly of the appendages. Finally, we will discuss the organization of the basal body and transition zone of cilia. Many key findings in the field come from studies in model organisms such as *Drosophila* or *C. elegans* (Marthiens and Basto, 2020; Schwarz et al., 2018), but in this Review we will mostly refer to the human (mammalian) system. We aim to highlight the orchestration of centriolar protein recruitment and removal during the cell cycle, which results in two molecularly distinct centrosomes. Remarkably, the built-in centrosome asymmetries that stem from the two centrosomes inheriting different centrioles are the underlying basis for spindle positioning and cell division being intrinsically asymmetric.

Instituto de Biología Molecular de Barcelona, Parc Científic de Barcelona, Baldiri i Reixac 20, Barcelona 08028, Spain.

*Author for correspondence (emgbmc@ibmb.csic.es)

E.M., 0000-0001-5839-7133

A pair of molecularly distinct centrioles form the core support structure of the centrosome

Centrioles and appendages

Centrioles are cylindrical structures that are ∼500 nm long and have a diameter of 250 nm in vertebrate cells (Winey and O'Toole, 2014). They are composed of triplets of microtubules (MTs) organized around a central cartwheel with an evolutionarily conserved nine-fold symmetry (Azimzadeh and Marshall, 2010) (Fig. 1). Typically, two centrioles are joined perpendicularly by their proximal ends, a connection that is sustained by the proteinaceous centrosome linker in conjunction with MT forces (Panic et al., 2015). Of these two centrioles, only one is fully mature, exhibiting two characteristic accessory structures, the distal appendages (DAs) and the subdistal appendages (SDAs); this centriole is termed the mother centriole. Both DAs and SDAs can be visualized by electron microscopy (EM) and are observed as electron-dense ring-like structures with a head that attaches to the centriole MTs through a stem, which in turn connects with two MT triplets (Bowler et al., 2019; Bystrevskaya et al., 1988; Paintrand et al., 1992). The classical view is that the DAs and SDAs have a similar centriolar distribution, shape and size, yet this now appears to be only partially true. In most cases, both appendages show the nine-fold symmetry of the centriole wall, with the head-like structures radially disposed around the MT triplets (Bowler et al., 2019; Ibrahim et al., 2009). However, although mother centrioles always have nine DAs around their walls (Uzbekov and Alieva, 2018), the number of SDAs can vary between different cell types (Bystrevskaya et al., 1988, 1992; Komesli et al., 1989). The heads of both the DA and SDA are ∼40 nm in length and extend for ∼100 nm from the centriole wall (Fig. 1) (Bowler et al., 2019; Ibrahim et al., 2009). In cilia, DAs (also known here as transition fibres) are the platform that allows a transition zone (TZ) to be established, which contains a ring-like protein structure that extends for ∼120 nm along the ciliary axis with a nine-fold symmetry, and which connects MTs with the ciliary membrane (Shi et al., 2017). The daughter centriole, the younger of the two centrioles, is less mature and lacks SDAs and DAs; however, it has several daughter centriolar proteins (DCPs) that are recruited to nascent centrioles in order to regulate their elongation and homeostasis (Li et al., 2012; Mahjoub et al., 2010; Zou et al., 2005).

Journal of Cell Science (2022) 135, jcs259395. doi:10.1242/jcs.259395

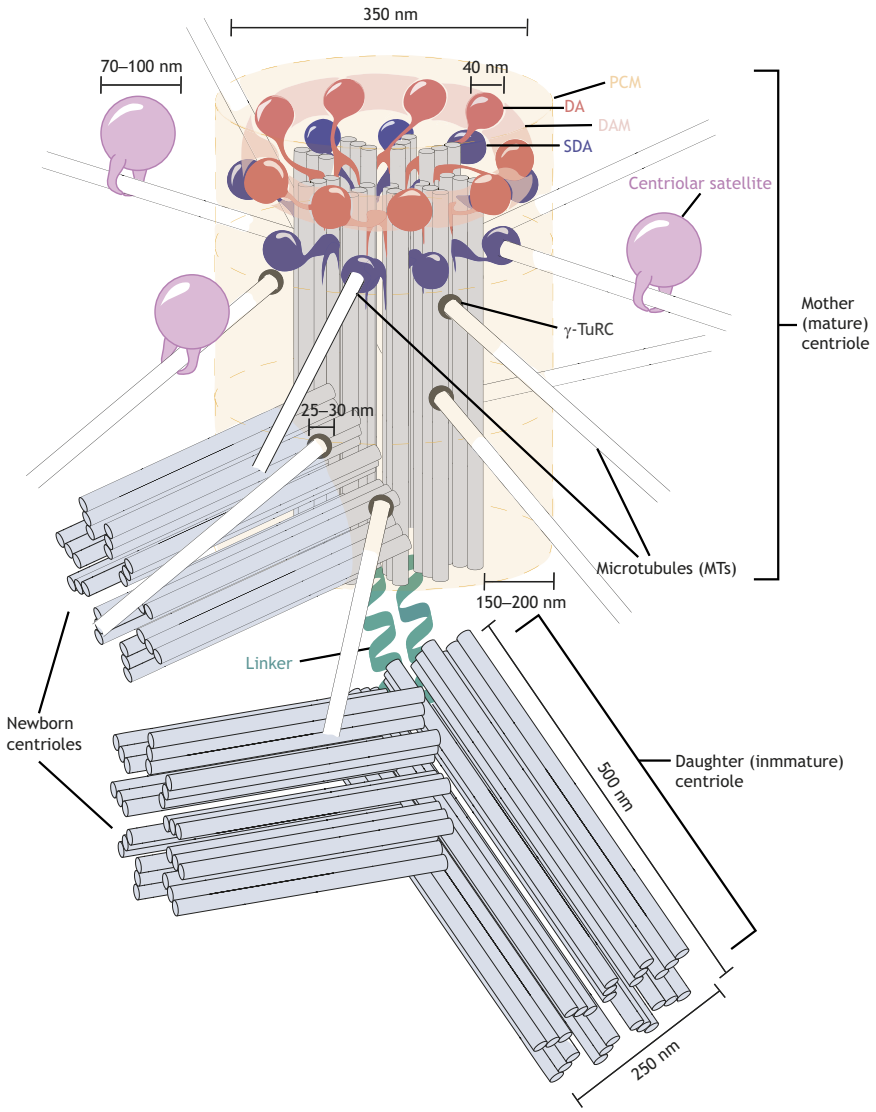

Fig. 1. 3D reconstruction of a mature centrosome in the G_2 phase of the cell cycle. The mother (mature) centriole is decorated with distal (DA, terracotta) and subdistal appendages (SDA, purple), as well as pericentriolar material (PCM, pale yellow). Proteins filling the space between DA constitute the distal appendage matrix (DAM, pale terracotta). Centriolar triplet microtubules are illustrated in grey-blue. Mother and daughter centrioles are connected through a proteinacous linker (green), and newborn centrioles emerge from each pre-existing centriole. Microtubules (MTs) nucleated by the mature centriole emerge from the γ-tubulin ring complex (γ-TuRC, dark grey) and centriolar satellites (lavender) travel along the MTs.

Pericentriolar material and centriolar satellites

The pericentriolar material (PCM), a proteinaceous material surrounding the mother centriole, forms a cylindrical structure devoid of MTs that assembles around the centriole and is the focal point of MT nucleation (Jana, 2021). Initially, the PCM was considered to be a disorganized proteinaceous matrix, and indeed, in the earliest examples of electron micrographs of centrosomes it is described as an amorphous pericentriolar halo arising from the highly structured centrioles (Robbins et al., 1968). However, super-resolution microscopy has revealed that the PCM is a highly organized structure located in the vicinity of the mother centriole (Fu and Glover, 2012; Lawo et al., 2012; Mennella et al., 2012; Sonnen et al., 2012). The PCM is organized into concentric protein layers that attach to the mother centriole via pericentrin, a large protein that forms fibrils orientated with its C-terminal domain adjacent to the centriole wall and its N-terminus extending outwards into the PCM (Lawo et al., 2012; Mennella et al., 2012; Woodruff et al., 2014). These PCM protein layers accommodate the γ-tubulin ring complex (γ-TuRC) (Moritz et al., 2000), which is ∼25–30 nm in diameter and the origin of MT nucleation (Conduit et al., 2015) (Fig. 1). The size of the PCM varies widely as it undergoes dynamic changes, with the proximal layer extending ∼150–200 nm from the centriole wall as cells proceed through the cell cycle (Fry et al., 2017a).

How protein exchange and replacement occur between the centrosome and the cytoplasm has long remained unclear. However, it now appears that centriolar satellites (CSs) (Fig. 1), spherical granular structures of ∼70–100 nm in diameter (Tollenaere et al., 2015), are responsible for centrosomal protein transport (Bärenz et al., 2011). These CSs travel towards the centrosome along the MTs and are thought to play important regulatory roles in centrosome biology (Bärenz et al., 2011; Prosser and

Pelletier, 2020). Indeed, CS depletion alters the composition of the PCM (Dammermann and Merdes, 2002; Hames et al., 2005) and basal body (Kim et al., 2008a; Sillibourne et al., 2013).

The centrosome replicates in coordination with the cell cycle

Centrosomes possess a self-replicative capacity that, like DNA replication, is coordinated with the cell cycle. In order to guarantee that there is a constant number of centrosomes in the cell, cycling cells establish two layers of control: (1) cell cycle control, whereby each centriole duplicates exactly once per cell cycle, and (2) copy number control, whereby only one new centriole forms alongside each pre-existing one (Nigg and Stearns, 2011). In most cells, centrosomes can form *de novo*, unless this is blocked by the pre-existing centrosomes (Heath et al., 1986; Khodjakov et al., 2002; Marshall, 2009). Here, we summarize the main events of canonical centrosome duplication during the cell cycle: procentriole formation during G_1, elongation of the procentriole during S phase, centrosome maturation during G_2, and centrosome separation as the cell enters mitosis. However, we note that there are some examples of non-canonical centrosome biogenesis where cells assemble *de novo* centrosomes without previous centriolar structures present in the cell (e.g. during the amoeba-to-flagellate transition in *Naegleria gruberi*, in parthenogenetic insect eggs and during oogenesis in most animal cells) (Nabais et al., 2017).

The procentriole forms during the G_1 phase of the cell cycle

As the structural backbone of the organelle, the centriole wall is the principal checkpoint for centrosome duplication. Upon duplication, the newborn centrioles, elongating from procentrioles, remain engaged with the pre-existing ones until the end of mitosis, preventing them from acting as a template for re-duplication and thereby guaranteeing cell cycle control (Tsou and Stearns, 2006). During G_1, the centrosomal proteins CEP192 and CEP152 make up the inner components of the PCM and are sequentially recruited to the wall of the daughter centriole, while in the case of the mother centriole, both proteins are inherited from the previous cell cycle (Fig. 2A). CEP192 is distributed in a barrel shape all along the proximo-distal axis, whereas CEP152 is restricted to the proximal end of the centriole (Sonnen et al., 2013). CEP192 promotes the recruitment of CEP152 and the Polo kinase PLK4 (Kim et al., 2013), and once at the centriole, CEP152 competes with CEP192 to restrict PLK4 to the CEP152-containing proximal end of the centriole (Park et al., 2014) (Fig. 2A). The activity of PLK4 controls the number of centrioles arising from each mother centriole, thereby regulating centriole copy number (Bettencourt-Dias et al., 2005; Habedanck et al., 2005).

At the G_1/S transition, exactly one procentriole is formed for each pre-existing centriole (Fig. 2B). The temporal restriction of this process depends on the availability of the protein STIL, which is controlled by the CDK1–cyclin-B complex (Zitouni et al., 2016) and proteolysis mediated by the anaphase-promoting complex/cyclosome containing FZR1 (Cdh1 in yeast) or CDC20 (APC/C^{FZR1} or APC/C^{CDC20}) (Arquint et al., 2012). PLK4 undergoes trans-autophosphorylation, and is thereby targeted for proteasomal degradation unless it binds to STIL (Cunha-Ferreira et al., 2009, 2013; Rogers et al., 2009). STIL is phosphorylated upon interaction with PLK4, allowing the centriolar loading of the coiled-coil protein SAS6 (encoded by *SASS6*) for cartwheel assembly (Moyer et al., 2015). Subsequently, the formation of a STIL–SAS6 complex establishes a negative-feedback loop by restricting PLK4 stabilization to a single focus, guaranteeing copy number control (Kim et al., 2016; Ohta et al., 2014). Moreover, STIL oligomerization could also contribute to the restriction of PLK4 to a single focal point (Banterle and Gönczy, 2017). SAS6 forms homodimers in the cytoplasm that, upon centriolar loading, undergo higher-order oligomerization to form a ring-like structure of nine homodimeric units (Keller et al., 2014). These ring-like oligomers then stack on top of each other to form the cartwheel structure (Fig. 2A).

The procentriole elongates during the S phase of the cell cycle

The cartwheel structure serves as a template for centriole elongation. Although this process is less well studied than procentriole formation, MT nucleation and its stabilization in the nine-fold symmetry requires the cartwheel–MT connection to be established, ensuring that elongation can occur during the S phase of the cell cycle. This connection probably takes place through CEP135, which can bind to SAS6 (Lin et al., 2013a) and to MTs (Kraatz et al., 2016) (Fig. 2B). Moreover, CEP135 recruits CPAP (also known as CENPJ), a protein implicated in MT stability, to the centriole wall (Lin et al., 2013a). In turn, CPAP will recruit CEP120, which allows CCDC52 (also known as SPICE1) to be incorporated into the complex (Comartin et al., 2013). Although CEP135 lies upstream of the other members of the complex in the recruitment hierarchy, some kind of positive feedback must exist between the different members of the complex, as depletion of CPAP, CEP120 or SPICE1 reduces CEP135 recruitment, ultimately impairing centriole elongation (Comartin et al., 2013). Centriole length is positively regulated by CPAP and CEP120 (Keller et al., 2009; Lin et al., 2013b; Schmidt et al., 2009) and negatively regulated by CCP110 and CEP97, which cap the distal end of centrioles (Schmidt et al., 2009; Spektor et al., 2007). The timely restriction of elongation is at least in part controlled through CPAP availability, which is regulated throughout the cell cycle by both APC/C^{FZR1}-driven proteolysis and degradation mediated by poly-ADP-ribosylation (PARsylation) (Kim et al., 2012; Tang et al., 2009).

Centrosome maturation takes place during the G_2 phase of the cell cycle

During late G_2 and the mitotic prophase, the centrosome increases in size from ∼500 nm in diameter during interphase to several micrometres at mitosis (Woodruff et al., 2017). This is mainly due to the recruitment of PCM components that enhance its MT-nucleating capacity to guarantee correct spindle pole formation during mitosis (Meraldi and Nigg, 2002). In addition to PCM recruitment, DAs and SDAs are assembled at the G2 phase of the cell cycle. This maturation process initiates the breaking of the intrinsic centrosome molecular asymmetries (Figs 2C and 3C).

Up until the G_2/M transition, centrosome separation is prevented by a flexible proteinaceous linker that bridges the centriole walls via CEP135 (Fig. 2B) (Lin et al., 2013a). Besides binding to the MT triplets of the centriole wall and the SAS6 cartwheel structure, CEP135 interacts with the linker protein CNAP1 (also known as CEP250) (Kim et al., 2008b). CNAP1 segregates into two pools at the proximal ends of the maternal and daughter centriole (Fry et al., 1998), which operate as anchor points for CROCC (also known as rootletin), a filamentous protein that forms the rootlet fibres that join the centrioles (Bahe et al., 2005; Yang et al., 2006). A further component of the proteinaceous linker is CEP68, which is a filament modulator that regulates the thickness of the rootlet fibres (Vlijm et al., 2018). Although CNAP1, CROCC and CEP68 are the best studied components of the linker, LRRC45 and CNTLN are also associated with this structure (Fang et al., 2014; He et al., 2013).

Journal of Cell Science (2022) 135, jcs259395. doi:10.1242/jcs.259395

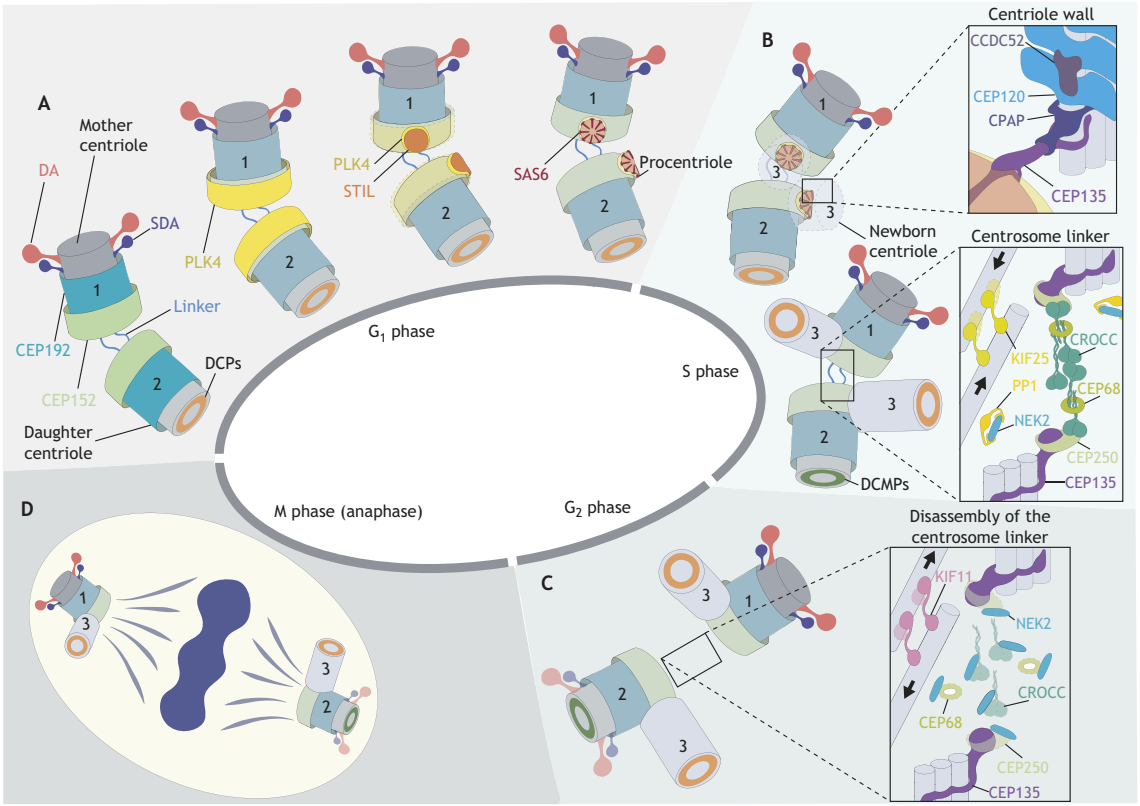

Fig. 2. Self-replication and maturation of the centrosome during the cell cycle. (A) In the mature centrosome, mother and daughter centrioles are connected through a proteinacous linker (mid-blue). The mother centriole (1) is decorated with distal (DA, terracotta) and subdistal appendages (SDA, dark-blue). Upon entering the cell cycle, CEP192 and CEP152 (inner components of the PCM), are recruited to the daughter centriole (2). On the daughter centriole, DCPs (orange ring) regulate centriole elongation. Restriction of PLK4 and STIL to a single focus ensures that only one procentriole cartwheel forms from a pre-existing centriole in G_1 phase. (B) Elongation of the newborn centriole (3) during S phase. The centriole wall expanded view shows proteins contributing to cartwheel–MT stabilization. Newborn centriole elongation terminates in S phase with the addition of DCPs. The transition from daughter to new mother centriole includes the loss of DCPs and the recruitment of new daughter centriole maturation proteins (DCMP, green ring). The expanded view shows proteins in the centrosome linker connecting centriolar MTs. (C) Daughter centriole maturation into a new 'mother' by the assembly of DAs and SDAs occurs during the G_2 phase of the cell cycle. Centrosome separation, caused by the disassembly of the linker (see expanded view) occurs at the end of G_2. (D) Two molecularly distinct centrosomes nucleate the mitotic spindle. Centriolar MTs and PCM are not shown for clarity.

In addition to the proteinaceous linker, MT fibres are also involved in preventing centrosome separation. As such, sliding of anti-parallel MTs is induced through the activity of the bipolar minus-end-directed kinesin KIF25, generating forces that tether the centrosomes together until mitosis (Decarreau et al., 2017; Jean et al., 1999).

Duplicated centrosomes separate on entering mitosis

At the end of G_2, the proteinaceous linker is disrupted to allow the two centrosomes to separate and polarize at mitosis (Fig. 2C,D). The stability of the proteinaceous linker is mainly regulated by the kinase NEK2 and the phosphatase PP1 (Helps et al., 2000). The balance between NEK2 and PP1 activities is determined by activation of the Polo kinase PLK1, which in turn relies on cyclinA2–Cdk activity that is mediated by Aurora kinase A (AURKA) (Gheghiani et al., 2017). Upon its activation, NEK2 phosphorylates CNAP1 (Fry et al., 1998; Hardy et al., 2014) and CROCC (Bahe et al., 2005), inducing their displacement from the proteinaceous linker and ultimately triggering its dissolution (Fig. 2C) (Agircan et al., 2014; Fry et al., 2017b). Besides the dissolution of the proteinaceous linker, mechanical forces exerted by the MTs contribute to centrosome separation. KIF11 (also known as EG5), a member of the kinesin-5 subfamily of motor proteins, generates outward forces that antagonize KIF25 activity and so induce the sliding of anti-parallel MTs of the centrosome linker in opposing directions (Kapitein et al., 2005). The two separated centrosomes nucleate the mitotic spindle (Fig. 2D). From centriole duplication until anaphase, centrioles remain tightly engaged such that the proximal end of the newborn centriole lies in opposition to the lateral portion of the proximal end of the pre-existing centriole. During anaphase, the protease separase is activated in order to guarantee sister chromatid separation, and it also acts on centrosomes, leading to centriole disengagement (Tsou and Stearns, 2006).

Centriole remodelling in cycling cells

As mentioned above, mature centrioles can be differentiated from immature (newborn and daughter) centrioles by the presence of their

Journal of Cell Science (2022) 135, jcs259395. doi:10.1242/jcs.259395

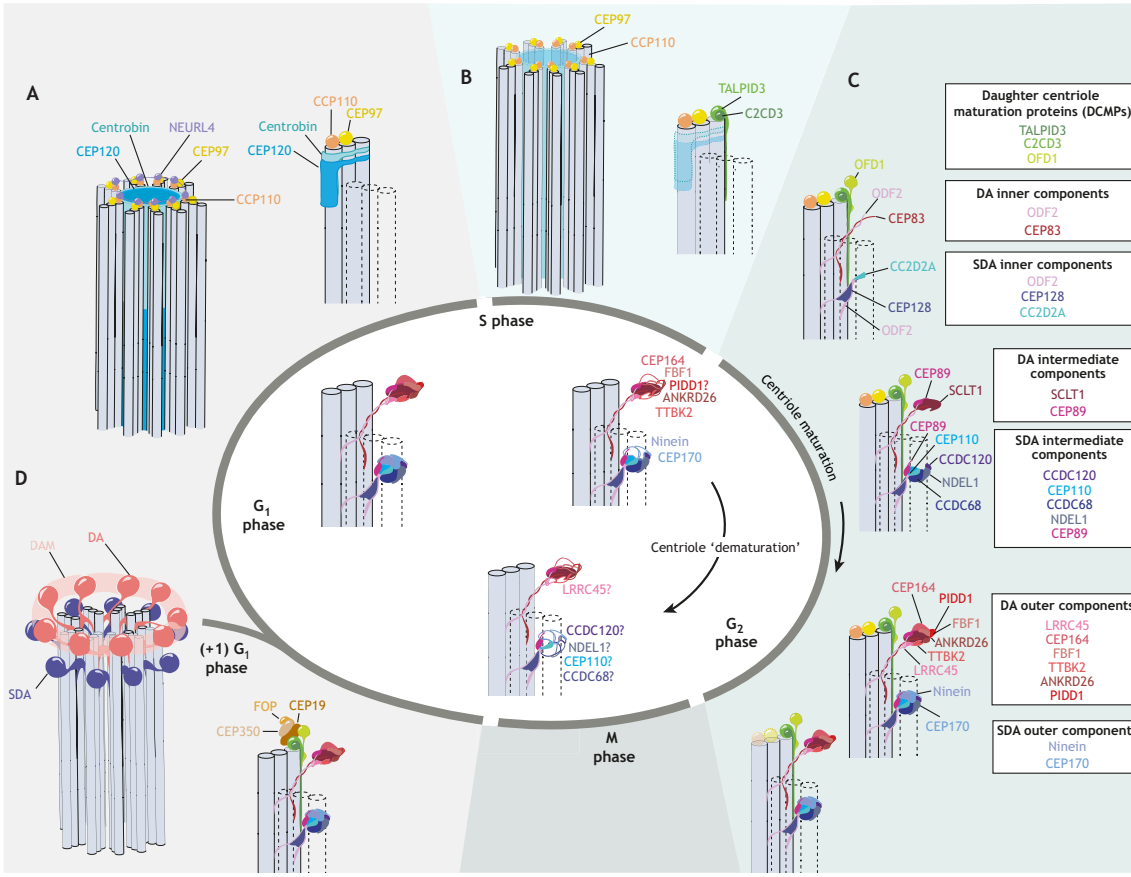

Fig. 3. Assembly and disassembly of protein complexes contributing to centriole maturation during the cell cycle. The assembly of protein complexes are depicted in the outer part of the circle. (A) MT triplets of the daughter centriole with proteins involved in centriole elongation (CEP120 and centrobin) and decorated with specific distal end capping proteins (CCP110, CEP97 and NEURL4). The scheme on the right illustrates a single MT triplet (grey) accommodating daughter centriole-specific proteins. (B) Daughter centriole maturation initiates at the end of S phase, with the removal of CEP120 and centrobin (pale blue), and the recruitment of daughter centriole maturation proteins (DCMPs) TALPID3 and C2CD3. (C) Daughter centriole maturation into a new mother centriole includes the sequential assembly of DAs and SDAs during the G2 phase of the cell cycle, and the disassembly of DCPs (CCP110, CEP97; spheres shown with transparency at the end of the G2). The text boxes indicate the specific proteins that are sequentially assembled within each indicated compartment. Partial disassembly of DAs and SDAs occurs as illustrated in the inner part of the circle (centriole 'dematuration'). During G2, proteins including CEP164, FBF1, ANKRD26 and TTBK2, disassemble from the DAs, while ninein and CEP170 disassemble from the SDAs. Proteins whose disassembly is predicted but has not been experimentally demonstrated are indicated with question marks. (D) After M phase, recruitment of the CEP350–FOP–CEP19 protein complex to the mature centriole contributes to its capacity to transform into a ciliary basal body, which contains DAs, SDAs and DAM.

appendages (DA and SDA) and the PCM (Fig. 1). These intrinsic centriole asymmetries are already present in the zygote, transmitted from the spermatozoan centrioles, since the oocyte does not have a functional centrosome (Avidor-Reiss and Fishman, 2019). Establishment of some of the best-understood molecular asymmetries of centrioles is co-ordinated with the cell cycle and generated by the recruitment and removal of relevant non-mature centriole proteins, as well as by appendage assembly and disassembly (Fig. 3).

Specific DCPs contribute to centriole elongation

Although non-mature centrioles lack SDAs and DAs, they are enriched in DCPs that are sequentially incorporated into the growing centriole (Fig. 3A). CEP120, a member of the MT-stabilization complex, is thought to be the first newborn centriole-associated protein to be incorporated into the elongating centrioles (Comartin et al., 2013). The presence of CEP120 in the centriole allows centrobin to become incorporated, which will interact with and prevent the degradation of CPAP, another member of the MT stabilization complex that is active during centriole elongation (Figs 2B and 3A) (Gudi et al., 2015; Wang and Dynlacht, 2018; Zou et al., 2005). As is the case for CEP120, centrobin follows the dynamics of the cell cycle and, during the G_1/S transition, is enriched at newborn centrioles. The longitudinal distribution of centrobin appears to be specifically enriched in the distal half of the centriole walls (Wang and Dynlacht, 2018; Zou et al., 2005), and the presence of both CEP120 and centrobin suppresses DA and SDA assembly (Fig. 3A) (Wang et al., 2018).

Subsequent to CEP120 and centrobin incorporation, NEURL4 localizes to the distal end of the daughter centrioles. NEURL4 is an

E3 ubiquitin ligase cofactor that interacts with CCP110 and thereby regulates its distal accumulation (Li et al., 2012; Loukil et al., 2017). CCP110 is a distal end-capping protein that contributes to centriole elongation and centrosome separation (Kim and Dynlacht, 2013; Schmidt et al., 2009; Spektor et al., 2007; Yadav et al., 2016). CCP110 interacts directly with CEP97 to form a DCP complex (Fig. 3A), which needs to be removed from the distal end of the daughter centriole before the final phase of centriole maturation (Spektor et al., 2007). Recent findings indicate that CEP97 not only acts as a recruitment factor for CCP110 (Spektor et al., 2007), but also contributes to the control of centriole length by regulating microtubule acetylation (Dobbelaere et al., 2020).

In addition to CCP110 and NEURL4, the poly(ADP-ribose) polymerase PARP3, which marks single-strand DNA breaks (Shall and de Murcia, 2000), preferentially interacts with the newborn centriole at its N-terminal domain (Augustin et al., 2003). Whether PARP3 is merely acting as part of a DNA-integrity checkpoint that controls the cell cycle, or whether it fulfils an additional role in centriole biogenesis and/or maturation remains to be elucidated. At the end of centriole elongation, the transition from newborn to daughter centriole is induced by the loss of specific newborn proteins, and the subsequent recruitment of new assembling proteins (Lin et al., 2013b; Mahjoub et al., 2010). Here, TALPID3 (also known as KIAA0586), which interacts with CCP110 (Kobayashi et al., 2014) and the distal part of CEP120, recruits C2CD3 and thus facilitates the removal of CEP120 and centrobin (Wu et al., 2014). C2CD3 also controls centriole elongation (Thauvin-Robinet et al., 2014) (Fig. 3B).

The assembly of DAs initiates maturation of the daughter centriole into a new mother centriole

The removal of specific newborn centriolar proteins allows OFD1, a centrosomal protein that modulates centriole length and the formation of distal appendages (Alfieri et al., 2020), to localize to the distal end of the daughter centriole (Fig. 3C); this is mediated by CEP90 and MNR (also known as PIBF1 and KIAA0753, respectively), protein components of the CSs (Kumar et al., 2021). OFD1 recruitment triggers DA formation, leading to the gradual maturation of the daughter centriole and it becoming a mother centriole in the next cell cycle (Wang et al., 2018). Components of DAs are assembled in a hierarchical manner, with first the inner, then the intermediate, and finally the outer components recruited to form a fully mature DA (Fig. 3C). OFD1 recruits the inner DA component CEP83 through a yet to be defined mechanism. This likely elicits events that lead to the incorporation of intermediate DA components, such as SCLT1 and CEP89 (Yang et al., 2018). The incorporation of SCLT1 subsequently triggers the recruitment of outer DA components, such as LRRC45 and probably CEP164; this in turn contributes to FBF1 recruitment, while CEP164 also recruits Tau tubulin kinase 2 (TTBK2) (Čajánek and Nigg, 2014; Kurtulmus et al., 2018; Tanos et al., 2013; Ye et al., 2014).

When fully mature, DAs adopt a pinwheel-like structure with a spherical head that connects through a thin stem to two MT triplets of the centriole wall (Wang et al., 2018). The connection with the centriole wall is thought to be established through ODF2, a SDA-associated protein that was also recently characterized as a proximal DA component (Chong et al., 2020; Huang et al., 2017; Kashihara et al., 2019; Tateishi et al., 2013), and through CEP83 (Yang et al., 2018). CEP83 is required for the recruitment of CEP89, SCLT1, FBF1 and CEP164 to appendages, without affecting the distribution of ODF2 (Tanos et al., 2013). Thus, ODF2 and CEP83 likely form the stem that joins the DA heads to the centriole wall (Figs 3C and 4C). CEP89, SCLT1, LRRC45, FBF1, CEP164, TTBK2 and the recently characterized centrosome protein ANKRD26, as well as PIDD1, are all known components of the DA head (Figs 3C and 4C) (Bowler et al., 2019; Burigotto et al., 2021; Evans et al., 2021; Lo et al., 2019; Tanos et al., 2013; Yang et al., 2018). In addition, super-resolution imaging of DAs has shown that there are also proteins filling the space between each pinwheel blade, constituting a new ultrastructural element, the distal appendage matrix (DAM) (Yang et al., 2018) (Fig. 4A). The correct localization of CEP164 and LRRC45 in the DA are required for DAM formation (Yang et al., 2018). Owing to its outer localization at the DA, ANKRD26 might also contribute to forming the DAM (Bowler et al., 2019).

The assembly of SDAs follows DA formation

Protein components of the SDA are also recruited gradually in a hierarchical manner; inner, intermediate and outer components are recruited to form fully mature SDAs with a spherical head that connects to two MT triplets of the centriole wall through a conical structure (Figs 3C and 4C). C2CD3 initiates the recruitment of ODF2 and likely a few additional inner SDA components (Thauvin-Robinet et al., 2014; Wang et al., 2018). However, it remains unknown whether this recruitment is mediated by direct interactions or through indirect mediators. The base of the conical SDA is formed by CC2D2A, ODF2 and CEP128, which form the inner SDA layer (Ishikawa et al., 2005; Kashihara et al., 2019; Tateishi et al., 2013; Veleri et al., 2014). Subsequently, CCDC120, CEP110 (also known as CNTRL), CCDC68 and NDEL1 interact with ODF2 and CEP128, establishing an intermediate layer (Chong et al., 2020; Huang et al., 2017; Kashihara et al., 2019; Tateishi et al., 2013). Interestingly, CEP89 is a DA protein implicated in ciliogenesis (Sillibourne et al., 2011; Tanos et al., 2013) and is also present in SDAs (Chong et al., 2020), highlighting that there is some overlap between DA and SDA composition. Finally, ninein and CEP170 form an outer layer, which interacts with at least CCDC120 and CCDC68 (Figs 3C and 4C) (Huang et al., 2017).

Some SDA proteins, such as CCDC68, CCDC120, ninein and CEP170, have also been detected at a second location, the proximal end of the centriole (Chong et al., 2020; Huang et al., 2017). Although the biological relevance of this dual distribution of some SDA components is not clear, we hypothesize that this secondary proximal site might serve as a rapid-access reservoir of factors, which would accelerate the maturation of the daughter centriole. As such, a delay owing to protein translation would be at least partially by-passed.

The assembly of the CEP350–FOP–CEP19 protein complex further contributes to centriole maturation and asymmetries

A protein complex formed by FOP (also known as CEP43), CEP350 and CEP19 has recently been reported to assemble in-between DAs and SDAs (Kanie et al., 2017; Mojarad et al., 2017; Nishijima et al., 2017) (Fig. 3D). C2CD3 contributes to the recruitment of CEP350 and FOP (Mojarad et al., 2017), while C2CD3, TALPID3 and OFD1 contribute to the specific localization of CEP19 during centriole maturation (Wang et al., 2018). Moreover, the recruitment of CEP19 appears to be linked to the removal of newborn centriole proteins, including CCP110, and contributes to the early steps of ciliary basal body formation through the recruitment of ciliary vesicles (Kanie et al., 2017; Mojarad et al., 2017; Wang et al., 2018). In summary, it appears that TALPID3 and C2CD3 are two main triggers of maturation, promoting assembly of the DA, SDA and the CEP350-FOP-CEP19 protein complex.

Journal of Cell Science (2022) 135, jcs259395. doi:10.1242/jcs.259395

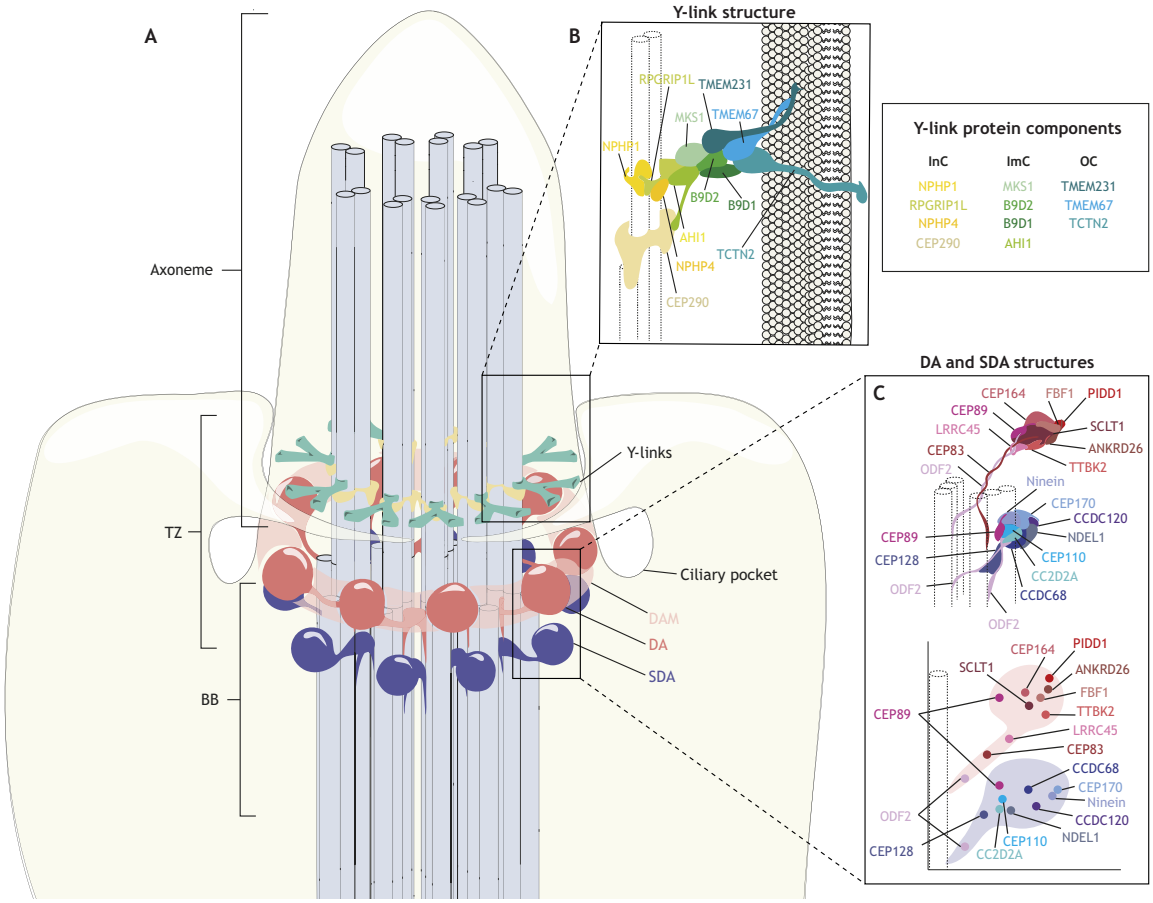

Fig. 4. Mature centriole organization at the basal body of the cilium. (A) Microtubule triplets of the basal body (BB) extend as doublets into the axoneme. This transition from triplets to doublets occurs at the transition zone (TZ), where Y-links connect microtubules to the extracellular membrane. (B) The relative position of protein complexes forming the Y-links that connect microtubule doublets to the plasma membrane. Proteins identified in the Y-link inner components (InC, in yellow/beige), the intermediate components (ImC, in greens), and the outer components (OC, in blues) are listed. (C) The relative positioning of DA (red) and SDA (blue) protein complexes as they associate to centriolar microtubule triplets.

Indeed, the recruitment of these proteins to the daughter centriole at the G_1/S transition represents the onset of the maturation process. Intriguingly, TALPID3 and C2CD3 are also present in the newborn centrioles, together with the CCP110 cap (Tsai et al., 2019), although they do not induce centriole maturation in growing newborn centrioles.

Centriole appendages partially disassemble on entering mitosis

CEP164 is displaced from the centriole just before mitosis (Schmidt et al., 2012), which suggests that, in part at least, mature centriole appendages are disassembled prior to entering division. EM data indicates that fewer DAs exist during mitosis and that there is a reduction in the head density due to transient displacement of the outer DA components FBF1, CEP164, ANKRD26 and TTBK2 (Bowler et al., 2019). However, inner components, such as CEP83 and SCLT1, maintain the nine-fold association with the mother centriole during mitosis (Bowler et al., 2019). Interestingly, SDAs retain this nine-fold symmetry but, as occurs in DAs, their head density is significantly reduced (Vorobjev and Chentsov, 1982). Moreover, it has been reported that both CEP170 and ninein association with the centrosome is reduced during division (Brunet et al., 2004; Chen et al., 2003); therefore, SDAs may undergo a similar transient remodelling during mitosis to that undertaken by their outer components. Further studies are needed to confirm such a SDA partial disassembly and to better characterize this process in DAs by assessing the behaviour of other components. The biological significance of the transient remodelling of the outer elements of DAs and SDAs is not yet clear, although it has been proposed that it might be a mechanism to equalize the age gap between the two mother centrioles of sister cells when DAs and SDAs re-assemble. Owing to the spatiotemporal correlation between the transient disassembly of DAs and SDAs on the older mother centriole and the maturation of the younger mother centriole (Bowler et al., 2019; Nakagawa et al., 2001; Piel et al., 2000), we propose that this process serves as a mechanism to transfer the maturation state. We hypothesize that the disassembled DA and SDA elements from the older mother centrioles could be distributed evenly between both daughter cells at mitosis, and that this could be

one of the mechanisms contributing to balancing out the built-in centrosome asymmetries in order to generate two daughter cells with identical fate and behaviour.

Cilia formation, a task for the mother centriole

One key function of centrosomes is to assemble cilia, MT-based organelles that protrude from the cell surface and can either be motile or non-motile. Motile cilia are required for cell locomotion and the propulsion of extracellular fluids, while non-motile primary cilia play critical roles in integrating signalling pathways (Mitchison and Valente, 2017). Particular attention has been paid recently to the role played by the primary cilium in the integration of growth factor signalling during neural development (Saade et al., 2018). Cilium assembly requires the transformation of the mother centriole into a basal body, which provides a template with nine-fold symmetry on which the axonemal structure of the cilium can be built (Fig. 4A). The basal body also dictates the position and orientation of the forming cilium. At the basal body, the centrosomal DA is involved in cilium assembly, while the SDA acts as a MT-anchoring point (Bornens, 2012; Clare et al., 2014). The TZ is situated just above the ciliary basal body and comprises the most proximal region of the cilium that separates the basal body from the axoneme. In functional cilia, the transport of molecules to the axoneme and ciliary membrane is tightly controlled, with the TZ acting as a ciliary gate that controls molecular access (Garcia-Gonzalo and Reiter, 2017).

Cilia are templated by mature centriolar structures

Like DAs and SDAs, the TZ adopts a ring-like protein structure composed of repetitive units, the Y-links, which bind to ciliary MT doublets and connect them to the ciliary membrane (Gilula and Satir, 1972). Y-links are organized in three layers: an inner layer of proteins located close to the MT doublets of the axoneme, an outer layer of transmembrane proteins in the ciliary membrane, and an intermediate layer of proteins in-between (Fig. 4B). In addition to these layers, CEP290 provides the base upon which Y-link components assemble by occupying the space between the axoneme and the plasma membrane (Yang et al., 2015). In the absence of CEP290, the distance between the MTs and ciliary membrane increases and the Y-link structure is lost (Craige et al., 2010) (Fig. 4B).

The inner components of the Y-links identified to date are RPGRIP1L (also known as NPHP8) and NPHP1 (Sang et al., 2011; Shi et al., 2017; Yang et al., 2015). RPGRIP1L dysfunction has been associated with a loss of Y-link integrity (Jensen et al., 2015), as well as with a reduction in NPHP1 and further components in other layers (e.g. AHI1, TCTN2 and TMEM231) (Shi et al., 2017). However, a reduction in NPHP1 only has a minor effect on RPGRP1L, with the intermediate and outer layers remaining unaffected (Shi et al., 2017). Thus, it appears that RPGRP1L is the main scaffold protein of Y-links. NPHP4 is a member of the RPGRIP1L–NPHP1–NPHP4 complex located above CEP290 in the TZ (Czarnecki and Shah, 2012; Sang et al., 2011; Williams et al., 2011). We propose NPHP4 to be another component of the Y-link inner layer given that it has been reported that it mediates the interaction between RPGRIP1L and NPHP1 (Sang et al., 2011) (Fig. 4B). Moreover, NPHP4 abrogation correlates with a displacement of NPHP1 from the TZ (Jauregui and Barr, 2005; Williams et al., 2011).

Although both RPGRIP1L and NPHP1 contain specific protein domains for membrane targeting (C2 domains), super-resolution imaging data shows that they form a ring structure around MT doublets with a radius that is too small to contact the ciliary membrane (Shi et al., 2017; Yang et al., 2015). Thus, C2 domains might be responsible for establishing protein–protein interaction modules that connect the different TZ proteins, rather than acting as direct membrane anchors (Remans et al., 2014). Indeed, one of the C2 domains of RPGRIP1L is thought to be responsible for its interaction with NPHP4 (Roepman et al., 2005).

For the intermediate layer of Y-links, so far only a single component has been characterized, MKS1 (Yang et al., 2015). Super-resolution data places MKS1 outside the RPGRIP1L ring and internal to some outer-layer components (TMEM67 and TCTN2) (Yang et al., 2015). As B9D1, B9D2 and AHI1 share some protein domains (B9 and C2) with MKS1, have no transmembrane regions and form a complex with MKS1 (MKS1–B9D1–B9D2–AHI1 complex) (Dowdle et al., 2011; Remans et al., 2014; Zhang and Aravind, 2012), this suggests that AHI1, B9D1 and B9D2 are part of the intermediate layer (Fig. 4B). Similar to the inner layer, these potential components of the intermediate layer have C2- and B9-type membrane-targeting domains. As suggested above, these domains could not only anchor the protein to the membrane, but also mediate the protein–protein interactions that help maintain the integrity of the Y-link structure.

Finally, TMEM231, TMEM67 and TCTN2 are outer components of Y-links (Shi et al., 2017; Yang et al., 2015); they are transmembrane proteins that, through their intracellular domains, likely interact with intermediate layer components (Yang et al., 2015). These proteins act as anchors that connect the Y-link base with the membrane, ultimately joining the ciliary membrane to the MT doublets and regulating the access of membrane proteins to the ciliary membrane (Yang et al., 2015). Future work will further elucidate the role of TZ and basal body components in ciliary biology, how cilia regulate cell signalling, both in organ development and tissue homeostasis, and also provide a better understanding as to how these components contribute to cilia-associated diseases (ciliopathies).

Concluding remarks and further considerations

The past decade of technological breakthroughs, including super-resolution microscopy, have paved the way for a detailed characterization of the 3D structure of the centrosome, as well as notable differences in the molecular composition of mother and daughter centrioles, thereby enhancing our understanding of relevant mechanisms underlying centrosome biology. This has led to our current view of the centrosome as a highly dynamic organelle that replicates in a semi-conservative manner in synchrony with the cell cycle. Indeed, the appendages that decorate the mother centriole are highly organized protein complexes that dynamically assemble and disassemble at the distal part of the centrioles during the late phases of the cell cycle. Because the assembly of these appendages in the new mother centriole is not fully acquired in one cell cycle, the organization of the mitotic spindle is intrinsically asymmetric. As a consequence, these built-in centrosome asymmetries establish the general rule that cell division is intrinsically asymmetric. This feature may be fundamental when cell division gives rise to two distinct cell types, such as when a stem cell divides to give rise to a stem cell and a cell that differentiates into another cell type. In addition, future research is needed to understand the mechanisms that a dividing cell utilizes to equalize these centrosome asymmetries in order to symmetrically divide.

The functional relevance of this small organelle in cell signalling, whether organized as a cilium basal body or as a mitotic spindle pole, in organ development and tissue homeostasis is only

beginning to be understood. Research in the coming years should pave the way to furthering our knowledge on the biology of this organelle and the pathological consequences of centrosome malfunction, such as seen in ciliopathies or neurodevelopmental congenital malformations.

Acknowledgements
The authors would like to apologise to those researchers whose primary data has not been directly cited in this Review article.

Competing interests
The authors declare no competing or financial interests.

Funding
The work in laboratory of E.M. is supported by the Spanish Ministry of Science and Innovation (grants nos PID2019-104134GB-I00 and RED2018-102553-T). J.B.A. is a recipient of a BES-2017-080050 PhD scholarship from the Spanish Ministry of Science and Innovation. P.L.F. is a recipient of a PRE2020-093886 PhD scholarship from the Spanish Ministry of Science and Innovation.

References

Agircan, F. G., Schiebel, E. and Mardin, B. R. (2014). Separate to operate: control of centrosome positioning and separation. *Philos. Trans. R. Soc. B Biol. Sci.* **369**, 20130461. doi:10.1098/rstb.2013.0461

Alfieri, M., Iaconis, D., Tammaro, R., Perone, L., Calì, G., Nitsch, L., Dougherty, G. W., Ragnini-Wilson, A. and Franco, B. (2020). The centrosomal/basal body protein OFD1 is required for microtubule organization and cell cycle progression. *Tissue Cell* **64**, 101369. doi:10.1016/j.tice.2020.101369

Arquint, C., Sonnen, K. F., Stierhof, Y.-D. and Nigg, E. A. (2012). Cell-cycle-regulated expression of STIL controls centriole number in human cells. *J. Cell Sci.* **125**, 1342-1352. doi:10.1242/jcs.099887

Arquint, C., Gabryjonczyk, A.-M. and Nigg, E. A. (2014). Centrosomes as signalling centres. *Philos. Trans. R. Soc. B Biol. Sci.* **369**, 20130464. doi:10.1098/rstb.2013.0464

Augustin, A., Spenlehauer, C., Dumond, H., Ménisier-de Murcia, J., Piel, M., Schmit, A.-C., Apiou, F., Vonesch, J.-L., Kock, M., Bornens, M. et al. (2003). PARP-3 localizes preferentially to the daughter centriole and interferes with the G1/S cell cycle progression. *J. Cell Sci.* **116**, 1551-1562. doi:10.1242/jcs.00341

Avidor-Reiss, T. and Fishman, E. L. (2019). It takes two to tango. *Soc. Reprod. Fertil.* **1**, 34.

Azimzadeh, J. and Marshall, W. F. (2010). Building the centriole. *Curr. Biol.* **20**, R816-R825. doi:10.1016/j.cub.2010.08.010

Bahe, S., Stierhof, Y.-D., Wilkinson, C. J., Leiss, F. and Nigg, E. A. (2005). Rootletin forms centriole-associated filaments and functions in centrosome cohesion. *J. Cell Biol.* **171**, 27-33. doi:10.1083/jcb.200504107

Banterle, N. and Gönczy, P. (2017). Centriole biogenesis: from identifying the characters to understanding the plot. *Annu. Rev. Cell Dev. Biol.* **33**, 23-49. doi:10.1146/annurev-cellbio-100616-060454

Bärenz, F., Mayilo, D. and Gruss, O. J. (2011). Centriolar satellites: busy orbits around the centrosome. *Eur. J. Cell Biol.* **90**, 983-989. doi:10.1016/j.ejcb.2011.07.007

Bettencourt-Dias, M., Rodrigues-Martins, A., Carpenter, L., Riparbelli, M., Lehmann, L., Gatt, M. K., Carmo, N., Balloux, F., Callaini, G. and Glover, D. M. (2005). SAK/PLK4 is required for centriole duplication and flagella development. *Curr. Biol.* **15**, 2199-2207. doi:10.1016/j.cub.2005.11.042

Bornens, M. (2012). The centrosome in cells and organisms. *Science* **335**, 422-426. doi:10.1126/science.1209037

Boveri, T. (1900). Zellen-Studien Vol. 4: Ueber die Natur der Centrosomen.

Bowler, M., Kong, D., Sun, S., Nanjundappa, R., Evans, L., Farmer, V., Holland, A., Mahjoub, M. R., Sui, H. and Loncarek, J. (2019). High-resolution characterization of centriole distal appendage morphology and dynamics by correlative STORM and electron microscopy. *Nat. Commun.* **10**, 993. doi:10.1038/s41467-018-08216-4

Brunet, S., Sardon, T., Zimmerman, T., Wittmann, T., Pepperkok, R., Karsenti, E. and Vernos, I. (2004). Characterization of the TPX2 domains involved in microtubule nucleation and spindle assembly in Xenopus egg extracts. *Mol. Biol. Cell* **15**, 5318-5328. doi:10.1091/mbc.e04-05-0385

Burigotto, M., Mattivi, A., Migliorati, D., Magnani, G., Valentini, C., Roccuzzo, M., Offterdinger, M., Pizzato, M., Schmidt, A., Villunger, A. et al. (2021). Centriolar distal appendages activate the centrosome-PIDDosome-p53 signalling axis via ANKRD26. *EMBO J.* **40**, 1-22. doi:10.15252/embj.2020104844

Bystrevskaya, V. B., Lichkun, V. V., Antonov, A. S. and Perov, N. A. (1988). An ultrastructural study of centriolar complexes in adult and embryonic human aortic endothelial cells. *Tissue Cell* **20**, 493-503. doi:10.1016/0040-8166(88)90052-3

Bystrevskaya, V. B., Lichkun, V. V., Krushinsky, A. V. and Smirnov, V. N. (1992). Centriole modification in human aortic endothelial cells. *J. Struct. Biol.* **109**, 1-12. doi:10.1016/1047-8477(92)90061-E

Čajánek, L. and Nigg, E. A. (2014). Cep164 triggers ciliogenesis by recruiting Tau tubulin kinase 2 to the mother centriole. *Proc. Natl. Acad. Sci. USA* **111**, E2841-E2850. doi:10.1073/pnas.1401777111

Chen, C.-H., Howng, S.-L., Cheng, T.-S., Chou, M.-H., Huang, C.-Y. and Hong, Y.-R. (2003). Molecular characterization of human ninein protein: Two distinct subdomains required for centrosomal targeting and regulating signals in cell cycle. *Biochem. Biophys. Res. Commun.* **308**, 975-983. doi:10.1016/S0006-291X(03)01510-9

Chong, W. M., Wang, W.-J., Lo, C.-H., Chiu, T.-Y., Chang, T.-J., Liu, Y.-P., Tanos, B., Mazo, G., Tsou, M.-F. B., Jane, W.-N. et al. (2020). Super-resolution microscopy reveals coupling between mammalian centriole subdistal appendages and distal appendages. *eLife* **9**, e53580. doi:10.7554/eLife.53580

Clare, D. K., Magescas, J., Piolot, T., Dumoux, M., Vesque, C., Pichard, E., Dang, T., Duvauchelle, B., Poirier, F. and Delacour, D. (2014). Basal foot MTOC organizes pillar MTs required for coordination of beating cilia. *Nat. Commun.* **5**, 4888. doi:10.1038/ncomms5888

Comartin, D., Gupta, G. D., Fussner, E., Coyaud, É., Hasegan, M., Archinti, M., Cheung, S. W. T., Pinchev, D., Lawo, S., Raught, B. et al. (2013). CEP120 and SPICE1 cooperate with CPAP in centriole elongation. *Curr. Biol.* **23**, 1360-1366. doi:10.1016/j.cub.2013.06.002

Conduit, P. T., Wainman, A. and Raff, J. W. (2015). Centrosome function and assembly in animal cells. *Nat. Rev. Mol. Cell Biol.* **16**, 611-624. doi:10.1038/nrm4062

Craige, B., Tsao, C.-C., Diener, D. R., Hou, Y., Lechtreck, K.-F., Rosenbaum, J. L. and Witman, G. B. (2010). CEP290 tethers flagellar transition zone microtubules to the membrane and regulates flagellar protein content. *J. Cell Biol.* **190**, 927-940. doi:10.1083/jcb.201006105

Cunha-Ferreira, I., Rodrigues-Martins, A., Bento, I., Riparbelli, M., Zhang, W., Laue, E., Callaini, G., Glover, D. M. and Bettencourt-Dias, M. (2009). The SCF/Slimb ubiquitin ligase limits centrosome amplification through degradation of SAK/PLK4. *Curr. Biol.* **19**, 43-49. doi:10.1016/j.cub.2008.11.037

Cunha-Ferreira, I., Bento, I., Pimenta-Marques, A., Jana, S. C., Lince-Faria, M., Duarte, P., Borrego-Pinto, J., Gilberto, S., Amado, T., Brito, D. et al. (2013). Regulation of autophosphorylation controls PLK4 self-destruction and centriole number. *Curr. Biol.* **23**, 2245-2254. doi:10.1016/j.cub.2013.09.037

Czarnecki, P. G. and Shah, J. V. (2012). The ciliary transition zone: From morphology and molecules to medicine. *Trends Cell Biol.* **22**, 201-210. doi:10.1016/j.tcb.2012.02.001

Dammermann, A. and Merdes, A. (2002). Assembly of centrosomal proteins and microtubule organization depends on PCM-1. *J. Cell Biol.* **159**, 255-266. doi:10.1083/jcb.200204023

Decarreau, J., Wagenbach, M., Lynch, E., Halpern, A. R., Vaughan, J. C., Kollman, J. and Wordeman, L. (2017). The tetrameric kinesin Kif25 suppresses pre-mitotic centrosome separation to establish proper spindle orientation. *Nat. Cell Biol.* **19**, 384-390. doi:10.1038/ncb3486

Dobbelaere, J., Schmidt Cernohorska, M., Huranova, M., Slade, D. and Dammermann, A. (2020). Cep97 is required for centriole structural integrity and cilia formation in Drosophila. *Curr. Biol.* **30**, 3045-3056.e7. doi:10.1016/j.cub.2020.05.078

Dowdle, W. E., Robinson, J. F., Kneist, A., Sirerol-Piquer, M. S., Frints, S. G. M., Corbit, K. C., Zaghloul, N. A., Van Lijnschoten, G., Mulders, L., Verver, D. E. et al. (2011). Disruption of a ciliary B9 protein complex causes meckel syndrome. *Am. J. Hum. Genet.* **89**, 589. doi:10.1016/j.ajhg.2011.09.013

Evans, L. T., Anglen, T., Scott, P., Lukasik, K., Loncarek, J. and Holland, A. J. (2021). ANKRD26 recruits PIDD1 to centriolar distal appendages to activate the PIDDosome following centrosome amplification. *EMBO J.* **40**, e105106. doi:10.15252/embj.2020105106

Fang, G., Zhang, D., Yin, H., Zheng, L., Bi, X. and Yuan, L. (2014). Centlein mediates an interaction between C-Nap1 and Cep68 to maintain centrosome cohesion. *J. Cell Sci.* **127**, 1631-1639. doi:10.1242/jcs.139451

Fry, A. M., Mayor, T., Meraldi, P., Stierhof, Y.-D., Tanaka, K. and Nigg, E. A. (1998). C-Nap1, a novel centrosomal coiled-coil protein and candidate substrate of the cell cycle-regulated protein kinase Nek2. *J. Cell Biol.* **141**, 1563-1574. doi:10.1083/jcb.141.7.1563

Fry, A. M., Sampson, J., Shak, C. and Shackleton, S. (2017a). Recent advances in pericentriolar material organization: ordered layers and scaffolding gels. *F1000Research* **6**, 1622. doi:10.12688/f1000research.11652.1

Fry, A. M., Bayliss, R. and Roig, J. (2017b). Mitotic regulation by NEK kinase networks. *Front. Cell Dev. Biol.* **5**, 102. doi:10.3389/fcell.2017.00102

Fu, J. and Glover, D. M. (2012). Structured illumination of the interface between centriole and peri-centriolar material. *Open Biol.* **2**, 120104. doi:10.1098/rsob.120104

Garcia-Gonzalo, F. R. and Reiter, J. F. (2017). Open Sesame: How transition fibers and the transition zone control ciliary composition. *Cold Spring Harb. Perspect. Biol.* **9**, a028134. doi:10.1101/cshperspect.a028134

Gheghiani, L., Loew, D., Lombard, B., Mansfeld, J. and Gavet, O. (2017). PLK1 activation in late G2 sets up commitment to mitosis. *Cell Rep.* **19**, 2060-2073. doi:10.1016/j.celrep.2017.05.031

Gilula, N. B. and Satir, P. (1972). The ciliary necklace: a ciliary membrane specialization. *J. Cell Biol.* **53**, 494-509. doi:10.1083/jcb.53.2.494

Gudi, R., Haycraft, C. J., Bell, P. D., Li, Z. and Vasu, C. (2015). Centrobin-mediated regulation of the centrosomal protein 4.1-associated protein (CPAP) level limits centriole length during elongation stage. *J. Biol. Chem.* **290**, 6890-6902. doi:10.1074/jbc.M114.603423

Habedanck, R., Stierhof, Y.-D., Wilkinson, C. J. and Nigg, E. A. (2005). The Polo kinase Plk4 functions in centriole duplication. *Nat. Cell Biol.* **7**, 1140-1146. doi:10.1038/ncb1320

Hames, R. S., Crookes, R. E., Straatman, K. R., Merdes, A., Hayes, M. J., Faragher, A. J. and Fry, A. M. (2005). Dynamic recruitment of Nek2 kinase to the centrosome involves microtubules, PCM-1, and localized proteasomal degradation. *Mol. Biol. Cell.* **16**, 1569-2127. doi:10.1091/mbc.e04-08-0688

Hardy, T., Lee, M., Hames, R. S., Prosser, S. L., Cheary, D.-M., Samant, M. D., Schultz, F., Baxter, J. E., Rhee, K. and Fry, A. M. (2014). Multisite phosphorylation of C-Nap1 releases it from Cep135 to trigger centrosome disjunction. *J. Cell Sci.* **127**, 2493-2506. doi:10.1242/jcs.142331

He, R., Huang, N., Bao, Y., Zhou, H., Teng, J. and Chen, J. (2013). LRRC45 is a centrosome linker component required for centrosome cohesion. *Cell Rep.* **4**, 1100-1107. doi:10.1016/j.celrep.2013.08.005

Heath, I. B., Kaminskyj, S. G. and Bauchop, T. (1986). Basal body loss during fungal zoospore encystment: evidence against centriole autonomy. *J. Cell Sci.* **83**, 135-140. doi:10.1242/jcs.83.1.135

Helps, N. R., Luo, X., Barker, H. M. and Cohen, P. T. W. (2000). NIMA-related kinase 2 (Nek2), a cell-cycle-regulated protein kinase localized to centrosomes, is complexed to protein phosphatase 1. *Biochem. J.* **349**, 509-518. doi:10.1042/bj3490509

Huang, N., Xia, Y., Zhang, D., Wang, S., Bao, Y., He, R., Teng, J. and Chen, J. (2017). Hierarchical assembly of centriole subdistal appendages via centrosome binding proteins CCDC120 and CCDC68. *Nat. Commun.* **8**, 15057. doi:10.1038/ncomms15057

Ibrahim, R., Messaoudi, C., Chichon, F. J., Celati, C. and Marco, S. (2009). Electron tomography study of isolated human centrioles. *Microsc. Res. Tech.* **72**, 42-48. doi:10.1002/jemt.20637

Ishikawa, H., Kubo, A., Tsukita, S. and Tsukita, S. (2005). Odf2-deficient mother centrioles lack distal/subdistal appendages and the ability to generate primary cilia. *Nat. Cell Biol.* **7**, 517-524. doi:10.1038/ncb1251

Jana, S. C. (2021). Centrosome structure and biogenesis: variations on a theme? *Semin. Cell Dev. Biol.* **110**, 123-138. doi:10.1016/j.semcdb.2020.10.014

Jauregui, A. R. and Barr, M. M. (2005). Functional characterization of the C. elegans nephrocystins NPHP-1 and NPHP-4 and their role in cilia and male sensory behaviors. *Exp. Cell Res.* **305**, 333-342. doi:10.1016/j.yexcr.2005.01.008

Jean, C., Tollon, Y., Raynaud-Messina, B. and Wright, M. (1999). The mammalian interphase centrosome: two independent units maintained together by the dynamics of the microtubule cytoskeleton. *Eur. J. Cell Biol.* **78**, 549-560. doi:10.1016/S0171-9335(99)80020-X

Jensen, V. L., Li, C., Bowie, R. V., Clarke, L., Mohan, S., Blacque, O. E. and Leroux, M. R. (2015). Formation of the transition zone by Mks5/Rpgrip1L establishes a ciliary zone of exclusion (CIZE) that compartmentalises ciliary signalling proteins and controls PIP2 ciliary abundance. *EMBO J.* **34**, 2537-2556. doi:10.15252/embj.201488044

Kanie, T., Abbott, K. L., Mooney, N. A., Plowey, E. D., Demeter, J. and Jackson, P. K. (2017). The CEP19-RABL2 GTPase complex binds IFT-B to initiate intraflagellar transport at the ciliary base. *Dev. Cell.* **42**, 22-36.e12. doi:10.1016/j.devcel.2017.05.016

Kapitein, L. C., Peterman, E. J. G., Kwok, B. H., Kim, J. H., Kapoor, T. M. and Schmidt, C. F. (2005). The bipolar mitotic kinesin Eg5 moves on both microtubules that it crosslinks. *Nature* **435**, 114-118. doi:10.1038/nature03503

Kashihara, H., Chiba, S., Kanno, S.-I., Suzuki, K., Yano, T. and Tsukita, S. (2019). Cep128 associates with Odf2 to form the subdistal appendage of the centriole. *Genes Cells* **24**, 231-243. doi:10.1111/gtc.12668

Keller, L. C., Geimer, S., Romijn, E., Yates, J., Zamora, I. and Marshall, W. F. (2009). Molecular architecture of the centriole proteome: the conserved WD40 domain protein POC1 is required for centriole duplication and length control. *Mol. Biol. Cell.* **20**, 1119-1267. doi:10.1091/mbc.e08-06-0619

Keller, D., Orpinell, M., Olivier, N., Wachsmuth, M., Mahen, R., Wyss, R., Hachet, V., Ellenberg, J., Manley, S. and Gönczy, P. (2014). Mechanisms of HsSAS-6 assembly promoting centriole formation in human cells. *J. Cell Biol.* **204**, 697-712. doi:10.1083/jcb.201307049

Khodjakov, A., Rieder, C. L., Sluder, G., Cassels, G., Sibon, O. and Wang, C.-L. (2002). De novo formation of centrosomes in vertebrate cells arrested during S phase. *J. Cell Biol.* **158**, 1171-1181. doi:10.1083/jcb.200205102

Kim, S. and Dynlacht, B. D. (2013). Assembling a primary cilium. *Curr. Opin. Cell Biol.* **25**, 506-511. doi:10.1016/j.ceb.2013.04.011

Kim, J., Krishnaswami, S. R. and Gleeson, J. G. (2008a). CEP290 interacts with the centriolar satellite component PCM-1 and is required for Rab8 localization to the primary cilium. *Hum. Mol. Genet.* **17**, 3796-3805. doi:10.1093/hmg/ddn277

Kim, K., Lee, S., Chang, J. and Rhee, K. (2008b). A novel function of CEP135 as a platform protein of C-NAP1 for its centriolar localization. *Exp. Cell Res.* **314**, 3692-3700. doi:10.1016/j.yexcr.2008.09.016

Kim, M. K., Dudognon, C. and Smith, S. (2012). Tankyrase 1 regulates centrosome function by controlling CPAP stability. *EMBO Rep.* **13**, 724-732. doi:10.1038/embor.2012.86

Kim, T.-S., Park, J.-E., Shukla, A., Choi, S., Murugan, R. N., Lee, J. H., Ahn, M., Rhee, K., Bang, J. K., Kim, B. Y. et al. (2013). Hierarchical recruitment of Plk4 and regulation of centriole biogenesis by two centrosomal scaffolds, Cep192 and Cep152. *Proc. Natl. Acad. Sci. USA* **110**, E4849-E4857. doi:10.1073/pnas.1319656110

Kim, M., O'Rourke, B. P., Soni, R. K., Jallepalli, P. V., Hendrickson, R. C. and Tsou, M.-F. B. (2016). Promotion and suppression of centriole duplication are catalytically coupled through PLK4 to ensure centriole homeostasis. *Cell Rep.* **16**, 1195-1203. doi:10.1016/j.celrep.2016.06.069

Kobayashi, T., Kim, S., Lin, Y.-C., Inoue, T. and Dynlacht, B. D. (2014). The CP110-interacting proteins talpid3 and cep290 play overlapping and distinct roles in cilia assembly. *J. Cell Biol.* **204**, 215-229. doi:10.1083/jcb.201304153

Komesli, S., Tournier, F., Paintrand, M., Margolis, R. L., Job, D. and Bornens, M. (1989). Mass isolation of calf thymus centrosomes: identification of a specific configuration. *J. Cell Biol.* **109**, 2869-2878. doi:10.1083/jcb.109.6.2869

Kraatz, S., Guichard, P., Obbineni, J. M., Olieric, N., Hatzopoulos, G. N., Hilbert, M., Sen, I., Missimer, J., Gönczy, P. and Steinmetz, M. O. (2016). The human centriolar protein CEP135 contains a two-stranded coiled-coil domain critical for microtubule binding. *Structure* **24**, 1358-1371. doi:10.1016/j.str.2016.06.011

Kumar, D., Rains, A., Herranz-Pérez, V., Lu, Q., Shi, X., Swaney, D. L., Stevenson, E., Krogan, N. J., Huang, B., Westlake, C. et al. (2021). A ciliopathy complex builds distal appendages to initiate ciliogenesis. *J. Cell Biol.* **220**, e202011133. doi:10.1083/jcb.202011133

Kurtulmus, B., Yuan, C., Schuy, J., Neuner, A., Hata, S., Kalamakis, G., Martin-Villalba, A. and Pereira, G. (2018). LRRC45 contributes to early steps of axoneme extension. *J. Cell Sci.* **131**, jcs223594. doi:10.1242/jcs.223594

Lawo, S., Hasegan, M., Gupta, G. D. and Pelletier, L. (2012). Subdiffraction imaging of centrosomes reveals higher-order organizational features of pericentriolar material. *Nat. Cell Biol.* **14**, 1148-1158. doi:10.1038/ncb2591

Li, J., Kim, S., Kobayashi, T., Liang, F.-X., Korzeniewski, N., Duensing, S. and Dynlacht, B. D. (2012). Neurl4, a novel daughter centriole protein, prevents formation of ectopic microtubule organizing centres. *EMBO Rep.* **13**, 547-553. doi:10.1038/embor.2012.40

Lin, Y.-C., Chang, C.-W., Hsu, W.-B., Tang, C.-J. C., Lin, Y.-N., Chou, E.-J., Wu, C.-T. and Tang, T.-K. (2013a). Human microcephaly protein CEP135 binds to hSAS-6 and CPAP, and is required for centriole assembly. *EMBO J.* **32**, 1141-1154. doi:10.1038/emboj.2013.56

Lin, Y.-N., Wu, C.-T., Lin, Y.-C., Hsu, W.-B., Tang, C.-J. C., Chang, C.-W. and Tang, T. K. (2013b). CEP120 interacts with CPAP and positively regulates centriole elongation. *J. Cell Biol.* **202**, 211-219. doi:10.1083/jcb.201212060

Lo, C.-H., Lin, I.-H., Yang, T. T., Huang, Y.-C., Tanos, B. E., Chou, P.-C., Chang, C.-W., Tsay, Y.-G., Liao, J.-C. and Wang, W.-J. (2019). Phosphorylation of CEP83 by TTBK2 is necessary for cilia initiation. *J. Cell Biol.* **218**, 3489-3505. doi:10.1083/jcb.201811142

Loukil, A., Tormanen, K. and Sütterlin, C. (2017). The daughter centriole controls ciliogenesis by regulating Neurl-4 localization at the centrosome. *J. Cell Biol.* **216**, 1287-1300. doi:10.1083/jcb.201608119

Mahjoub, M. R., Xie, Z. and Stearns, T. (2010). Cep120 is asymmetrically localized to the daughter centriole and is essential for centriole assembly. *J. Cell Biol.* **191**, 331-346. doi:10.1083/jcb.201003009

Marshall, W. F. (2009). Centriole Evolution. *Curr. Opin. Cell Biol.* **21**, 14-19. doi:10.1016/j.ceb.2009.01.008

Marthiens, V. and Basto, R. (2020). Centrosomes: the good and the bad for brain development. *Biol. Cell* **112**, 153-172. doi:10.1111/boc.201900090

Mennella, V., Keszthelyi, B., Mcdonald, K. L., Chhun, B., Kan, F., Rogers, G. C., Huang, B. and Agard, D. A. (2012). Subdiffraction-resolution fluorescence microscopy reveals a domain of the centrosome critical for pericentriolar material organization. *Nat. Cell Biol.* **14**, 1159-1168. doi:10.1038/ncb2597

Meraldi, P. and Nigg, E. A. (2002). The centrosome cycle. *FEBS Lett.* **521**, 9-13. doi:10.1016/S0014-5793(02)02865-X

Mitchison, H. M. and Valente, E. M. (2017). Motile and non-motile cilia in human pathology: from function to phenotypes. *J. Pathol.* **241**, 294-309. doi:10.1002/path.4843

Mojarad, B. A., Gupta, G. D., Hasegan, M., Goudiam, O., Basto, R., Gingras, A.-C. and Pelletier, L. (2017). CEP19 cooperates with FOP and CEP350 to drive early steps in the ciliogenesis programme. *Open Biol.* **7**, 170114. doi:10.1098/rsob.170114

Moritz, M., Braunfeld, M. B., Guénebaut, V., Heuser, J. and Agard, D. A. (2000). Structure of the γ-tubulin ring complex: a template for microtubule nucleation. *Nat. Cell Biol.* **2**, 365-370. doi:10.1038/35014058

Moyer, T. C., Clutario, K. M., Lambrus, B. G., Daggubati, V. and Holland, A. J. (2015). Binding of STIL to Plk4 activates kinase activity to promote centriole assembly. *J. Cell Biol.* **209**, 863-878. doi:10.1083/jcb.201502088

Nabais, C., Pereira, S. G. and Bettencourt-Dias, M. (2017). Noncanonical biogenesis of centrioles and basal bodies. *Cold Spring Harb. Symp. Quant. Biol.* **82**, 123-135. doi:10.1101/sqb.2017.82.034694

Nakagawa, Y., Yamane, Y., Okanoue, T., Tsukita, S. and Tsukita, S. (2001). Outer dense fiber 2 is a widespread centrosome scaffold component preferentially associated with mother centrioles: Its identification from isolated centrosomes. *Mol. Biol. Cell.* **12**, 1541-1910. doi:10.1091/mbc.12.6.1687

Nigg, E. A. and Stearns, T. (2011). The centrosome cycle: centriole biogenesis, duplication and inherent asymmetries. *Nat. Cell Biol.* **13**, 1154-1160. doi:10.1038/ncb2345

Nishijima, Y., Hagiya, Y., Kubo, T., Takei, R., Katoh, Y. and Nakayama, K. (2017). RABL2 interacts with the intraflagellar transport-B complex and CEP19 and participates in ciliary assembly. *Mol. Biol. Cell.* **28**, 1591-1711. doi:10.1091/mbc.e17-01-0017

Ohta, M., Ashikawa, T., Nozaki, Y., Kozuka-Hata, H., Goto, H., Inagaki, M., Oyama, M. and Kitagawa, D. (2014). Direct interaction of Plk4 with STIL ensures formation of a single procentriole per parental centriole. *Nat. Commun.* **5**, 5267. doi:10.1038/ncomms6267

Paintrand, M., Moudjou, M., Delacroix, H. and Bornens, M. (1992). Centrosome organization and centriole architecture: Their sensitivity to divalent cations. *J. Struct. Biol.* **108**, 107-128. doi:10.1016/1047-8477(92)90011-X

Panic, M., Hata, S., Neuner, A. and Schiebel, E. (2015). The centrosomal linker and microtubules provide dual levels of spatial coordination of centrosomes. *PLoS Genet.* **11**, e1005243. doi:10.1371/journal.pgen.1005243

Park, S.-Y., Park, J.-E., Kim, T.-S., Kim, J. H., Kwak, M.-J., Ku, B., Tian, L., Murugan, R. N., Ahn, M., Komiya, S. et al. (2014). Molecular basis for unidirectional scaffold switching of human Plk4 in centriole biogenesis. *Nat. Struct. Mol. Biol.* **21**, 696-703. doi:10.1038/nsmb.2846

Piel, M., Meyer, P., Khodjakov, A., Rieder, C. L. and Bornens, M. (2000). The respective contributions of the mother and daughter centrioles to centrosome activity and behavior in vertebrate cells. *J. Cell Biol.* **149**, 317-330. doi:10.1083/jcb.149.2.317

Prosser, S. L. and Pelletier, L. (2020). Centriolar satellite biogenesis and function in vertebrate cells. *J. Cell Sci.* **133**, jcs239566. doi:10.1242/jcs.239566

Remans, K., Bürger, M., Vetter, I. R. and Wittinghofer, A. (2014). C2 domains as protein-protein interaction modules in the ciliary transition zone. *Cell Rep.* **8**, 1-9. doi:10.1016/j.celrep.2014.05.049

Robbins, E., Jentzsch, G. and Micali, A. (1968). The centriole cycle in synchronized HeLa cells. *J. Cell Biol.* **36**, 329-339. doi:10.1083/jcb.36.2.329

Roepman, R., Letteboer, S. J. F., Arts, H. H., Van Beersum, S. E. C., Lu, X., Krieger, E., Ferreira, P. A. and Cremers, F. P. M. (2005). Interaction of nephrocystin-4 and RPGRIP1 is disrupted by nephronophthisis or Leber congenital amaurosis-associated mutations. *Proc. Natl. Acad. Sci. USA* **102**, 18520-18525. doi:10.1073/pnas.0505774102

Rogers, G. C., Rusan, N. M., Roberts, D. M., Peifer, M. and Rogers, S. L. (2009). The SCF Slimb ubiquitin ligase regulates Plk4/Sak levels to block centriole reduplication. *J. Cell Biol.* **184**, 225-229. doi:10.1083/jcb.200808049

Saade, M., Blanco-Ameijeiras, J., Gonzalez-Gobartt, E. and Martı, E. (2018). A centrosomal view of CNS growth. *Dev* **145**, dev170613. doi:10.1242/dev.170613

Sang, L., Miller, J. J., Corbit, K. C., Giles, R. H., Brauer, M. J., Otto, E. A., Baye, L. M., Wen, X., Scales, S. J., Kwong, M. et al. (2011). Mapping the NPHP-JBTS-MKS protein network reveals ciliopathy disease genes and pathways. *Cell* **145**, 513-528. doi:10.1016/j.cell.2011.04.019

Schmidt, K. N., Kuhns, S., Neuner, A., Hub, B., Zentgraf, H. and Pereira, G. (2012). Cep164 mediates vesicular docking to the mother centriole during early steps of ciliogenesis. *J. Cell Biol.* **199**, 1083-1101. doi:10.1083/jcb.201202126

Schmidt, T. I., Kleylein-Sohn, J., Westendorf, J., Le Clech, M., Lavoie, S. B., Stierhof, Y. D. and Nigg, E. A. (2009). Control of centriole length by CPAP and CP110. *Curr. Biol.* **19**, 1005-1011. doi:10.1016/j.cub.2009.05.016

Schwarz, A., Sankaralingam, P., O'Connell, K. and Müller-Reichert, T. (2018). Revisiting centrioles in nematodes—historic findings and current topics. *Cells* **7**, 101. doi:10.3390/cells7080101

Shall, S. and de Murcia, G. (2000). Poly(ADP-ribose) polymerase-1: what have we learned from the deficient mouse model? *Mutat. Res. DNA Repair* **460**, 1-15. doi:10.1016/S0921-8777(00)00016-1

Shi, X., Garcia, G., Van De Weghe, J. C., McGorty, R., Pazour, G. J., Doherty, D., Huang, B. and Reiter, J. F. (2017). Super-resolution microscopy reveals that disruption of ciliary transition-zone architecture causes Joubert syndrome. *Nat. Cell Biol.* **19**, 1178-1188. doi:10.1038/ncb3599

Sillibourne, J. E., Specht, C. G., Izeddin, I., Hurbain, I., Tran, P., Triller, A., Darzacq, X., Dahan, M. and Bornens, M. (2011). Assessing the localization of centrosomal proteins by PALM/STORM nanoscopy. *Cytoskeleton* **68**, 619-627. doi:10.1002/cm.20536

Sillibourne, J. E., Hurbain, I., Grand-Perret, T., Goud, B., Tran, P. and Bornens, M. (2013). Primary ciliogenesis requires the distal appendage component Cep123. *Biol. Open* **2**, 535-545. doi:10.1242/bio.20134457

Sonnen, K. F., Schermelleh, L., Leonhardt, H. and Nigg, E. A. (2012). 3D-structured illumination microscopy provides novel insight into architecture of human centrosomes. *Biol. Open* **1**, 965-976. doi:10.1242/bio.20122337

Sonnen, K. F., Gabryjonczyk, A.-M., Anselm, E., Stierhof, Y.-D. and Nigg, E. A. (2013). Human cep192 and cep152 cooperate in plk4 recruitment and centriole duplication. *J. Cell Sci.* **126**, 3223-3233. doi:10.1242/jcs.129502

Spektor, A., Tsang, W. Y., Khoo, D. and Dynlacht, B. D. (2007). Cep97 and CP110 suppress a cilia assembly program. *Cell* **130**, 678-690. doi:10.1016/j.cell.2007.06.027

Tang, C.-J. C., Fu, R.-H., Wu, K.-S., Hsu, W.-B. and Tang, T. K. (2009). CPAP is a cell-cycle regulated protein that controls centriole length. *Nat. Cell Biol.* **11**, 825-831. doi:10.1038/ncb1889

Tanos, B. E., Yang, H.-J., Soni, R., Wang, W.-J., Macaluso, F. P., Asara, J. M. and Tsou, M.-F. B. (2013). Centriole distal appendages promote membrane docking, leading to cilia initiation. *Genes Dev.* **27**, 163-168. doi:10.1101/gad.207043.112

Tateishi, K., Yamazaki, Y., Nishida, T., Watanabe, S., Kunimoto, K., Ishikawa, H. and Tsukita, S. (2013). Two appendages homologous between basal bodies and centrioles are formed using distinct Odf2 domains. *J. Cell Biol.* **203**, 417-425. doi:10.1083/jcb.201303071

Thauvin-Robinet, C., Lee, J. S., Lopez, E., Herranz-Pérez, V., Shida, T., Franco, B., Jego, L., Ye, F., Pasquier, L., Loget, P. et al. (2014). The oral-facial-digital syndrome gene C2CD3 encodes a positive regulator of centriole elongation. *Nat. Genet.* **46**, 905-911. doi:10.1038/ng.3031

Tollenaere, M. A. X., Mailand, N. and Bekker-Jensen, S. (2015). Centriolar satellites: key mediators of centrosome functions. *Cell. Mol. Life Sci.* **72**, 11-23. doi:10.1007/s00018-014-1711-3

Tsai, J.-J., Hsu, W.-B., Liu, J.-H., Chang, C.-W. and Tang, T. K. (2019). CEP120 interacts with C2CD3 and Talpid3 and is required for centriole appendage assembly and ciliogenesis. *Sci. Rep.* **9**, 6037. doi:10.1038/s41598-019-42577-0

Tsou, M.-F. B. and Stearns, T. (2006). Mechanism limiting centrosome duplication to once per cell cycle. *Nature* **442**, 947-951. doi:10.1038/nature04985

Uzbekov, R. and Alieva, I. (2018). Who are you, subdistal appendages of centriole? *R. Soc. Open Sci.* **8**, 180062. doi:10.1098/rsob.180062

Veleri, S., Manjunath, S. H., Fariss, R. N., May-Simera, H., Brooks, M., Foskett, T. A., Gao, C., Longo, T. A., Liu, P., Nagashima, K. et al. (2014). Ciliopathy-associated gene Cc2d2a promotes assembly of subdistal appendages on the mother centriole during cilia biogenesis. *Nat. Commun.* **5**, 4207. doi:10.1038/ncomms5207

Vlijm, R., Li, X., Panic, M., Rüthnick, D., Hata, S., Herrmannsdörfer, F., Kuner, T., Heilemann, M., Engelhardt, J., Hell, S. W. et al. (2018). STED nanoscopy of the centrosome linker reveals a CEP68-organized, periodic rootletin network anchored to a C-Nap1 ring at centrioles. *Proc. Natl. Acad. Sci. USA* **115**, E2246-E2253. doi:10.1073/pnas.1716840115

Vorobjev, I. A. and Chentsov, Y. S. (1982). Centrioles in the cell cycle. I. Epithelial cells. *J. Cell Biol.* **93**, 938-949. doi:10.1083/jcb.93.3.938

Wang, L. and Dynlacht, B. D. (2018). The regulation of cilium assembly and disassembly in development and disease. *Development* **145**, dev151407. doi:10.1242/dev.151407

Wang, L., Failler, M., Fu, W. and Dynlacht, B. D. (2018). A distal centriolar protein network controls organelle maturation and asymmetry. *Nat. Commun.* **9**, 3938. doi:10.1038/s41467-018-06286-y

Williams, C. L., Li, C., Kida, K., Inglis, P. N., Mohan, S., Semenec, L., Bialas, N. J., Stupay, R. M., Chen, N., Blacque, O. E. et al. (2011). MKS and NPHP modules cooperate to establish basal body/transition zone membrane associations and ciliary gate function during ciliogenesis. *J. Cell Biol.* **192**, 1023-1041. doi:10.1083/jcb.201012116

Winey, M. and O'Toole, E. (2014). Centriole structure. *Philos. Trans. R. Soc. B Biol. Sci.* **369**, 20130457. doi:10.1098/rstb.2013.0457

Woodruff, J. B., Wueseke, O. and Hyman, A. A. (2014). Pericentriolar material structure and dynamics. *Philos. Trans. R. Soc. B Biol. Sci.* **369**, 20130459. doi:10.1098/rstb.2013.0459

Woodruff, J. B., Ferreira Gomes, B., Widlund, P. O., Mahamid, J., Honigmann, A. and Hyman, A. A. (2017). The centrosome is a selective condensate that nucleates microtubules by concentrating tubulin. *Cell* **169**, 1066-1077.e10. doi:10.1016/j.cell.2017.05.028

Wu, C., Yang, M., Li, J., Wang, C., Cao, T., Tao, K. and Wang, B. (2014). Talpid3-binding centrosomal protein Cep120 is required for centriole duplication and proliferation of cerebellar granule neuron progenitors. *PLoS ONE* **9**, e107943. doi:10.1371/journal.pone.0107943

Yadav, S. P., Sharma, N. K., Liu, C., Dong, L., Li, T. and Swaroop, A. (2016). Centrosomal protein CP110 controls maturation of the mother centriole during cilia biogenesis. *Development* **143**, 1491-1501. doi:10.1242/dev.130120

Yang, J., Adamian, M. and Li, T. (2006). Rootletin interacts with C-Nap1 and may function as a physical linker between the pair of centrioles/basal bodies in cells. *Mol. Biol. Cell.* **17**, 555-1040. doi:10.1091/mbc.e05-10-0943

Yang, T. T., Su, J., Wang, W.-J., Craige, B., Witman, G. B., Bryan Tsou, M.-F. and Liao, J.-C. (2015). Superresolution pattern recognition reveals the architectural map of the ciliary transition zone. *Sci. Rep.* **5**, 14096. doi:10.1038/srep14096

Yang, T. T., Chong, W. M., Wang, W.-J., Mazo, G., Tanos, B., Chen, Z., Tran, T. M. N., Chen, Y.-D., Weng, R. R., Huang, C.-E. et al. (2018). Super-resolution architecture of mammalian centriole distal appendages reveals distinct

blade and matrix functional components. *Nat. Commun.* **9**, 2023. doi:10.1038/s41467-018-04469-1

Ye, X., Zeng, H., Ning, G., Reiter, J. F. and Liu, A. (2014). C2cd3 is critical for centriolar distal appendage assembly and ciliary vesicle docking in mammals. *Proc. Natl. Acad. Sci. USA* **111**, 2164-2169. doi:10.1073/pnas.1318737111

Zhang, D. and Aravind, L. (2012). Novel transglutaminase-like peptidase and C2 domains elucidate the structure, biogenesis and evolution of the ciliary compartment. *Cell Cycle* **11**, 3861-3875. doi:10.4161/cc.22068

Zitouni, S., Francia, M. E., Leal, F., Montenegro Gouveia, S., Nabais, C., Duarte, P., Gilberto, S., Brito, D., Moyer, T., Kandels-Lewis, S. et al. (2016). CDK1 prevents unscheduled PLK4-STIL complex assembly in centriole biogenesis. *Curr. Biol.* **26**, 1127-1137. doi:10.1016/j.cub.2016.03.055

Zou, C., Li, J., Bai, Y., Gunning, W. T., Wazer, D. E., Band, V. and Gao, Q. (2005). Centrobin: a novel daughter centriole-associated protein that is required for centriole duplication. *J. Cell Biol.* **171**, 437-445. doi:10.1083/jcb.200506185